

Isotope Geochemistry of Natural Gas from the Horn River Basin: Understanding Gas Origin,
Storage and Transport in an Unconventional Shale Play

by

Giselle Norville

A thesis submitted in partial fulfillment of the requirements for the degree of

Doctor of Philosophy

Department of Earth and Atmospheric Sciences
University of Alberta

© Giselle Norville, 2014

Abstract

Devonian shales of the Horn River Basin, northeast British Columbia are recognized key targets for unconventional shale gas production in Canada. Recent studies show gas isotope geochemistry in several unconventional shale plays worldwide differ from conventional hydrocarbon reservoirs and carbon isotope reversal between hydrocarbon gas components is a common phenomenon. Geochemical properties of natural gases hold clues to origin, storage and transport within the shale and may assist in elucidation of the shale gas system; however limited published work exists on stable isotope geochemistry of Horn River Basin shale gases. Over four hundred mud gas and production gas samples were obtained from Phanerozoic formations in the Dilly Creek area of the basin and chemical and stable isotope compositions were measured.

Carbon isotope depth profiles of Horn River Basin gases (methane, ethane and propane) from surface depth to the target formation provide a geochemical template applicable for use in environmental remediation. Isotope signatures ($\delta^{13}\text{C}_{\text{methane}}$, $\delta^{13}\text{C}_{\text{ethane}}$ and $\delta^{13}\text{C}_{\text{propane}}$) of surface casing vent gas and soil gas at six leaking well sites in the basin were matched to isotope depth profiles which allow identification of formations from which gas leaks occurred. Carbon isotope lateral profiles map the subsurface variation within shale gas target formations and serve as a proxy for flow connectivity within the shale. Inter- and intra-formational variations in $\delta^{13}\text{C}_{\text{methane}}$ values of Horn River Group gases are observed and carbon isotope data purports greater connectivity in the Muskwa Formation than in the Otter Park Formation. Time series data show stable isotope compositional

changes during shale gas production and fluctuations in $\delta^{13}\text{C}$ values of produced Muskwa, Otter Park and Evie gases occur with unique trends for each well. In the early stage of production Horn River Group gases generally show more negative $\delta^{13}\text{C}_{\text{methane}}$ values, while increases in $\delta^{13}\text{C}_{\text{methane}}$ values are observed in after periods of well 'shut in' and overall $\delta^{13}\text{C}_{\text{methane}}$ values ranged from approximately -38‰ to -28‰.

Horn River Group gas isotope signatures indicate gases are dry, mature and thermogenic in origin and several shale gas samples exhibit isotopically reversed gas signatures. Few cases of carbon isotope reversal were observed in mud gases while most produced gases showed partial isotope reversal among gas components or full isotope reversals where $\delta^{13}\text{C}_{\text{methane}} > \delta^{13}\text{C}_{\text{ethane}} > \delta^{13}\text{C}_{\text{propane}}$. It is plausible that carbon isotope fractionation occurs during shale gas production as hydrocarbon molecules traverse tortuous pathways within the complex shale fabric which alters the carbon isotope signature of produced gases. Spatial and temporal stable isotope variations occur in Devonian shale gases in the Horn River Basin and this should be taken into consideration during interpretation of isotope data obtained from unconventional shale gas reservoirs.

To William and Enid

Acknowledgements

I would like to extend sincere thanks to my supervisor Karlis Muehlenbachs for his guidance and support provided throughout my research. Karlis was always extremely willing to share his knowledge and give generously of his time which I greatly appreciated. Special thanks to my supervisory and examination committee members and John-Paul Zonneveld, Murray Gingras, Ben Rostron and Murray Gray for their advice and thoughtful comments. I would like to acknowledge Nexen for financial support and providing samples for this study and offer thanks to Jon Dola and Doug Bearinger for their assistance. I also wish to thank Dean Rokosh, Tom Chacko, Barb Tilley, Olga Levner and staff of the Earth and Atmospheric Science Department.

Table of Contents

Chapter 1 - Introduction	1
1.1 Introduction.....	1
1.2 Thesis Approach	6
References Cited	10
Chapter 2 –Carbon isotope depth profiles as a forensic tool for source identification in leaking gas wells in the Horn River Basin	19
2.1 Introduction.....	19
2.1.1 <i>The Horn River Basin</i>	22
2.2 Methods.....	22
2.3 Results and Discussion	23
2.4 Conclusions.....	28
References Cited	29
Chapter 3 – Characterization of Muskwa and Otter Park gas shales in the Horn River Basin using Mud Gas Isotope Depth Profiles	33
3.1 Introduction.....	33
3.1.1 <i>Flow connectivity in gas shales</i>	34
3.1.2 <i>Isotope reversals</i>	36
3.1.3 <i>Geologic setting</i>	36
3.2 Methodology	38
3.2.1 <i>Sample collection</i>	38
3.2.2 <i>Sample analysis</i>	41
$\delta^{13}C$ analysis	41
δD analysis	41
<i>X-ray fluorescence (XRF) analysis</i>	42
3.3 Results and Discussion	42
3.3.1 <i>Mineralogy</i>	42

3.3.2	<i>Stable isotope geochemistry</i>	49
3.3.3	<i>Isotope cross-plots</i>	53
3.3.4	<i>The natural gas plot</i>	54
3.4	Conclusions.....	68
	References Cited	70

Chapter 4 – Gas generation and transport in Devonian gas shales of the Horn River Basin- Insights using carbon isotope geochemistry78

4.1	Introduction.....	78
4.1.1	<i>The Horn River Basin</i>	81
4.1.2	<i>Gas flow mechanisms in shale</i>	81
4.1.3	<i>Chemical and isotope composition of shale gas</i>	83
4.2	Methods.....	84
4.3	Results and Discussion	85
4.4	Conclusions.....	102
	References Cited	104

Chapter 5 – Understanding Temporal Variations in Carbon and Hydrogen Isotope Ratios during Devonian Shale Gas Production112

5.1	Introduction.....	112
5.1.1	<i>Geological background</i>	115
5.1.2	<i>Natural gas generation</i>	116
5.1.3	<i>Isotope Fractionation effects during gas transport through the shale matrix</i>	118
5.2	Methods.....	120
5.3	Results and Discussion	122
5.4	Conclusions.....	135
	References Cited	136

Chapter 6 – Conclusions	145
6.1 Conclusions.....	145
6.1.1 <i>Environmental remediation</i>	145
6.1.2 <i>Flow connectivity in shale gas target formations</i>	146
6.1.3 <i>Isotope fractionation effects during degassing of the shale reservoir</i>	147
6.1.4 <i>Carbon isotope ratios of mud gas vs production gases</i> ...	148
6.2 Future Work	149
References Cited	151
 References Cited	 154
 Appendix A –Time Series Chemical composition	 171
Appendix B1 –Time Series Stable isotope composition	183
Appendix B2 – Isotope crossplots	189
Appendix C1 –Time Series Gas production	194
Appendix C2 –Time Series Gas production and stable isotopes	197
Appendix D –Natural Gas Plots	203

List of Tables

Table 1.1 List of Horn River Basin wells from which natural gas samples were obtained for this study	8
Table 2.1 Depth and location data for Well HZ TSEA B-018-I/094-O-08	23
Table 4.1 Shale gas target formations for Horn River Group Wells 1 to 8	85
Table 4.2 Perforation and fracture treatment for Horn River Group Wells 1 to 8 (Horizontal well length~2km)	85
Table 5.1 Carbon isotope data for mud gases and production gases from the Horn River Basin (Muskwa and Otter Park Formations)	122
Table 5.2 Classification scheme for shale gases based on their carbon isotope signatures	133
Table B1.1 Carbon isotope ratios of methane and ethane for production gases from 18 wells located at the b-77-H multi-well pad site.	187

List of Figures

Figure 1.1 Location map showing the Horn River Basin, northeast British Columbia.....	5
Figure 1.2 Schematic showing stratigraphy of the Horn River Basin and placement of laterals of wells in the Muskwa and Otter Park target formations	9
Figure 2.1 Location map showing the study area and the HZ TSEA B-018-I/094-O-08 well in the Horn River Basin, NE British Columbia	21
Figure 2.2 Carbon isotopic depth profiles for methane, ethane and propane gas components for the HZ TSEA B-018-I/094-O-08 well	25
Figure 2.3 Carbon isotope signatures ($\delta^{13}\text{C}_{\text{methane}}$, $\delta^{13}\text{C}_{\text{ethane}}$, $\delta^{13}\text{C}_{\text{propane}}$) of six samples of soil gases and surface casing vent flow gases from leaking wells in the Horn River Basin	26
Figure 2.4 Carbon isotope depth profiles indicating formations from which leaking soil gases and surface casing vent gases originated	27
Figure 3.1 Location map of the Horn River Basin, Northeast British Columbia. The study site is indicated by a star symbol within NTS map 94O/8	38
Figure 3.2 Stratigraphy of the Middle Devonian NE British Columbia in the Horn River Basin area	39
Figure 3.3 Schematic showing well placements in the Horn River Basin. Mud gas isotope profiles are created for laterals of Wells 1 and 2 (b-18-I and b-A18I	

respectively). The horizontal well leg for Well 1 is within the Otter Park Formation and for Well 2 within the Muskwa Formation	40
Figure 3.4 Variation in shale mineralogy for Horn River wells measured along the horizontal well legs (a) bA18I (Muskwa Formation) (b) b18I (Otter Park formation)	44
Figure 3.5 Relationship between mineral (wt. %) and the mud gas concentration for bA18I (Muskwa Formation) and b18I (Otter Park formation) wells. Minerals (a) Quartz (b) Clay minerals- Illite and Kaolinite (c) Calcite (d) Brittle components of shale –quartz , feldspar and carbonate.	46
Figure 3.6 Variation in mineral (wt. %) and the mud gas concentration for the b18I (Otter Park formation) wells along horizontal well paths	47
Figure 3.7 Variation in mineral (wt. %) and the mud gas concentration for the bA18I (Muskwa Formation) well along horizontal well paths	48
Figure 3.8 Mud gas isotope profiles for the Muskwa and Otter Park Formations (a) Carbon isotope profiles of methane (b) Carbon isotope profiles of ethane (c) Carbon isotope profiles of propane	51
Figure 3.9 Variation in mud gas concentration (gas units) along horizontal wellbore paths in the Muskwa and Otter Park Formations.....	52
Figure 3.10 Hydrogen isotope profiles of methane for the Muskwa and Otter Park Formations	53

Figure 3.11 (a) Isotope cross-plot showing $\delta^{13}\text{C}_{\text{ethane}}$ vs $\delta^{13}\text{C}_{\text{methane}}$ for the Muskwa and Otter Park Formations (b) Isotope cross-plot showing $\delta^{13}\text{C}_{\text{propane}}$ vs $\delta^{13}\text{C}_{\text{ethane}}$ for the Muskwa and Otter Park Formation54

Figure 3.12 (a) Natural gas plot of mud gases from the Muskwa Formation sampled along the horizontal well leg (b) Natural gas plot of mud gases from the Otter Park Formation sampled along the horizontal well leg54

Figure 3.13 Cross-plot of $\delta^{13}\text{C}_{\text{methane}}$ vs $\delta\text{D}_{\text{methane}}$ for the Muskwa and Otter Park Formations56

Figure 3.14 The Schoell plot for natural gas classification (after (Schoell, 1983) B and M denotes biogenic and mixed gas respectively. To, Tc and Td denotes thermogenic with oil, condensate and dry56

Figure 3.15 Cross-plots of isotope composition vs mud gas concentration for the Otter Park and Muskwa Formations (a) $\delta^{13}\text{C}_{\text{methane}}$ vs mud gas concentration (b) $\delta^{13}\text{C}_{\text{ethane}}$ vs mud gas concentration (c) $\delta^{13}\text{C}_{\text{propane}}$ vs mud gas concentration (d) $\delta\text{D}_{\text{methane}}$ vs mud gas concentration58

Figure 3.16 (a) Carbon isotope profiles for the Muskwa Formation and corresponding mud gas concentration (gas units) (b) Carbon isotope profiles for the Otter Park Formation and corresponding mud gas concentration (gas units).60

Figure 3.17 (a) Variation in $\delta^{13}\text{C}_{\text{ethane}} - \delta^{13}\text{C}_{\text{methane}}$ and mud gas concentration for well bA18I (Muskwa Formation) (b) Variation in $\delta^{13}\text{C}_{\text{ethane}} - \delta^{13}\text{C}_{\text{methane}}$ and mud gas concentration for well b18I (Otter Park Formation)62

Figure 3.18 Relationship between $\delta^{13}\text{C}_{\text{ethane}} - \delta^{13}\text{C}_{\text{methane}}$ and mud gas concentration for well bA18I (Muskwa Formation) and well b18I (Otter Park Formation)63

Figure 3.19 Variation in clay mineralogy along lateral of well b18I. Distinct regions are identified where high or low clays content is measured in the shale from laterals of well b18I (Otter Park). The red lines subdivide the length into sections based on the variation in the clay content.64

Figure 3.20 Relationship between $\delta^{13}\text{C}_{\text{ethane}} - \delta^{13}\text{C}_{\text{methane}}$ and mud gas concentration for well b18I (Otter Park Formation). Depth intervals based on mineralogy variations in the shale65

Figure 3.21 Relationship between $\delta^{13}\text{C}_{\text{methane}}$ and mineral composition for well bA18I (Muskwa Formation) and well b18I (Otter Park Formation)67

Figure 3.22 Relationship between $\delta^{13}\text{C}_{\text{ethane}} - \delta^{13}\text{C}_{\text{methane}}$ and mineral composition for well bA18I (Muskwa Formation) and well b18I (Otter Park Formation).68

Figure 4.1 Location map showing the study area in the Horn River Basin, NE British Columbia80

Figure 4.2 Stratigraphic chart of Devonian Horn River Basin Formations82

Figure 4.3(a) Horn River Basin Production decline curves for Wells 1 to 6 showing long term fluctuations in gas rate ~ 1250 days b) Horn River Basin Production decline curves for Wells 7 and Well 8 wells showing short term fluctuations in gas rate ~ 20 days c) Gas production decline curves for Horn River Group shale gases from Wells 1 to 8 shown on a logarithmic time scale87

Figure 4.4 Variation of methane concentration (mole fraction) for Horn River Group shale gases from Wells 1 to 889

Figure 4.5(a) Variation in the $\delta^{13}\text{C}_{\text{methane}}$ values of Horn River Group shale gases for Wells 1 to 6 indicating long term fluctuations b) Variation in the $\delta^{13}\text{C}_{\text{methane}}$ values of Horn River Group shale gases for Wells 1 to 8 shown on a logarithmic time scale c) Variation in the $\delta^{13}\text{C}_{\text{ethane}}$ values of Horn River Group shale gases for Wells 1 to 8 shown on a logarithmic time scale d) Variation in the $\delta^{13}\text{C}_{\text{propane}}$ values of Horn River Group shale gases for Wells 1 to 8 shown on a logarithmic time scale91

Figure 4.6(a) Plot of $\delta^{13}\text{C}_{\text{ethane}} - \delta^{13}\text{C}_{\text{methane}}$ shown on a logarithmic time scale. Gases which show isotope reversal plot below the dashed line. b) Plot of $\delta^{13}\text{C}_{\text{propane}} - \delta^{13}\text{C}_{\text{ethane}}$ shown on a logarithmic time scale. Gases which show isotope reversal plot below the dashed line.93

Figure 4.7(a) Overlay plot of gas production rate and methane carbon isotope values ($\delta^{13}\text{C}_{\text{methane}}$) vs time for Well 1 (a16I –Muskwa) b) Overlay plot of gas production rate and methane carbon isotope values ($\delta^{13}\text{C}_{\text{methane}}$) vs time for Well 2 (aC16I –Evie) c) Overlay plot of gas production rate and methane carbon isotope values ($\delta^{13}\text{C}_{\text{methane}}$) vs time for Well 3 (aE16I –Muskwa-Otter Park) d) Overlay plot of gas production rate and methane carbon isotope values ($\delta^{13}\text{C}_{\text{methane}}$) vs time for Well 4 (c16I –Muskwa) e) Overlay plot of gas production rate and methane carbon isotope values ($\delta^{13}\text{C}_{\text{methane}}$) vs time for Well 5 (b93A –Muskwa) f) Overlay plot of gas production rate and methane carbon isotope values ($\delta^{13}\text{C}_{\text{methane}}$) vs time for Well 6 (c93A –Muskwa) g) Overlay plot of gas production rate and methane carbon isotope values ($\delta^{13}\text{C}_{\text{methane}}$) vs time for Well 7 (c1J –Muskwa) h) Overlay plot of gas production rate and methane carbon isotope values ($\delta^{13}\text{C}_{\text{methane}}$) vs time for Well 8 (dA1J–Evie)95

Figure 4.8 Crossplot of gas production rate vs methane carbon isotope values $\delta^{13}\text{C}_{\text{methane}}$ for 8 Horn River Basin wells	100
Figure 4.9(a) Gas rate vs methane carbon isotope values $\delta^{13}\text{C}_{\text{methane}}$ for wells located at well pad 1 b) Gas rate vs methane carbon isotope values $\delta^{13}\text{C}_{\text{methane}}$ for wells located at well pad 2 c) Gas rate vs methane carbon isotope values $\delta^{13}\text{C}_{\text{methane}}$ for wells located at well pad 3	100
Figure 5.1 Location map showing the study area in the Horn River Basin, Northeast British Columbia using the National Topographic System	114
Figure 5.2 Stratigraphic chart showing the Mid-Late Devonian period for the Horn River Basin	116
Figure 5.3 Burial curves highlighting Devonian strata in the Sukunka area northeast British Columbia	117
Figure 5.4 (a) Relationship between the relative changes in $\delta^{13}\text{C}$ values of methane, ethane and propane and the fraction of shale gas desorbed from the core (b) Variation in carbon isotope ratios due to isotope fractionation effects during methane gas diffusion in a sample of shale. The dashed line indicates changes over time until the $\delta^{13}\text{C}$ values approach that of the source where $\delta^{13}\text{C}_{\text{methane}}$ is - 39‰	119
Figure 5.5 Location map indicating the sites of the three well pads in the Horn River Basin. The map (NTS 94/O) shows a section of the NTS 1:50000 map sheet. The horizontal well legs are within the Muskwa and Otter Park Formations of the Horn River Group.....	121

Figure 5.6 The James maturity diagram illustrating Muskwa mud gas (after James, 1983). The plot shows the average $\delta^{13}\text{C}$ values of methane, ethane, propane and butane for all Muskwa mud gases. Isotopic separations between components determine the level of organic maturity (LOM)126

Figure 5.7(a) Crossplot of $\delta^{13}\text{C}_{\text{ethane}}$ vs $\delta^{13}\text{C}_{\text{methane}}$ gases from the Muskwa. $\delta^{13}\text{C}$ values of methane and ethane for samples of mud gas and production gas are shown for the 5 well locations in the HRB b) Crossplot of $\delta^{13}\text{C}_{\text{propane}}$ vs $\delta^{13}\text{C}_{\text{ethane}}$ gases from the Muskwa. $\delta^{13}\text{C}$ values of methane and ethane for samples of mud gas and production gas are shown for the 5 well locations in the HRB127

Figure 5.8(a) Crossplot of $\delta^{13}\text{C}_{\text{ethane}}$ vs $\delta^{13}\text{C}_{\text{methane}}$ gases from the Otter Park $\delta^{13}\text{C}$ values of methane and ethane for samples of mud gas and production gas are shown for the 5 well locations in the HRB b) Crossplot of $\delta^{13}\text{C}_{\text{propane}}$ vs $\delta^{13}\text{C}_{\text{ethane}}$ gases from the Otter Park. $\delta^{13}\text{C}$ values of methane and ethane for samples of mud gas and production gas are shown for the 5 well locations in the HRB128

Figure 5.9 (a) The Natural gas plot for Muskwa mud gases. $\delta^{13}\text{C}$ values (C1- C4 components) vs $1/n$ are plot where n represents the number of carbon atoms in the hydrocarbon (b) The Natural gas plot for Muskwa production gas. $\delta^{13}\text{C}$ values (C1- C4 components) vs $1/n$ are plot where n represents the number of carbon atoms in the hydrocarbon130

Figure 5.10 Natural gas plots for Muskwa production gases. $\delta^{13}\text{C}$ values (C1-C4 components) vs $1/n$ are plot where n represents the number of carbon atoms in the hydrocarbon131

Figure 5.11 (a) The Natural gas plot for Otter Park mud gases. $\delta^{13}\text{C}$ values (C1- C4 components) vs $1/n$ are plot where n represents the number of carbon atoms in the hydrocarbon (b) The Natural gas plot for Otter Park production gas. $\delta^{13}\text{C}$

values (C1- C4 components) vs 1/n are plot where n represents the number of carbon atoms in the hydrocarbon	132
Figure A.1. Variation in methane concentration (mole fraction) for Horn River Group shale gases from 8 well locations- NTS 94/08	171
Figure A.2. Variation in ethane concentration (mole fraction) for Horn River Group shale gases from 8 well locations - NTS 94/08	172
Figure A.3. Variation in propane concentration (mole fraction) for Horn River Group shale gases from 6 well locations - NTS 94/08	173
Figure A.4. Variation in carbon dioxide concentration (mole fraction) for Horn River Group shale gases from 8 well locations - NTS 94/08	174
Figure A.5. Variation in nitrogen concentration (mole fraction) for Horn River Group shale gases from 8 well locations - NTS 94/08	175
Figure A.6. Variation in gas wetness for Horn River Group shale gases from 8 well locations - NTS 94/08	176
Figure A.7. Overlay plot showing variation in methane concentration (mole fraction) for Horn River Group shale gases from 8 well locations - NTS 94/08.	177
Figure A.8. Overlay plot showing variation in ethane concentration (mole fraction) for Horn River Group shale gases from 8 well locations - NTS 94/08.	177
Figure A.9. Overlay plot showing variation in propane concentration (mole fraction) for Horn River Group shale gases from 8 well locations - NTS 94/08.	178

Figure A.10. Overlay plot showing variation in carbon dioxide concentration (mole fraction) for Horn River Group shale gases from 8 well locations - NTS 94/08	178
Figure A.11. Overlay plot showing variation in carbon dioxide concentration (mole fraction) for Horn River Group shale gases from 8 well locations - NTS 94/08	179
Figure A.12. Overlay plot showing variation in gas wetness for Horn River Group shale gases from 8 well locations - NTS 94/08.....	179
Figure A.13. Overlay plot showing variation in methane concentration (mole fraction) on a logarithmic time scale for Horn River Group shale gases from 8 well locations - NTS 94/08	180
Figure A.14. Overlay plot showing variation in ethane concentration (mole fraction) on a logarithmic time scale for Horn River Group shale gases from 8 well locations - NTS 94/08	180
Figure A.15. Overlay plot showing variation in propane concentration (mole fraction) on a logarithmic time scale for Horn River Group shale gases from 8 well locations - NTS 94/08	181
Figure A.16. Overlay plot showing variation in carbon dioxide concentration (mole fraction) on a logarithmic time scale for Horn River Group shale gases from 8 well locations - NTS 94/08	181
Figure A.17. Overlay plot showing variation in nitrogen concentration (mole fraction) on a logarithmic time scale for Horn River Group shale gases from 8 well locations - NTS 94/08	182

Figure A.18. Overlay plot showing variation in propane concentration (mole fraction) on a logarithmic time scale for Horn River Group shale gases from 8 well locations - NTS 94/08	182
Figure B1.1. Variation in $\delta^{13}\text{C}_{\text{methane}}$ values for Horn River Group shale gases from 8 well locations - NTS 94/08	183
Figure B1.2. Variation in $\delta^{13}\text{C}_{\text{ethane}}$ values for Horn River Group shale gases from 8 well locations - NTS 94/08	184
Figure B1.3. Variation in $\delta^{13}\text{C}_{\text{propane}}$ values for Horn River Group shale gases from 8 well locations - NTS 94/08	185
Figure B1.4. Variation in $\delta\text{D}_{\text{methane}}$ values for Horn River Group shale gases from 8 well locations - NTS 94/08	186
Figure B1.5. Overlay plot of $\delta^{13}\text{C}_{\text{ethane}} - \delta^{13}\text{C}_{\text{methane}}$ for Horn River Group shale gases from 8 well locations - NTS 94/08.....	188
Figure B1.6. Overlay plot of $\delta^{13}\text{C}_{\text{propane}} - \delta^{13}\text{C}_{\text{ethane}}$ for Horn River Group shale gases from 8 well locations - NTS 94/08.....	188
Figure B2.1. Isotope cross-plot showing $\delta^{13}\text{C}_{\text{ethane}}$ vs $\delta^{13}\text{C}_{\text{methane}}$ for Horn River Group shale gases from 8 well locations - NTS 94/08	189
Figure B2.2. Isotope cross-plot showing $\delta^{13}\text{C}_{\text{propane}}$ vs $\delta^{13}\text{C}_{\text{ethane}}$ for Horn River Group shale gases from 8 well locations - NTS 94/08	190
Figure B2.3. Isotope cross-plot showing $\delta^{13}\text{C}_{\text{propane}}$ vs $\delta^{13}\text{C}_{\text{methane}}$ for Horn River Group shale gases from 8 well locations - NTS 94/08	191

Figure B2.4. Overlay plot of $\delta^{13}\text{C}_{\text{ethane}} - \delta^{13}\text{C}_{\text{methane}}$ for Horn River Group shale gases from 8 well locations - NTS 94/08.....	192
Figure B2.5. Overlay plot of $\delta^{13}\text{C}_{\text{propane}} - \delta^{13}\text{C}_{\text{ethane}}$ for Horn River Group shale gases from 8 well locations - NTS 94/08.....	192
Figure B2.6. Overlay plot of $\delta^{13}\text{C}_{\text{propane}} - \delta^{13}\text{C}_{\text{methane}}$ for Horn River Group shale gases from 8 well locations - NTS 94/08.....	193
Figure B2.7. Overlay plot of $\delta^{13}\text{C}_{\text{methane}}$ vs gas wetness for Horn River Group shale gases from 8 well locations - NTS 94/08.....	193
Figure C1.1. Gas production decline curves for Horn River Group shale gases from 8 well locations - NTS 94/08	194
Figure C1.2. Variation in tubing pressure for Horn River Group shale gases from 6 well locations - NTS 94/08	195
Figure C1.3. Gas production decline curves for Horn River Group shale gases from 8 well locations - NTS 94/08	196
Figure C1.4. Gas production decline curves for Horn River Group shale gases from 6 well locations - NTS 94/08	196
Figure C2.1. 3D plot showing variation in gas flow rate and $\delta^{13}\text{C}_{\text{methane}}$ with time for well a16I - NTS 94/08.....	197
Figure C2.2. 3D plot showing variation in gas flow rate and $\delta^{13}\text{C}_{\text{methane}}$ with time for well aC16I - NTS 94/08	197

Figure C2.3. 3D plot showing variation in gas flow rate and $\delta^{13}\text{C}_{\text{methane}}$ with time for well aE16I - NTS 9.....	198
Figure C2.4. Overlay 3D plot showing variation in gas flow rate and $\delta^{13}\text{C}_{\text{methane}}$ with time for wells a16I and aC16I - NTS 94/08.....	198
Figure C2.5. Overlay 3D plot showing variation in gas flow rate and $\delta^{13}\text{C}_{\text{methane}}$ with time for three wells at the a16I multi-well pad site (a16I and aC16I and aE16I) - NTS 94/08.....	199
Figure C2.6. Overlay plots of gas production rate and methane carbon isotope values ($\delta^{13}\text{C}_{\text{methane}}$) vs time for Horn River Group shale gases from 8 well locations - NTS 94/08	200
Figure C2.7. Gas rate vs methane carbon isotope values ($\delta^{13}\text{C}_{\text{methane}}$) for Horn River Group shale gases from 6 well locations - NTS 94/08	201
Figure C2.8. Overlay plot showing methane carbon isotope values ($\delta^{13}\text{C}_{\text{methane}}$) vs gas rate for Horn River Group shale gases from 6 well locations - NTS 94/08 ..	202
Figure D.1. The natural gas plot for well a16I (NTS 94/08). $\delta^{13}\text{C}$ values vs $1/n$ are shown where n represents the number of carbon atoms in the hydrocarbon	203
Figure D.2. The natural gas plot for well aC16I (NTS 94/08). $\delta^{13}\text{C}$ values vs $1/n$ are shown where n represents the number of carbon atoms in the hydrocarbon .	203
Figure D.3. The natural gas plot for well aE16I (NTS 94/08). $\delta^{13}\text{C}$ values vs $1/n$ are shown where n represents the number of carbon atoms in the hydrocarbon .	204

Figure D.4. The natural gas plot for well c16I (NTS 94/08). $\delta^{13}\text{C}$ values vs $1/n$ are shown where n represents the number of carbon atoms in the hydrocarbon204

Figure D.5. The natural gas plot for well b93A (NTS 94/08). $\delta^{13}\text{C}$ values vs $1/n$ are shown where n represents the number of carbon atoms in the hydrocarbon .205

Figure D.6. The natural gas plot for well c93A (NTS 94/08). $\delta^{13}\text{C}$ values vs $1/n$ are shown where n represents the number of carbon atoms in the hydrocarbon .205

Figure D.7. The natural gas plot for well c1J (NTS 94/08). $\delta^{13}\text{C}$ values vs $1/n$ are shown where n represents the number of carbon atoms in the hydrocarbon206

Figure D.8. The natural gas plot for well dA1J (NTS 94/08). $\delta^{13}\text{C}$ values vs $1/n$ are shown where n represents the number of carbon atoms in the hydrocarbon .206

Figure D.9. Natural gas plots for well a16I (NTS 94/08) showing variation in carbon isotope signatures of gases over time. $\delta^{13}\text{C}$ values vs $1/n$ are shown where n represents the number of carbon atoms in the hydrocarbon207

Figure D.10. 3D natural gas plot for well a16I (NTS 94/08) showing variation in carbon isotope signatures of gases over time. $\delta^{13}\text{C}$ values vs $1/n$ are shown where n represents the number of carbon atoms in the hydrocarbon208

CHAPTER 1

1.1 INTRODUCTION

The Horn River Basin, northeast British Columbia (Fig. 1.1) is a major Canadian unconventional shale gas play (NTS 94I, 94J, 94O and 94P) which covers an area of approximately 1.3 million hectares with estimated gas in place (GIP) reserves of 448 trillion cubic feet (Tcf) (Adams, 2012; Close et al., 2012). Increased demand for new sources of energy, a decline in conventional resources and advances in technologies for recovery of hydrocarbon reserves have prompted development of shale gas reservoirs. Gas shales are prolific, continuous, self-contained hydrocarbon systems where shales function as the source, seal and reservoir (Hill and Nelson, 2000; Curtis, 2002; Law and Curtis, 2002; Schmoker, 2002; Cardott, 2006). Natural gas production from shale plays provide new challenges due to the ultra-low porosity and permeability of these fine grained sedimentary rocks which may extend into the nano-scale range (Loucks et al., 2009; Nelson, 2009; Curtis et al., 2010; Sondergeld et al., 2010; Ambrose et al., 2010). Shale gas reservoirs require multi-stage hydraulic fracturing for economic gas production. Artificial fractures generated intercept natural fractures and provide additional flow pathways from the shale matrix to the wellbore.

Understanding the shale gas system is critical for successful reservoir exploration and development and this study involves a geochemical approach for evaluation. Stable isotope geochemistry is widely used for natural gas analysis in conventional hydrocarbon reservoirs (Stahl, 1974; Fuex, 1977; Schoell, 1980; Rice and Claypool, 1981; James, 1983; Schoell, 1983; Berner and Faber, 1988; Chung et al., 1988a; Clayton, 1991; Jenden et al., 1993; Prinzhofer and Huc, 1995; Rowe and Muehlenbachs, 1999; Tilley and Muehlenbachs, 2006; Norville and Dawe, 2007) and others; however few publications exist on application of isotope geochemistry to unconventional gas plays. Exploration and production in the Horn River Basin is still in the early stages and at present there exist gaps in

current knowledge with regard to gas generation, storage and transport within shale formations.

In this study, natural gas geochemistry is applied and stable isotope compositions of gases from Phanerozoic Horn River Basin formations measured. Isotope signatures of natural gases are determined by the parent organic matter, gas generation processes and subsequent post generation processes which occur in the reservoir. Isotope fractionation effects may be a result of biological, chemical or physical processes which alter the gas stable isotope composition. In conventional hydrocarbon reservoirs, the natural gas carbon isotope signature generally shows methane (C1) with the most negative $\delta^{13}\text{C}$ value and higher homologues; ethane (C2), propane (C3) and butane (C4) show increasing ^{13}C enrichment (Fuex, 1977; Sackett, 1978; Chung et al., 1988b). These ‘normal’ thermogenic gases generally have carbon isotope compositions where $\delta^{13}\text{C}_{\text{methane}} < \delta^{13}\text{C}_{\text{ethane}} < \delta^{13}\text{C}_{\text{propane}} < \delta^{13}\text{C}_{\text{butane}}$. Carbon isotope reversal between hydrocarbon components of natural gas is uncommon in conventional reservoirs and reversal between methane and ethane ($\delta^{13}\text{C}_{\text{methane}} > \delta^{13}\text{C}_{\text{ethane}}$) is very rare (Fuex, 1977). Smith et al. (1971) and Fuex (1977) theorize cases of isotope reversals including complete reversal can be attributed to late stages of gas generation and indicate ‘a late high-maturity increment of gas produced by its source’.

Unconventional shale gas systems frequently show deviation from the ‘normal’ trend in gas carbon isotope signature. In hydrocarbon reservoirs, carbon stable isotope gas signatures may be ‘isotopically reversed’ where $\delta^{13}\text{C}$ values of ethane and / or propane are more negative than $\delta^{13}\text{C}$ of methane (Jenden et al., 1993; Seewald and Whelan, 2005; Burruss and Laughrey, 2010; Rodriguez and Philp, 2010; Tilley et al., 2011; Zumberge et al., 2012; Tilley and Muehlenbachs, 2013). Carbon isotope signatures of gases may be (i) partially reversed where some deviation from the normal trend occurs or (ii) fully reversed where there is complete deviation from the normal trend and $\delta^{13}\text{C}_{\text{methane}} > \delta^{13}\text{C}_{\text{ethane}} > \delta^{13}\text{C}_{\text{propane}}$ (Burruss and Laughrey, 2010; Tilley et al., 2011; Tilley and Muehlenbachs, 2013). In the literature, possible explanations to account for isotope reversals

observed include wet gas cracking, mixing of gases from different sources and complex redox reactions involving transition metals and water (Jenden et al., 1993; Ni et al., 2009; Burruss and Laughrey, 2010; Tilley et al., 2011; Xia et al., 2012; Zumberge et al., 2012), however further investigation is necessary.

Carbon and hydrogen stable isotope composition of natural gases reflect biogenic or thermogenic gas origin and gas maturity which is influenced by the history of the sedimentary basin. In gas shales, the hydrocarbons remain in situ trapped in the shale matrix after generation and often the reservoir is considered to be a 'closed system'. Experimental studies document changes in stable isotope composition which occur during thermogenic gas generation in open and closed system conditions and the corresponding carbon isotope signatures of these highly mature natural gases (Arneth, 1984; Arneth and Matzigkeit, 1986; Ungerer and Pelet, 1987; Rullkötter et al., 1988; Behar et al., 1992; Horsfield et al., 1992; Mycke et al., 1994; Behar et al., 1995; Lewan, 1997; Behar et al., 1997; Schenk et al., 1997; Lorant et al., 1998; Dieckmann et al., 1998; Waples, 2000; Lorant and Behar, 2002; Odden et al., 2002; Hill et al., 2003; Kotarba and Lewan, 2013).

Carbon isotope fractionation may also occur during gas transport through shales (Zhang and Krooss, 2001; Strapoć et al., 2010; Zhang et al., 2012; Amann-Hildenbrand et al., 2012) and may have implications during shale gas production as natural gas travels from the reservoir to the wellbore. Changes in the isotope ratios which occur during diffusion and desorption from shales may cause produced gases and in situ gas to differ in their isotope signatures. Theoretical models (Tang and Xia, 2011; Xia and Tang, 2012) show the isotope changes expected during natural gas production as degassing of low permeability shales occurs. Freeman et al. (2012, 2013) demonstrate evidence of compositional changes in natural gases during production from North American shale gas wells.

Givetian- Frasnian shales of the Horn River group include the Muskwa, Otter Park and Evie Formations; basinal sediments deposited during periods of marine transgression (Gray and Kassube, 1963; Oldale and Munday, 1994; Weissenberger and Potma, 2001; Ross and Bustin, 2008). Grey to black siliceous shales of the Muskwa Formation are overlain conformably by the Fort Simpson

Formation. The Otter Park Formation is dark grey, calcareous and underlies the Muskwa Formation and overlies the shales of the Evie Formation.

Stable isotope compositions of carbon ($^{13}\text{C}/^{12}\text{C}$) and hydrogen (D/H) shale gases components are determined using gas chromatography isotope ratio mass spectroscopy (GC IRMS). Natural gas samples selected for this study were obtained from twenty-eight wells located at multi-well pad sites in the Dilly Creek area of the Horn River Basin. Samples include mud gases from Paleozoic to Cretaceous strata obtained while drilling and prior to the process of hydraulic fracturing. Produced shale gas samples were collected as time series during various stages of gas production from wells completed in the Muskwa, Otter Park and Evie Formations.

The main objectives of this thesis research are: (i) to use the chemical composition and stable isotope ratios of carbon and hydrogen for characterization of natural gases in the Horn River Basin (ii) to create a geochemical fingerprint in the Horn River Basin using carbon isotope depth profiles which is applicable for use in environmental remediation (iii) to map stable isotope subsurface lateral variations in target formations to determine flow connectivity and any links between isotope signature, mineralogy and mud gas concentration (iv) to monitor the chemical and stable isotope compositional changes which occur during shale gas production and evaluate these changes in conjunction with corresponding reservoir data (v) to develop further understanding of the phenomenon known as ‘isotope reversal’ commonly observed in shale gas plays worldwide.

Stable isotope subsurface variations within Horn River shale gas target Formations are unknown; however they may be proxies for flow connectivity in the reservoir or reflect differences gas storage in the shale. In addition, any chemical and stable isotope compositional changes which may occur during Horn River Basin shale gas production remain unknown. Such information may be valuable in exploration and development of these unconventional plays including determination of the hydrocarbon potential, well completion strategies and optimization of techniques used for gas recovery.

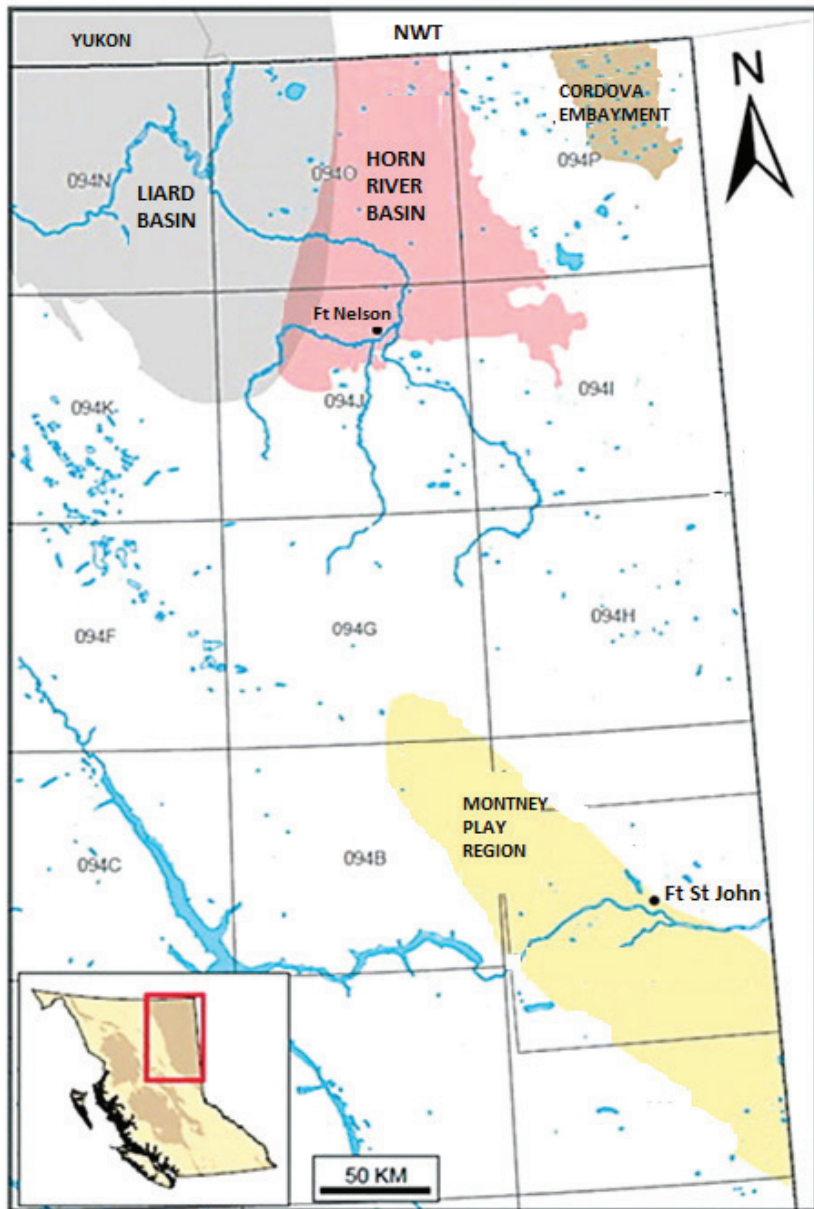


Figure 1.1 Location map showing the Horn River Basin, northeast British Columbia (modified from Adams, 2012)

1.2 Thesis approach

This thesis is prepared in the paper format. The study location is within the Dilly Creek region of the Horn River Basin, northeast British Columbia. The Horn River Basin wells from which natural gas samples were obtained are listed in Table 1.1. Carbon and hydrogen stable isotope analysis was performed at the Stable Isotope Laboratory at University of Alberta. Chemical compositions of gases were determined at an external commercial laboratory and the well data was provided by Nexen Energy ULC.

Chapter 2: This chapter examines the application of stable carbon isotopes for environmental remediation purposes in the Horn River Basin. Carbon isotope depth profiles of methane, ethane and propane are presented from surface depths to the Devonian Otter Park Formation; one of the target zones for shale gas production in the Basin. Isotope depth profiles map vertical carbon isotope variations in methane, ethane and propane ($\delta^{13}\text{C}_{\text{methane}}$, $\delta^{13}\text{C}_{\text{ethane}}$ and $\delta^{13}\text{C}_{\text{propane}}$) through Phanerozoic strata. Carbon isotope signatures of six representative problem gas samples (surface casing vent flow gases and soil gases) from other leaking wells at various sites in the Horn River Basin were obtained and the carbon isotope depth profiles were used to identify geologic formations and depths from which the natural gas leaks occurred.

Chapter 3: In this chapter, mud gas isotope profiles along lateral legs of horizontal wells are used to investigate flow connectivity of Horn River Group shales. Carbon and hydrogen isotope depth profiles map subsurface variation along horizontal legs of wells completed in the Devonian Muskwa and Otter Park Formations (Fig. 1.2). Carbon ($^{13}\text{C}/^{12}\text{C}$) and hydrogen isotope ratios (D/H) of gas components (methane, ethane, propane and butane) were measured and the stable isotope profiles compared to the corresponding mud gas concentrations and mineral composition.

Chapter 4: This chapter presents temporal changes in chemical and stable isotope compositions of shale gases during production from Devonian Horn River Group shales. Chemical and stable isotope compositions of Horn River shale gases were evaluated for eight horizontal wells completed in the Muskwa, Otter Park and Evie Formations. Variations in shale gas composition are examined over short term (25 to 50 days) and long term periods (~ 1500 days) to create time series for each well. Carbon and hydrogen stable isotope and chemical compositional trends were evaluated in conjunction with the gas production decline curves for these wells.

Chapter 5: A comparison of stable isotope compositions of mud gas and production gas data is performed in this chapter. Muskwa and Otter Park production gases and mud gases were assessed to determine the differences in the stable isotope composition of gas in place in the shale versus the production gas isotope composition. This may provide further insight into stable isotope changes which occur during degassing of ultra-low permeability shales and the phenomenon known as isotope reversal commonly observed in shale plays.

Chapter 6: In this chapter, a summary of the main conclusions of this thesis are presented and recommendations for future work are provided.

Appendix A to D: These contain time series showing variation in chemical composition and stable isotope composition of natural gas from Horn River Basin wells and isotope cross-plots. The production decline curves for wells and the associated stable isotope ratios of gases are shown in addition to the natural gas plots for wells.

Table 1.1 List of Horn River Basin wells from which natural gas samples were obtained for this study

Well Name	Well Authorization (WA)
Nexen Inc. HZ TSEA A-16-I/94-O-08	024773
Nexen Inc. HZ TSEA A-C16-I/94-O-08	025127
Nexen Inc. HZ TSEA A-E16-I/94-O-08	025174
Nexen Inc. HZ TSEA C-16-I/94-O-08	027360
Nexen Inc. HZ Komie C-93-A/94-O-08	024220
Nexen Inc. HZ Komie B-93-A/94-O-08	024219
Nexen Inc. HZ TSEA B-18-I/94-O-08	025702
Nexen Inc. HZ Komie B-A18-I/94-O-08	025938
Nexen Inc. HZ Komie C-1-J/94-O-08	026026
Nexen Inc. HZ Komie D-A1-J/94-O-08	026765
Nexen Inc. HZ Komie B-77-H/94-O-08	026175
Nexen Inc. HZ Komie B-A77-H/94-O-08	026925
Nexen Inc. HZ Komie B-B77-H/94-O-08	026926
Nexen Inc. HZ Komie B-C77-H/94-O-08	026927
Nexen Inc. HZ Komie B-D77-H/94-O-08	026928
Nexen Inc. HZ Komie B-E77-H/94-O-08	026929
Nexen Inc. HZ Komie B-F77-H/94-O-08	026930
Nexen Inc. HZ Komie B-G77-H/94-O-08	026931
Nexen Inc. HZ Komie B-H77-H/94-O-08	026932
Nexen Inc. HZ Komie B-I77-H/94-O-08	026933
Nexen Inc. HZ Komie B-J77-H/94-O-08	026934
Nexen Inc. HZ Komie B-K77-H/94-O-08	026935
Nexen Inc. HZ Komie B-L77-H/94-O-08	026936
Nexen Inc. HZ Komie B-M77-H/94-O-08	026937
Nexen Inc. HZ Komie B-N77-H/94-O-08	026938
Nexen Inc. HZ Komie B-O77-H/94-O-08	026939
Nexen Inc. HZ Komie B-P77-H/94-O-08	026940
Nexen Inc. HZ Komie B-Q77-H/94-O-08	026941

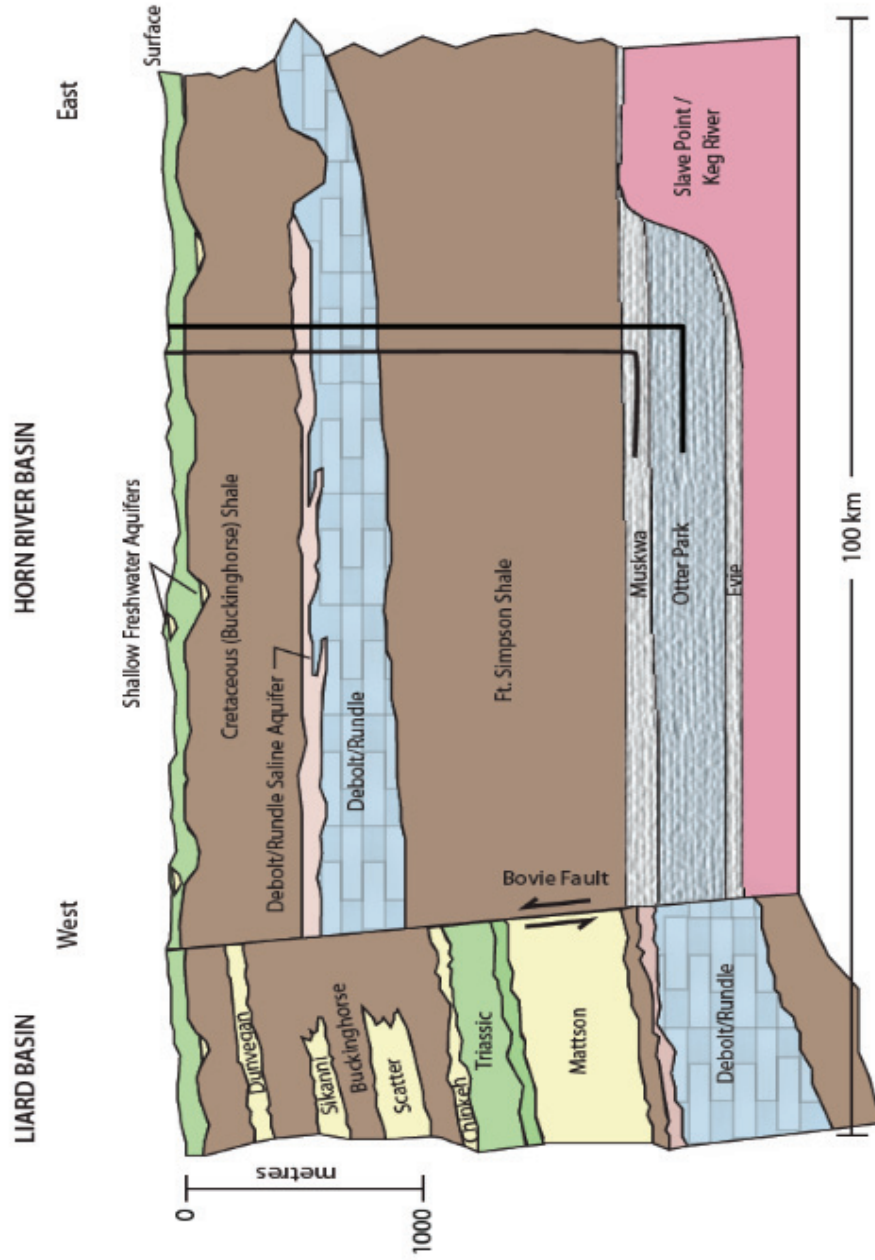


Figure 1.2 Schematic showing stratigraphy of the Horn River Basin and placement of laterals of wells in the Muskwa and Otter Park target formations (modified from B.C. Oil and Gas Commission, 2012)

References Cited

Adams, C., 2012, Summary of Shale Gas Activity in Northeast British Columbia 2011 Oil and Gas Reports 2012-1, BC Ministry of Energy and Mines, Geoscience and Strategic Initiatives Branch.

Amann-Hildenbrand, A., A. Ghanizadeh, and B. M. Krooss, 2012, Transport properties of unconventional gas systems, *Marine and Petroleum Geology*, vol. 31, no. 1, p. 90-99.

Ambrose, R., R. Hartman, M. Diaz Campos, I. Y. Akkutlu, and C. Sondergeld, 2010, New pore-scale considerations for shale gas in place calculations, SPE Unconventional Gas Conference, 23-25 February 2010, Pittsburgh, Pennsylvania, USA.

Arneth, J., 1984, Stable isotope and organo-geochemical studies on phanerozoic sediments of the Williston Basin, North America, *Chemical Geology*, vol. 46, no. 2, p. 113-140.

Arneth, J. and U. Matzigkeit, 1986, Variations in the carbon isotope composition and production yield of various pyrolysis products under open and closed system conditions, *Organic Geochemistry*, vol. 10, no. 4-6, p. 1067-1071.

British Columbia Oil and Gas Commission, 2012, Investigation of observed seismicity in the Horn River Basin, <<http://www.bcogc.ca/node/8046/download>> Accessed 06/04, 2013.

Behar, F., S. Kressmann, J. Rudkiewicz, and M. Vandenbroucke, 1992, Experimental simulation in a confined system and kinetic modelling of kerogen and oil cracking, *Organic Geochemistry*, vol. 19, no. 1, p. 173-189.

Behar, F., M. Vandenbroucke, S. Teermann, P. Hatcher, C. Leblond, and O. Lerat, 1995, Experimental simulation of gas generation from coals and a marine kerogen, *Chemical Geology*, vol. 126, no. 3, p. 247-260.

Behar, F., M. Vandenbroucke, Y. Tang, F. Marquis, and J. Espitalie, 1997, Thermal cracking of kerogen in open and closed systems: determination of kinetic parameters and stoichiometric coefficients for oil and gas generation, *Organic Geochemistry*, vol. 26, no. 5, p. 321-339.

Berner, U. and E. Faber, 1988, Maturity related mixing model for methane, ethane and propane, based on carbon isotopes, *Organic Geochemistry*, vol. 13, no. 1-3, p. 67-72.

Burruss, R. C. and C. D. Laughrey, 2010, Carbon and hydrogen isotopic reversals in deep basin gas: Evidence for limits to the stability of hydrocarbons, *Organic Geochemistry*, vol. 41, no. 12, p. 1285-1296.

Cardott, B., 2006, Gas shales tricky to understand: *AAPG Explorer*, vol. 27, no.11, p 48, 49.

Chung, H. M., J. R. Gormly, and R. M. Squires, 1988a, Origin of gaseous hydrocarbons in subsurface environments: Theoretical considerations of carbon isotope distribution, *Chemical Geology*, vol. 71, no. 1-3, p. 97-104.

Chung, H. M., J. R. Gormly, and R. M. Squires, 1988b, Origin of gaseous hydrocarbons in subsurface environments: Theoretical considerations of carbon isotope distribution, *Chemical Geology*, vol. 71, no. 1-3, p. 97-104.

Clayton, C., 1991, Carbon isotope fractionation during natural gas generation from kerogen, *Marine and Petroleum Geology*, vol. 8, no. 2, p. 232-240.

Close, D., M. Perez, B. Goodway, and G. Purdue, 2012, Integrated workflows for shale gas and case study results for the Horn River Basin, British Columbia, Canada, *The Leading Edge*, vol. 31, no. 5, p. 556-569.

Curtis, M., R. Ambrose, C. Sondergeld, and C. Sondergeld, 2010, Structural characterization of gas shales on the micro-and nano-scales, *Canadian Unconventional Resources and International Petroleum Conference*, 19-21 October 2010, Calgary, Alberta, Canada.

Curtis, J. B., 2002, Fractured Shale-Gas Systems, *AAPG Bulletin*, vol. 86, no. 11, p. 1921-1938.

Dieckmann, V., H. J. Schenk, B. Horsfield, and D. H. Welte, 1998, Kinetics of petroleum generation and cracking by programmed-temperature closed-system pyrolysis of Toarcian Shales, *Fuel*, vol. 77, no. 1-2, p. 23-31.

Freeman, C., G. Moridis, and T. Blasingame, 2013, Modeling and Performance Interpretation of Flowing Gas Composition Changes in Shale Gas Wells with Complex Fractures, *6th International Petroleum Technology Conference*, Mar 26 - 28, 2013, Beijing, China.

Freeman, C., G. J. Moridis, G. E. Michael, and T. A. Blasingame, 2012, Measurement, Modeling, and Diagnostics of Flowing Gas Composition Changes in Shale Gas Wells, *SPE Latin America and Caribbean Petroleum Engineering Conference*, 16-18 April 2012, Mexico City, Mexico.

Fuex, A. N., 1977, The use of stable carbon isotopes in hydrocarbon exploration, *Journal of Geochemical Exploration*, vol. 7, p. 155-188.

Gray, F. F. and J. Kassube, 1963, Geology and stratigraphy of Clarke Lake gas field, British Columbia, *AAPG Bulletin*, vol. 47, no. 3, p. 467-483.

- Hill, D. G. and C. R. Nelson, 2000, Gas Productive Fractured Shales: An Overview and Update, Gas TIPS, vol. 6, no. No.2, p. 4-13.
- Hill, R. J., Y. Tang, and I. R. Kaplan, 2003, Insights into oil cracking based on laboratory experiments, Organic Geochemistry, vol. 34, no. 12, p. 1651-1672.
- Horsfield, B., H. Schenk, N. Mills, and D. Welte, 1992, An investigation of the in-reservoir conversion of oil to gas: compositional and kinetic findings from closed-system programmed-temperature pyrolysis, Organic Geochemistry, vol. 19, no. 1, p. 191-204.
- James, A. T., 1983, Correlation of natural gas by use of carbon isotopic distribution between hydrocarbon components, AAPG Bulletin, vol. 67, no. 7, p. 1176-1191.
- Jenden, P. D., D. J. Drazan, and I. R. Kaplan, 1993, Mixing of thermogenic natural gases in northern Appalachian Basin, AAPG Bulletin, vol. 77, no. 6, p. 980-998.
- Kotarba, M. J. and M. D. Lewan, 2013, Sources of natural gases in Middle Cambrian reservoirs in Polish and Lithuanian Baltic Basin as determined by stable isotopes and hydrous pyrolysis of Lower Palaeozoic source rocks, Chemical Geology, vol. 345, p. 62-76.
- Law, B. E. and J. B. Curtis, 2002, Introduction to Unconventional Petroleum Systems, AAPG Bulletin, vol. 86, no. 11, p. 1851-1852.
- Lewan, M., 1997, Experiments on the role of water in petroleum formation, Geochimica et Cosmochimica Acta, vol. 61, no. 17, p. 3691-3723.
- Lorant, F. and F. Behar, 2002, Late generation of methane from mature kerogens, Energy & Fuels, vol. 16, no. 2, p. 412-427.

- Lorant, F., A. Prinzhofer, F. Behar, and A. Huc, 1998, Carbon isotopic and molecular constraints on the formation and the expulsion of thermogenic hydrocarbon gases, *Chemical Geology*, vol. 147, no. 3-4, p. 249-264.
- Loucks, R. G., R. M. Reed, S. C. Ruppel, and D. M. Jarvie, 2009, Morphology, genesis, and distribution of nanometer-scale pores in siliceous mudstones of the Mississippian Barnett Shale, *Journal of Sedimentary Research*, vol. 79, no. 12, p. 848-861.
- Mycke, B., K. Hall, and P. Leplat, 1994, Carbon isotopic composition of individual hydrocarbons and associated gases evolved from micro-scale sealed vessel (MSSV) pyrolysis of high molecular weight organic material, *Organic Geochemistry*, vol. 21, no. 6-7, p. 787-800.
- Nelson, P. H., 2009, Pore-throat sizes in sandstones, tight sandstones, and shales, *AAPG Bulletin*, vol. 93, no. 3, p. 329-340.
- Ni, Y., J. Dai, X. Yang, Y. Tang, Y. Jin, and J. Chen, 2009, Kinetic modeling of post-mature gas generation: Constraints from high-pressure thermal-cracking of nC₂₄, *Geochimica et Cosmochimica Acta*, vol. 73, no. 13 supplement 1, p. A940.
- Norville, G. A. and R. A. Dawe, 2007, Carbon and hydrogen isotopic variations of natural gases in the southeast Columbus basin offshore southeastern Trinidad, West Indies – clues to origin and maturity, *Applied Geochemistry*, vol. 22, no. 9, p. 2086-2094.
- Odden, W., T. Barth, and M. Talbot, 2002, Compound-specific carbon isotope analysis of natural and artificially generated hydrocarbons in source rocks and petroleum fluids from offshore Mid-Norway, *Organic Geochemistry*, vol. 33, no. 1, p. 47-65.

Oldale, H. and R. Munday, 1994, Devonian Beaverhill Lake Group of the western Canada sedimentary basin, Geological Atlas of the Western Canada Sedimentary Basin, p. 149-164.

Prinzhofer, A. A. and A. Y. Huc, 1995, Genetic and post-genetic molecular and isotopic fractionations in natural gases, Chemical Geology, vol. 126, no. 3-4, p. 281-290.

Rice, D. D. and G. E. Claypool, 1981, Generation, accumulation, and resource potential of biogenic gas, AAPG Bulletin, vol. 65, no. 1, p. 5-25.

Rodriguez, N. D. and R. P. Philp, 2010, Geochemical characterization of gases from the Mississippian Barnett Shale, Fort Worth Basin, Texas, AAPG Bulletin, vol. 94, no. 11, p. 1641-1656.

Ross, D. J. K. and R. M. Bustin, 2008, Characterizing the shale gas resource potential of Devonian Mississippian strata in the Western Canada sedimentary basin: Application of an integrated formation evaluation, AAPG Bulletin, vol. 92, no. 1, p. 87-125.

Rowe, D. and K. Muehlenbachs, 1999b, Isotopic fingerprints of shallow gases in the Western Canadian sedimentary basin: tools for remediation of leaking heavy oil wells, Organic Geochemistry, vol. 30, no. 8, Part 1, p. 861-871.

Rullkötter, J., D. Leythaeuser, B. Horsfield, R. Littke, U. Mann, P. Müller, M. Radke, R. Schaefer, H. Schenk, and K. Schwochau, 1988, Organic matter maturation under the influence of a deep intrusive heat source: a natural experiment for quantitation of hydrocarbon generation and expulsion from a petroleum source rock (Toarcian shale, northern Germany), Organic Geochemistry, vol. 13, no. 4, p. 847-856.

Sackett, W. M., 1978, Carbon and hydrogen isotope effects during the thermocatalytic production of hydrocarbons in laboratory simulation experiments, *Geochimica et Cosmochimica Acta*, vol. 42, no. 6, Part 1, p. 571-580.

Schenk, H., R. Di Primio, and B. Horsfield, 1997, The conversion of oil into gas in petroleum reservoirs. Part 1: Comparative kinetic investigation of gas generation from crude oils of lacustrine, marine and fluviodeltaic origin by programmed-temperature closed-system pyrolysis, *Organic Geochemistry*, vol. 26, no. 7, p. 467-481.

Schmoker, J. W., 2002, Resource-Assessment Perspectives for Unconventional Gas Systems, *AAPG Bulletin*, vol. 86, no. 11, p. 1993-1999.

Schoell, M., 1980, The hydrogen and carbon isotopic composition of methane from natural gases of various origins, *Geochimica et Cosmochimica Acta*, vol. 44, no. 5, p. 649-661.

Schoell, M., 1983, Genetic characterization of natural gases, *AAPG Bulletin*, vol. 67, no. 12, p. 2225-2238.

Seewald, J. and J. Whelan, 2005, Isotopic and chemical composition of natural gas from the Potato Hills Field, Southeastern Oklahoma: Evidence for an Abiogenic Origin?
<http://www.searchanddiscovery.com/documents/abstracts/2005research_calgary/abstracts/extended/seewald/seewald.htm> Accessed 10/18, 2013.

Smith, J. E., D. A. Morris, and J. G. Erdman, 1971, Migration, Accumulation and Retention of Petroleum in the Earth, *Proc. 8th World Petroleum Congress*, vol. 2, p. 13-26.

Sondergeld, C., R. Ambrose, C. Rai, and J. Moncrieff, 2010, Micro-Structural Studies of Gas Shales. Paper SPE 131771 presented at the SPE Unconventional Gas Conference, Pittsburg, Pennsylvania, USA, 23–25 February 2010.

Stahl, W., 1974, Carbon isotope fractionations in natural gases, *Nature*, vol. 251, no. 5471, p. 134-135.

Strapoć, D., G. Michael, J. Roper, and Maguire Matt, 2010, Insights into Shale Gas Production & Storage From Gas Chemistry – What Is It Telling Us? <http://www.searchanddiscovery.com/abstracts/pdf/2011/hedberg-texas/abstracts/ndx_strapoc.pdf> Accessed 09/13, 2013.

Tang, Y. and D. Xia, 2011, Predicting Original Gas in Place and Optimizing Productivity by Isotope Geochemistry of Shale Gas, <http://www.cspg.org/documents/Conventions/Archives/Annual/2011/204-Predicting_Original_Gas_in_Place_and_Optimizing_Productivity.pdf> Accessed 09/13, 2013.

Tilley, B. and K. Muehlenbachs, 2006, Gas maturity and alteration systematics across the Western Canada Sedimentary Basin from four mud gas isotope depth profiles, *Organic Geochemistry*, vol. 37, no. 12, p. 1857-1868.

Tilley, B., S. McLellan, S. Hiebert, B. Quartero, B. Veilleux, and K. Muehlenbachs, 2011, Gas isotope reversals in fractured gas reservoirs of the western Canadian Foothills: Mature shale gases in disguise, *AAPG Bulletin*, vol. 95, no. 8, p. 1399-1422.

Tilley, B. and K. Muehlenbachs, 2013, Isotope reversals and universal stages and trends of gas maturation in sealed, self-contained petroleum systems, *Chemical Geology*, vol. 339, p. 194-204.

Ungerer, P. and R. Pelet, 1987, Extrapolation of the kinetics of oil and gas formation from laboratory experiments to sedimentary basins, .

Waples, D. W., 2000, The kinetics of in-reservoir oil destruction and gas formation: constraints from experimental and empirical data, and from thermodynamics, *Organic Geochemistry*, vol. 31, no. 6, p. 553-575.

Weissenberger, J. A. W. and K. Potma, 2001, The Devonian of western Canada -- aspects of a petroleum system: Introduction, *Bulletin of Canadian Petroleum Geology*, vol. 49, no. 1, p. 1-6.

Xia, X., J. Chen, R. Braun, and Y. Tang, 2012, Isotopic reversals with respect to maturity trends due to mixing of primary and secondary products in source rocks, *Chemical Geology*.

Xia, X. and Y. Tang, 2012, Isotope fractionation of methane during natural gas flow with coupled diffusion and adsorption/desorption, *Geochimica et Cosmochimica Acta*, vol. 77, p. 489-503.

Zhang, T. and B. M. Krooss, 2001, Experimental investigation on the carbon isotope fractionation of methane during gas migration by diffusion through sedimentary rocks at elevated temperature and pressure, *Geochimica et Cosmochimica Acta*, vol. 65, no. 16, p. 2723-2742.

Zhang, T., G. S. Ellis, S. C. Ruppel, K. Milliken, and R. Yang, 2012, Effect of organic-matter type and thermal maturity on methane adsorption in shale-gas systems, *Organic Geochemistry*, vol. 47, p. 120-131.

Zumberge, J., K. Ferworn, and S. Brown, 2012, Isotopic reversal ('rollover') in shale gases produced from the Mississippian Barnett and Fayetteville formations, *Marine and Petroleum Geology*, vol. 31, no. 1, p. 43-52.

CHAPTER 2

CARBON ISOTOPE DEPTH PROFILES AS A FORENSIC TOOL FOR SOURCE IDENTIFICATION IN LEAKING GAS WELLS IN THE HORN RIVER BASIN

2.1 Introduction

The Horn River Basin is a large Canadian shale gas play located in northeast British Columbia, north of Ft. Nelson. Devonian marine Horn River Group shales are prolific, gas-rich and key formations for shale gas production in this region (Adams, 2012). Development unconventional gas reservoirs varies from conventional hydrocarbon reservoirs and a major concern during shale gas exploration and production is impact on the environment and human health (Chermak and Schreiber, 2012; Carpenter, 2013; Duggan-Haas et al., 2013; Jackson et al., 2013; Orem et al., 2013; Vengosh, 2013). During commercial production from shale gas reservoirs several horizontal wells are usually drilled from a multi-well pad and multi-stage hydraulic fracturing is employed to create permeable pathways for gas flow in the shale. Gas leakage from wells may occur as a result of poor cement jobs or casing damage which may develop during hydraulic fracturing and cause natural gas migration to the surface environment (De Wit, 2011). Potential contamination of aquifers, groundwater wells and the surface environment by stray gas migration as well as short and long-term effects on public health and safety are fundamental issues associated with shale gas recovery. Shale gas plays worldwide exhibit highly variable characteristics; hence during assessment of environmental and human health impacts there exists the need for collection of site-specific geochemical data (Chermak and Schreiber, 2012).

In this paper, the main objective is to use the carbon isotope signatures of Horn River Basin gases to generate a subsurface geochemical isotope fingerprint in this region, applicable for purposes of environmental remediation. Stable isotope analysis is presented as a diagnostic tool for determination of the source of natural gas at leaking well sites in the Horn River Basin.

Carbon isotope signatures of natural gas are determined by the organic matter source, gas generation processes (biogenic or thermogenic) and other factors which may alter the isotope composition of gas subsequent to its generation (Stahl, 1974; Fuex, 1977; Schoell, 1980; Rice and Claypool, 1981; Claypool and Kvenvolden, 1983; James, 1983; Schoell, 1983; Berner and Faber, 1988; Clayton, 1991; Jenden et al., 1993; Norville and Dawe, 2007; Close et al., 2012). Carbon isotope depth profiles are valuable to show subsurface variation in the carbon isotope composition of hydrocarbon components of natural gases (Rowe and Muehlenbachs, 1999; Wilhelms et al., 2001; Tilley et al., 2001; Ellis et al., 2003; Tilley and Muehlenbachs, 2006).

Carbon isotope depth profiles were generated for the HZ TSEA B-018-I/094-O-08 well in the Horn River Basin located within the National Topographic System (NTS) Map sheet 94/O (Fig.2.1). Carbon isotope ratios ($^{13}\text{C}/^{12}\text{C}$) of methane (CH_4), ethane (C_2H_6) and propane (C_3H_8) of mud gas samples from Horn River Basin formations from the surface to the target formation for shale gas production were determined. Carbon isotope analysis of natural gases obtained from sedimentary rocks from the Devonian to the Cretaceous map vertical variation in carbon isotope ratios ($^{13}\text{C}/^{12}\text{C}$) of natural gas components. Carbon isotope depth profiles of methane, ethane and propane of natural gas are used to identify formation depths from which gas leaks were derived based on the isotope signature of the gas.

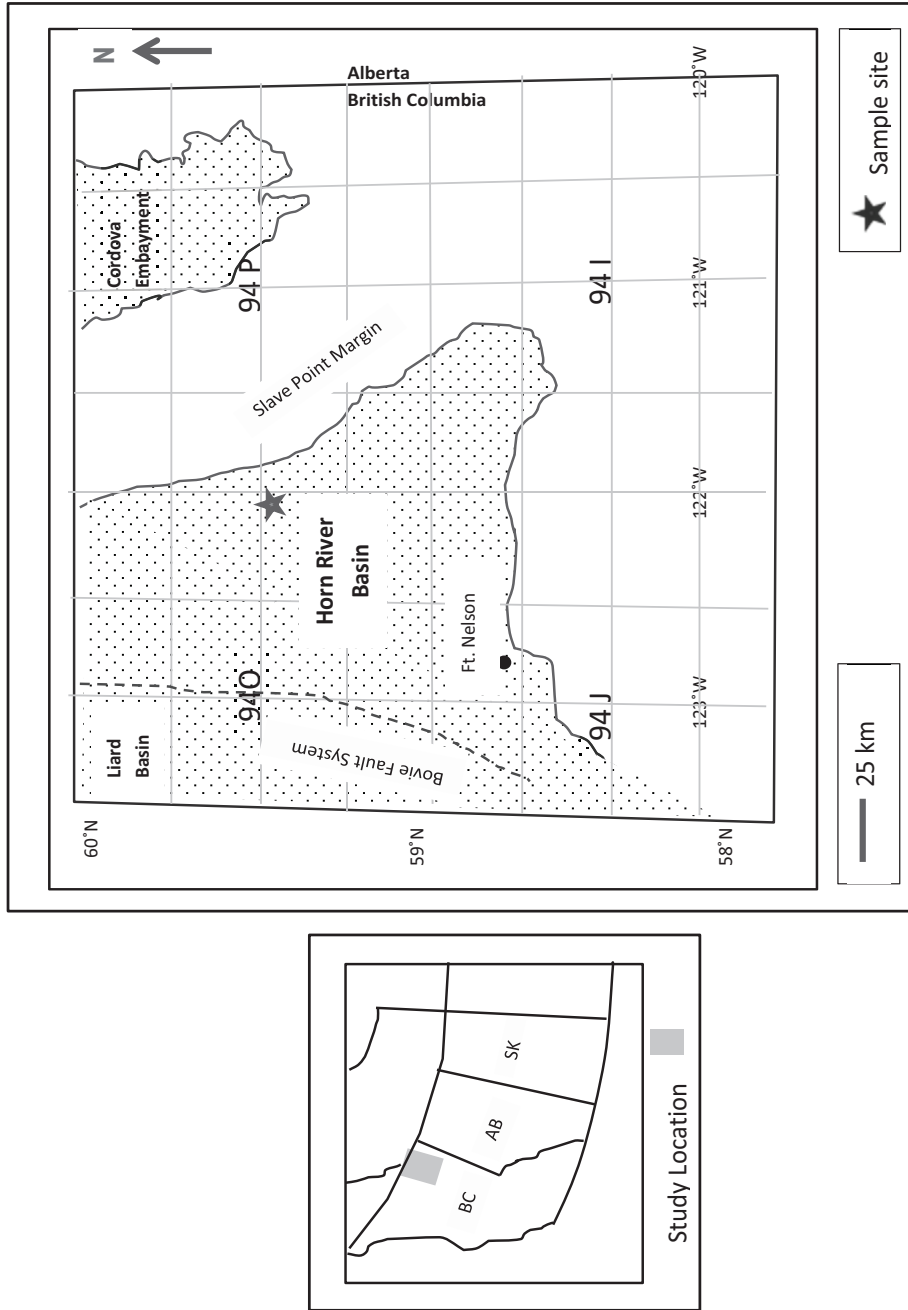


Figure 2.1 Location map showing the study area and the HZ TSEA B-018-I/094-O-08 well in the Horn River Basin, NE British Columbia (modified from Oldale and Mundav, 1994).

2.1.1 *The Horn River Basin*

The Horn River Basin is located north of Ft. Nelson, northeast British Columbia forms part of the Western Canada Sedimentary Basin. The Horn River Basin is bounded by the Liard Basin in the west and the Slave point carbonate platform in the east and covers an area of approximately 1.3 million hectares (Close et al., 2012; Adams, 2012). Sedimentary rocks in the Horn River Basin reflect various changes during tectonic basin evolution (Price, 1994). Devonian Horn River Group shales were deposited in a passive margin setting on the western edge of the continent where transgression and increasing water depths resulted in deposition of these marine sediments (Williams, 1983; Oldale and Munday, 1994; Weissenberger and Potma, 2001; Ross and Bustin, 2008).

2.2 Methods

Gas samples for stable isotope analysis were obtained from the HZ TSEA B-018-I/094-O-08 well in the Dilly Creek area of the Horn River Basin, northeast British Columbia (Table 2.1). Mud gases were sampled at the wellhead after separation from the drill fluid and collected in single-use IsoTube® containers (IsoTech Laboratories, Champaign IL) representing depth intervals of twenty-five metres. One hundred and seventy-five gas samples were collected from surface depth to the Otter Park Formation which is the target for shale gas production. These samples of natural gases were obtained from Cretaceous to Devonian sedimentary rocks which include the Dunvegan, Sully, Sikanni, Buckingham, Spirit River, Debolt, Shunda, Pekisko, Banff, Exshaw, Kotcho, Tetcho, Trout River, Kakisa, Red Knife, Jean Marie, Fort Simpson, Muskwa and Otter Park Formations (Fig. 2.2).

Carbon isotope analysis was performed at the University of Alberta Stable Isotope Laboratory, Department of Earth and Atmospheric Sciences. Carbon isotope ratios ($^{12}\text{C}/^{13}\text{C}$) of Horn River Basin mud gases were analysed by gas chromatography- combustion- continuous flow isotope ratio mass spectrometer (GC-C CF-IRMS). Carbon isotopic compositions of gas components; methane,

ethane and propane ($\delta^{13}\text{C}_{\text{methane}}$, $\delta^{13}\text{C}_{\text{ethane}}$, $\delta^{13}\text{C}_{\text{propane}}$) were reported using standard $\delta^{13}\text{C}$ notation (per mil) relative to the Vienna Pee Dee Belemnite (VPDB) standard. Reproducibility of $\delta^{13}\text{C}$ values are $\pm 0.1\%$ for methane, $\pm 0.2\%$ for ethane and $\pm 0.8\%$ for propane.

Table 2.1 Depth and location data for Well HZ TSEA B-018-I/094-O-08

UWI	00/B-096-H/094-O-08/0
Surface UWI	200B018I094O0800
Latitude °N	59
Longitude °W	122
True Vertical Depth (m)	2485.4
Total Depth (m)	4600
KB Elevation (m)	685.5
Ground Elevation (m)	674.1
Well Authorization (WA)	025702

2.3 Results and Discussion

HZ TSEA B-018-I/094-O-08 is a horizontal well with the lateral leg completed in the Devonian Otter Park Formation of the Horn River Basin. Carbon isotope depth profiles for methane, ethane and propane ($\delta^{13}\text{C}_{\text{methane}}$, $\delta^{13}\text{C}_{\text{ethane}}$, $\delta^{13}\text{C}_{\text{propane}}$) of Horn River mud gases from HZ TSEA B-018-I/094-O-08 are presented in Fig. 2.2. Carbon isotope depth profiles for natural gas hydrocarbon components (methane, ethane and propane) depict vertical variation in isotope composition through Devonian to Cretaceous formations. The isotope depth profiles represent only the vertical portion of the well and include carbon isotope signatures of natural gases from both the shale gas target and non-target formations. $\delta^{13}\text{C}_{\text{methane}}$ values of gases range widely from approximately -52% near the surface to -28% in the shale gas target formation. $\delta^{13}\text{C}$ values of

methane greater than -50‰ usually indicate a thermogenic gas origin (Norville and Dawe, 2007), hence all Horn River Basin gases appear to be thermogenic even at shallow subsurface depths. Variations in $\delta^{13}\text{C}$ values reflect differences in thermal maturity of gases from various Formations the Horn River Basin from the Devonian to the Cretaceous. In general, carbon isotope values ($\delta^{13}\text{C}$) of gas components are expected to show ^{13}C enrichment with increasing maturity. $\delta^{13}\text{C}_{\text{ethane}}$ values of gases range from approximately -37‰ to -27‰ and $\delta^{13}\text{C}_{\text{propane}}$ values range from -37‰ to -26‰.

In Fig. 2.3 carbon isotope signatures ($\delta^{13}\text{C}_{\text{methane}}$, $\delta^{13}\text{C}_{\text{ethane}}$ and $\delta^{13}\text{C}_{\text{propane}}$) of six natural gas samples from other leaking wells in the Horn River Basin are presented. Three of these samples of natural gas were from surface casing vent (SCV) gas leaks and the other three samples were soil gases collected near the surface. Each natural gas sample obtained was from a different problem well located in Horn River Basin and the gas origin was unknown.

The carbon isotope depth profiles (Fig. 2.4) were used to determine the source of gas by identifying the location at which carbon isotope signature of the leaking gas matches the carbon isotope signature of formation gas. Carbon isotope depth profiles and isotope signatures of natural gas samples from well leaks indicate that the soil gas sample 1 and soil gas sample 2 were gases which originated from formation depths between 200 and 400m (Upper Cretaceous Sikanni Formation). Soil gas sample 3 was derived from the deeper Debolt Formation at approximately 700m. Source formations for surface casing vent (SCV) gases (Fig. 2.3) indicate SCV 1 is a highly mature gas obtained from the Devonian Redknife Formation at depth of 1700m. Natural gas obtained from the SCV 2 well leak originated from the Upper Devonian Kotcho Formation and the sample of SCV 3 gas was originally from the Debolt Formation of the Horn River Basin.

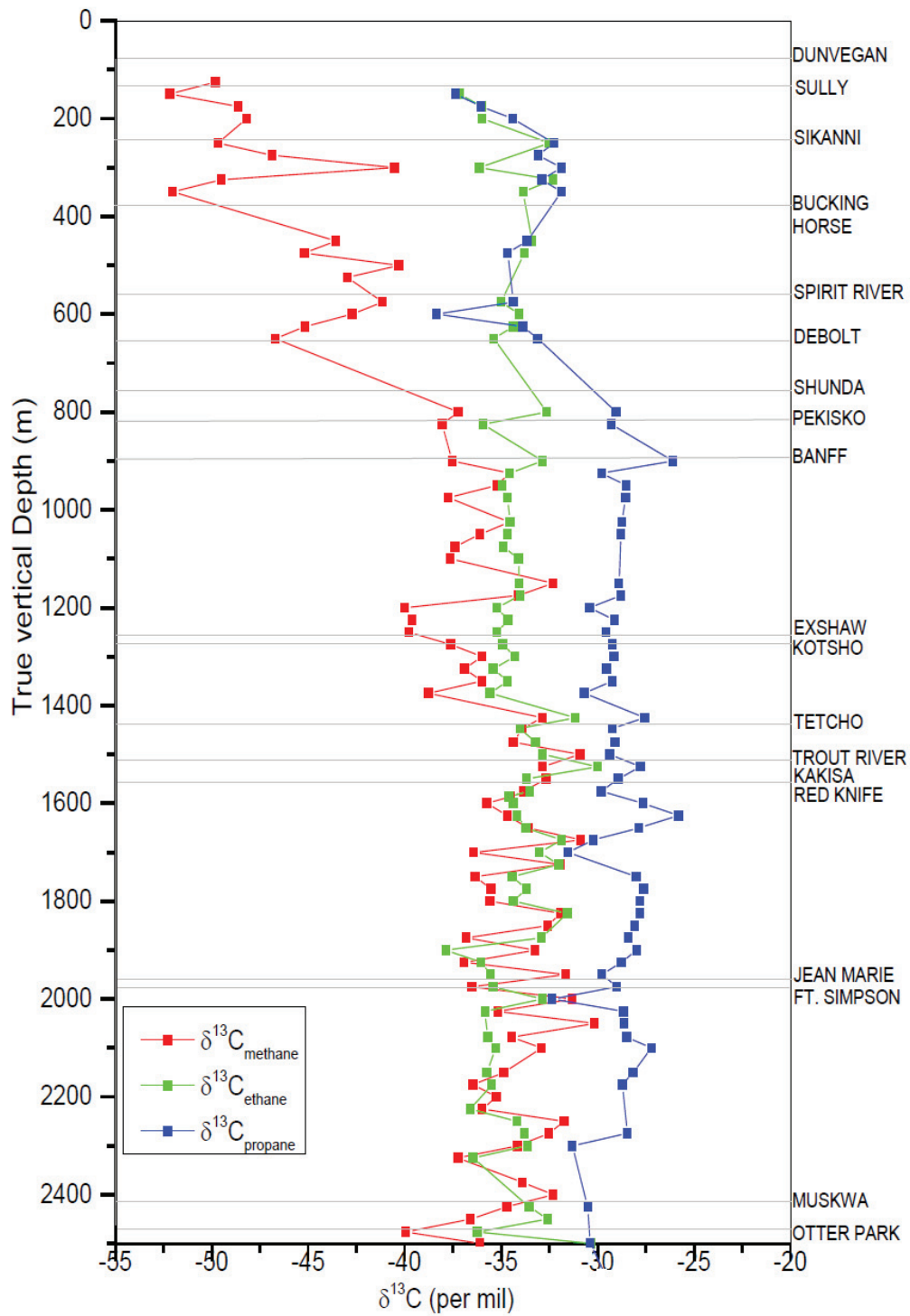


Figure 2.2 Carbon isotopic depth profiles for methane, ethane and propane gas components for the Hz TSEA B-018-I/094-O-08 well.

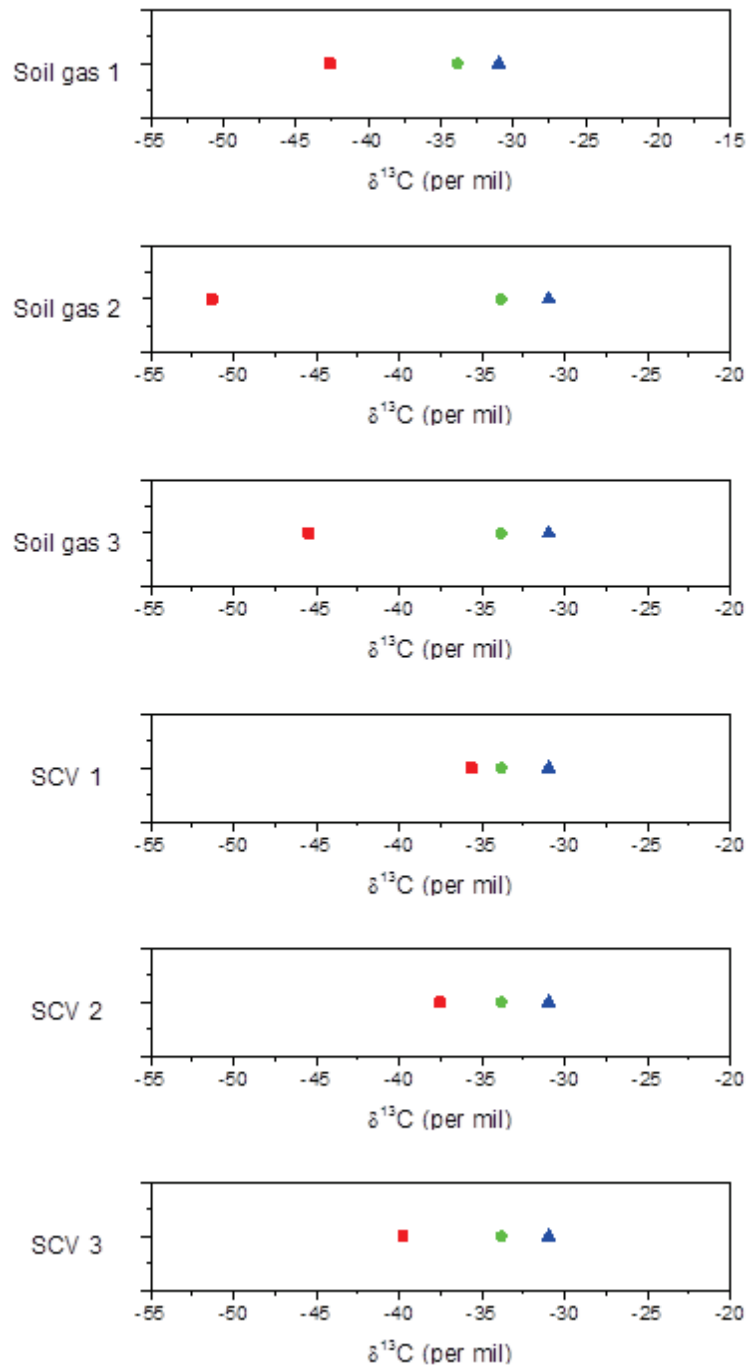


Figure 2.3 Carbon isotope signatures ($\delta^{13}\text{C}_{\text{methane}}$, $\delta^{13}\text{C}_{\text{ethane}}$, $\delta^{13}\text{C}_{\text{propane}}$) of six samples of soil gases and surface casing vent flow gases from leaking wells in the Horn River Basin.

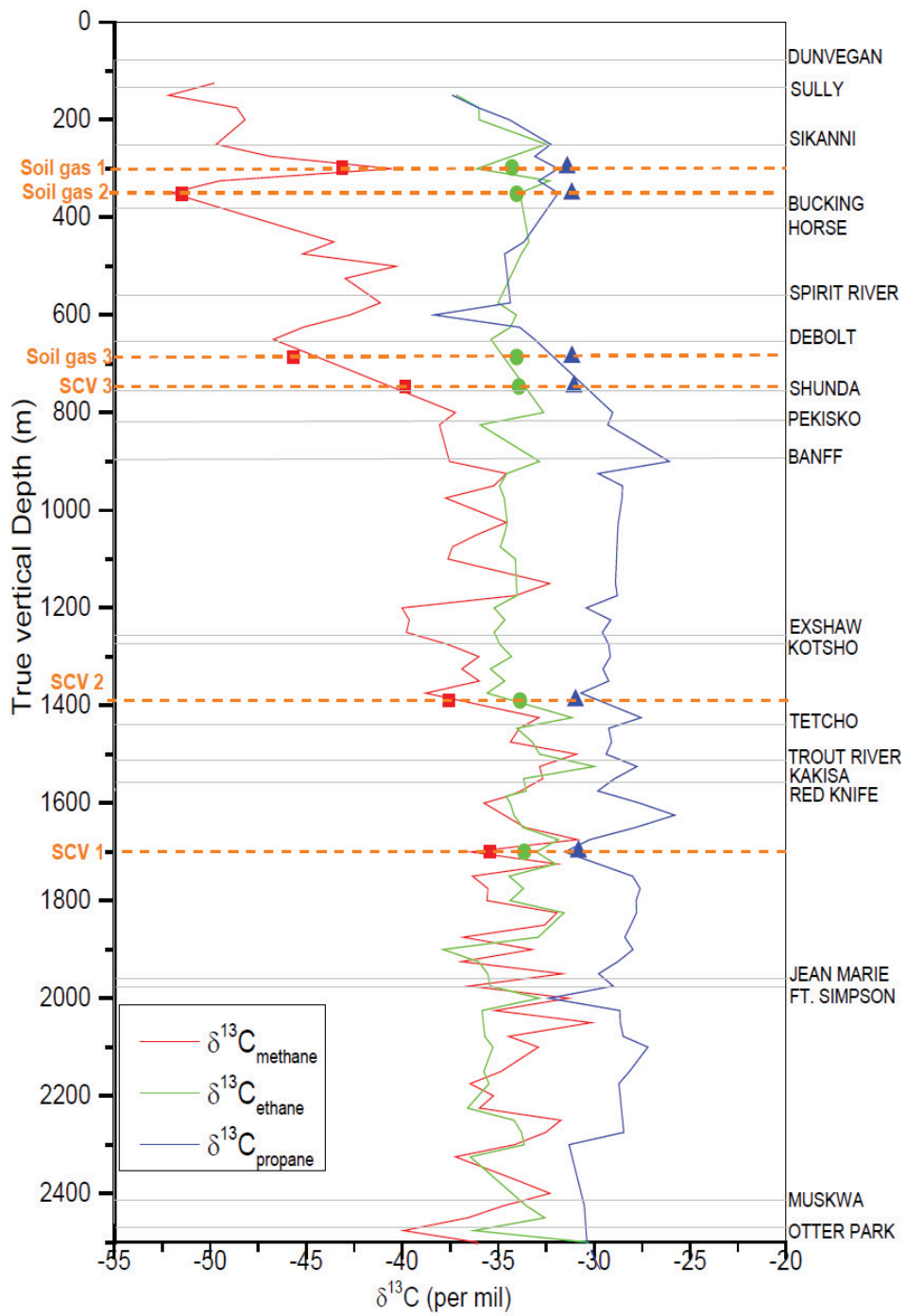


Figure 2.4 Carbon isotope depth profiles indicating Horn River Basin formations from which leaking soil gases and surface casing vent gases originated.

2.4 Conclusions

Natural gas maturity is influenced by the thermal history of a sedimentary basin and carbon isotope signatures of gases within formations and carbon isotope ratios ($^{13}\text{C}/^{12}\text{C}$) of gases reflect high thermal maturity in this region of the Horn River Basin. Natural gases from the Horn River Basin are thermogenic in origin where $\delta^{13}\text{C}_{\text{methane}} > -55\text{‰}$. Carbon isotope depth profiles were valuable to show the stable carbon isotope variation through Devonian to Cretaceous formations in the Basin and provided a geochemical isotope fingerprint for natural gas in the Horn River Basin. Formations from which soil and surface casing vent gas leaks occurred from wells in the Horn River were identified. Stable isotope geochemistry is a useful technique for environmental remediation purposes and can assist in locating the source depths from which gas leaks occur and so zones where cement damage exists can be sealed in leaking gas wells.

References Cited

- Adams, C., 2012, Summary of Shale Gas Activity in Northeast British Columbia 2011 Oil and Gas Reports 2012-1, BC Ministry of Energy and Mines, Geoscience and Strategic Initiatives Branch.
- Berner, U. and E. Faber, 1988, Maturity related mixing model for methane, ethane and propane, based on carbon isotopes, *Organic Geochemistry*, vol. 13, no. 1-3, p. 67-72.
- Carpenter, D. O., 2013, Public health implications of hydraulic fracturing, *Abstracts with Programs - Geological Society of America*, vol. 45, no. 7; 7, p. 182-182.
- Chermak, J. and M. E. Schreiber, 2012, Environmental impact evaluation of hydrocarbon extraction from shales, *Abstracts with Programs - Geological Society of America*, vol. 44, no. 7; 7, p. 313-313.
- Claypool, G. E. and K. A. Kvenvolden, 1983, Methane and other hydrocarbon gases in marine sediment, *Annual Review of Earth and Planetary Sciences*, vol. 11, p. 299.
- Clayton, C., 1991, Carbon isotope fractionation during natural gas generation from kerogen, *Marine and Petroleum Geology*, vol. 8, no. 2, p. 232-240.
- Close, D., M. Perez, B. Goodway, and G. Purdue, 2012, Integrated workflows for shale gas and case study results for the Horn River Basin, British Columbia, Canada, *The Leading Edge*, vol. 31, no. 5, p. 556-569.
- De Wit, M. J., 2011, The great shale debate in the Karoo, *S Afr J Sci*, vol. 107, no. 7/8.

Duggan-Haas, D., R. M. Ross, and K. E. Cronin, 2013, What do you need to understand to teach about hydrofracking? Abstracts with Programs - Geological Society of America, vol. 45, no. 7; 7, p. 284-284.

Ellis, L., A. Brown, M. Schoell, and S. Uchytel, 2003, Mud gas isotope logging (MGIL) assists in oil and gas drilling operation, The Oil and Gas Journal, vol. 101, no. 21, p. 32(8).

Fuex, A. N., 1977, The use of stable carbon isotopes in hydrocarbon exploration, Journal of Geochemical Exploration, vol. 7, p. 155-188.

Jackson, R. B., A. Vengosh, T. H. Darrah, A. Down, and N. Warner, 2013, Drinking water and shale gas extraction; evidence for water contamination in some locations but not others, Abstracts with Programs - Geological Society of America, vol. 45, no. 7; 7, p. 181-181.

James, A. T., 1983, Correlation of natural gas by use of carbon isotopic distribution between hydrocarbon components, AAPG Bulletin, vol. 67, no. 7, p. 1176-1191.

Jenden, P. D., D. J. Drazan, and I. R. Kaplan, 1993, Mixing of thermogenic natural gases in northern Appalachian Basin, AAPG Bulletin, vol. 77, no. 6, p. 980-998.

Norville, G. A. and R. A. Dawe, 2007, Carbon and hydrogen isotopic variations of natural gases in the southeast Columbus basin offshore southeastern Trinidad, West Indies – clues to origin and maturity, Applied Geochemistry, vol. 22, no. 9, p. 2086-2094.

Oldale, H. and R. Munday, 1994, Devonian Beaverhill Lake Group of the western Canada sedimentary basin, Geological Atlas of the Western Canada Sedimentary Basin, p. 149-164.

Orem, W. H., L. M. Crosby, C. Tatu, M. S. Varonka, C. DeVera, and M. Engle, 2013, Produced water from shale gas production; organic substances and toxicity testing, Abstracts with Programs - Geological Society of America, vol. 45, no. 7; 7, p. 181-181.

Price, R., 1994, Cordilleran tectonics and the evolution of the Western Canada Sedimentary Basin, Geological Atlas of the Western Canada Sedimentary Basin, p. 13-24.

Rice, D. D. and G. E. Claypool, 1981, Generation, accumulation, and resource potential of biogenic gas, AAPG Bulletin, vol. 65, no. 1, p. 5-25.

Ross, D. J. K. and R. M. Bustin, 2008, Characterizing the shale gas resource potential of Devonian Mississippian strata in the Western Canada sedimentary basin: Application of an integrated formation evaluation, AAPG Bulletin, vol. 92, no. 1, p. 87-125.

Rowe, D. and K. Muehlenbachs, 1999b, Isotopic fingerprints of shallow gases in the Western Canadian sedimentary basin: tools for remediation of leaking heavy oil wells, Organic Geochemistry, vol. 30, no. 8, Part 1, p. 861-871.

Schoell, M., 1980, The hydrogen and carbon isotopic composition of methane from natural gases of various origins, Geochimica et Cosmochimica Acta, vol. 44, no. 5, p. 649-661.

Schoell, M., 1983, Genetic characterization of natural gases, AAPG Bulletin, vol. 67, no. 12, p. 2225-2238.

Stahl, W., 1974, Carbon isotope fractionations in natural gases, Nature, vol. 251, no. 5471, p. 134-135.

Tilley, B. J., K. Muehlenbachs, and B. J. Szatkowski, 2001, Compartmentalization of Gas Reservoirs: Insights From Carbon Isotope Ratios,

<<http://www.cspg.org/documents/Conventions/Archives/Annual/2001/14-102.pdf>> Accessed 09/11, 2013.

Tilley, B. and K. Muehlenbachs, 2006, Gas maturity and alteration systematics across the Western Canada Sedimentary Basin from four mud gas isotope depth profiles, *Organic Geochemistry*, vol. 37, no. 12, p. 1857-1868.

Vengosh, A., 2013, Tracing the impacts of fossil fuels production on the quality of water resources in the United States, *Abstracts with Programs - Geological Society of America*, vol. 45, no. 7; 7, p. 181-181.

Weissenberger, J. A. W. and K. Potma, 2001, The Devonian of western Canada -- aspects of a petroleum system: Introduction, *Bulletin of Canadian Petroleum Geology*, vol. 49, no. 1, p. 1-6.

Wilhelms, A., E. Rein, C. Zwach, and A. S. Steen, 2001, Application and implication of horizontal well geochemistry, *Petroleum Geoscience*, vol. 7, no. 1, p. 75-79.

Williams, G. K., 1983, What does the term 'Horn River Formation' mean? *Bulletin of Canadian Petroleum Geology*, vol. 31, no. 2, p. 117-122.

CHAPTER 3

CHARACTERIZATION OF MUSKWA AND OTTER PARK GAS SHALES IN THE HORN RIVER BASIN USING MUD GAS ISOTOPE LATERAL PROFILES

3.1 Introduction

Organic-rich Devonian shales of the Horn River Basin, northeast British Columbia contain significant natural gas reserves trapped within fine grained marine sedimentary rock with gas-in-place volume estimates which range from 448 to 1000 Tcf (Ross and Bustin, 2008; Adams, 2012). Givetian-Frasnian Muskwa and Otter Park Formations of the Horn River Group are major targets for shale gas exploration and production in this region of the basin. Gas recovery from ultra-low porosity and permeability unconventional reservoirs provides new challenges and integration of various geological, geophysical and geochemical techniques is necessary for accurate reservoir depiction.

This study focuses on stable isotope analysis as a tool for evaluation of Horn River Basin shale gases and provides a snapshot of subsurface isotope geochemistry along laterals of horizontal wells in the Muskwa and Otter Park Formations. Carbon and hydrogen isotope signatures of natural gas components ($\delta^{13}\text{C}_{\text{methane}}$, $\delta^{13}\text{C}_{\text{ethane}}$, $\delta^{13}\text{C}_{\text{propane}}$ and $\delta\text{D}_{\text{methane}}$) provide insight into these geofluids and the reservoir. Stable carbon and hydrogen isotope ratios ($^{13}\text{C}/^{12}\text{C}$ and D/H) of natural gas are widely used to indicate gas origin, source, thermal maturity, reservoir continuity / compartmentalization and gas ‘families’ in conventional reservoirs (Stahl, 1974; Fuex, 1977; Schoell, 1983; James, 1983; Chung et al., 1988; Schoell, 1988; Berner and Faber, 1988; Clayton, 1991; Jenden et al., 1993; Prinzhofer and Huc, 1995; Rowe and Muehlenbachs, 1999a; Norville and Dawe, 2007; Tilley and Muehlenbachs, 2007). Additionally, stable isotope analysis of mud gases is valuable in hydrocarbon exploration to map subsurface variations in gas isotope composition (Rowe and Muehlenbachs, 1999a; Rowe and Muehlenbachs, 1999b; Wilhelms et al., 2001; Ellis et al., 2003; Tilley and Muehlenbachs, 2006; Dawson and Murray, 2011). Carbon isotope profiles are

used to characterize natural gas in the Upper Cretaceous to Mississippian rocks of the Western Canada Sedimentary Basin (Rowe and Muehlenbachs, 1999a; Rowe and Muehlenbachs, 1999b; Tilley and Muehlenbachs, 2006); however applications can also be extended to unconventional shale gas reservoirs.

In this study shale gas samples were obtained from two wells at the b18I multi-well pad in the Dilly Creek area of the Horn River Basin and horizontal legs of these shale gas wells were drilled and completed within the gas rich Muskwa and Otter Park shale formations. Mud gases for carbon and hydrogen stable isotope analysis were collected at the well head representing pre-determined intervals from Horn River Group Formations and the corresponding gas concentrations recorded as gas units (GU). Carbon isotope ratios ($^{13}\text{C}/^{12}\text{C}$) and hydrogen isotope ratios (D/H) ratios of hydrocarbon components (methane, ethane, propane and butane) of shale gases were measured. The main objectives are to determine (i) the isotope signatures of shale gases and gas maturity of Muskwa and Otter Park gases (ii) the flow connectivity in shales of the Muskwa and Otter Park Formations using the carbon stable isotope profiles (iii) if any relationship exists between isotopically reversed gases and the mud gas concentration. Carbon and hydrogen isotope lateral profiles for two horizontal wells in the Horn River Basin are presented. Interpretation of geochemical data is performed utilizing various isotope plots for evaluation of the shale gases.

3.1.1 Flow connectivity in gas shales

Gas shales are organic-rich, fine grained and heterogeneous in nature with complex pore networks (Javadpour et al., 2007; Wang and Reed, 2009; Sondergeld et al., 2010; Ambrose et al., 2010; Curtis et al., 2010; Chalmers et al., 2012). Economic recovery in these unconventional reservoirs depends on natural gas transport from the shale matrix and fracture network (stimulated and natural) to the well bore. In Givetian / Frasnian shales of Horn River Basin pore sizes extend to the nanometer scale (Ross and Bustin, 2008; Dong and Harris, 2012; Chalmers et al., 2012; Harris and Dong, 2013). Understanding pore systems

within gas shales is necessary since effective porosity affects the natural gas flow within the shale and low pore connectivity can impede the rate of gas diffusion (Curtis, 2002; Hu et al., 2012). The microstructure of shale is not homogeneous and consequently porosity and permeability variations may also occur within shale formations. Permeability is an important parameter in shale gas reservoirs, but various challenges are associated with obtaining reliable measurements in these sedimentary rocks (Passey et al., 2010; Sondergeld et al., 2010; Amann-Hildenbrand et al., 2012; Glorioso and Rattia, 2012; Aguilera, 2013). Scanning electron microscopy (SEM) imaging techniques (Curtis et al., 2010), mercury injection capillary pressure (MICP) and nuclear magnetic resonance (NMR) measurements have been employed for observing the structure and determination of pore connectivity in shales. Methods used for measurement each have individual limitations, however certain techniques routinely used for analysis in conventional reservoirs may not be suitable for shale gas reservoirs due to the nature of these extremely fine grained sedimentary rocks. In addition, lack of standardization exists at present which may pose further challenges in measurement of porosity and permeability in gas shales.

Mud gas isotope geochemistry can be used as a complementary technique to provide insight into the flow connectivity of gas shales within formations targeted for shale gas production. Mud gas isotope profiles are useful to map isotopic variation of natural gas in the subsurface (Tilley and Muehlenbachs, 2006). Carbon isotope profiles show $\delta^{13}\text{C}$ variations with depth and can assist in determination of pore connectivity in the reservoir. Uniformity in carbon isotope profiles may indicate connectivity while geochemical variations imply barriers to diffusion (Wilhelms et al., 2001; Tilley et al., 2001; Elshahawi et al., 2010). The use of a stable isotope mud log is advantageous since real time geologic data is obtained while the well is drilled and it removes the problem of collecting very small rock samples which may not provide a complete depiction at the wellbore scale.

3.1.2 Isotope reversals

Isotope reversal is a common phenomenon observed in several shale gas plays worldwide (Zumberge et al., 2009; Burruss and Laughrey, 2010; Rodriguez and Philp, 2010; Burruss and Laughrey, 2011; Tilley et al., 2011; Tilley and Muehlenbachs, 2012; Zumberge et al., 2012; Tilley and Muehlenbachs, 2013). In these plays carbon isotope signatures of natural gases may show deviation from the ‘normal’ gas isotope trend established in conventional hydrocarbon reservoirs where $\delta^{13}\text{C}_{\text{methane}} < \delta^{13}\text{C}_{\text{ethane}} < \delta^{13}\text{C}_{\text{propane}} < \delta^{13}\text{C}_{\text{butane}}$. In some cases the most productive wells appear to be those which exhibit isotope reversals (Zumberge et al., 2012). In the Horn River Basin many wells contain shale gases which show isotope reversals among gas components (Tilly and Muehlenbachs, 2013). Identification of specific regions where ‘isotope reversals’ are observed might therefore provide additional information useful for development of the shale gas play. In this study isotope reversal is investigated at the wellbore scale to determine if there exists any relationship between the isotope reversals and the gas concentrations observed for gases from the Givetian / Frasnian Otter Park and Muskwa Formations.

3.1.3 Geologic setting

The Horn River Basin, British Columbia (Fig. 3.1) covers an area approximately 3 million acres (Reynolds and Munn, 2010) located north of Fort Nelson and surrounded by the Keg River and Slave point carbonate platforms and the Bovie Lake Fault (Williams, 1983; Morrow et al., 2002; Ness et al., 2010). In the early Devonian an inland seaway formed due to tectonic and eustatic changes which resulted in the sea encroaching from the northwest (Oldale and Munday, 1994; Root, 2001; Corlett and Jones, 2011). During the middle Devonian, shallow epicontinental seas with well-circulated sea water existed in the Presqu’ile barrier reef area, while further west, in deeper marine and suboxic conditions of the Horn

River Basin, clays, siliceous muds and dead plankton were deposited (B.C. Ministry of Energy and Mines and National Energy Board, 2011). The Givetian / Frasnian Horn River Group includes the Muskwa, Otter Park and Evie Formations; ramp and basinal marine shales. Paleozoic Muskwa and Otter Park and Evie shales; originally members of the Horn River Formation (Gray and Kassube, 1963) were later elevated to Formation status (Williams, 1983; Morrow et al., 2002; Ross and Bustin, 2008). Horn River group shales are interpreted to be a series of clinoform beds which thinned to the west (Pelzer, 1966; Williams, 1983). The Otter Park Formation is overlain by the Muskwa Formation and overlies shales of the Evie Formation (Fig. 3.2). Muskwa shales are overlain conformably by the Fort Simpson Formation. In the southeast, the Middle Devonian Otter Park shale is medium to dark grey, calcareous with lower radioactivity and resistivity than in the northwest where it thins and turns black, siliceous and radioactive (Oldale and Munday, 1994). Upper Devonian Muskwa shales are grey to black, pyritic, siliceous and ranges in thickness from approximately thirty to sixty metres. Pelagic fauna present in the shale suggests a deep water origin (Williams, 1983). The Muskwa Formation is highly radioactive and represents a large scale transgression across the Basin (Oldale and Munday, 1994; Weissenberger and Potma, 2001; Ross and Bustin, 2008). Devonian shales of the Horn River Basin are thermally mature with reported vitrinite reflectance (Ro) values of 2.5% for the Muskwa (Reynolds and Munn, 2010).

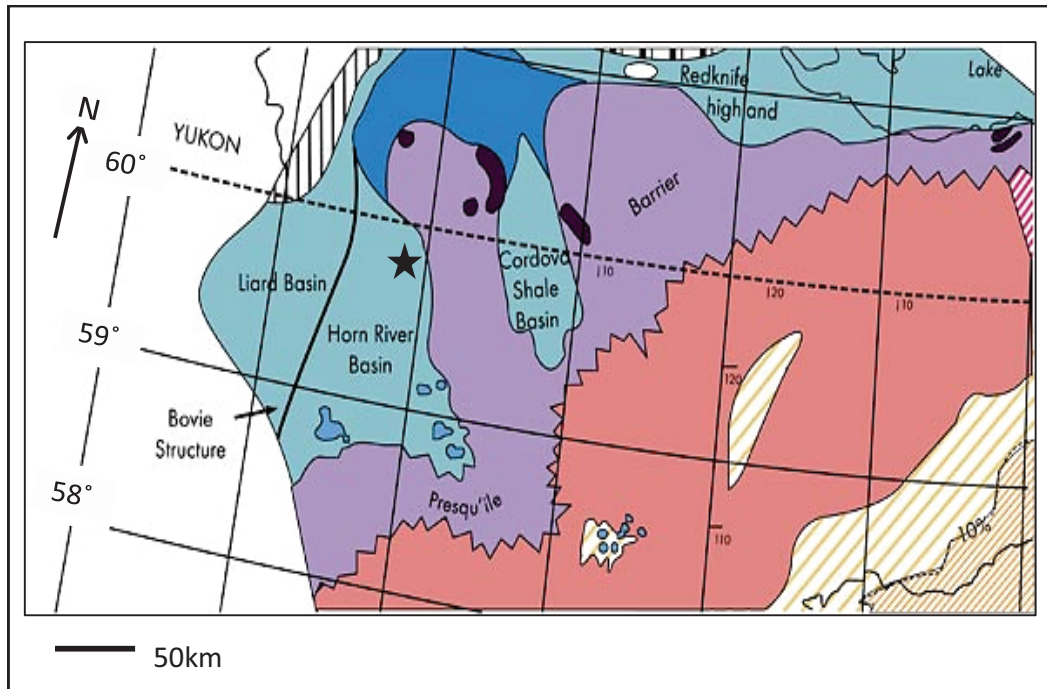


Figure 3.1 Location map of the Horn River Basin, Northeast British Columbia. The study site is indicated by a star symbol within NTS map 94O/8 (modified from British Columbia Ministry of Energy, 2011).

3.2 Methodology

3.2.1 Sample collection

The sample site for this study is located in the Dilly Creek area of the Horn River Basin, northeast of Ft. Nelson, British Columbia within map sheet 94O/8 in the National Topographic System (NTS). Shale gas samples for carbon and hydrogen stable isotope analysis were collected at fixed intervals along laterals legs of two horizontal wells (Nexen Komie b-A18-I/94-O-08 and Nexen TSEA b-18-I/94-O-08) drilled from a multi-well pad with horizontal displacement well paths in the Muskwa and Otter Park Formations (Fig.3.3). The target zone for shale gas production for Nexen Komie b-A18-I/94-O-08 is the Muskwa ‘C’ package; approximately 12m thick and for Nexen TSEA b-18-I/94-O-08 the target is the Otter Park ‘B’ package approximately 24m in thickness. Lateral legs of wells are

approximately 2 km and true vertical depths (TVD) are 2429m and 2485m for the Muskwa and Otter Park wells respectively.

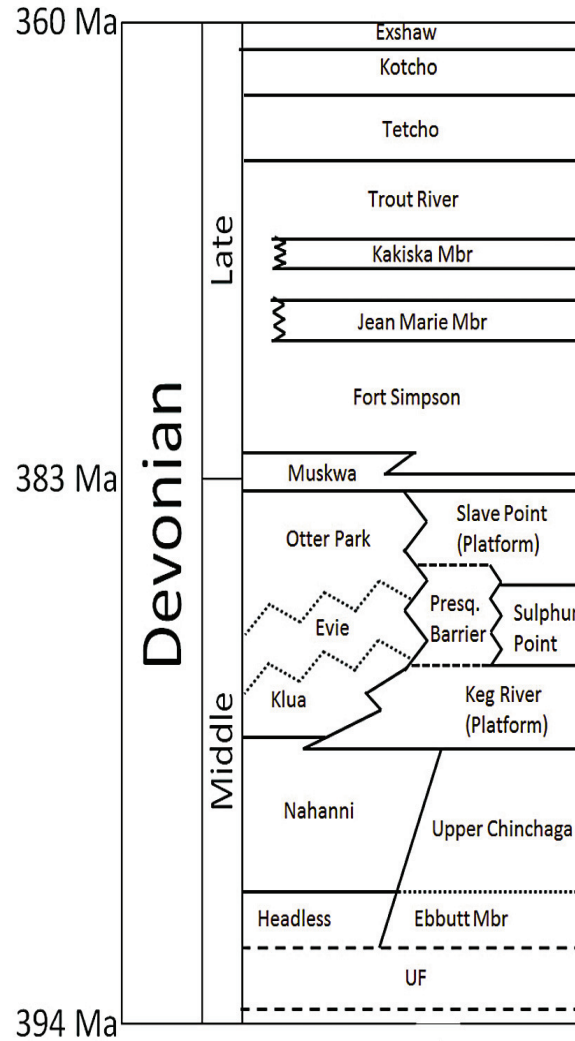


Figure 3.2 Stratigraphy of the Devonian NE British Columbia in the Horn River Basin area (after Close et al., 2012).

During drilling of the wells over one hundred Muskwa and Otter Park mud gas samples were collected for stable isotope analysis as gas samples were separated from the mud stream on its return to the surface. Mud gases were collected in IsoTubes[®] (IsoTech Laboratories, Champaign IL) inserted into the sampling manifold at the wellhead which allow samples to be collected directly from flow lines and maintain gas integrity. The well information, measured depth (m) and corresponding gas concentration (gas units) for each sample was recorded.

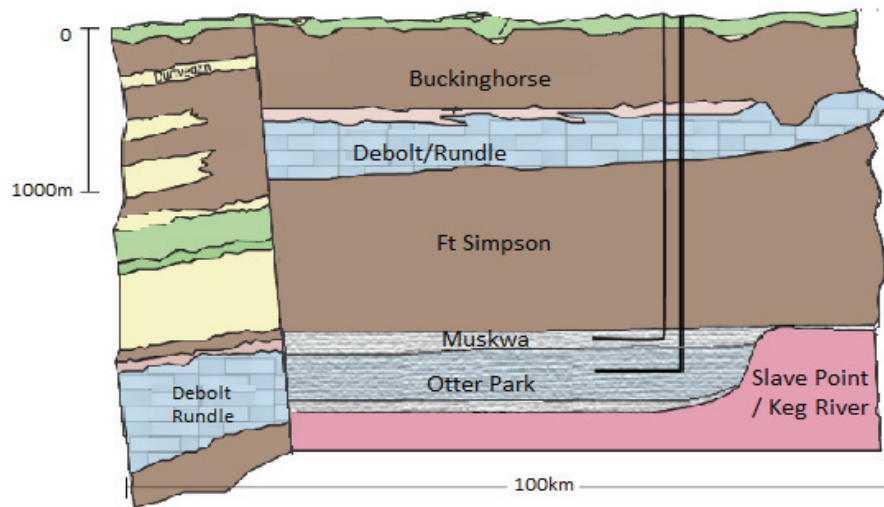


Figure 3.3 Schematic showing well placements at well pad b18I in the Horn River Basin. Mud gas isotope profiles are created for laterals of two wells (b-18-I and b-A18I). The horizontal well leg of well b-18-I is completed within the Otter Park Formation and well b-A18I is within the Muskwa Formation (modified from B.C. Oil and Gas Commission, 2012)

3.2.2 Sample analysis

Carbon and hydrogen stable isotope analysis of mud gas samples was performed at the Stable Isotope Laboratory at University of Alberta and isotope ratios were expressed using the standard δ -notation.

$\delta^{13}\text{C}$ analysis

Carbon isotope ratios ($^{13}\text{C}/^{12}\text{C}$) of mud gas hydrocarbon components; methane (C1), ethane (C2), propane (C3) and butane (C4) were measured using the Finnigan-MAT 252 mass spectrometer. A gas chromatography combustion continuous-flow isotope ratio mass spectrometry (GC-C CF-IRMS) system was used. Natural gases were separated into individual components by GC and converted to CO_2 by combustion. Isotope ratios of these gases were measured against a CO_2 lab reference standard. Instrument settings and conditions for the GC-C CF-IRMS are outlined in Rowe and Muehlenbachs (1999b). The $\delta^{13}\text{C}$ values of gas components (C1 to C4) were reported in per mil (‰) relative to the Vienna Pee Dee Belemnite (VPDB) standard. Reproducibility of $\delta^{13}\text{C}$ values in the analysis of gases are $\pm 0.1\text{‰}$ for methane, $\pm 0.2\text{‰}$ for ethane and $\pm 0.8\text{‰}$ propane.

δD analysis

$\delta\text{D}_{\text{methane}}$ values for methane in mud gas samples were obtained by isotope analysis of hydrogen gas. Hydrocarbon components of mud gases were separated using the Agilent 6890 Series gas chromatograph with the methane fraction later reacting in a CuO furnace at $\sim 1000^\circ\text{C}$ to produce H_2O and CO_2 . H_2O and CO_2 were separated using liquid nitrogen. The H_2O collected was subsequently reduced to H_2 by reaction with Zn metal at $\sim 480^\circ\text{C}$ using similar techniques to those outlined in Coleman (1982) for preparation of hydrogen gas by reduction of water. Hydrogen isotope ratios (D/H) of gases were measured using the Finnigan MAT 252 IRMS. The $\delta\text{D}_{\text{methane}}$ values were reported in per mil (‰) relative to the

VSMOW (Standard Mean Ocean Water) standard. The overall average reproducibility of $\delta D_{\text{methane}}$ values for gases is $\pm 2.5\%$.

X-ray fluorescence (XRF) analysis

An X-ray Fluorescence (XRF) spectrometer was used for elemental analysis samples of drill cuttings by a commercial company and interpretation to determine mineralogy. Shale samples were obtained from along the horizontal well legs and analysis was performed at 5m intervals in the target Muskwa and Otter Park formations. The minerals include orthoclase (Or), quartz (Q), illite (Ill), kaolinite (Kn), chlorite (Chl), Apatite (Ap), dolomite (DI), ankerite (Ank), siderite (Sd), serpentine (Srp), halite (Ht), pyrolusite (Prl), pyrite (Pr) and rutile (Rt).

3.3 Results and Discussion

3.3.1 Mineralogy

Muskwa and Otter Park shales obtained from the drill cuttings along laterals lengths of wells are dark grey to black in colour and contain calcareous as well as silty zones, low amounts of microcrystalline plus nodular pyrite and fractures cemented with calcite or quartz (Nexen Geological Wellsite Report-NEXEN INC HZ TSEA b-18-I/94-O-8). Fig. 3.4 illustrates the mineral content (wt %) of shales for wells b-18-I (Otter Park) and b-A18I (Muskwa) determined by X-ray Fluorescence (XRF) analysis. Muskwa and Otter Park shales vary in mineral composition between formations and within each formation along the horizontal lengths of the wells. Otter Park shales showed greater compositional heterogeneity than shales the Muskwa Formation. Major minerals present in these formations were quartz, clay minerals (illite and kaolinite) and calcite. Muskwa shales were enriched in quartz compared to the shales of the Otter Park and average quartz wt % values were $\sim 73\%$ and $\sim 51\%$ respectively. Higher clay content (illite and kaolinite) was measured in the Otter Park shale where average

wt % values were ~24% while shales of the Muskwa contained ~15%. Overall higher percentages of calcite were present in the Otter Park formation.

The percentage mineral composition in the shale is an important parameter since it determines which shale formations are suitable for creation of successful hydraulic fractures which are necessary for economic shale gas production. Mineral composition may also play a role in the distribution of gas within the shale and hence will affect the gas deliverability during production. Figs. 3.5 to 3.7 show the relationship between the mineral composition (wt %) for Muskwa and Otter Park shales and the corresponding mud gas concentrations. In Fig 3.5 the mud gas concentrations for the Otter Park and Muskwa are illustrated and the main minerals present in shales from these two formations. The graphs show overall higher mud gas concentrations with increased quartz % and decreased % clay (illite and kaolinite). Fig 3.6 and 3.7 show both the variation in mineralogy and mud gas concentrations along the laterals legs of the wells and regions of elevated gas concentration can be identified and the associated mineral content of the shale.

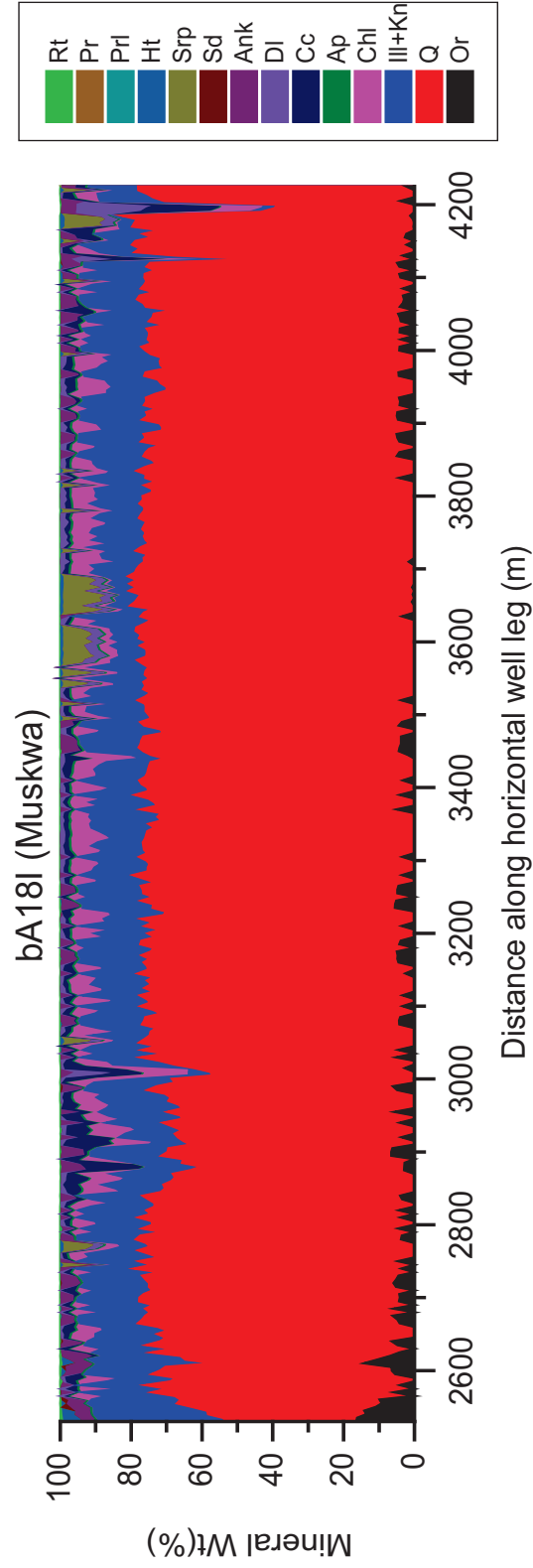


Figure 3.4 (a) Variation in shale mineralogy for bA18I (Muskwa Formation) measured along the horizontal length of the well. The minerals shown are orthoclase (Or), quartz (Q), illite (Ill), kaolinite (Kn), chlorite (Chl), Apatite (Ap), dolomite (DI), ankerite (Ank), siderite (Sd), serpentine (Srp), halite (Ht), pyrolusite. (Pr), pyrite (Pr) and rutile (Rt).

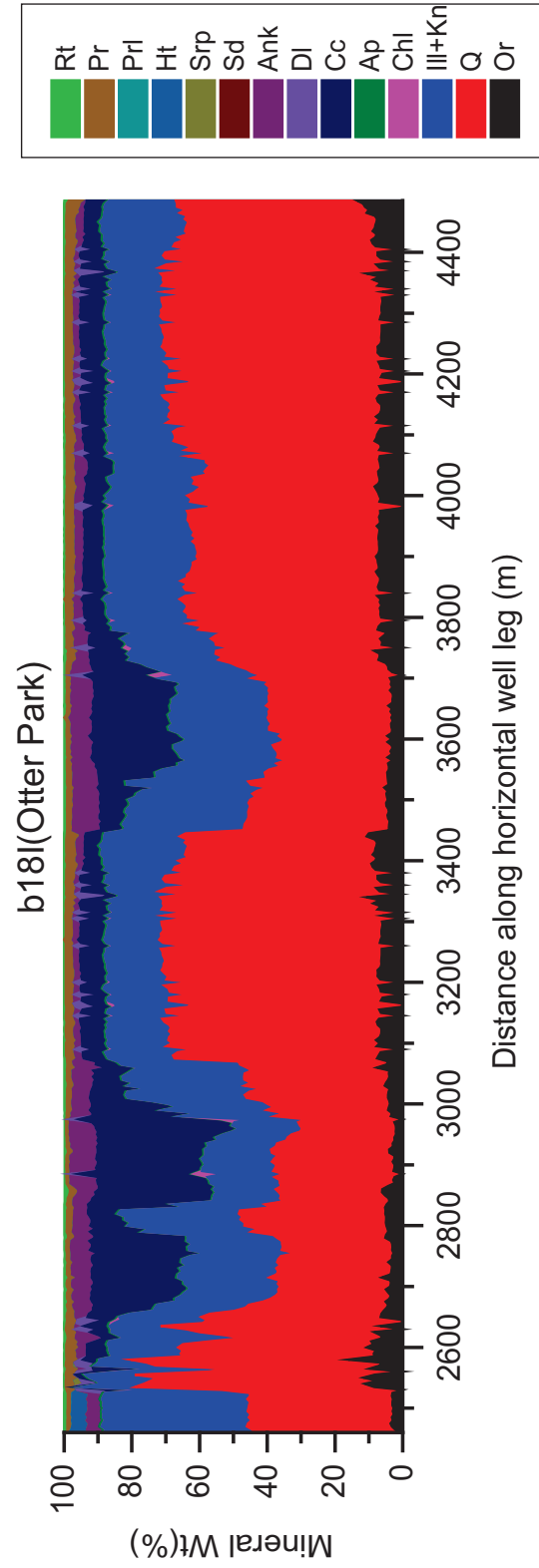


Figure 3.4 (b) Variation in shale mineralogy for b181 (Otter Park Formation) measured along the horizontal length of the well. The minerals shown are orthoclase (Or), quartz (Q), illite (Ill), kaolinite (Kn), chlorite (Chl), Apatite (Ap), dolomite (DI), ankerite (Ank), siderite (Sd), serpentine (Srp), halite (Ht), pyrolusite (PrI), pyrite (Pr) and rutile (Rt).

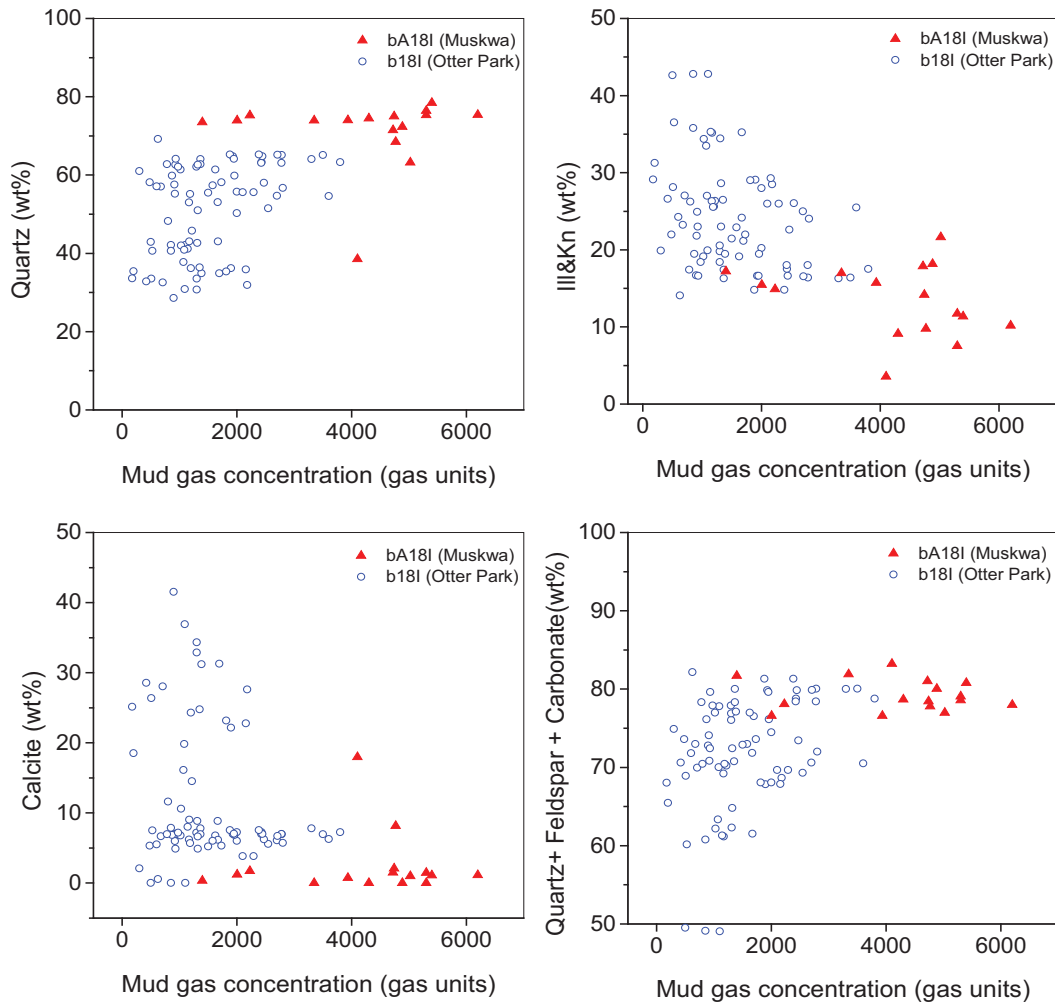


Figure 3.5 Relationship between mineral (wt. %) and the mud gas concentration for bA18I (Muskwa Formation) and b18I (Otter Park formation) wells. Minerals (a) Quartz (b) Clay minerals- Illite and Kaolinite (c) Calcite (d) Brittle components of shale –quartz , feldspar and carbonate.

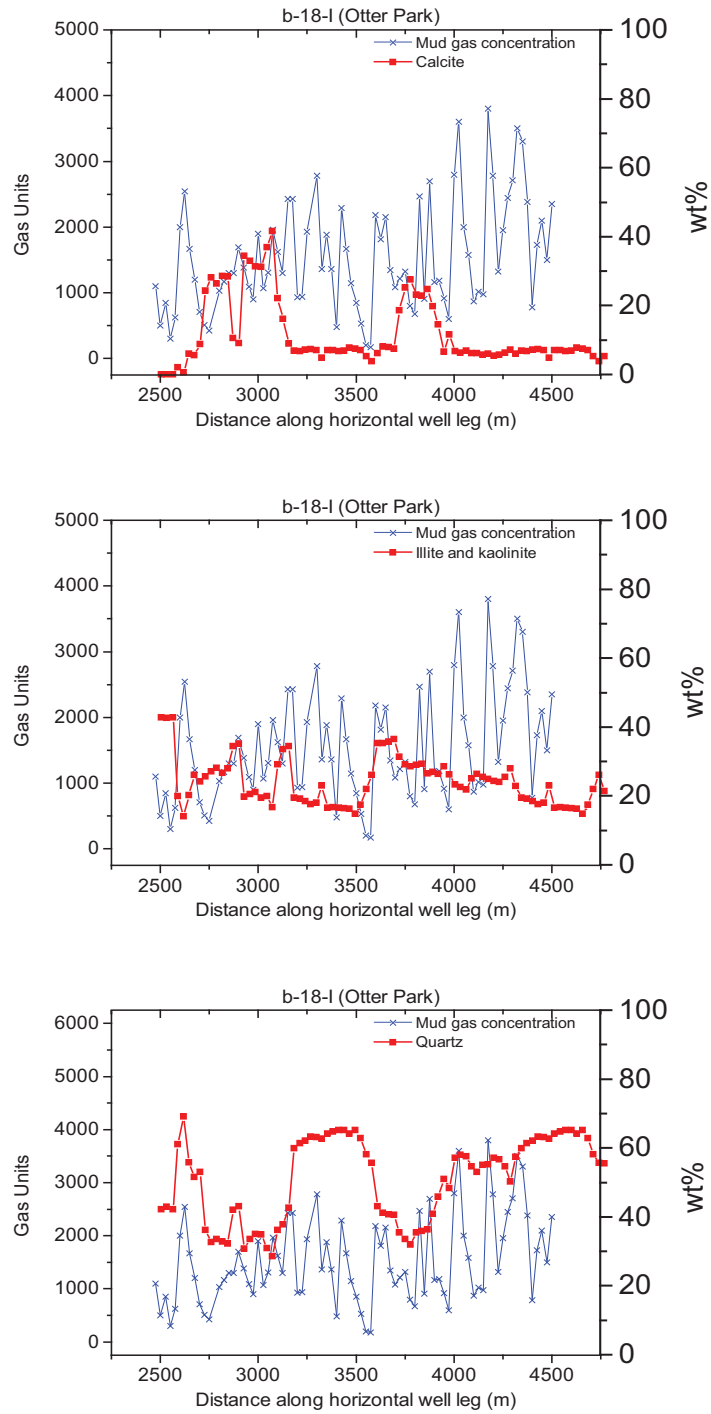


Figure 3.6 Variation in mineral (wt. %) and the mud gas concentration for the b18I (Otter Park formation) wells along horizontal well paths

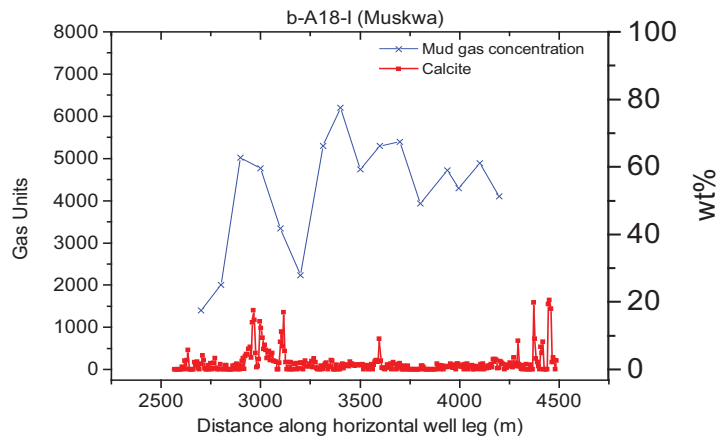
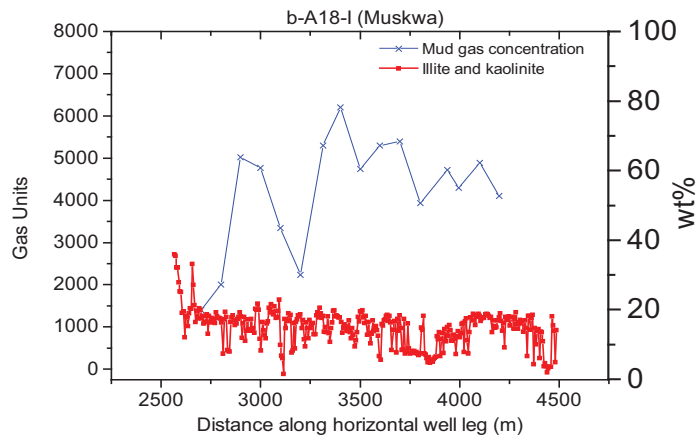
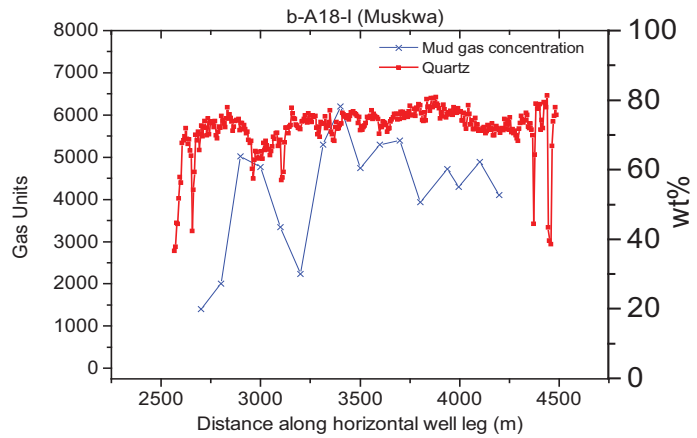


Figure 3.7 Variation in mineral (wt. %) and the mud gas concentration for the bA18I (Muskwa Formation) well along horizontal well paths

3.3.2 Stable isotope geochemistry

Carbon isotope profiles for the Upper Devonian Muskwa Formation and underlying Middle Devonian Otter Park Formation are presented. Variation in the stable isotope composition ($\delta^{13}\text{C}_{\text{methane}}$, $\delta^{13}\text{C}_{\text{ethane}}$ and $\delta^{13}\text{C}_{\text{propane}}$) of mud gas hydrocarbon components is evident along the horizontal displacement paths of both well bores (Fig. 3.8a to Fig. 3.8c). Individual carbon isotope profiles were created for the hydrocarbon components methane, ethane and propane (C1 to C3) and inspection of isotope data from Muskwa and Otter Park mud gases analysis clearly exhibit isotopic compositional differences between these two formations.

The Otter Park Formation exhibited a wider range in $\delta^{13}\text{C}$, most obvious in the carbon isotope ratios of methane which ranged from -36.9‰ to -31.9‰, whereas Muskwa gases showed $\delta^{13}\text{C}_{\text{methane}}$ values between -35.5‰ and -34.5‰ (Fig 3.8a). The higher uniformity in carbon isotope profiles for methane, ethane and propane in the Muskwa shales suggest greater lateral flow connectivity between pores of the Muskwa Formation than in the Otter Park shale for these two wells. Carbon isotope data results are in agreement with other published work in which higher overall permeability in shales of the Muskwa compared to the Otter Park Formation is reported (Ness et al., 2010; Dong and Harris, 2012). The higher flow connectivity for the Muskwa shales is likely to be a key contributing factor to the overall higher gas concentration observed in drilling mud from the Muskwa Formation (Fig. 3.9).

In the Otter Park shale average $\delta^{13}\text{C}_{\text{methane}}$, $\delta^{13}\text{C}_{\text{ethane}}$, $\delta^{13}\text{C}_{\text{propane}}$ values were -35.0‰, -33.8‰ and -28.9‰ respectively, while average $\delta^{13}\text{C}_{\text{methane}}$, $\delta^{13}\text{C}_{\text{ethane}}$, $\delta^{13}\text{C}_{\text{propane}}$ values in the Muskwa shales were -34.9‰, -34.2‰ and -30.3‰ respectively. Although wide variations occur in carbon isotope values of the Otter Park, the results indicate overall $\delta^{13}\text{C}_{\text{methane}}$, $\delta^{13}\text{C}_{\text{ethane}}$ and $\delta^{13}\text{C}_{\text{propane}}$ values for both Formations were comparable suggesting similar maturities for these lithologic units. $\delta^{13}\text{C}_{\text{methane}}$ values indicate gases are thermogenic in origin ($\delta^{13}\text{C}_{\text{methane}} > -55\text{‰}$) which is expected considering the high thermal maturity of

Devonian Horn River shales where Ro values are approximately 2.5% for the Muskwa shale (Reynolds and Munn, 2010). Along the well bore of the Otter Park some gas samples are more enriched in the ‘heavier’ ^{13}C isotope while others show ^{13}C depletion. These results suggest that isolated pore systems may present in the Otter Park and responsible for the differences observed in the $\delta^{13}\text{C}_{\text{methane}}$ values. The variation in carbon isotope values along the well path indicates a high degree of lateral heterogeneity within the shale. Stable isotope fingerprints of mud gases may reflect the differences in the mineralogy, fabric and natural fractures present in the shale. More natural fractures are present in the ‘brittle’ siliceous quartz rich Muskwa shale in contrast to the Otter Park shale (Chalmers et al., 2012) and these may have contributed to enhanced pore connectivity in the shales of the Muskwa Formation.

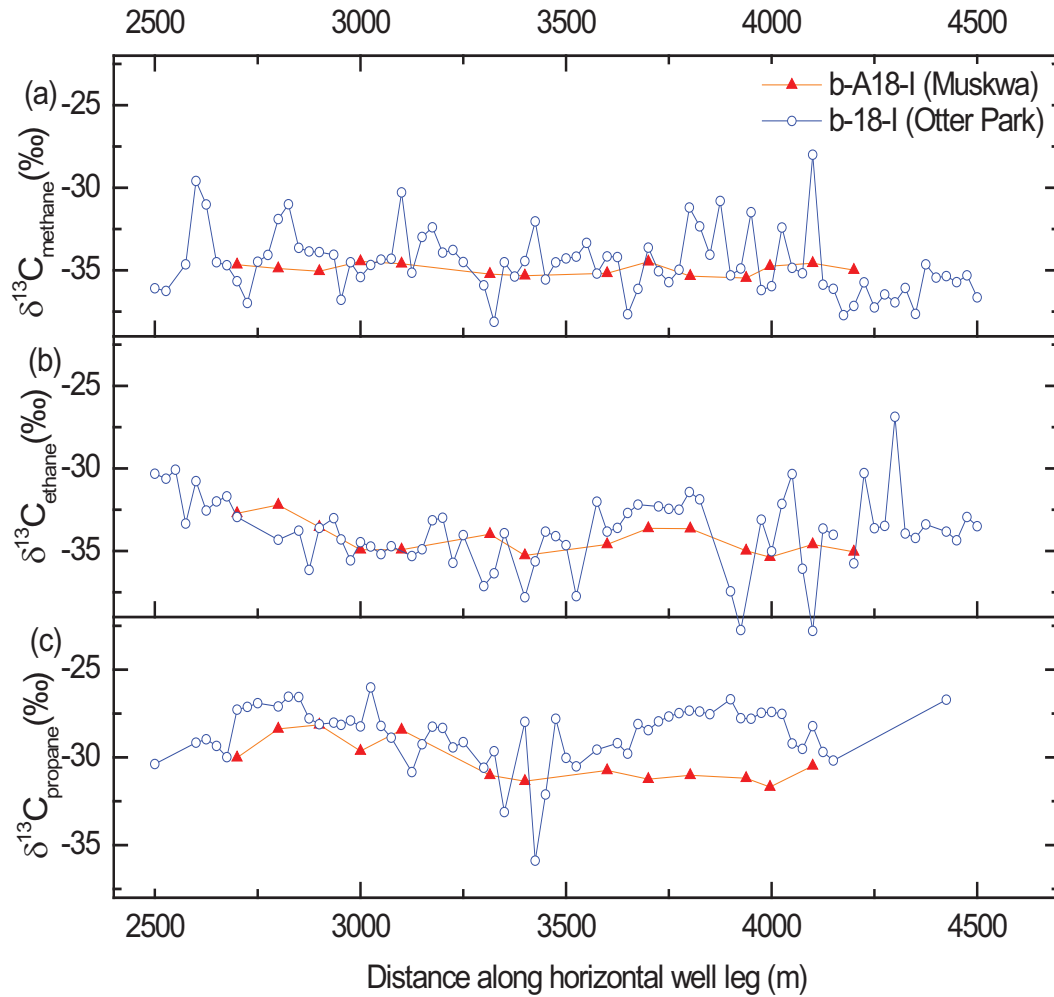


Figure 3.8 Mud gas isotope profiles for the Muskwa and Otter Park Formations (a) Carbon isotope profiles of methane (b) Carbon isotope profiles of ethane (c) Carbon isotope profiles of propane.

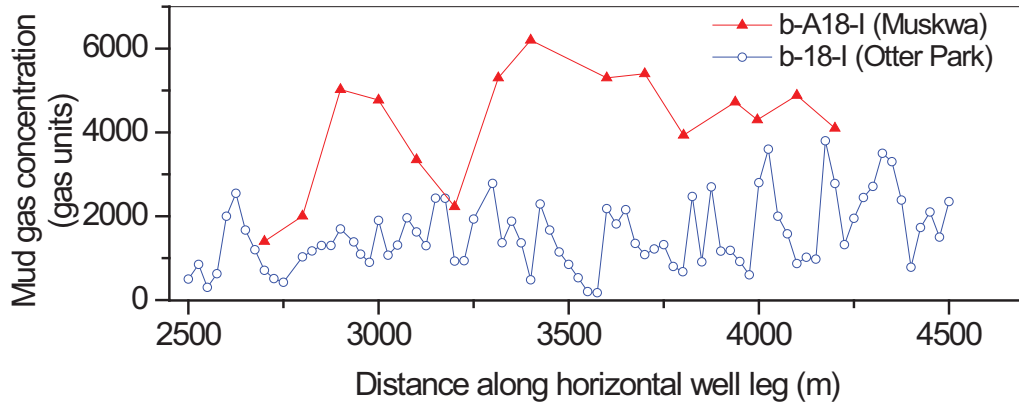


Figure 3.9 Variation in mud gas concentration (gas units) along horizontal wellbore paths in the Muskwa and Otter Park Formations.

Variation in the hydrogen isotope composition of methane ($\delta D_{\text{methane}}$) along the horizontal displacement of wellbores in Muskwa and Otter Park shales is shown in Fig. 3.10. In the Muskwa Formations the range of $\delta D_{\text{methane}}$ values measured was approximately -165‰ to -150‰ while $\delta D_{\text{methane}}$ values of Otter Park gases ranged from -165‰ to -135‰.

Hydrogen isotopes compositions of natural gases vary with subsurface depth and δD values of n-alkanes show overall D-enrichment with increasing subsurface depth (Pedentchouk et al., 2006). δD of formation water affects the δD of natural gas however δD values of formation water are unknown for this region of the Horn River Basin. In general, the δD values were more negative for the gases from the Muskwa Formation than for the Otter Park Formation. Muskwa gases had an average $\delta D_{\text{methane}}$ of -159.5‰ while the average value for the Otter Park gases was -153.5‰. This suggests slightly overall higher maturity of the Otter Park which is expected considering the stratigraphy of the Horn River Group where shales of the Muskwa Formation overlie the Otter Park Formation.

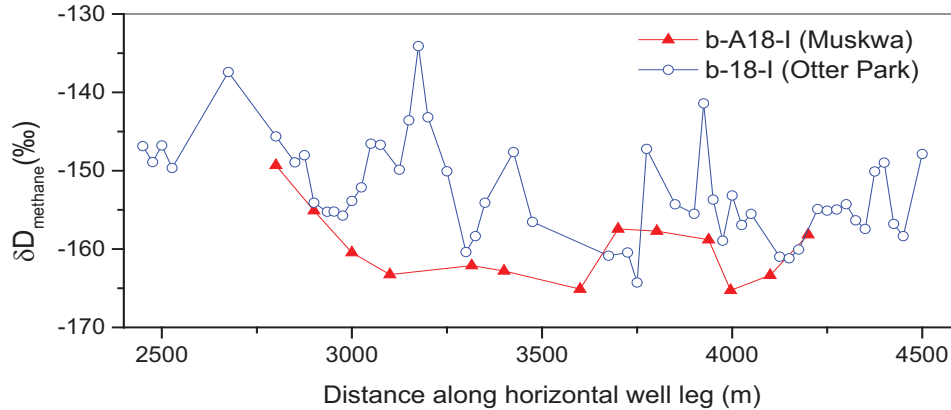


Figure 3.10 Hydrogen isotope profiles of methane for the Muskwa and Otter Park Formations.

3.3.3 Isotope cross-plots

The $\delta^{13}\text{C}_{\text{ethane}}$ vs $\delta^{13}\text{C}_{\text{methane}}$ isotope cross-plot (Fig. 3.11a) and $\delta^{13}\text{C}_{\text{propane}}$ vs $\delta^{13}\text{C}_{\text{ethane}}$ isotope cross-plot (Fig. 3.11b) reflect the high maturity of shale gases from the Muskwa and Otter Park Formations. Gases showing isotope reversals between components are separated from gases without isotope reversals by the dashed lines. Isotopically reversed gases fall below the dashed lined and arrows point in the general direction of increasing maturity. Devonian Horn River Group shales are thermally mature with R_o values of $\sim 2\%$ for the Muskwa and Otter Park Formations and carbon isotope values reflect the high maturity of these gases and indicates thermal origin. Isotope cross-plots indicate similar gas maturity in both formations and show that gas isotope reversals occur mainly between $\delta^{13}\text{C}_{\text{methane}}$ and $\delta^{13}\text{C}_{\text{ethane}}$. In the $\delta^{13}\text{C}_{\text{ethane}}$ vs $\delta^{13}\text{C}_{\text{methane}}$ cross-plot (Fig. 3.11a) there was a cluster in the carbon isotope values of methane and ethane for Muskwa gases; however, Otter Park gases show a high degree of scatter in the carbon isotope values of methane and ethane. The $\delta^{13}\text{C}_{\text{propane}}$ vs $\delta^{13}\text{C}_{\text{ethane}}$ isotope cross-plot (Fig. 3.11b) shows that the majority of mud gases from the Muskwa and Otter Park Formations lack isotope reversal between propane and ethane components.

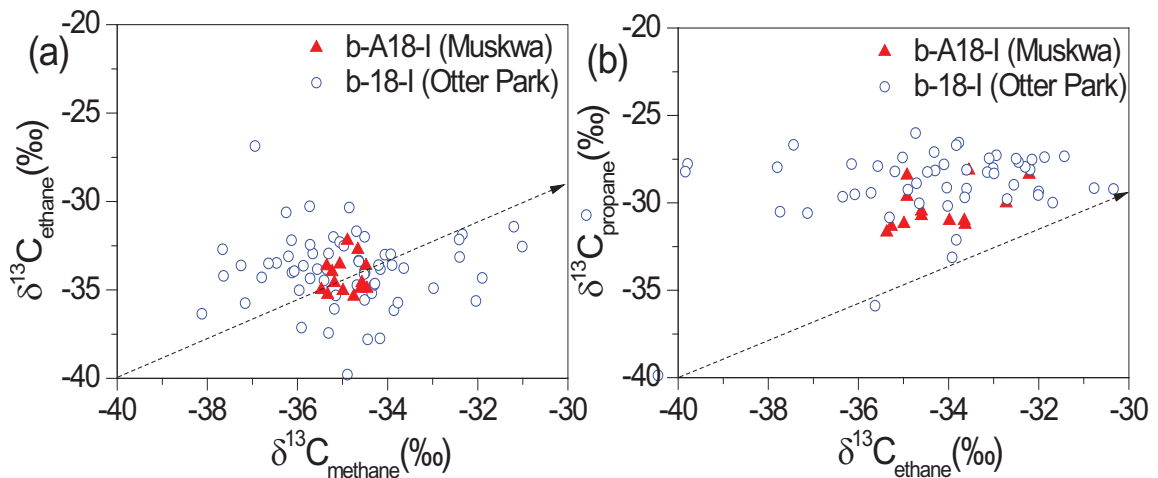


Figure 3.11 (a) Isotope cross-plot showing $\delta^{13}\text{C}_{\text{ethane}}$ vs $\delta^{13}\text{C}_{\text{methane}}$ for the Muskwa and Otter Park Formations (b) Isotope cross-plot showing $\delta^{13}\text{C}_{\text{propane}}$ vs $\delta^{13}\text{C}_{\text{ethane}}$ for the Muskwa and Otter Park Formations.

3.3.4 The natural gas plot

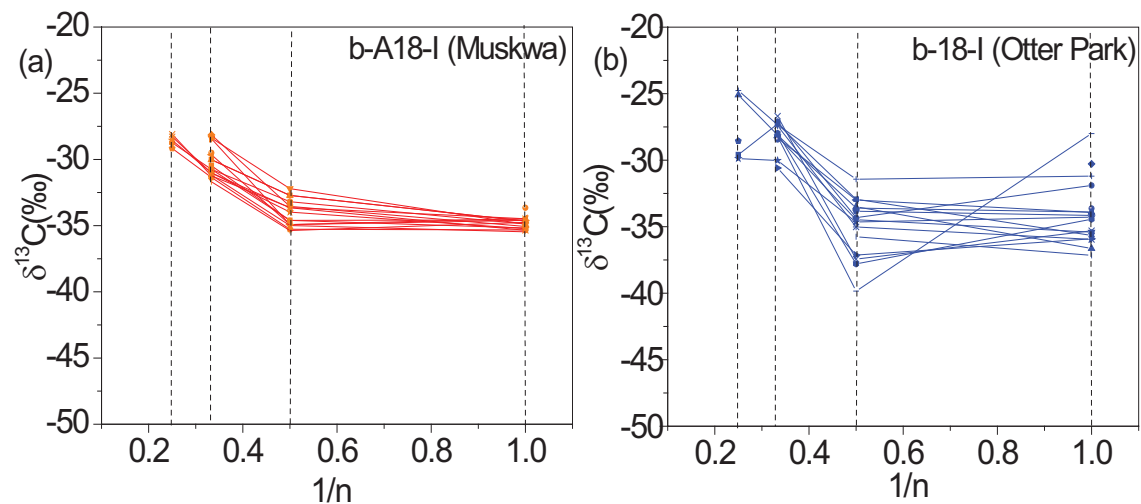


Figure 3.12 (a) Natural gas plot of mud gases from the Muskwa Formation sampled along the horizontal well leg (b) Natural gas plot of mud gases from the Otter Park Formation sampled along the horizontal well leg.

Mud gas isotope data for the Muskwa and Otter Park Formations (Fig. 3.12a and Fig. 3.12b) are shown using natural gas plots. In conventional hydrocarbon reservoirs a straight line on the gas plot indicates ‘pure’ natural gas while mixing of gases from different sources causes deviation from linearity (Chung et al., 1988). In the natural gas plot Muskwa and Otter Park gases show digression from a straight line. The trends on both plots (where methane is enriched in ^{13}C) are likely due to wet gas cracking which alters the ‘normal’ trend in isotope values of the gas components. However, the exact mechanism involved during the process of wet gas cracking is unknown and further investigation is required (Ni et al., 2009; Tilley and Muehlenbachs, 2013). In shale gas systems reversed/ partially reversed isotope gas signatures indicate advanced thermal maturity (Tilley et al., 2011; Tilley and Muehlenbachs, 2013). In this study some instances of partial isotope reversals are observed and reversals are seen mainly between methane and ethane components where $\delta^{13}\text{C}_{\text{methane}} > \delta^{13}\text{C}_{\text{ethane}}$. In conventional hydrocarbon systems the natural gas plot has been used for identification of the $\delta^{13}\text{C}$ values of the source organic matter. In unconventional shale gases from the Horn River Basin, $\delta^{13}\text{C}$ values of ethane, propane and butane generally form a straight line on the natural gas plot (Fig. 3.12a and Fig. 3.12b). If average values for $\delta^{13}\text{C}_{\text{ethane}}$, $\delta^{13}\text{C}_{\text{propane}}$ and $\delta^{13}\text{C}_{\text{butane}}$ components are used and the line extrapolated this results in $\delta^{13}\text{C}$ values of approximately -23‰ for the organic matter source. These $\delta^{13}\text{C}$ values lie within the expected range for kerogen in the shales of the Horn River Basin which were deposited in a marine environment (Gray and Kassube, 1963). Typical marine organic matter has average $\delta^{13}\text{C}$ values between -20‰ to -25‰ (Fuex, 1977). Natural gas plots highlight the differences in carbon isotope signatures between mud gases from the Muskwa and Otter Park Formations with Muskwa gases showing less variation in $\delta^{13}\text{C}$ values of methane, ethane and propane.

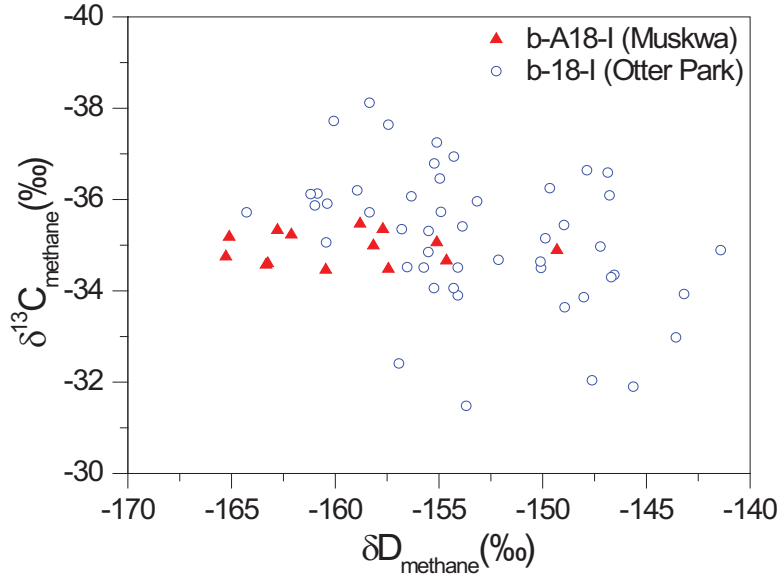


Figure 3.13 Cross-plot of $\delta^{13}\text{C}_{\text{methane}}$ vs $\delta\text{D}_{\text{methane}}$ for the Muskwa and Otter Park Formations.

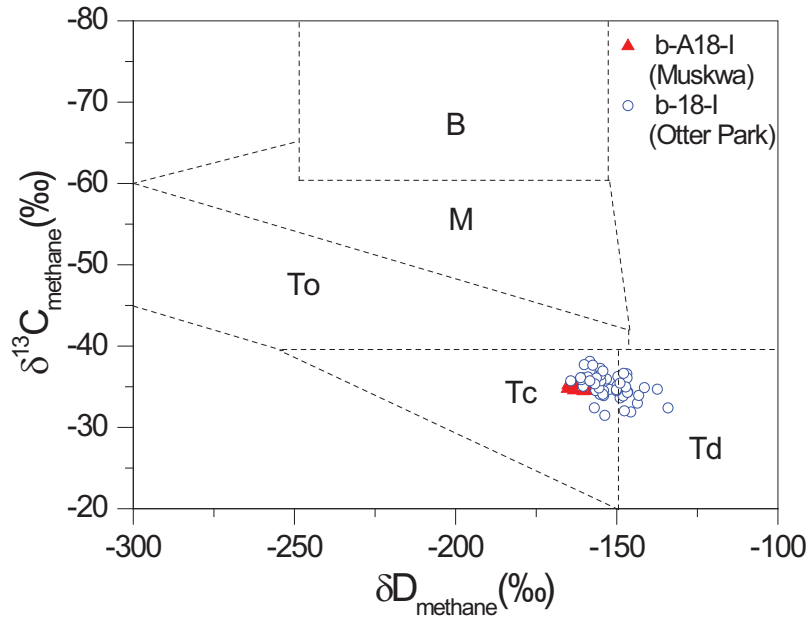


Figure 3.14 The Schoell plot for natural gas classification (after (Schoell, 1983) B and M denotes biogenic and mixed gas respectively. To, Tc and Td denotes thermogenic with oil, condensate and dry.

The $\delta^{13}\text{C}_{\text{methane}}$ vs $\delta\text{D}_{\text{methane}}$ cross-plot (Fig. 3.13) shows the relationship between carbon and hydrogen isotope ratios of methane from the Muskwa and Otter Park shales. In the Otter Park Formation mud gas samples which show ^{13}C enrichment also appear enriched in the D isotope. The carbon and hydrogen isotope compositions of methane suggest gases may have been compartmentalized or isolated pore systems exist within the shales of the Otter Park Formation. In hydrocarbon reservoirs kinetic isotope effects may occur causing preferential breaking of $^{12}\text{C}-^{12}\text{C}$ over $^{12}\text{C}-^{13}\text{C}$ and $^{13}\text{C}-^{13}\text{C}$ bonds during the gas generation process. Methane which showed ^{13}C depletion also appeared depleted in D. It is likely that ^{13}C enriched methane present may correspond to high total organic carbon (TOC) regions within the Otter Park shale. Muskwa shales which exhibit low variation $\delta^{13}\text{C}_{\text{methane}}$ values showed no correlation between $\delta^{13}\text{C}_{\text{methane}}$ and $\delta\text{D}_{\text{methane}}$. These data suggest a higher degree of flow connectivity between the shales of the Muskwa than in the Otter Park shales and are consistent with reports by Dong and Harris (2012) and Dong and Harris (2013) which show connected pore systems in the Muskwa and unconnected pores and lower permeability for shales in the Otter Park in the Horn River Basin.

The Schoell plot (Fig. 3.14) is commonly used for the determination of natural gas origin; biogenic, thermogenic or mixed. In the Schoell plot gases fall within the thermogenic region as expected given the high thermal maturity of the Givetian/ Frasnian Horn River shales ($R_o > 2\%$). However, Devonian gases in this region of the Horn River are deep and very dry gases.

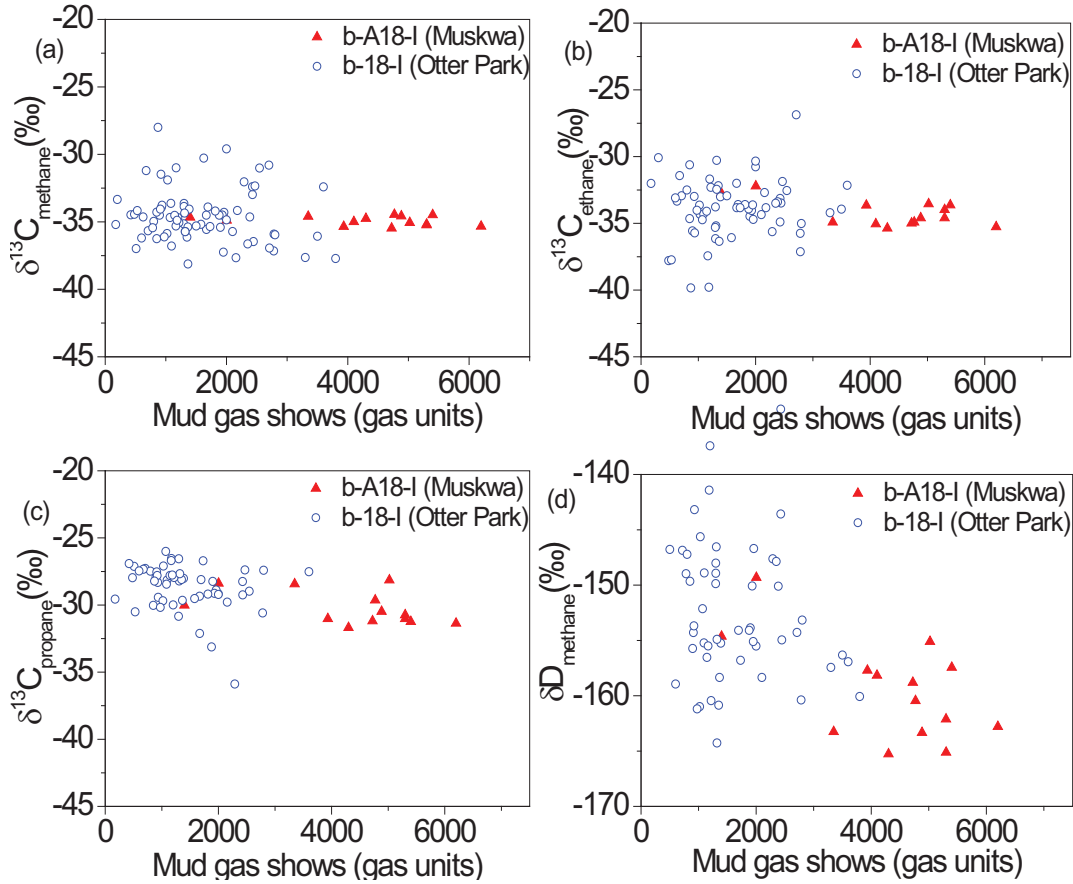


Figure 3.15 Cross-plots of isotope composition vs mud gas concentration for the Otter Park and Muskwa Formations (a) $\delta^{13}\text{C}_{\text{methane}}$ vs mud gas concentration (b) $\delta^{13}\text{C}_{\text{ethane}}$ vs mud gas concentration (c) $\delta^{13}\text{C}_{\text{propane}}$ vs mud gas concentration (d) $\delta\text{D}_{\text{methane}}$ vs mud gas concentration.

Fig. 3.15a to Fig. 3.15c demonstrate the relationship between $\delta^{13}\text{C}$ values of hydrocarbon components (methane, ethane and propane) and the mud gas concentration for the Muskwa and Otter Park Formations. During drilling, elevated hydrocarbon concentrations are reported in arbitrary gas units (GU). Average mud gas concentrations for the Muskwa was approximately double that of the Otter Park shale (Fig. 3.9). In both formations there appears to be some correlation between the magnitude of the gas show and the stable isotope values of carbon and hydrogen ($\delta^{13}\text{C}$ and δD). The Pearson's correlation coefficients (r) of $\delta^{13}\text{C}$ and mud gas concentration (GU) for the Muskwa (Fig. 3.15a to Fig 3.15c)

are -0.3, -0.6 and -0.6 respectively. The observed trend was increased mud gas concentration with depletion of ^{13}C and lower gas concentration with ^{13}C enrichment. In the Otter Park shale the higher gas concentration seems to be associated with the ^{13}C depleted methane and lower gas concentrations occur with ^{13}C methane enrichment. Similar trends exist for both ethane and propane carbon isotope values ($\delta^{13}\text{C}_{\text{ethane}}$ and $\delta^{13}\text{C}_{\text{propane}}$) which are related to magnitude of the gas show recorded / gas concentration observed.

The plots (Fig. 3.15a to Fig. 3.15c) may reflect the differences in the diffusivity of methane, ethane and propane between the two formations. Stable isotope data may be able to assist in identification of low/ high permeability regions if overall elevated gas concentration is observed where gases are depleted in the ^{13}C of methane, ethane and propane. It is evident that each formation must be considered separately. In Fig. 3.15d there is a fairly strong correlation between the $\delta\text{D}_{\text{methane}}$ values and the measured gas concentration and the Pearson correlation coefficient (r) is -0.6. As $\delta\text{D}_{\text{methane}}$ values decreased there was a corresponding increase in the magnitude of the mud gas concentration. Mud gas samples which are depleted in D (more negative $\delta\text{D}_{\text{methane}}$ values) have the lowest gas concentration in both the Muskwa and Otter Park Formations.

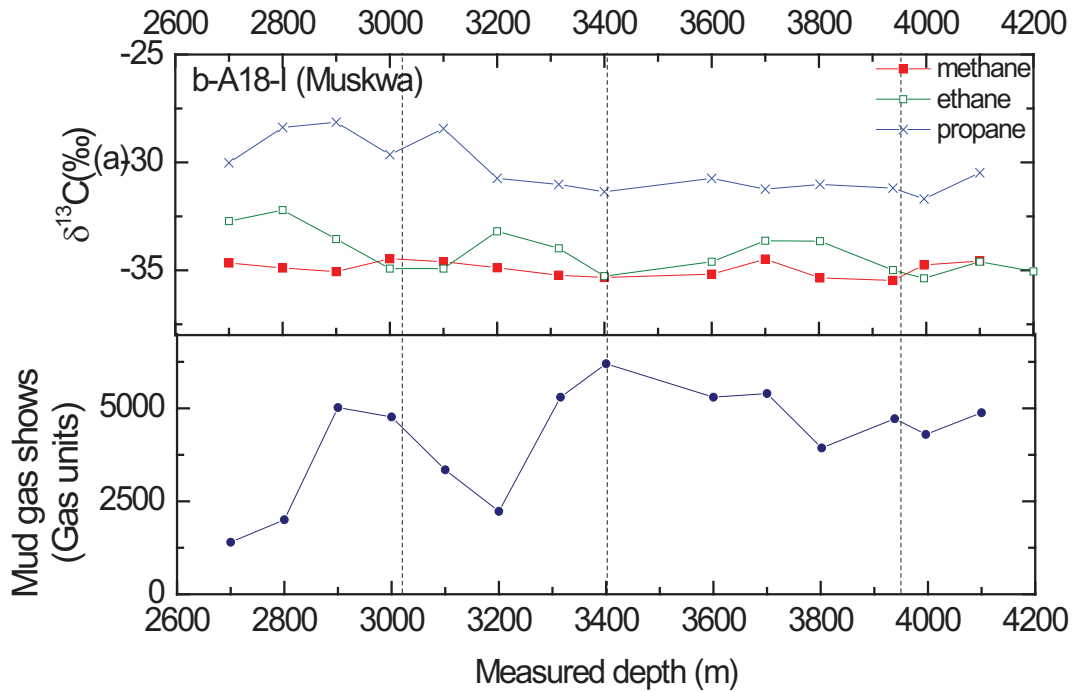


Figure 3.16 (a) Carbon isotope profiles for the Muskwa Formation and corresponding mud gas concentration (gas units). Dashed lines indicate regions where $\delta^{13}C_{\text{methane}} > \delta^{13}C_{\text{ethane}}$ (isotope reversal)

In Fig. 3.16a and Fig. 3.16b dashed lines indicate regions in the shale profile where isotope reversals are present and associated mud gas concentrations. In the majority of cases isotope reversals are found to be associated with regions of high gas concentration in both the Muskwa and the Otter Park Formations. In shale gas plays it is necessary to fracture the reservoir in order to produce gas in economic quantities. Artificial fractures must intercept natural fractures and high permeability flow paths to produce gas; hence zones where reversals occur may identify regions of high diffusivity in the shale and hence allow selection of particular sites to be targeted for fracturing within formations.

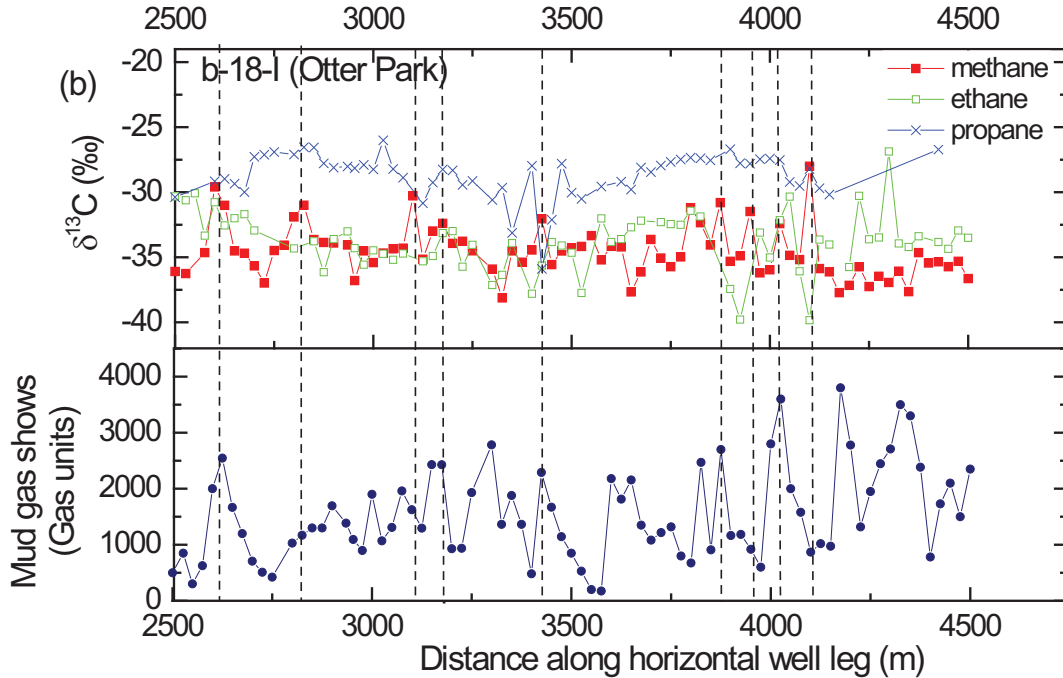


Figure 3.16 (b) Carbon isotope profiles for the Otter Park Formation and corresponding mud gas concentration (gas units). Dashed lines indicate regions where $\delta^{13}\text{C}_{\text{methane}} > \delta^{13}\text{C}_{\text{ethane}}$ (isotope reversal)

Variation in the magnitude of isotope reversals between methane and ethane and the associated mud gas concentrations for the Otter Park and Muskwa and Otter Park are shown in Fig 3.17a and 3.17b. Gases showing isotope reversals $\delta^{13}\text{C}_{\text{ethane}} - \delta^{13}\text{C}_{\text{methane}} < 0$, fall below the dashed lines. These plots show the variation along the horizontal lengths of wells. Fig. 3.17a shows the relationship between isotope reversals and Muskwa mud gas concentrations. Low concentrations of Muskwa gases are observed at distances approximately 2700m and 3200m and these gases showed no isotope reversals between methane and ethane. The relationship between isotope reversal ($\delta^{13}\text{C}_{\text{ethane}}$ and $\delta^{13}\text{C}_{\text{methane}}$) and mud gas concentration for the Otter Park formation is complex (Fig.3.17).

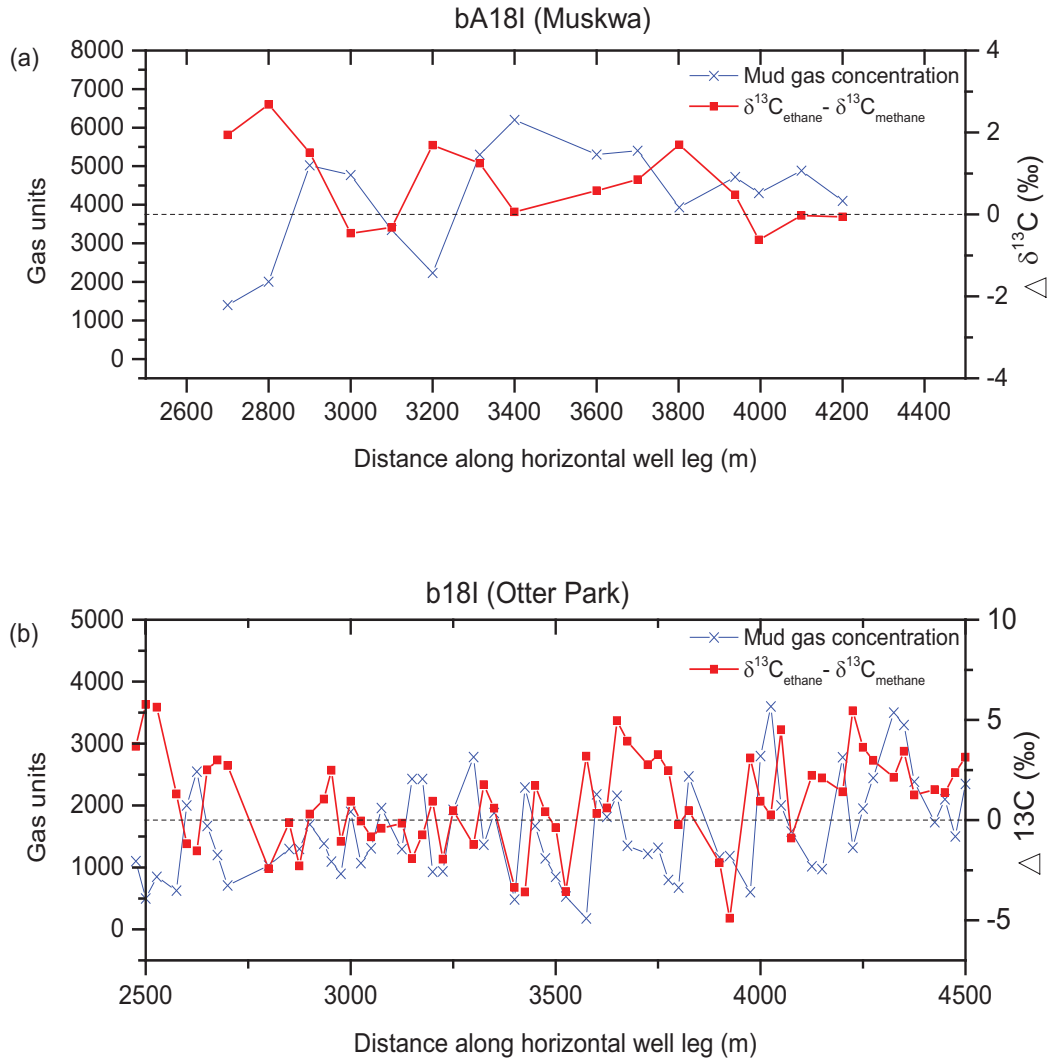


Figure 3.17 (a) Variation in $\delta^{13}C_{\text{ethane}} - \delta^{13}C_{\text{methane}}$ and mud gas concentration for well bA18I (Muskwa Formation) (b) Variation in $\delta^{13}C_{\text{ethane}} - \delta^{13}C_{\text{methane}}$ and mud gas concentration for well b18I (Otter Park Formation).

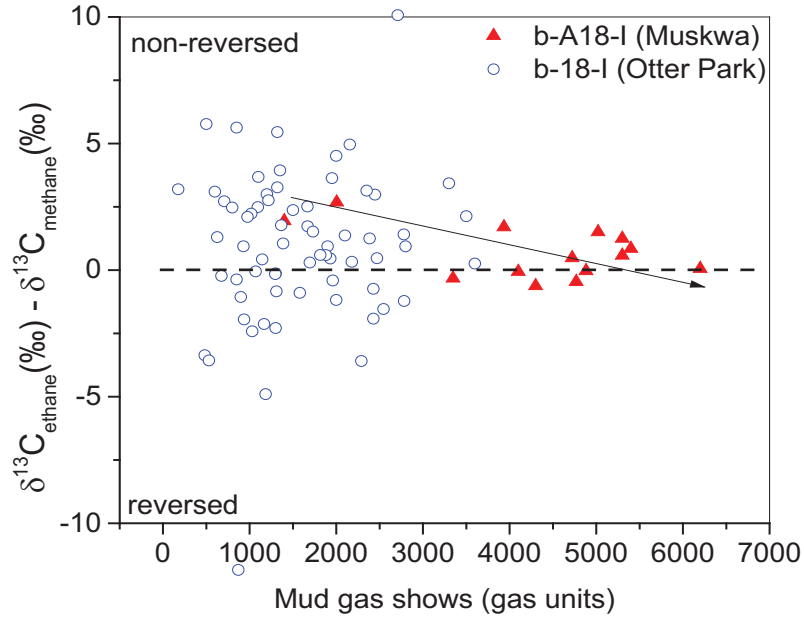


Figure 3.18 Relationship between $\delta^{13}\text{C}_{\text{ethane}} - \delta^{13}\text{C}_{\text{methane}}$ and mud gas concentration for well bA18I (Muskwa Formation) and well b18I (Otter Park Formation).

The $\delta^{13}\text{C}_{\text{ethane}} - \delta^{13}\text{C}_{\text{methane}}$ vs mud gas concentration plot (Fig. 3.18) shows comparison between the Muskwa and Otter Park Formations. In this plot in regions where $\delta^{13}\text{C}_{\text{ethane}} - \delta^{13}\text{C}_{\text{methane}} < 0$, gases have ‘reversed’ isotope signatures and where $\delta^{13}\text{C}_{\text{ethane}} - \delta^{13}\text{C}_{\text{methane}} > 0$, ‘normal’ thermogenic gas signatures are observed. The plot is used to demonstrate if reversed isotope signatures were associated with elevated gas concentration. The Muskwa and the Otter Park both show ‘reversed’ and ‘normal’ gas isotope signatures. In the Muskwa Formation highest gas concentrations occur when $\delta^{13}\text{C}_{\text{ethane}} - \delta^{13}\text{C}_{\text{methane}}$ approaches zero and the arrow shows the change from normal to reversed signature. Interpretation for the Otter Park is more difficult and the high degree of scatter may be expected if there is compartmentalization in the Otter Park (Fig.3.18). In the Muskwa all gases showing isotope reversals have elevated gas concentration.

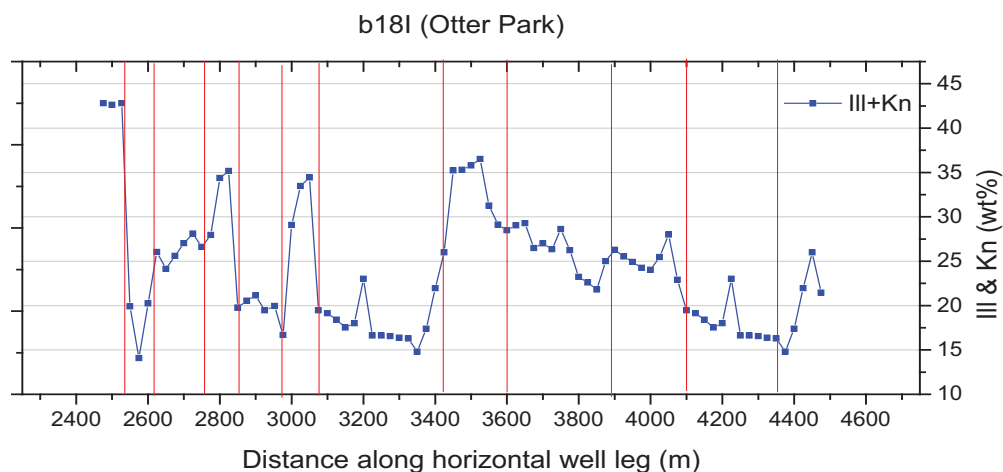


Figure 3.19 Distinct regions are identified where high or low clay content is measured in the shale from laterals of well b18I (Otter Park). The red lines subdivide the length into sections based on the variation in the clay content.

In Fig. 3.19 the variation in clay mineralogy for the Otter Park shale is shown for the lateral of well b18I. Regions of high and low clay content are identified and subdivisions create separate zones used for the isotope/ mud gas concentration cross-plots (Fig. 3.20). In Fig. 3.20 some of the plots show negative correlation between the $\delta^{13}\text{C}_{\text{ethane}} - \delta^{13}\text{C}_{\text{methane}}$ and the mud gas concentration of Otter Park gases. In the majority of instances the $\delta^{13}\text{C}_{\text{ethane}} - \delta^{13}\text{C}_{\text{methane}}$ values decrease the mud gas concentration increases and the anomalies may reflect bias in the intervals selected for zone identification or missed zones not included. The linearity observed in some of the plots (Fig. 3.20) suggests compartmentalization in the Otter Park shale.

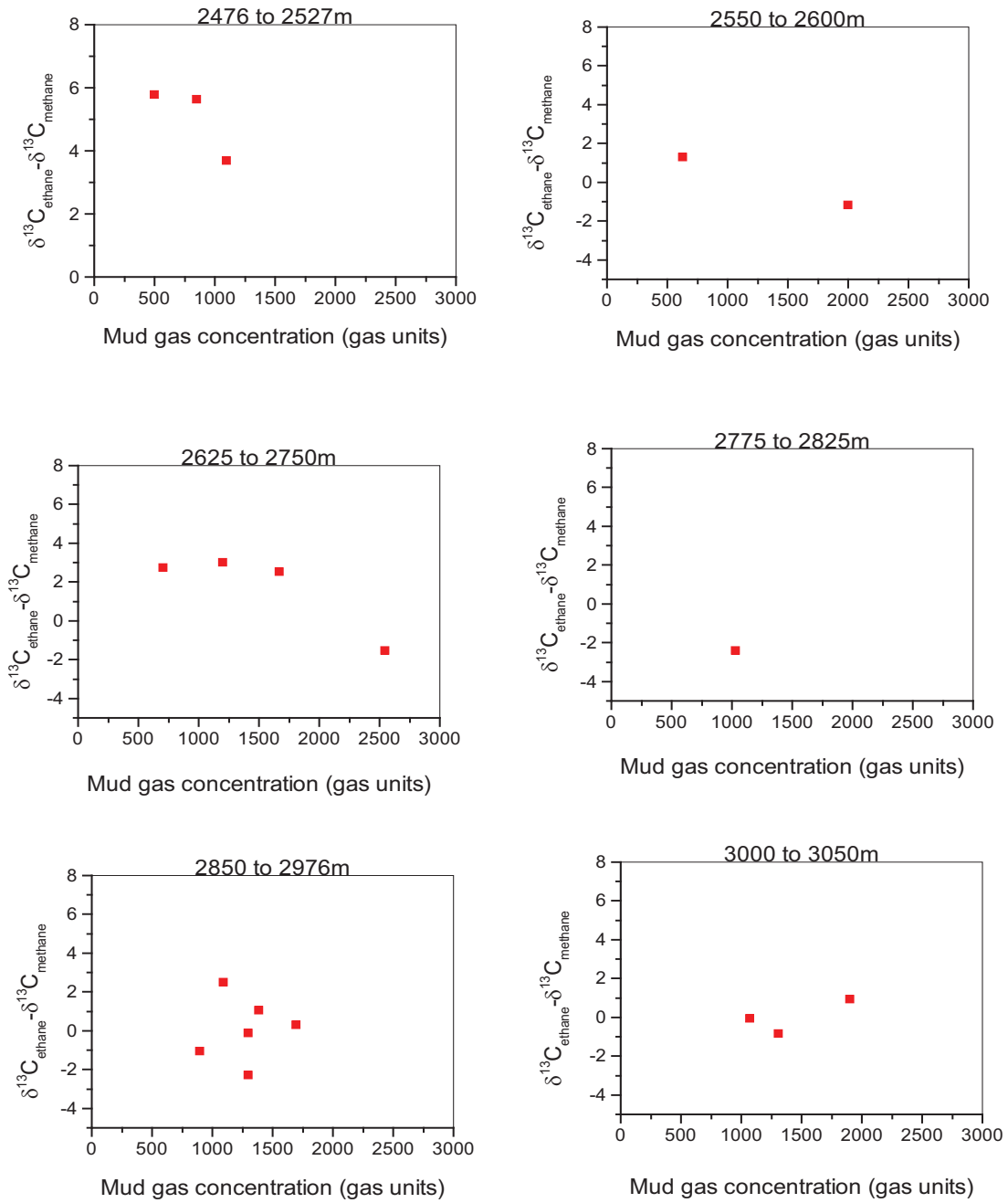
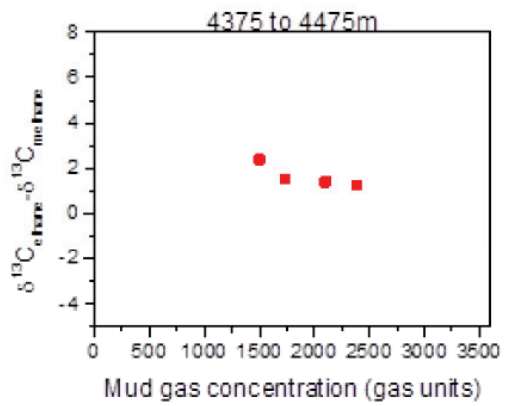
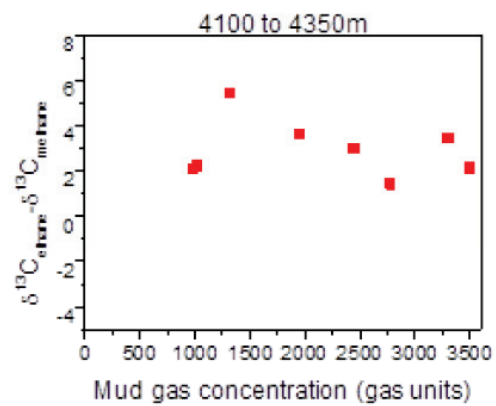
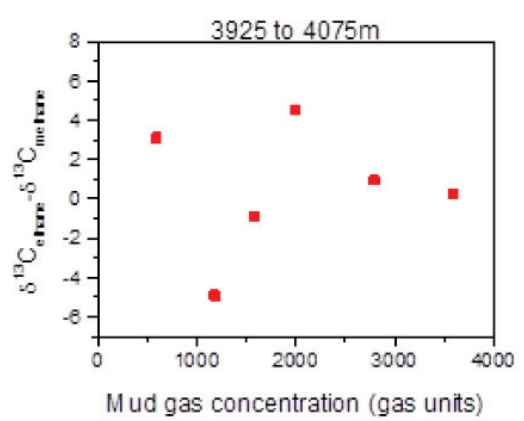
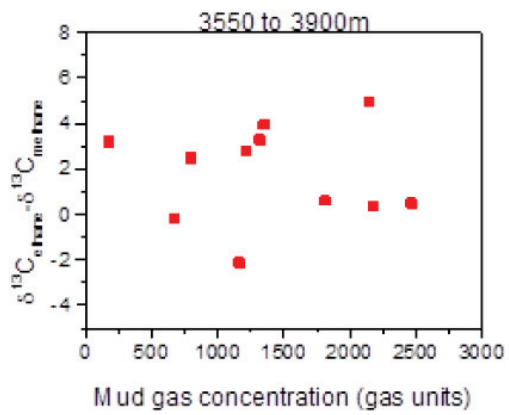
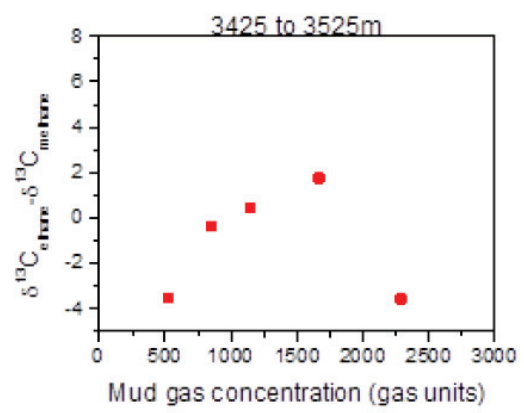
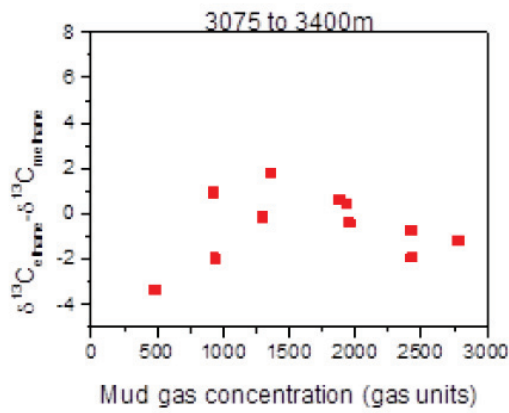


Figure 3.20 Relationship between $\delta^{13}\text{C}_{\text{ethane}} - \delta^{13}\text{C}_{\text{methane}}$ and mud gas concentration for well b18I (Otter Park Formation). Depth intervals based on mineralogy variations in the shale



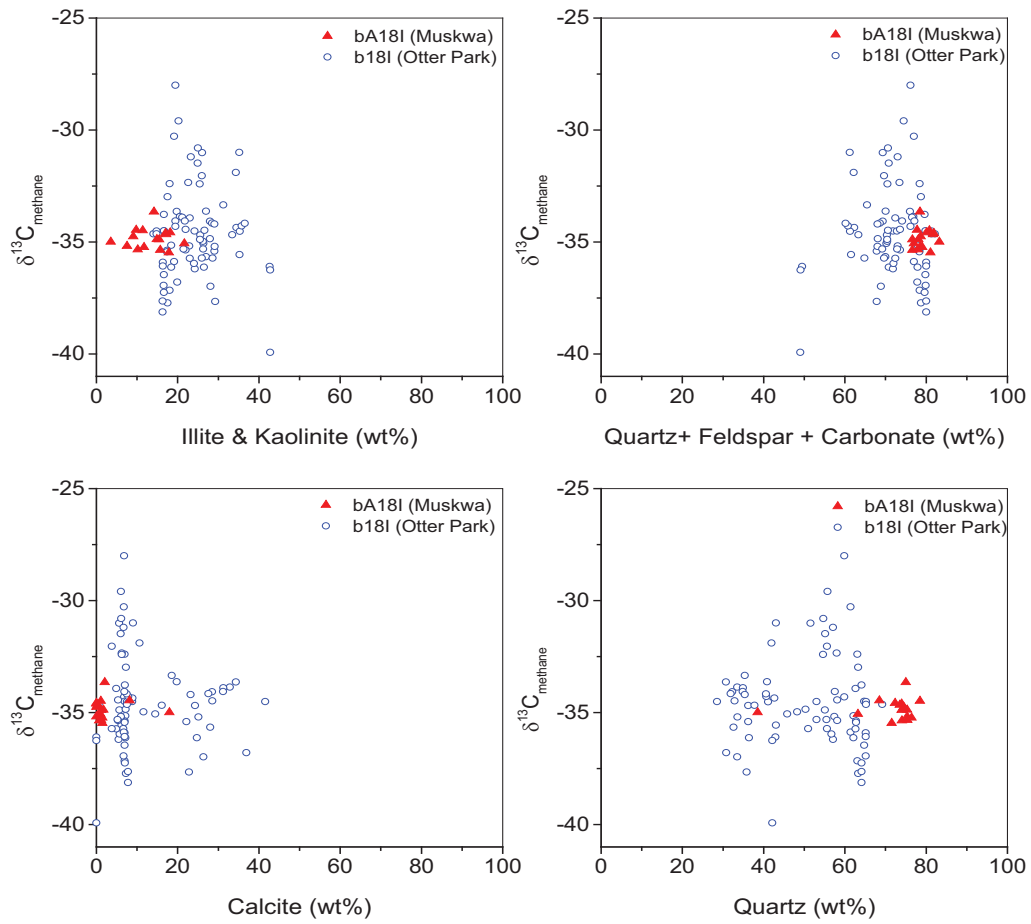


Figure 3.21 Relationship between $\delta^{13}\text{C}_{\text{methane}}$ and mineral composition for well bA18I (Muskwa Formation) and well b18I (Otter Park Formation).

In Fig. 3.21 plots indicate the methane isotope composition in the Otter Park and Muskwa shales and the corresponding major mineral compositions (clays, quartz, calcite and feldspar). $\delta^{13}\text{C}_{\text{ethane}} - \delta^{13}\text{C}_{\text{methane}}$ and mineral composition for shales is shown in Fig. 3.22. In both plots (Fig 3.21 and Fig. 3.22) there is no direct relationship between the mineral composition and the observed isotope ratios.

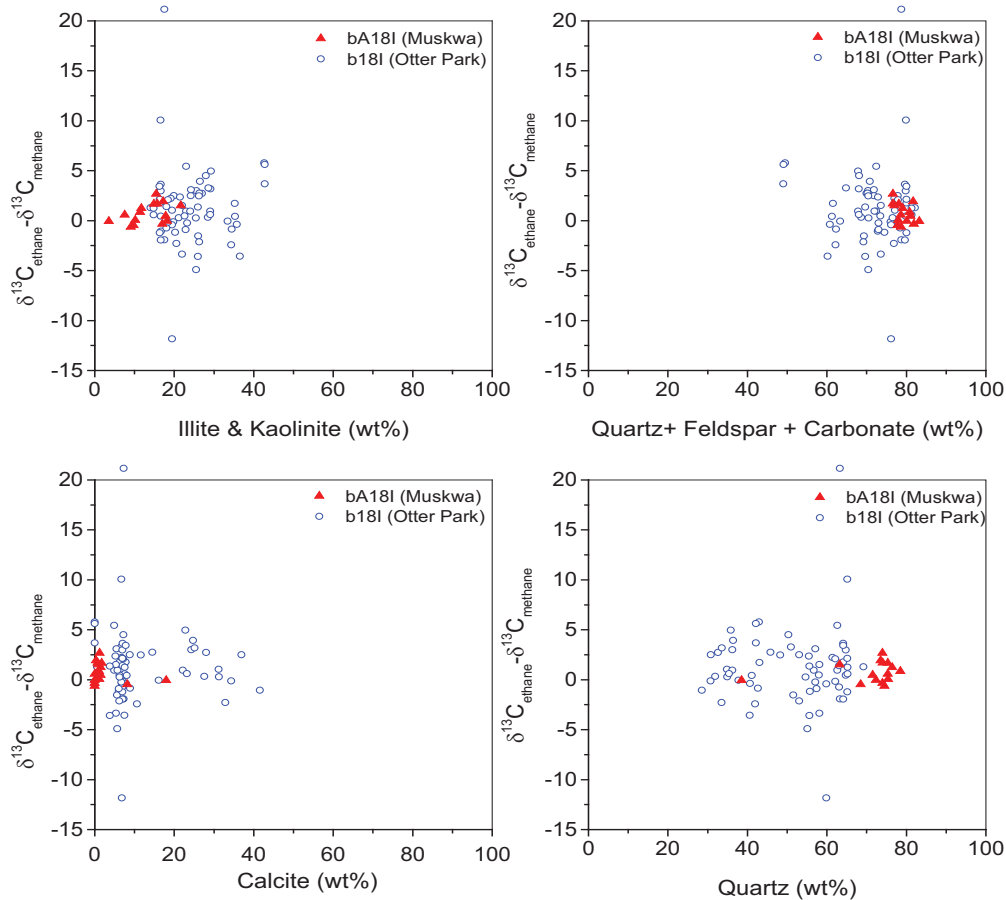


Figure 3.22 Relationship between $\delta^{13}\text{C}_{\text{ethane}} - \delta^{13}\text{C}_{\text{methane}}$ and mineral composition for well bA18I (Muskwa Formation) and well b18I (Otter Park Formation).

3.4 Conclusions

Mud gas isotope profiles along horizontal well paths of the b18I and bA18I wells completed in the Givetian-Frasnian gas shales of the Muskwa and Otter Park Formations document stable isotope variations ($\delta^{13}\text{C}$ and δD) and establish heterogeneity in isotope composition along the wellbores in these Formations. Methane (C1) carbon isotope lateral profiles were more suitable than

ethane (C2) or propane (C3) lateral profiles to determine flow connectivity within gas shales. Carbon isotope data along horizontal well paths suggest greater lateral connectivity in the shales of the Muskwa Formation than in the Otter Park shale. The shale matrix plays an important role in gas diffusivity and influences transport of natural gas during production. Correlation between the $\delta^{13}\text{C}_{\text{methane}}$ and $\delta\text{D}_{\text{methane}}$ of Otter Park gases also suggests gas ‘pockets’ exist in shales of this Formation. Carbon isotope profiles are a useful tool to estimate flow connectivity between pores of gas shales.

Hydrogen isotope composition ($\delta\text{D}_{\text{methane}}$) of mud gases proved to be more useful than carbon isotope composition ($\delta^{13}\text{C}$) for distinguishing gas from the Muskwa from that of the Otter Park Formation (average $\delta\text{D}_{\text{methane}}$ of -159.5‰ and -153.5‰, respectively). Hydrogen isotope ratios (D/H) may be useful in identification of high gas show regions along the well bore since the highest gas concentration (GU) were recorded when the $\delta\text{D}_{\text{methane}}$ values were most negative, though further investigation is necessary.

Carbon and hydrogen isotope values of shale gas and the presence of isotope reversals between gas components suggest an advanced stage of maturity for gases in the Muskwa and Otter Park Formations which is expected in this region in the Horn River Basin. No clear trend was observed between carbon isotope reversals and gas concentration; although in the Muskwa many reversed gases had elevated gas concentration. In both the Otter Park and Muskwa Formations, as ^{13}C and D enrichment occurred, the overall gas concentration decreased suggesting diffusivity differences between isotopologues in gases from these formations. Stable isotope signatures of shale gases can indicate gas origin and thermal maturity useful for evaluation and development of shale gas plays; however additional value may be realized in their use as a proxy for flow connectivity within low permeability gas shale reservoirs.

References Cited

Adams, C., 2012, Summary of Shale Gas Activity in Northeast British Columbia 2011 Oil and Gas Reports 2012-1, BC Ministry of Energy and Mines, Geoscience and Strategic Initiatives Branch.

Aguilera, R., 2013, Flow Units: From Conventional to Tight Gas to Shale Gas to Tight Oil to Shale Oil Reservoirs, SPE Western Regional & AAPG Pacific Section Meeting, 2013 Joint Technical Conference, Apr 19 - 25, 2013 2013, Monterey, CA, USA.

Amann-Hildenbrand, A., A. Ghanizadeh, and B. M. Krooss, 2012, Transport properties of unconventional gas systems, *Marine and Petroleum Geology*, vol. 31, no. 1, p. 90-99.

Ambrose, R., R. Hartman, M. Diaz Campos, I. Y. Akkutlu, and C. Sondergeld, 2010, New pore-scale considerations for shale gas in place calculations, SPE Unconventional Gas Conference, 23-25 February 2010, Pittsburgh, Pennsylvania, USA.

B.C. Ministry of Energy and Mines and National Energy Board, 2011, Ultimate Potential for Unconventional Natural Gas in Northeastern British Columbia's Horn River Basin. Oil and Gas Reports 2011-1, <<http://www.empr.gov.bc.ca/OG/Documents/HornRiverEMA.pdf>> Accessed 10/11, 2013.

British Columbia Oil and Gas Commission, 2012, Investigation of observed seismicity in the Horn River Basin, <<http://www.bcogc.ca/node/8046/download>> Accessed 06/04, 2013.

Berner, U. and E. Faber, 1988, Maturity related mixing model for methane, ethane and propane, based on carbon isotopes, *Organic Geochemistry*, vol. 13, no. 1-3, p. 67-72.

Burruss, R. C. and C. D. Laughrey, 2010, Carbon and hydrogen isotopic reversals in deep basin gas: Evidence for limits to the stability of hydrocarbons, *Organic Geochemistry*, vol. 41, no. 12, p. 1285-1296.

Burruss, R. C. and C. D. Laughrey, 2011, Isotope reversals and rollovers: The last gasp of shale gas?

<http://www.searchanddiscovery.com/abstracts/pdf/2011/hedberg-beijing/abstracts/ndx_burruss.pdf> Accessed 09/13, 2013.

Chalmers, G. R., D. J. Ross, and R. M. Bustin, 2012, Geological controls on matrix permeability of Devonian Gas Shales in the Horn River and Liard basins, northeastern British Columbia, Canada, *International Journal of Coal Geology*, vol. 103, p. 120-131.

Chung, H. M., J. R. Gormly, and R. M. Squires, 1988, Origin of gaseous hydrocarbons in subsurface environments: Theoretical considerations of carbon isotope distribution, *Chemical Geology*, vol. 71, no. 1-3, p. 97-104.

Clayton, C., 1991, Carbon isotope fractionation during natural gas generation from kerogen, *Marine and Petroleum Geology*, vol. 8, no. 2, p. 232-240.

Coleman, M. L., T. J. Shepherd, J. J. Durham, J. E. Rouse, and G. R. Moore, 1982, Reduction of water with zinc for hydrogen isotope analysis, *Analytical Chemistry*, vol. 54, no. 6, p. 993-995.

Corlett, H. and B. Jones, 2011, The influence of paleogeography in epicontinental seas: A case study based on Middle Devonian strata from the MacKenzie Basin, Northwest Territories, Canada, *Sedimentary Geology*, vol. 239, no. 3-4, p. 199-216.

Curtis, M., R. Ambrose, C. Sondergeld, and C. Sondergeld, 2010, Structural characterization of gas shales on the micro-and nano-scales, *Canadian*

Unconventional Resources and International Petroleum Conference, 19-21 October 2010, Calgary, Alberta, Canada.

Curtis, J. B., 2002, Fractured Shale-Gas Systems, AAPG Bulletin, vol. 86, no. 11, p. 1921-1938.

Dawson, D. and A. Murray, 2011, Applications of Mud Gas Isotope Logging in Petroleum Systems Analysis,

http://www.searchanddiscovery.com/abstracts/pdf/2011/hedberg-beijing/abstracts/ndx_dawson.pdf Accessed 10/01, 2013.

Dong, T. and N. Harris, 2012, Porosity and Pore Sizes in the Horn River Shales,

https://docs.google.com/viewer?a=v&q=cache:bxCSVjGXi2gJ:www.empr.gov.bc.ca/OG/oilandgas/petroleumgeology/UnconventionalGas/Documents/N%2520Harris.pdf+otter+park,+mukswa,+harris&hl=en&gl=ca&pid=bl&srcid=ADGEESgRYliGiaqTy7MdvSBrdar6afQXqASw0wOa-FaI_yENUQfAU6IBbKKBv6gTJCJhm88m0yVI29TAxjOvTfzpbY55mcQRXRbh-LPMDwXGG6NqSJEEnECxMkdoL4-N_r6mV4_g6I5Tp&sig=AHIEtbRIOyNJ2CIFNLK8KBaAWcRCnFiNgw

Accessed 09/11, 2013.

Ellis, L., A. Brown, M. Schoell, and S. Uchytel, 2003, Mud gas isotope logging (MGIL) assists in oil and gas drilling operation, The Oil and Gas Journal, vol. 101, no. 21, p. 32(8).

Elshahawi, H., O. C. Mullins, M. Hows, S. Colacelli, M. Flannery, J. Zuo, and C. Dong, 2010, Reservoir fluid analysis as a proxy for connectivity in deepwater reservoirs, Petrophysics, vol. 51, no. 2.

Fuex, A. N., 1977, The use of stable carbon isotopes in hydrocarbon exploration, Journal of Geochemical Exploration, vol. 7, p. 155-188.

Glorioso, J. C. and A. J. Rattia, 2012, Unconventional Reservoirs: Basic Petrophysical Concepts for Shale Gas, SPE/EAGE European Unconventional Resources Conference and Exhibition, 20-22 March 2012, Vienna, Austria.

Gray, F. F. and J. Kassube, 1963, Geology and stratigraphy of Clarke Lake gas field, British Columbia, AAPG Bulletin, vol. 47, no. 3, p. 467-483.

Harris, N. B. and T. Dong, 2013, Characterizing porosity in the Horn River shale, northeastern British Columbia,
<http://www.empr.gov.bc.ca/OG/oilandgas/petroleumgeology/Geoscience_Publications/Geoscience%20Reports%202013%20Web.pdf> Accessed 09/13, 2013.

Hu, Q., Z. Gao, S. Peng, and R. Ewing, 2012, Pore Structure Inhibits Gas Diffusion in the Barnett Shale,
<http://www.searchanddiscovery.netwww.searchanddiscovery.net/documents/2012/50609hu/ndx_hu.pdf> Accessed 09/11, 2012.

James, A. T., 1983, Correlation of natural gas by use of carbon isotopic distribution between hydrocarbon components, AAPG Bulletin, vol. 67, no. 7, p. 1176-1191.

Javadpour, F., D. Fisher, and M. Unsworth, 2007, Nanoscale gas flow in shale gas sediments, Journal of Canadian Petroleum Technology, vol. 46, no. 10, p. 55-61.

Jenden, P. D., D. J. Drazan, and I. R. Kaplan, 1993, Mixing of thermogenic natural gases in northern Appalachian Basin, AAPG Bulletin, vol. 77, no. 6, p. 980-998.

Morrow, D. W., M. Zhao, and L. D. Stasiuk, 2002, The Gas-Bearing Devonian Presqu'ile Dolomite of the Cordova Embayment Region of British Columbia, Canada: Dolomitization and the Stratigraphic Template, AAPG Bulletin, vol. 86, no. 9, p. 1609-1638.

- Ness, S., R. Benteau, and S. Leggitt, 2010, Horn River Shales ...Boring and Black? ...or...Beautifully Complex?
<http://cseg.ca/assets/files/resources/abstracts/2010/core/1069_GC2010_Horn_River_Shales.pdf> Accessed 09/11, 2013.
- Ni, Y., J. Dai, X. Yang, Y. Tang, Y. Jin, and J. Chen, 2009, Kinetic modeling of post-mature gas generation: Constraints from high-pressure thermal-cracking of nC₂₄, *Geochimica et Cosmochimica Acta*, vol. 73, no. 13 supplement 1, p. A940.
- Norville, G. A. and R. A. Dawe, 2007, Carbon and hydrogen isotopic variations of natural gases in the southeast Columbus basin offshore southeastern Trinidad, West Indies – clues to origin and maturity, *Applied Geochemistry*, vol. 22, no. 9, p. 2086-2094.
- Oldale, H. and R. Munday, 1994, Devonian Beaverhill Lake Group of the western Canada sedimentary basin, *Geological Atlas of the Western Canada Sedimentary Basin*, p. 149-164.
- Passey, Q. R., K. Bohacs, W. L. Esch, R. Klimentidis, and S. Sinha, 2010, From oil-prone source rock to gas-producing shale reservoir—geologic and petrophysical characterization of unconventional shale-gas reservoirs, SPE-131350, CPS/SPE International Oil & Gas Conference and Exhibition in China (2010) June 8–10, 2010, Beijing, China
- Pedentchouk, N., K. H. Freeman, and N. B. Harris, 2006, Different response of δD values of n-alkanes, isoprenoids, and kerogen during thermal maturation, *Geochimica et Cosmochimica Acta*, vol. 70, no. 8, p. 2063-2072.
- Pelzer, E. E., 1966, Mineralogy, geochemistry, and stratigraphy of Besa River Shale, British Columbia, *Bulletin of Canadian Petroleum Geology*, vol. 14, no. 2, p. 273-321.

Prinzhofer, A. A. and A. Y. Huc, 1995, Genetic and post-genetic molecular and isotopic fractionations in natural gases, *Chemical Geology*, vol. 126, no. 3-4, p. 281-290.

Reynolds, M. M. and D. L. Munn, 2010, Development Update for an Emerging Shale Gas Giant Field - Horn River Basin, British Columbia, Canada, .

Rodriguez, N. D. and R. P. Philp, 2010, Geochemical characterization of gases from the Mississippian Barnett Shale, Fort Worth Basin, Texas, *AAPG Bulletin*, vol. 94, no. 11, p. 1641-1656.

Root, K. G., 2001, Devonian Antler fold and thrust belt and foreland basin development in the southern Canadian Cordillera: implications for the Western Canada Sedimentary Basin, *Bulletin of Canadian Petroleum Geology*, vol. 49, no. 1, p. 7-36.

Ross, D. J. K. and R. M. Bustin, 2008, Characterizing the shale gas resource potential of Devonian Mississippian strata in the Western Canada sedimentary basin: Application of an integrated formation evaluation, *AAPG Bulletin*, vol. 92, no. 1, p. 87-125.

Rowe, D. and A. Muehlenbachs, 1999a, Low-temperature thermal generation of hydrocarbon gases in shallow shales, *Nature*, vol. 398, no. 6722, p. 61-63.

Rowe, D. and K. Muehlenbachs, 1999b, Isotopic fingerprints of shallow gases in the Western Canadian sedimentary basin: tools for remediation of leaking heavy oil wells, *Organic Geochemistry*, vol. 30, no. 8, Part 1, p. 861-871.

Schoell, M., 1983, Genetic characterization of natural gases, *AAPG Bulletin*, vol. 67, no. 12, p. 2225-2238.

Schoell, M., 1988, Multiple origins of methane in the Earth, *Chemical Geology*, vol. 71, no. 1-3, p. 1-10.

- Sondergeld, C., R. Ambrose, C. Rai, and J. Moncrieff, 2010, Micro-Structural Studies of Gas Shales. Paper SPE 131771 presented at the SPE Unconventional Gas Conference, Pittsburg, Pennsylvania, USA, 23–25 February 2010.
- Stahl, W., 1974, Carbon isotope fractionations in natural gases, *Nature*, vol. 251, no. 5471, p. 134-135.
- Stasiuk, L. D. and M. G. Fowler, 2004, Organic facies in Devonian and Mississippian strata of Western Canada Sedimentary Basin: relation to kerogen type, paleoenvironment, and paleogeography, *Bulletin of Canadian Petroleum Geology*, vol. 52, no. 3, p. 234-255.
- Tilley, B. and K. Muehlenbachs, 2007, Isotopically Determined Mannville Group Gas Families, *Let it Flow: CSPG/CSEG 2007 Convention, Abstracts Volume*, p. 67-69.
- Tilley, B. and K. Muehlenbachs, 2012, Isotope Systematics of High Maturity Shale Gases in the WCSB Compared to Other North American Shale Gases, http://www.cspg.org/documents/Conventions/Archives/Annual/2012/026_GC2012_Isotope_Systematics_of_High_Maturity_Shale_Gases.pdf Accessed 09/11, 2013.
- Tilley, B. J., K. Muehlenbachs, and B. J. Szatkowski, 2001, Compartmentalization of Gas Reservoirs: Insights From Carbon Isotope Ratios, <http://www.cspg.org/documents/Conventions/Archives/Annual/2001/14-102.pdf> Accessed 09/11, 2013.
- Tilley, B. and K. Muehlenbachs, 2006, Gas maturity and alteration systematics across the Western Canada Sedimentary Basin from four mud gas isotope depth profiles, *Organic Geochemistry*, vol. 37, no. 12, p. 1857-1868.
- Tilley, B., S. McLellan, S. Hiebert, B. Quintero, B. Veilleux, and K. Muehlenbachs, 2011, Gas isotope reversals in fractured gas reservoirs of the

western Canadian Foothills: Mature shale gases in disguise, AAPG Bulletin, vol. 95, no. 8, p. 1399-1422.

Tilley, B. and K. Muehlenbachs, 2013, Isotope reversals and universal stages and trends of gas maturation in sealed, self-contained petroleum systems, *Chemical Geology*, vol. 339, p. 194-204.

Wang, F. P. and R. M. Reed, 2009, Pore Networks and Fluid Flow in Gas Shales, *SPWPE Annual Technical Conference and Exhibition*, 4-7 October 2009, New Orleans, Louisiana, 2009, Society of Petroleum Engineers, New Orleans, Louisiana.

Weissenberger, J. A. W. and K. Potma, 2001, The Devonian of western Canada -- aspects of a petroleum system: Introduction, *Bulletin of Canadian Petroleum Geology*, vol. 49, no. 1, p. 1-6.

Wilhelms, A., E. Rein, C. Zwach, and A. S. Steen, 2001, Application and implication of horizontal well geochemistry, *Petroleum Geoscience*, vol. 7, no. 1, p. 75-79.

Williams, G. K., 1983, What does the term 'Horn River Formation' mean? *Bulletin of Canadian Petroleum Geology*, vol. 31, no. 2, p. 117-122.

Zumberge, J., K. Ferworn, and J. Curtis, 2009, Gas character anomalies found in highly productive shale gas wells, *Geochimica et Cosmochimica Acta Supplement*, vol. 73, p. A1539.

Zumberge, J., K. Ferworn, and S. Brown, 2012, Isotopic reversal ('rollover') in shale gases produced from the Mississippian Barnett and Fayetteville formations, *Marine and Petroleum Geology*, vol. 31, no. 1, p. 43-52.

CHAPTER 4

UNDERSTANDING TEMPORAL TRENDS IN CARBON ISOTOPE RATIOS DURING DEVONIAN SHALE GAS PRODUCTION

4.1 Introduction

Compositional changes in geofluids occur over time during hydrocarbon production as fluids travel from pores and fractures in formations to the wellbore and the reservoir is depleted. Variations in fluid composition in conventional reservoirs usually reflect phase changes concomitant with pressure decline during production (Gray and Dawe, 1991; Danesh, 1998; Freeman et al., 2012; Blasingame et al., 2013). Stable isotope geochemistry is routinely employed for analysis of these reservoir fluids and geochemical techniques used for characterization of natural gas and evaluation of hydrocarbon reservoirs (Fuex, 1977; Schoell, 1980; Rice and Claypool, 1981; Claypool and Kvenvolden, 1983; James, 1983; Schoell, 1983; Berner and Faber, 1988; Chung et al., 1988; Schoell, 1988; James, 1990; Clayton, 1991; Jenden et al., 1993; Prinzhofer and Huc, 1995; Rowe and Muehlenbachs, 1999a; Rowe and Muehlenbachs, 1999b; Norville and Dawe, 2007) and others. Chemical composition and stable isotope ratios indicate natural gas origin, thermal maturity and reservoir compartmentalization; however few studies evaluate temporal changes in fluid composition which may occur as natural gas is produced from complex unconventional shale gas reservoirs.

Commercial production of natural gas from shale provides new challenges due to ultra-low porosity and permeability which extends to the nano-scale and impacts gas flow from the reservoir (Soeder, 1988; Javadpour et al., 2007; Wang and Reed, 2009; Javadpour, 2009; Loucks et al., 2009; Nelson, 2009; Sondergeld et al., 2010; Ambrose et al., 2010; Curtis et al., 2010; Bustin and Bustin, 2012). Unconventional gas shales require stimulation for economic gas production and multi-stage hydraulic fracturing is used to create permeable pathways for gas transport. Production decline curves are commonly used in evaluation of shale gas well performance and employed during production forecasts and calculation of

OGIP (original gas in place). Gas transport through pores and fractures of the shale may alter the fluid composition of produced shale gas and the profiles of production decline curves. In this study chemical and stable isotope compositional changes during gas production from Devonian shale gas wells in the Horn River Basin, northeast British Columbia (Fig. 4.1) are evaluated.

Givetian-Frasnian Horn River Group shales are organic-rich, thermally mature and key targets for shale gas production in the Horn River Basin (Adams, 2012); however chemical and stable isotope changes in gases during production are currently unknown. The study location is within the Dilly Creek area, north of Ft. Nelson (NTS map sheet 094O/8). Produced gas samples were obtained from eight hydraulically fractured horizontal wells completed in Muskwa, Otter Park and Evie Formations (Fig.4.2). Shale permeability of Devonian Horn River Group Formations in this region of the Basin ranges from approximately 150 to 450 nano-darcy (Nexen Corporate Update, 2011).

In Chapter 3 the spatial stable isotope subsurface variations prior to hydraulic fracturing for the Muskwa and Otter Park Formations are documented for wells b18I and bA18I using lateral isotope depth profiles. In this study the objective is to create time series for Devonian shale gas wells (after hydraulic fracturing and completion when the well is put on production) to determine chemical and stable isotope compositional changes in hydrocarbons components (methane, ethane and propane) at various stages of shale gas production. Temporal changes in carbon isotope values of methane ($\delta^{13}\text{C}_{\text{methane}}$), ethane ($\delta^{13}\text{C}_{\text{ethane}}$) and propane ($\delta^{13}\text{C}_{\text{propane}}$) and chemical composition of methane (mol fraction) will be evaluated in conjunction with gas production data and completion designs for these wells. General trends among shale gas wells in the Horn River Group as well as any correlation between gas production rate and gas composition is investigated. Knowledge gained may be useful to provide insight into gas transport, predict which wells are good producers and assist in development of the shale play.

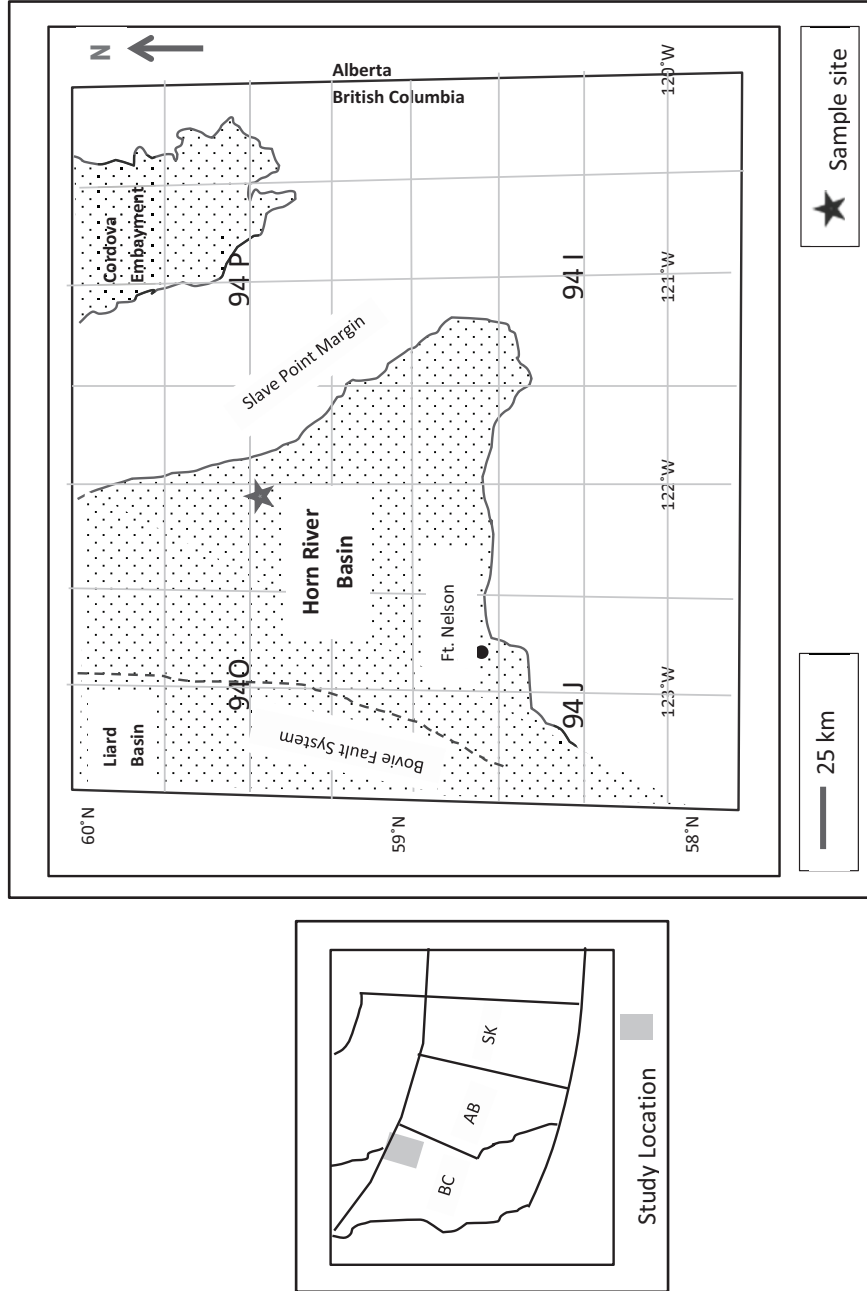


Figure 4.1 Location map showing the study area in the Horn River Basin, NE British Columbia (modified from Oldale and Mundav, 1994).

4.1.1 The Horn River Basin

The Horn River Basin, northeast British Columbia is a major unconventional shale gas play in Canada with estimated natural gas reserves up to 1000 trillion cubic feet (TCF) (Ross and Bustin, 2008; Reynolds and Munn, 2010; Adams, 2012). The Basin is located in northeast British Columbia, north of Fort Nelson and covers an area of over 1.3 million hectares (Close et al., 2012). The Givetian-Frasnian Horn River Group includes the Muskwa, Otter Park and Evie Formations which is overlain by the Fort Simpson shale (Williams, 1983; Oldale and Munday, 1994). Devonian shallow marine Horn River Group shales were deposited in a passive margin setting during periods of transgression in the Basin (Weissenberger and Potma, 2001; Morrow et al., 2002; Corlett and Jones, 2011). Horn River Group shale thickness in the Dilly Creek region is approximately 175m.

4.1.2 Gas flow mechanisms in shale

Complex pore networks in sedimentary shale rocks create tortuous pathways for flow of fluids to the wellbore during production and affects shale gas deliverability. Pore sizes in shales may be in the order of nanometers in ultra-low permeability shale formations. In shale gas reservoirs the gas is usually classified into free gas, adsorbed gas and solution gas (Curtis, 2002; Ramos, 2004; Montgomery et al., 2005; Ambrose et al., 2010).

Typical production decline curves in shale gas reservoirs show a steep initial decline in gas production rate which slows and becomes more uniform over time. Produced gas likely reflects a varying admixture of these components over time. In the initial stages of production the gas in fractures, commonly termed 'free gas' in the literature, may flow to the wellbore provided fractures are interconnected. At later stages of production an increase in desorbed gas fraction may be expected as gas is transferred from pores in the shale matrix to the fracture system during production. It is likely classification of shale gas into these strict categories may not reflect intrinsic compositional differences in natural gas but

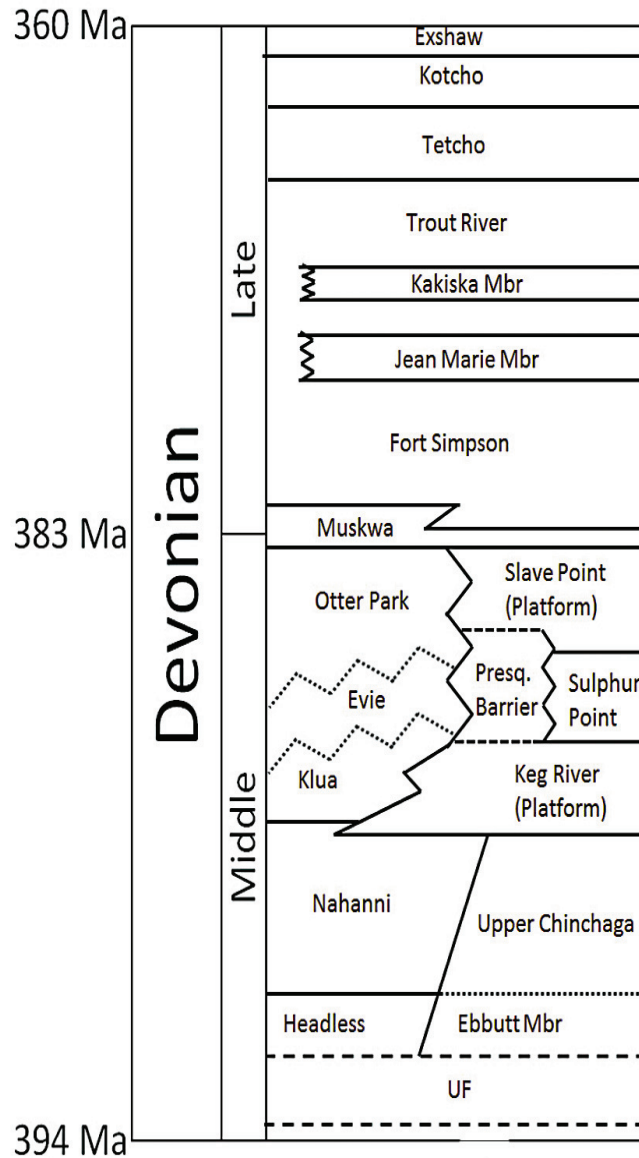


Figure 4.2 Stratigraphy of the Devonian NE British Columbia in the Horn River Basin area (after Close et al., 2012).

instead spatial differences dependent on the location of gas within the shale. In gas recovery from shale desorbed gas moves from the matrix and enters the fracture system for production. Gas transport in nanoporous shales differs from that in conventional hydrocarbon reservoirs and flow mechanisms are not fully understood at present (Javadpour et al., 2007; Javadpour, 2009; Wang and Reed,

2009; Moridis et al., 2010; Akkutlu and Fathi, 2012; Amann-Hildenbrand et al., 2012; Freeman et al., 2012; Hu et al., 2012; Liang et al., 2012; Freeman et al., 2013; Wei et al., 2013; Aguilera, 2013).

4.1.3 Chemical and Isotope composition of shale gas

Devonian shales in the Horn River Basin contain dry thermogenic gases (Chapter 2 and Chapter 3) and the true vertical depths (TVD) for Horn River wells in this region are approximately 2.5 km. The source organic matter and generation processes are factors which influence the carbon isotope signatures of shale gas in the reservoir. In unconventional shale gas plays, gas transport processes which occur as natural gas moves from the reservoir to the wellbore during production may cause carbon isotope fractionation which alters the isotope signature of in situ shale gas. Diffusion and desorption processes through shale may change the carbon isotope signature of natural gas (Zhang and Krooss, 2001; Xia and Tang, 2012). Isotope signatures of produced gases may be different from those of in situ natural gas within the reservoir. Theoretical models predict changes in carbon isotope composition during production from shales (Tang and Xia, 2011; Xia and Tang, 2012). In early phases of production ^{12}C enrichment should be expected due to the diffusivity differences between $^{12}\text{CH}_4$ and $^{13}\text{CH}_4$ molecules.

Stable isotope signature of thermogenic natural gases generally show a characteristic signature where $\delta^{13}\text{C}_{\text{methane}} < \delta^{13}\text{C}_{\text{ethane}} < \delta^{13}\text{C}_{\text{propane}}$, however in many shale gas plays worldwide isotope reversals occur between gas components (Zumberge et al., 2009; Burruss and Laughrey, 2010; Rodriguez and Philp, 2010; Tilley et al., 2011; Burruss and Laughrey, 2011; Tilley and Muehlenbachs, 2012; Zumberge et al., 2012).

4.2 Methods

One hundred and seventy two production gas samples were obtained from eight Devonian shale gas wells in the Horn River Basin. Horizontal legs of wells are approximately 2km in length and completion design information including number and spacing of perforation clusters and the number of fracture stages is shown in Table 4.2. Production gases were sampled in duplicate for compositional analysis and collected as time series in 1L steel containers at the well heads. Shale gas wells were located in Township 94, including 2 multi-well pads. Targets for these wells include the Devonian Muskwa, Otter Park and Evie Formations (Figure 4.2). Wells 1 to 3 (a16I, aC16I and aE16I) were located at well pad a16I and Well 4 (c16I) was also located near well pad a16I. Wells 5 and HR 6 (b93A and c93A respectively) were closely spaced and located roughly 12 km southeast of well pad a16I. Wells 7 and 8 (c1J and dA1J respectively) were located on Well Pad c1J approximately 2 km west of Well pad a16I. Wells 1 to 6 (a16I, aC16I, aE16I, c16I, b93A, c93A) were sampled monthly over a time period of 12 months then re-sampled at pre-determined time intervals up to ~36 months into production. Wells 7 and 8 (c1J and dA1J) were sampled daily over a time periods of ~25 days and 50 days.

The chemical compositions of methane (C1 Mole fraction) from produced gas samples were determined using gas chromatography at a commercial laboratory. Carbon isotope compositions of methane ($\delta^{13}\text{C}_{\text{methane}}$), ethane ($\delta^{13}\text{C}_{\text{ethane}}$) and propane ($\delta^{13}\text{C}_{\text{propane}}$) of shale gases were measured in triplicate at the University of Alberta Stable Isotope Laboratory using gas chromatography-combustion –continuous flow isotope ratio mass spectrometry (GC-C CF- IRMS). A Finnigan Mat 252 mass spectrometer was used for stable isotope analysis and the reference gas was calibrated to the Vienna Pee Dee Belemnite (VPDB) scale using NBS-18 and NBS-19 standards. Carbon isotope compositions were reported in per mil using standard δ notation relative to the VPDB standard. The reproducibility for methane, ethane and propane were ± 0.1 , ± 0.2 and ± 0.8 respectively.

Table 4.1 Shale gas target formations for Horn River Group Wells 1 to 8

Well#	Well	Well Authorization	Well pad	Target Formation
1	a16I	024773	1	Muskwa C
2	aC16I	025127	1	Evie A/B
3	aE16I	025174	1	Muskwa to Otter Park C
4	c16I	027360	1	Muskwa C
5	b93A	024219	2	Muskwa
6	c93A	024220	2	Muskwa
7	c1J	026026	3	Muskwa C
8	dA1J	026765	3	Evie

Table 4.2 Perforation and fracture treatment for Horn River Group Wells 1 to 8
(Horizontal well length~2km)

Well#	Well	Well Authorization	Well pad	Target Formation
1	a16I	024773	1	Muskwa C
2	aC16I	025127	1	Evie A/B
3	aE16I	025174	1	Muskwa to Otter Park C
4	c16I	027360	1	Muskwa C
5	b93A	024219	2	Muskwa
6	c93A	024220	2	Muskwa
7	c1J	026026	3	Muskwa C
8	dA1J	026765	3	Evie

4.3 Results and Discussion

Gases from Devonian shales in the Horn River Basin show variation in chemical composition and carbon isotope ratios ($\delta^{13}\text{C}$) of gas components even among wells completed in the same formation and drilled from a single well pad.

Shale gas wells undergo stimulation prior to gas production in which holes are punched (perforation clusters) to allow connection to the reservoir and multi-stage hydraulic fracturing is performed in a number of stages (Table 4.2). Production decline curves for shale gas wells 1 to 8 shown in Figs. 4.3a to 4.3c indicate changes in gas rate over time. Long term production decline curves (Fig. 4.3a) show gas production rates for 6 wells (a16I, aC16I, aE16I, c16I, b93A and c93A) monitored for time periods up to approximately 3 years. Initial decline rates in gas production are steep for time periods of up to approximately 250 days before more steady gas production rates are observed for these wells. It is evident that these 6 wells show variations in the production rates especially in the early phases of production (~250 days). Wells 1 to 4 were located at well pad 1 and target formations for these wells are shown in Table 4.1. Wells 7 (c1J) and 8 (dA1J) are completed in the Muskwa and Evie Formations respectively; Fig. 4.3b shows short term gas production curves for these wells. In Fig 4.3c superpositioning of production decline curves of all wells show dissimilarity in gas production rate between Wells 1 to 6 and Wells 7, 8. Overall higher gas production rates in well 7 and 8 may be attributed to differences in well completion design for wells at well pad 3 (Table 4.2).

Produced shale gases from the Muskwa and Evie Formations differ in the concentration of methane (C1) (Fig. 4.4). The chemical composition of gas components (C1, C2, C3, CO₂ and N₂) from these wells are presented in Appendix A. Wells 2 and 8 are completed in the Evie shale while the remainder of wells produce gas from the Muskwa formation, with the exception of well 3 in which both Muskwa and Otter Park Formations are targeted for production (Table 4.1). In Muskwa gases the concentration of methane is approximately 90% while Evie gases are less dry and the percentage of methane ranges between 80 and 85%. The chemical compositions of shale gases from these wells are presented in Appendix A.

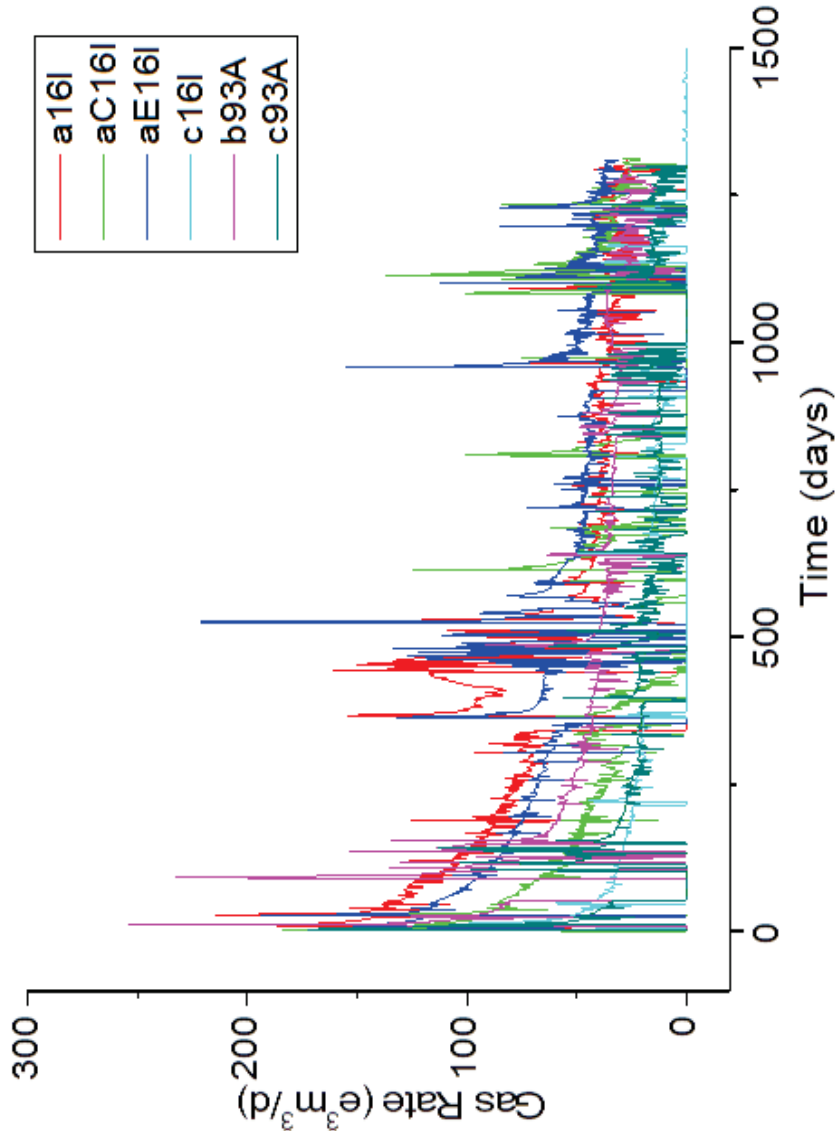


Figure 4.3(a) Horn River Basin production decline curves for Wells 1 to 6 showing long term fluctuations in gas rate ~1250days.

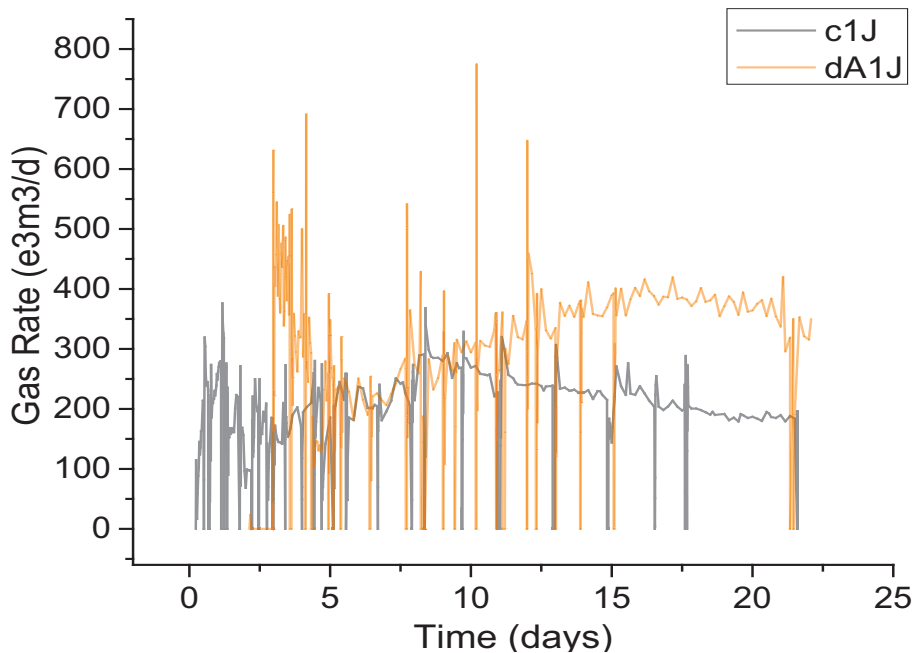


Figure 4.3(b) Horn River Basin production decline curves for Wells 7 and Well 8 wells showing short term fluctuations in gas rate ~20days.

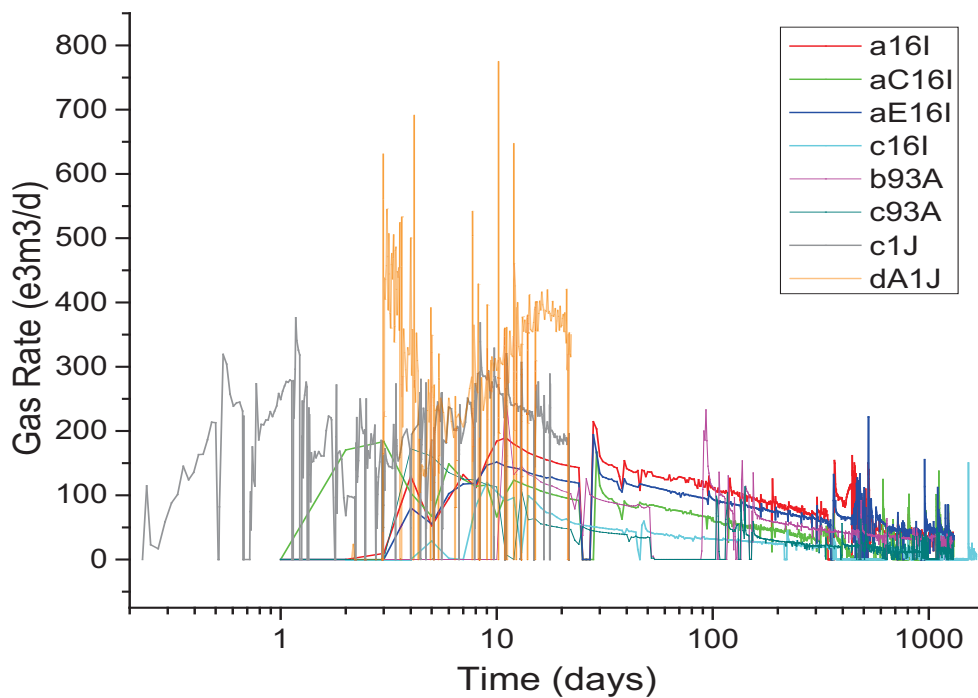


Figure 4.3(c) Gas production decline curves for Horn River Group shale gases from Wells 1 to 8 shown on a logarithmic time scale.

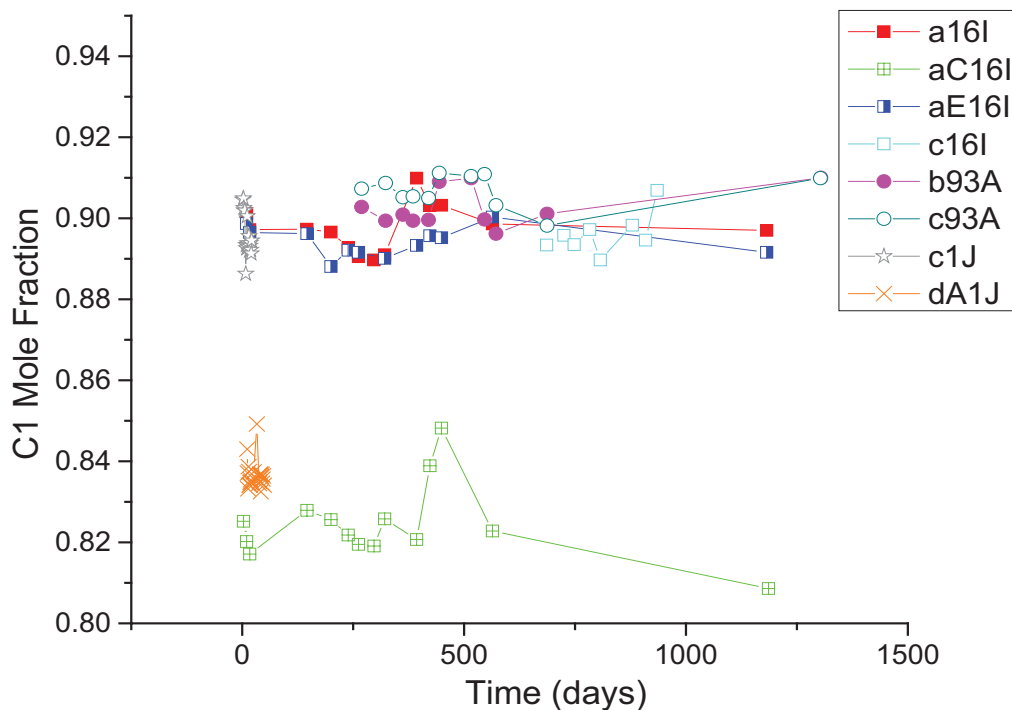


Figure 4.4 Variation in methane concentration (mole fraction) for Horn River Group shale gases from Wells 1 to 8.

Time series show long term variations in the carbon isotope ratios of methane ($\delta^{13}\text{C}_{\text{methane}}$) for wells 1 to 6 (Fig. 4.5). It is evident large fluctuations in $\delta^{13}\text{C}_{\text{methane}}$ values of natural gases occur during production from these six Horn River Group shale gas wells. Over the time period of approximately three years the stable carbon isotope ratios of methane varied up to $\sim 8\%$. Gases from wells 1 to 3 (a16I, aC16I and aE16I) were sampled in the early phase of production. These early gases show $\delta^{13}\text{C}_{\text{methane}}$ only ranging from approximately -35% to -36% . During initial gas production a larger fraction of the ‘free gas’ component is released after hydraulic fracturing which creates permeability pathways in shale. The enrichment in ^{12}C in shale gases observed during early stages of production may be caused by diffusivity differences in $^{12}\text{CH}_4$ and $^{13}\text{CH}_4$ methane isotopologues. Theoretical models for carbon isotope changes during production from shale reservoirs also indicate this trend may be expected (Tang and Xia,

2011). No clear distinction is observed in gas carbon isotope signatures between formations and differentiation of Muskwa, Otter Park and Evie produced gases based on carbon isotope ratios is not possible.

Carbon isotope ratios of methane ($\delta^{13}\text{C}_{\text{methane}}$), ethane ($\delta^{13}\text{C}_{\text{ethane}}$) and propane ($\delta^{13}\text{C}_{\text{propane}}$) for Wells 1 to 8 during production are shown in Fig. 4.5b to 4.5d. Short-term (wells 7 and 8) and long-term (wells 1 to 6) carbon isotope changes are shown and a log time scale is selected to represent time due to the difference in sample density in the short term (daily) compared to long term (monthly scale). In shale gases from wells 7 and 8 (Muskwa and Evie gases respectively) a similar trend in ^{12}C enrichment of methane is observed compared to methane produced in later stages of production (Fig 4.5b). Produced gas samples from these two wells were obtained over time periods of approximately 25 and 50 days and $\delta^{13}\text{C}_{\text{methane}}$ values in these formations also show ^{12}C enrichment with the most negative value of $\sim -38\%$. Wells 7 and 8 are located at well pad 3 and the well completion design differed from the other wells. The number of fracture stages and the number and spacing of perforation clusters were also greater than for wells located at well pad 1 (Table 4.2). The overall ^{12}C enrichment in methane for gases from wells 7 and 8 may be indicative of higher connectivity created in the shale by the process of hydraulic fracturing.

In Fig. 4.6a and Fig. 4.6b differences in the carbon isotope ratios of methane- ethane and ethane-propane are presented as a function of time shown on a logarithmic scale. Carbon isotope data for wells 1 to 8 are shown in these plots and the dashed lines separate gases showing isotope reversals from those without isotope reversal between hydrocarbon gas components. The $\delta^{13}\text{C}_{\text{ethane}} - \delta^{13}\text{C}_{\text{methane}}$ vs time plot illustrates that in the early stages of production the $\delta^{13}\text{C}_{\text{methane}} < \delta^{13}\text{C}_{\text{ethane}}$ (Fig 4.6a) and isotope reversals between methane and ethane are observed at later stages of production. The $\delta^{13}\text{C}_{\text{propane}} - \delta^{13}\text{C}_{\text{ethane}}$ vs time plot illustrates that most gases show isotope reversals between ethane and propane. Isotope reversals are commonly observed in shale gas plays worldwide (Zumberge et al., 2009; Burruss and Laughrey, 2010; Rodriguez and Philp, 2010; Tilley et al., 2011; Burruss and Laughrey, 2011; Tilley and Muehlenbachs, 2012;

Zumberge et al., 2012). Although the cause of the isotope reversal is still debated in the literature it is evident that produced gases from the Muskwa, Otter Park and Evie Horn River Group Formations may show partial or full isotope reversal in the carbon isotope gas signature.

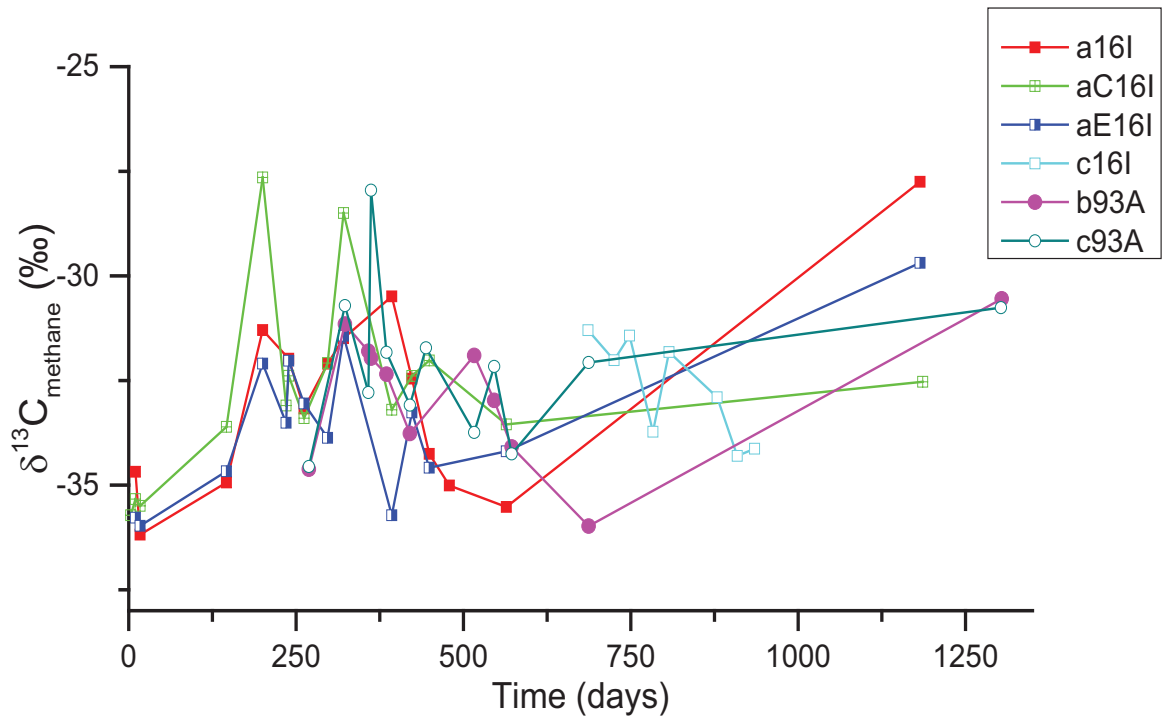


Figure 4.5(a) Variation in the $\delta^{13}\text{C}_{\text{methane}}$ values of Horn River Group shale gases for Wells 1 to 6 indicating long term fluctuations.

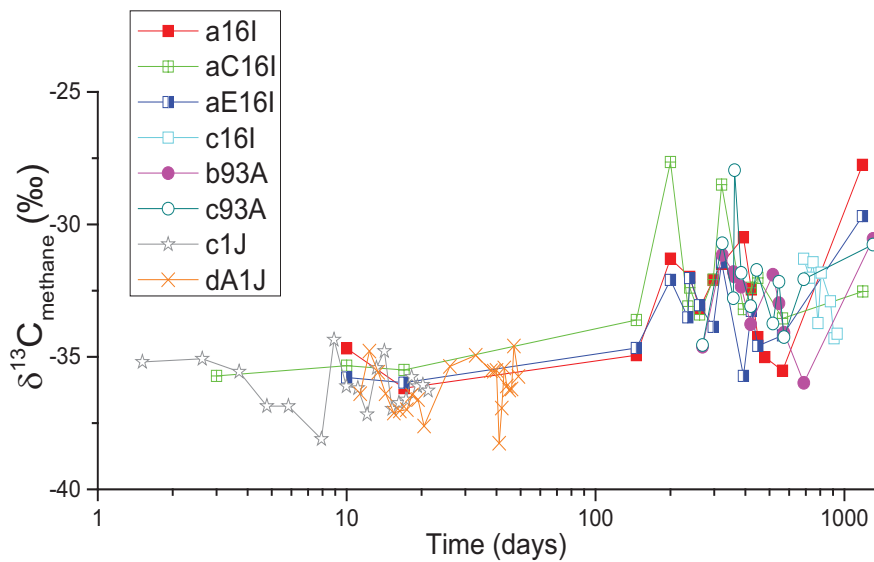


Figure 4.5(b) Variation in the $\delta^{13}\text{C}_{\text{methane}}$ values of Horn River Group shale gases for Wells 1 to 8 shown on a logarithmic time scale.

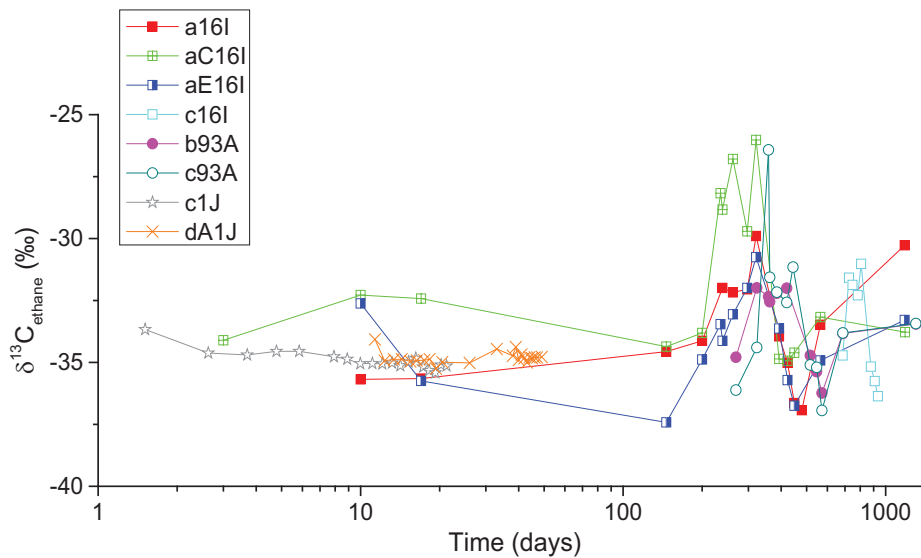


Figure 4.5(c) Variation in the $\delta^{13}\text{C}_{\text{ethane}}$ values of Horn River Group shale gases for Wells 1 to 8 shown on a logarithmic time scale.

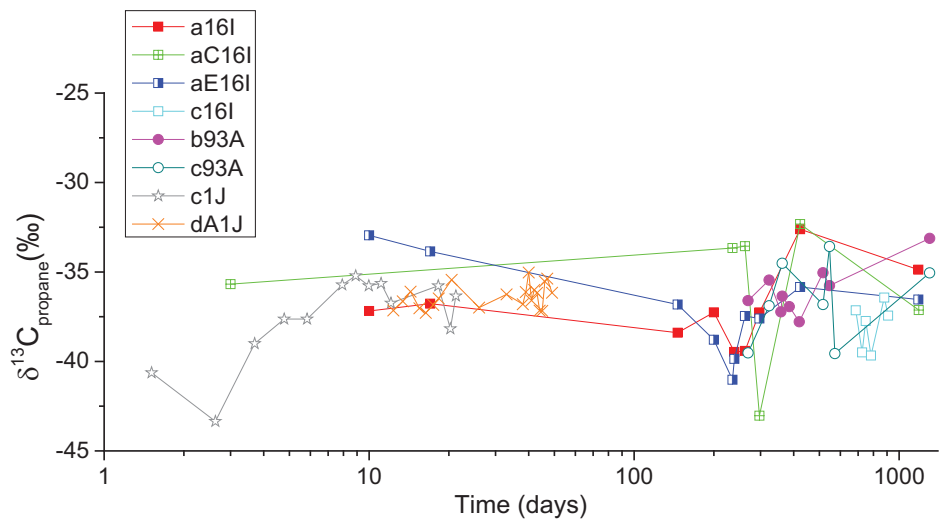


Figure 4.5(d) Variation in the $\delta^{13}\text{C}_{\text{propane}}$ values of Horn River Group shale gases for Wells 1 to 8 shown on a logarithmic time scale.

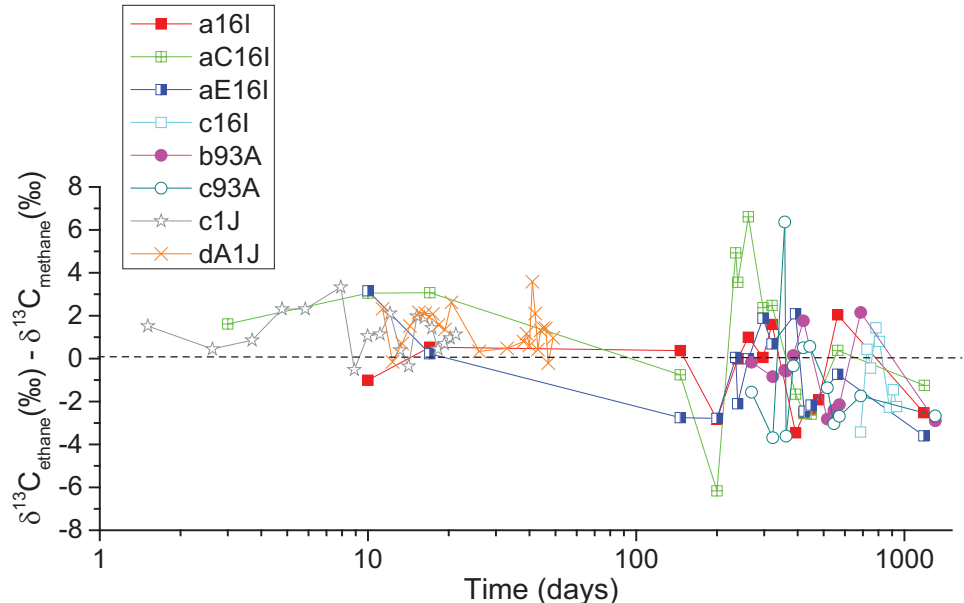


Figure 4.6(a) Plot of $\delta^{13}\text{C}_{\text{ethane}} - \delta^{13}\text{C}_{\text{methane}}$ shown on a logarithmic time scale. Gases which show isotope reversal plot below the dashed line.

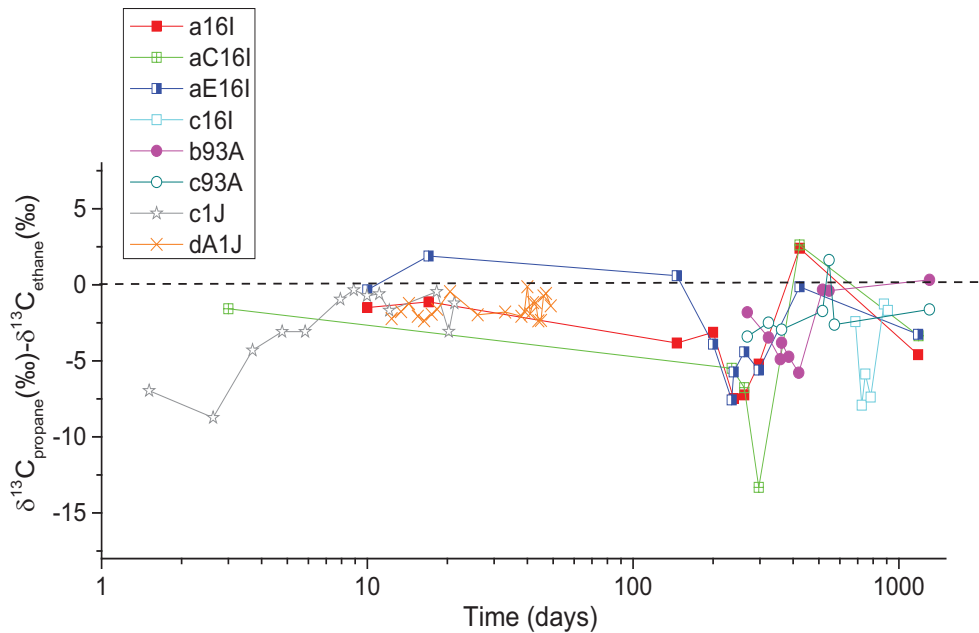


Figure 4.6(b) Plot of $\delta^{13}\text{C}_{\text{propane}} - \delta^{13}\text{C}_{\text{ethane}}$ shown on a logarithmic time scale. Gases which show isotope reversal plot below the dashed line.

Gas production rate and the corresponding changes in the $\delta^{13}\text{C}_{\text{methane}}$ values over time are presented in Fig. 4.7a to Fig. 4.7h. Shale gases demonstrate subtle temporal changes in isotope composition of methane as gas is produced from the reservoir. After periods of well ‘shut in’ methane showed ^{13}C enrichment. Time series for Muskwa gases from wells 1 (a16I) and 5 (b93A) clearly indicate this ^{13}C enrichment at times of approximately 400 days and 500 days respectively. Decreases in the carbon isotope values of methane generally occur after the production is restarted in these wells (Fig.4.7a and Fig. 4.7e). It is possible that during shut in periods gases are desorbed from the matrix which likely contributes to the ^{13}C enrichment observed. In wells which showed greater fluctuation in their gas production rate (wells 3 and well 7) more variations were also observed in the carbon isotope methane values of gases (Fig. 4.7c and 4.7f). In wells 1 and 5 two distinct phases of decline in gas production occurred. In well 1 the initial gas

production rates decreased from ~ 180 to $70 \text{ e}^3 \text{ m}^3/\text{d}$ after which shut in occurs and the rates return to $\sim 160 \text{ e}^3 \text{ m}^3/\text{d}$ then decline occurs for a second time. A similar trend is observed for well 5 after shut in. In both wells 1 and 5 there appears to be a relationship between the decline in rate and the decline in $\delta^{13}\text{C}_{\text{methane}}$ values of produced gas (Fig.4.7a and Fig. 4.7e).

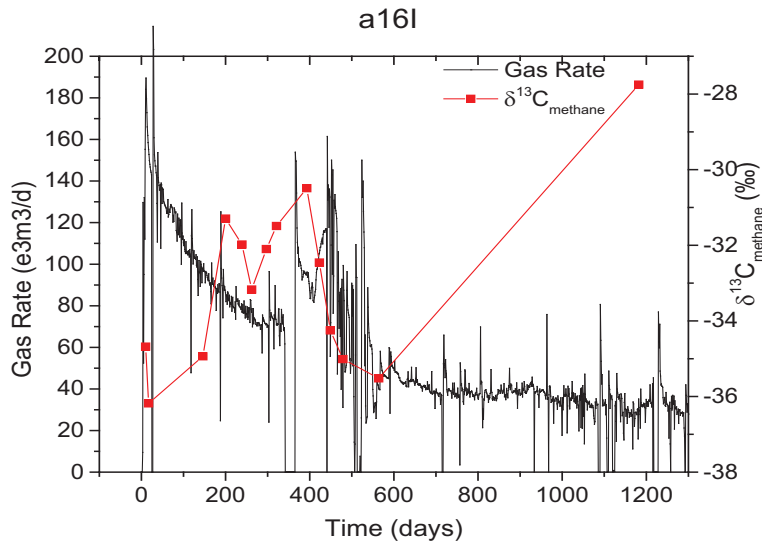


Figure 4.7(a) Overlay plot of gas production rate and methane carbon isotope values ($\delta^{13}\text{C}_{\text{methane}}$) vs time for Well 1 (a16I –Muskwa).

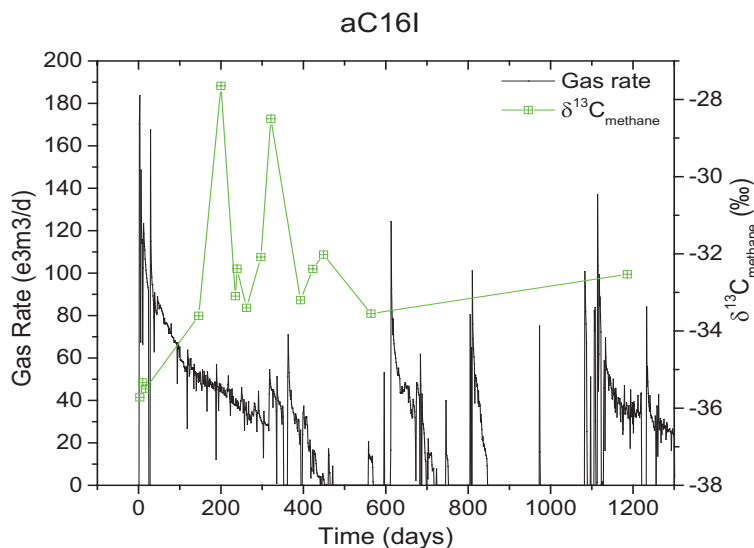


Figure 4.7(b) Overlay plot of gas production rate and methane carbon isotope values ($\delta^{13}\text{C}_{\text{methane}}$) vs time for Well 2 (aC16I –Evie).

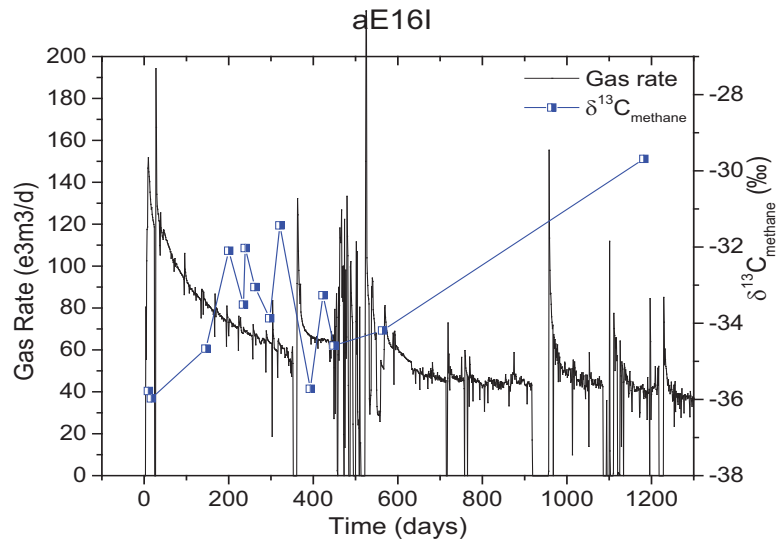


Figure 4.7(c) Overlay plot of gas production rate and methane carbon isotope values ($\delta^{13}\text{C}_{\text{methane}}$) vs time for Well 3 (aE16I –Muskwa-Otter Park).

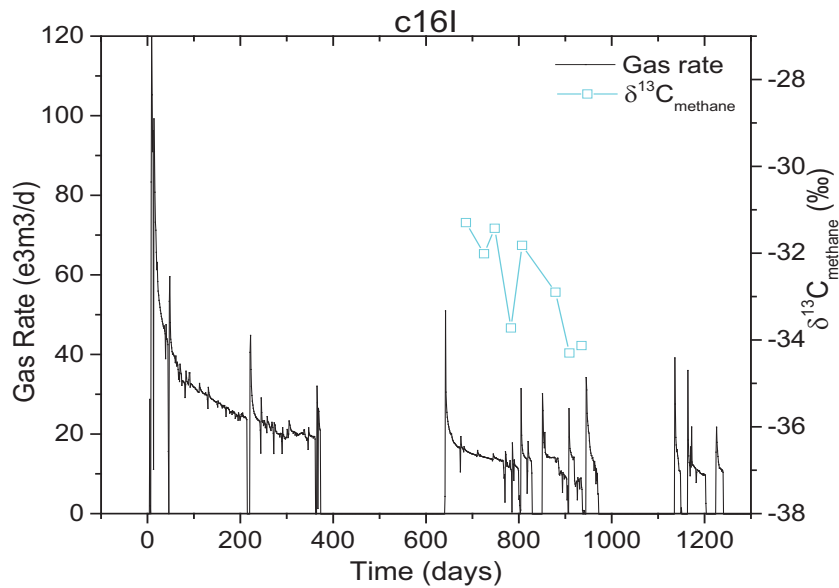


Figure 4.7(d) Overlay plot of gas production rate and methane carbon isotope values ($\delta^{13}\text{C}_{\text{methane}}$) vs time for Well 4 (c16I –Muskwa).

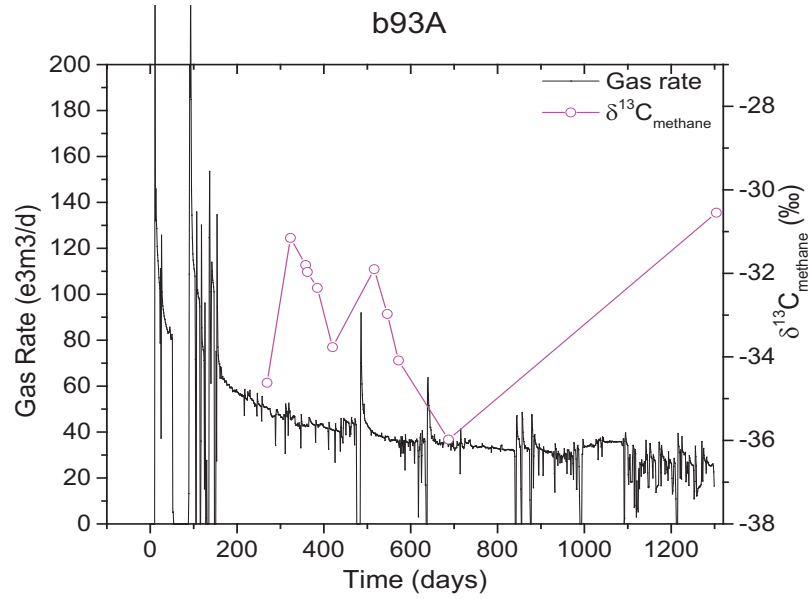


Figure 4.7(e) Overlay plot of gas production rate and methane carbon isotope values ($\delta^{13}\text{C}_{\text{methane}}$) vs time for Well 5 (b93A –Muskwa).

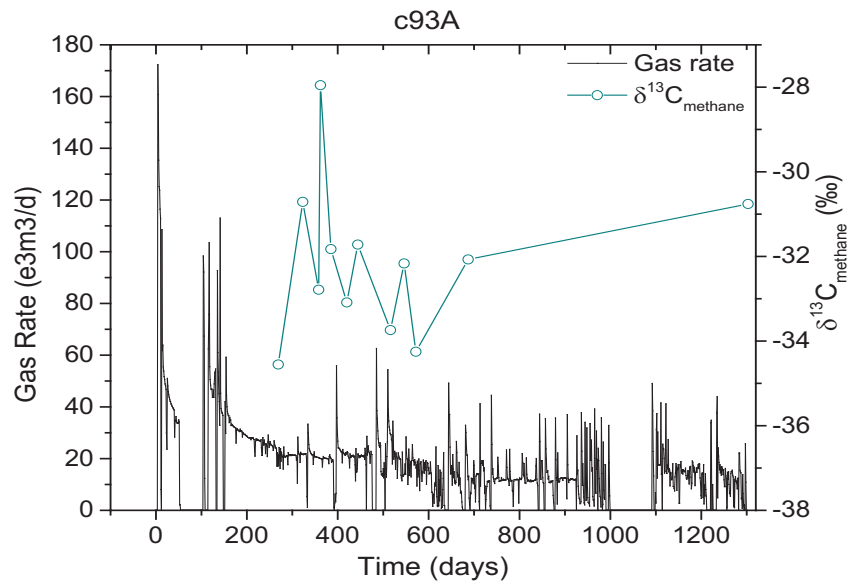


Figure 4.7(f) Overlay plot of gas production rate and methane carbon isotope values ($\delta^{13}\text{C}_{\text{methane}}$) vs time for Well 6 (c93A –Muskwa).

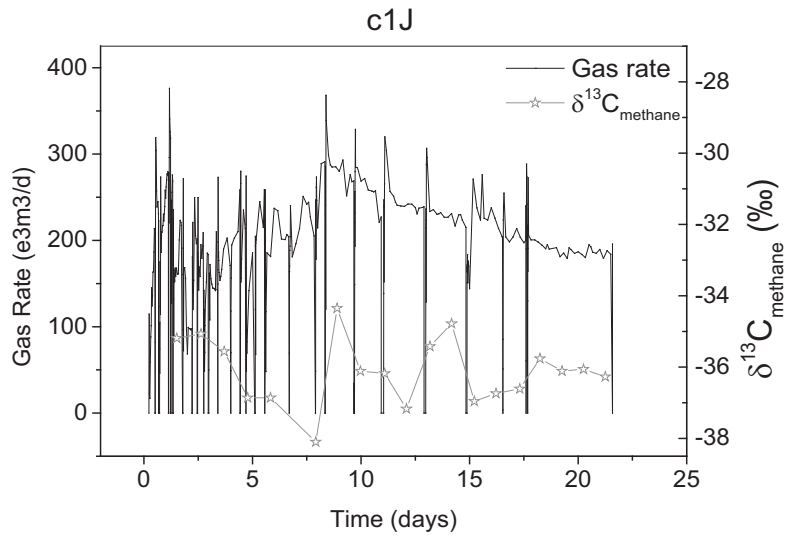


Figure 4.7(g) Overlay plot of gas production rate and methane carbon isotope values ($\delta^{13}\text{C}_{\text{methane}}$) vs time for Well 7 (c1J –Muskwa).

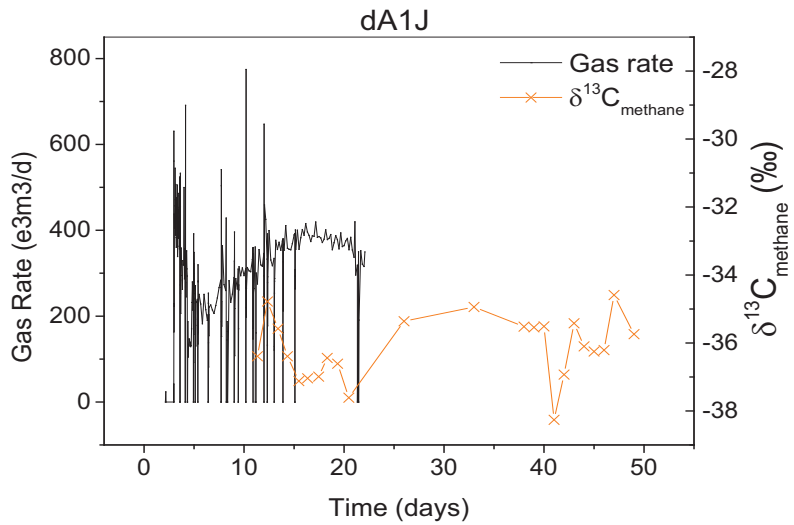


Figure 4.7(h) Overlay plot of gas production rate and methane carbon isotope values ($\delta^{13}\text{C}_{\text{methane}}$) vs time for Well 8 (dA1J–Evie).

The relationship between carbon isotope values of methane and the produced gas rate for wells 1 to 8 is shown in Fig. 4.8. In general highest rates of production are observed where gases are most depleted in ^{13}C however the production time is not taken into account in this plot and may also be useful in analysis of carbon isotope data as indicated in earlier time series plots. In Fig. 4.9a to Fig 4.9c the wells have been grouped depending on location for comparison. Wells 1 to 4 (a16I, aC16I, aE16I and c16I) were situated at well pad 1 and the variation in $\delta^{13}\text{C}_{\text{methane}}$ values for these is shown in (Fig. 4.9a). Well 1(a16I) completed in the Muskwa formation had the most hydraulic fracture stages of wells at this site and highest initial gas production rates and most negative $\delta^{13}\text{C}_{\text{methane}}$ value at the start of production. Wells 2 (aC16I) and 3 (aE16I) were completed in the Evie and Muskwa / Otter Park shales respectively. The perforation and hydraulic fracturing treatment was similar for these two wells (Table 4.1) and the overall range of $\delta^{13}\text{C}_{\text{methane}}$ values for well 2 (aC16I) was $\sim 5\text{‰}$ and for well 3 (aE16I) $\sim 7\text{‰}$.

Carbon isotope and gas production data for Wells 5 (b93A) and 6 (c93A) are shown in Fig. 4.9b. These wells were located at well pad 2 and showed similar gas production rates. Wells 7 (c1J) and 8 (dA1J) completed in the Muskwa and Evie formations at well pad 3 showed highest ^{12}C methane enrichment and the gas rates up to $\sim 400\text{e}^3\text{m}^3/\text{d}$.

Time series data presented establish the chemical and isotope behavior of Horn River Group shale gas at various stages during production. It is evident that the carbon isotope composition of the natural gas varies as the gas is released from pores and fractures of the shale.

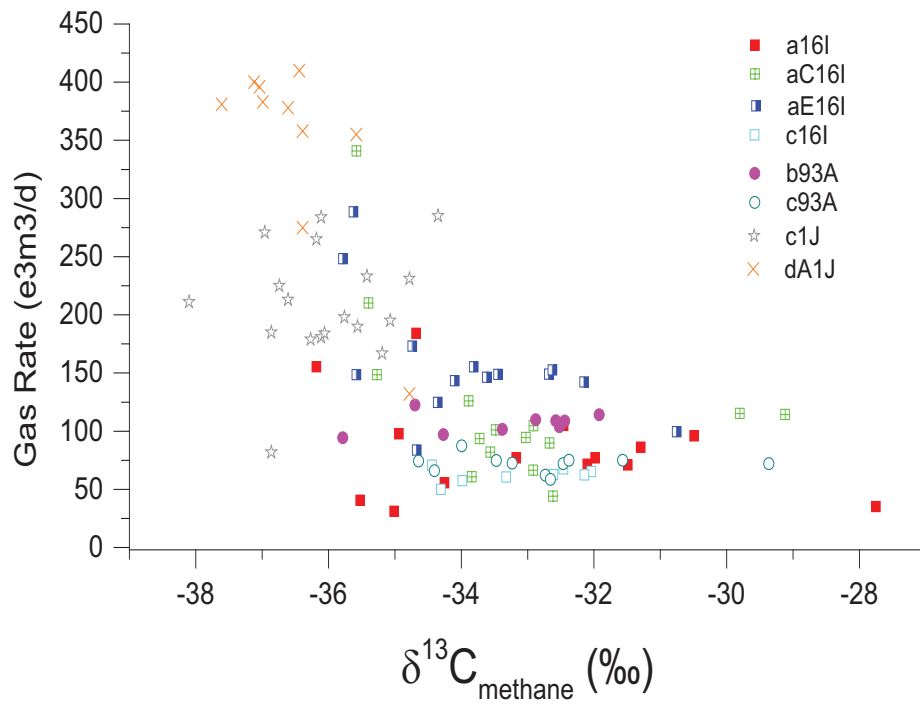


Figure 4.8 Cross-plots of gas production rate vs methane carbon isotope values ($\delta^{13}\text{C}_{\text{methane}}$) for 8 Horn River Basin wells.

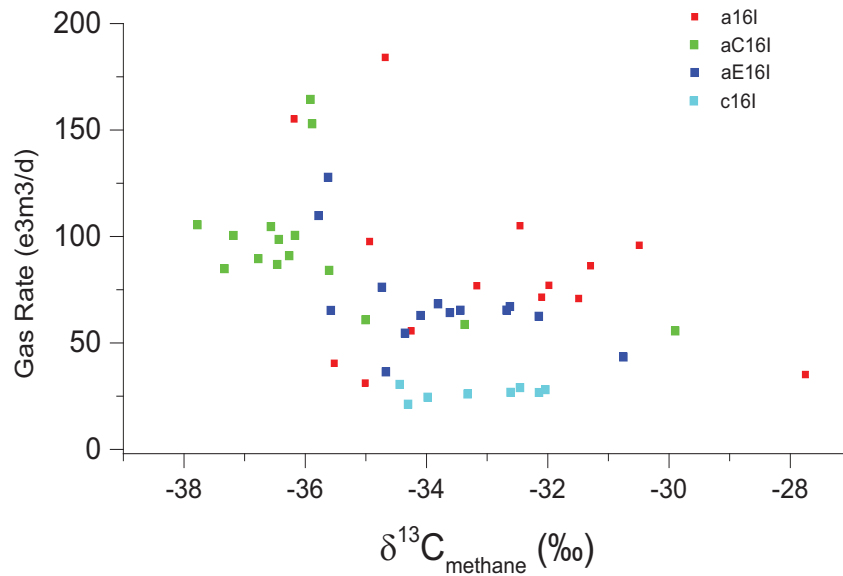


Figure 4.9(a) Gas rate vs methane carbon isotope values ($\delta^{13}\text{C}_{\text{methane}}$) for wells located at well pad 1.

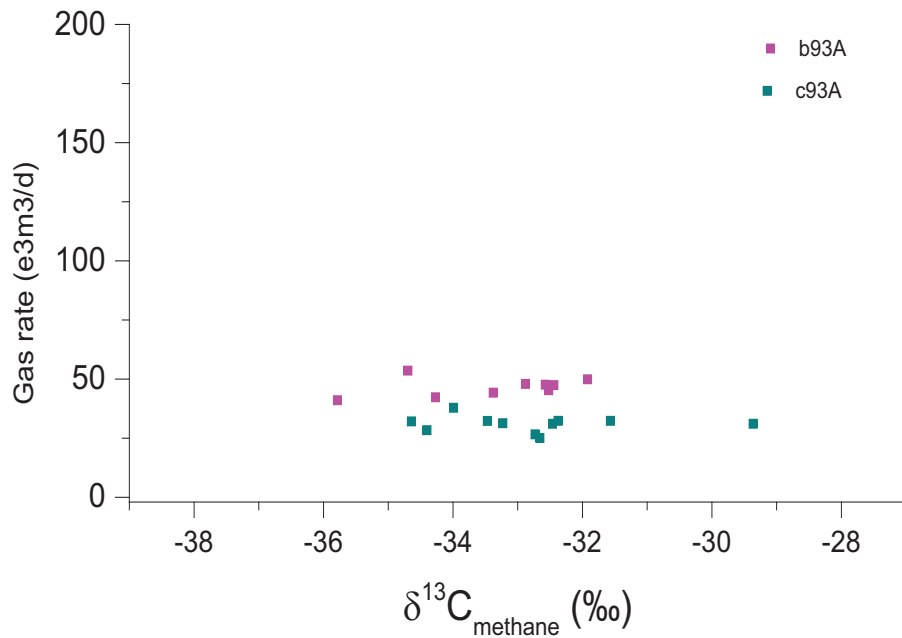


Figure 4.9(b) Gas rate vs methane carbon isotope values $\delta^{13}\text{C}_{\text{methane}}$ for wells located at well pad 2.

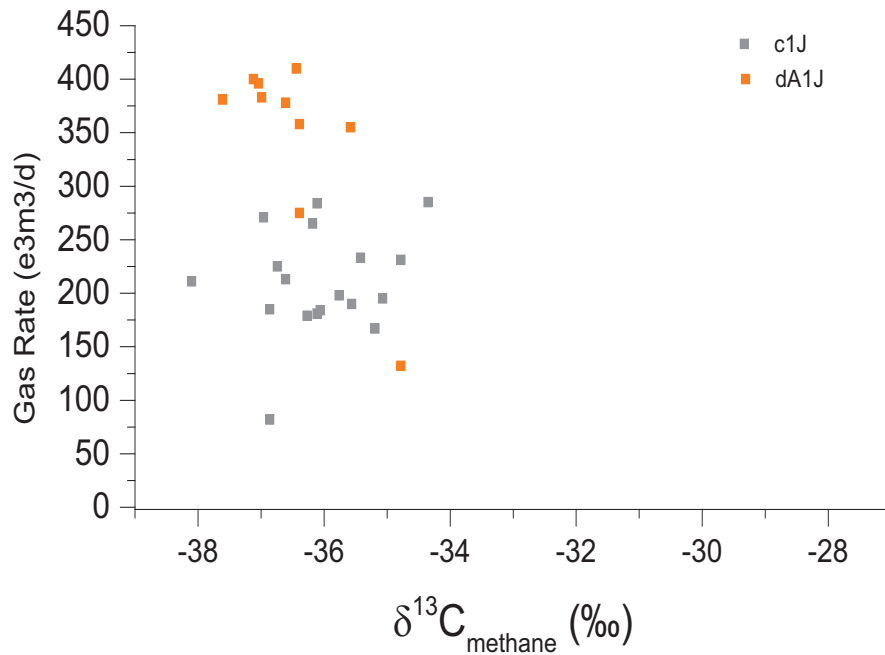


Figure 4.9(c) Gas rate vs methane carbon isotope values $\delta^{13}\text{C}_{\text{methane}}$ for wells located at well pad 3.

4.4 Conclusions

Unconventional shale gas systems differ from conventional hydrocarbon systems due to the intricate nature of the shale matrix and complexities in the stable isotope data were also revealed in analysis of Horn River Group gases. Produced gases from the Horn River show partial or fully reversed carbon isotope signatures indicative of high thermal maturity in this shale play. Chemical composition and stable isotope ratios of produced gases indicate temporal variations in carbon isotope signature occur during shale gas production from Horn River Group Formations. Changes in the stable isotope composition of methane ($\delta^{13}\text{C}_{\text{methane}}$), ethane ($\delta^{13}\text{C}_{\text{ethane}}$) and propane ($\delta^{13}\text{C}_{\text{propane}}$) occur over long term periods during shale gas production. Carbon isotope composition of the gases cannot be used to differentiate produced gases from the Muskwa, Otter Park and Evie Formations, however the Evie Formation differed in chemical composition from the other formations with overall higher amounts of carbon dioxide measured.

It is evident from the stable carbon isotope values of methane that the shale gas system does not follow a simple degassing model in which ^{13}C enrichment of gases occur over time. The variation in the carbon isotope values observed is likely to reflect the changes in produced gas during diffusion and desorption and depends on the location of gas in the shale and the connectivity of the fracture network both natural and artificially created during hydraulic fracturing. 'Free gas' may show methane which is ^{13}C depleted; as observed in early stages of gas production where $\delta^{13}\text{C}_{\text{methane}}$ values are most negative due to the differences in diffusivity of molecules. In general time series show during later phases of gas production from Horn River Group shales there is enrichment in ^{13}C of methane. The fluctuation in carbon isotope ratio of gases that occurs after the initial production decline phase in the reservoir reflect changes during desorption processes which are known to influence the $\delta^{13}\text{C}$ values during gas transport in shale.

Periods of well 'shut in' during gas production can be easily identified in some wells where ^{13}C enrichment of methane occurs. Carbon isotope gas signatures of gases from wells with different completion designs (perforation and fracture treatment) suggest stable carbon isotopes may be useful as diagnostic tool in shale gas reservoirs to signal an effective fracture job. Diffusive isotope fractionation might be important in shale gas plays altering the carbon isotope signature of natural gas as it transported from the low permeability nanoporous shale matrix during production. Gas chemical composition and stable isotope analysis is important for gas characterization and this study enhances our understanding of the geochemical aspects of the shale gas system.

References Cited

Adams, C., 2012, Summary of Shale Gas Activity in Northeast British Columbia 2011 Oil and Gas Reports 2012-1, BC Ministry of Energy and Mines, Geoscience and Strategic Initiatives Branch.

Aguilera, R., 2013, Flow Units: From Conventional to Tight Gas to Shale Gas to Tight Oil to Shale Oil Reservoirs, SPE Western Regional & AAPG Pacific Section Meeting, 2013 Joint Technical Conference, Apr 19 - 25, 2013 2013, Monterey, CA, USA.

Akkutlu, I. Y. and E. Fathi, 2012, Multiscale Gas Transport in Shales With Local Kerogen Heterogeneities, SPE Journal, no. 12, p. pp. 1002-1011.

Amann-Hildenbrand, A., A. Ghanizadeh, and B. M. Krooss, 2012, Transport properties of unconventional gas systems, Marine and Petroleum Geology, vol. 31, no. 1, p. 90-99.

Ambrose, R., R. Hartman, M. Diaz Campos, I. Y. Akkutlu, and C. Sondergeld, 2010, New pore-scale considerations for shale gas in place calculations, SPE Unconventional Gas Conference, 23-25 February 2010, Pittsburgh, Pennsylvania, USA.

Berner, U. and E. Faber, 1988, Maturity related mixing model for methane, ethane and propane, based on carbon isotopes, Organic Geochemistry, vol. 13, no. 1-3, p. 67-72.

Burruss, R. C. and C. D. Laughrey, 2010, Carbon and hydrogen isotopic reversals in deep basin gas: Evidence for limits to the stability of hydrocarbons, Organic Geochemistry, vol. 41, no. 12, p. 1285-1296.

Burruss, R. C. and C. D. Laughrey, 2011, Isotope reversals and rollovers: The last gasp of shale gas?

http://www.searchanddiscovery.com/abstracts/pdf/2011/hedberg-beijing/abstracts/ndx_burruss.pdf> Accessed 09/13, 2013.

Bustin, A. M. M. and R. M. Bustin, 2012, Importance of rock properties on the producibility of gas shales, *International Journal of Coal Geology*, vol. 103, p. 132-147.

Chung, H. M., J. R. Gormly, and R. M. Squires, 1988, Origin of gaseous hydrocarbons in subsurface environments: Theoretical considerations of carbon isotope distribution, *Chemical Geology*, vol. 71, no. 1-3, p. 97-104.

Claypool, G. E. and K. A. Kvenvolden, 1983, Methane and other hydrocarbon gases in marine sediment, *Annual Review of Earth and Planetary Sciences*, vol. 11, p. 299.

Clayton, C., 1991, Carbon isotope fractionation during natural gas generation from kerogen, *Marine and Petroleum Geology*, vol. 8, no. 2, p. 232-240.

Close, D., M. Perez, B. Goodway, and G. Purdue, 2012, Integrated workflows for shale gas and case study results for the Horn River Basin, British Columbia, Canada, *The Leading Edge*, vol. 31, no. 5, p. 556-569.

Corlett, H. and B. Jones, 2011, The influence of paleogeography in epicontinental seas: A case study based on Middle Devonian strata from the MacKenzie Basin, Northwest Territories, Canada, *Sedimentary Geology*, vol. 239, no. 3-4, p. 199-216.

Curtis, M., R. Ambrose, C. Sondergeld, and C. Sondergeld, 2010, Structural characterization of gas shales on the micro-and nano-scales, *Canadian Unconventional Resources and International Petroleum Conference*, 19-21 October 2010, Calgary, Alberta, Canada.

Curtis, J. B., 2002, Fractured Shale-Gas Systems, AAPG Bulletin, vol. 86, no. 11, p. 1921-1938.

Danesh, A., 1998, PVT and phase behaviour of petroleum reservoir fluids, vol. 47. Elsevier.

Freeman, C., G. Moridis, and T. Blasingame, 2013, Modeling and Performance Interpretation of Flowing Gas Composition Changes in Shale Gas Wells with Complex Fractures, 6th International Petroleum Technology Conference, Mar 26 - 28, 2013 2013, Beijing, China.

Freeman, C., G. J. Moridis, G. E. Michael, and T. A. Blasingame, 2012, Measurement, Modeling, and Diagnostics of Flowing Gas Composition Changes in Shale Gas Wells, SPE Latin America and Caribbean Petroleum Engineering Conference, 16-18 April 2012, Mexico City, Mexico.

Fuex, A. N., 1977, The use of stable carbon isotopes in hydrocarbon exploration, Journal of Geochemical Exploration, vol. 7, p. 155-188.

Geoscience BC Report 2012-4, 2013, Results from a Pilot Airborne Electromagnetic Survey, Horn River Basin, British Columbia, <<http://www.geosciencebc.com/s/Report2012-04.asp>> Accessed 10/29, 2013.

Gray, J. and R. Dawe, 1991, Modeling low interfacial tension hydrocarbon phenomena in porous media, SPE Reservoir Engineering, vol. 6, no. 3, p. 353-359.

Hu, Q., Z. Gao, S. Peng, and R. Ewing, 2012, Pore Structure Inhibits Gas Diffusion in the Barnett Shale, <http://www.searchanddiscovery.netwww.searchanddiscovery.net/documents/2012/50609hu/ndx_hu.pdf> Accessed 09/11, 2012.

James, A. T., 1983, Correlation of natural gas by use of carbon isotopic distribution between hydrocarbon components, AAPG Bulletin, vol. 67, no. 7, p. 1176-1191.

James, A. T., 1990, Correlation of reservoir gases using the carbon isotopic compositions of wet gas components, AAPG Bulletin, vol. 74, no. 9, p. 1441-1458.

Javadpour, F., 2009, Nanopores and apparent permeability of gas flow in mudrocks (shales and siltstone), Journal of Canadian Petroleum Technology, vol. 48, no. 8, p. 16-21.

Javadpour, F., D. Fisher, and M. Unsworth, 2007, Nanoscale gas flow in shale gas sediments, Journal of Canadian Petroleum Technology, vol. 46, no. 10.

Jenden, P. D., D. J. Drazan, and I. R. Kaplan, 1993, Mixing of thermogenic natural gases in northern Appalachian Basin, AAPG Bulletin, vol. 77, no. 6, p. 980-998.

Liang, P., J. M. Thompson, and L. Mattar, 2012, Importance of the Transition Period to Compound Linear Flow in Unconventional Reservoirs, SPE Canadian Unconventional Resources Conference, 30 October-1 November, Calgary, Alberta, Canada.

Loucks, R. G., R. M. Reed, S. C. Ruppel, and D. M. Jarvie, 2009, Morphology, genesis, and distribution of nanometer-scale pores in siliceous mudstones of the Mississippian Barnett Shale, Journal of Sedimentary Research, vol. 79, no. 12, p. 848-861.

Montgomery, S. L., D. M. Jarvie, K. A. Bowker, and R. M. Pollastro, 2005, Mississippian Barnett Shale, Fort Worth basin, north-central Texas: Gas-shale play with multi-trillion cubic foot potential, AAPG Bulletin, vol. 89, no. 2, p. 155-175.

Moridis, G., T. Blasingame, and C. Freeman, 2010, Analysis of mechanisms of flow in fractured tight-gas and shale-gas reservoirs, SPE Latin American and Caribbean Petroleum Engineering Conference. Society of Petroleum Engineers, 2010.

Morrow, D. W., M. Zhao, and L. D. Stasiuk, 2002, The Gas-Bearing Devonian Presqu'ile Dolomite of the Cordova Embayment Region of British Columbia, Canada: Dolomitization and the Stratigraphic Template, AAPG Bulletin, vol. 86, no. 9, p. 1609-1638.

Nelson, P. H., 2009, Pore-throat sizes in sandstones, tight sandstones, and shales, AAPG Bulletin, vol. 93, no. 3, p. 329-340.

Nexen Corporate Update, 2011,

http://www.nexenco.com/~media/Files/Presentations/PDF/Nexen_IRRoaddshow_UBS.ashx> Accessed 01/27, 2014.

Norville, G. A. and R. A. Dawe, 2007, Carbon and hydrogen isotopic variations of natural gases in the southeast Columbus basin offshore southeastern Trinidad, West Indies – clues to origin and maturity, Applied Geochemistry, vol. 22, no. 9, p. 2086-2094.

Oldale, H. and R. Munday, 1994, Devonian Beaverhill Lake Group of the western Canada sedimentary basin, Geological Atlas of the Western Canada Sedimentary Basin, p. 149-164.

Prinzhofer, A. A. and A. Y. Huc, 1995, Genetic and post-genetic molecular and isotopic fractionations in natural gases, Chemical Geology, vol. 126, no. 3-4, p. 281-290.

Ramos, S., 2004, The effect of shale composition on the gas sorption potential of organic-rich mudrocks in the Western Canadian sedimentary basin, M.Sc. thesis University of British Columbia, Vancouver, Canada (2004).

- Reynolds, M. M. and D. L. Munn, 2010, Development Update for an Emerging Shale Gas Giant Field - Horn River Basin, British Columbia, Canada, SPE Unconventional Gas Conference. Society of Petroleum Engineers, 2010.
- Rice, D. D. and G. E. Claypool, 1981, Generation, accumulation, and resource potential of biogenic gas, AAPG Bulletin, vol. 65, no. 1, p. 5-25.
- Rodriguez, N. D. and R. P. Philp, 2010, Geochemical characterization of gases from the Mississippian Barnett Shale, Fort Worth Basin, Texas, AAPG Bulletin, vol. 94, no. 11, p. 1641-1656.
- Ross, D. J. K. and R. M. Bustin, 2008, Characterizing the shale gas resource potential of Devonian Mississippian strata in the Western Canada sedimentary basin: Application of an integrated formation evaluation, AAPG Bulletin, vol. 92, no. 1, p. 87-125.
- Rowe, D. and A. Muehlenbachs, 1999a, Low-temperature thermal generation of hydrocarbon gases in shallow shales, Nature, vol. 398, no. 6722, p. 61-63.
- Rowe, D. and K. Muehlenbachs, 1999b, Isotopic fingerprints of shallow gases in the Western Canadian sedimentary basin: tools for remediation of leaking heavy oil wells, Organic Geochemistry, vol. 30, no. 8, Part 1, p. 861-871.
- Schoell, M., 1980, The hydrogen and carbon isotopic composition of methane from natural gases of various origins, Geochimica et Cosmochimica Acta, vol. 44, no. 5, p. 649-661.
- Schoell, M., 1983, Genetic characterization of natural gases, AAPG Bulletin, vol. 67, no. 12, p. 2225-2238.
- Schoell, M., 1988, Multiple origins of methane in the Earth, Chemical Geology, vol. 71, no. 1-3, p. 1-10.

Soeder, D. J., 1988, Porosity and Permeability of Eastern Devonian Gas Shale, , vol. 3, no. 1, p. 116-116-124.

Sondergeld, C., R. Ambrose, C. Rai, and J. Moncrieff, 2010, Micro-Structural Studies of Gas Shales. Paper SPE 131771 presented at the SPE Unconventional Gas Conference, Pittsburg, Pennsylvania, USA, 23–25 February 2010.

Stasiuk, L. D. and M. G. Fowler, 2004, Organic facies in Devonian and Mississippian strata of Western Canada Sedimentary Basin: relation to kerogen type, paleoenvironment, and paleogeography, Bulletin of Canadian Petroleum Geology, vol. 52, no. 3, p. 234-255.

Tang, Y. and D. Xia, 2011, Predicting Original Gas in Place and Optimizing Productivity by Isotope Geochemistry of Shale Gas, <http://www.cspg.org/documents/Conventions/Archives/Annual/2011/204-Predicting_Original_Gas_in_Place_and_Optimizing_Productivity.pdf> Accessed 09/13, 2013.

Tilley, B. and K. Muehlenbachs, 2012, Isotope Systematics of High Maturity Shale Gases in the WCSB Compared to Other North American Shale Gases, <http://www.cspg.org/documents/Conventions/Archives/Annual/2012/026_GC2012_Isotope_Systematics_of_High_Maturity_Shale_Gases.pdf> Accessed 09/11, 2013.

Tilley, B., S. McLellan, S. Hiebert, B. Quatero, B. Veilleux, and K. Muehlenbachs, 2011, Gas isotope reversals in fractured gas reservoirs of the western Canadian Foothills: Mature shale gases in disguise, AAPG Bulletin, vol. 95, no. 8, p. 1399-1422.

Wang, F. P. and R. M. Reed, 2009, Pore Networks and Fluid Flow in Gas Shales, reeSPE Annual Technical Conference and Exhibition, 4-7 October 2009, New Orleans, Louisiana, 2009, Society of Petroleum Engineers, New Orleans, Louisiana.

Wei, M., Y. Duan, Q. Fang, R. Wang, B. Yu, and C. Yu, 2013, Mechanism model for shale gas transport considering diffusion, adsorption/desorption and Darcy flow, *Journal of Central South University*, vol. 20, no. 7, p. 1928-1937.

Weissenberger, J. A. W. and K. Potma, 2001, The Devonian of western Canada -- aspects of a petroleum system: Introduction, *Bulletin of Canadian Petroleum Geology*, vol. 49, no. 1, p. 1-6.

Williams, G. K., 1983, What does the term 'Horn River Formation' mean? *Bulletin of Canadian Petroleum Geology*, vol. 31, no. 2, p. 117-122.

Xia, X. and Y. Tang, 2012, Isotope fractionation of methane during natural gas flow with coupled diffusion and adsorption/desorption, *Geochimica et Cosmochimica Acta*, vol. 77, p. 489-503.

Zhang, T. and B. M. Krooss, 2001, Experimental investigation on the carbon isotope fractionation of methane during gas migration by diffusion through sedimentary rocks at elevated temperature and pressure, *Geochimica et Cosmochimica Acta*, vol. 65, no. 16, p. 2723-2742.

Zumberge, J., K. Ferworn, and J. Curtis, 2009, Gas character anomalies found in highly productive shale gas wells, *Geochimica et Cosmochimica Acta Supplement*, vol. 73, p. A1539.

Zumberge, J., K. Ferworn, and S. Brown, 2012, Isotopic reversal ('rollover') in shale gases produced from the Mississippian Barnett and Fayetteville formations, *Marine and Petroleum Geology*, vol. 31, no. 1, p. 43-52.

CHAPTER 5

GAS GENERATION AND TRANSPORT IN DEVONIAN GAS SHALES OF THE HORN RIVER BASIN- INSIGHTS USING CARBON ISOTOPE GEOCHEMISTRY

5.1 Introduction

The Horn River Basin is located in northeast British Columbia, north of Ft. Nelson and covers an area approximately 1.3 million hectares (Adams, 2012). Organic-rich, marine Devonian Horn River Group Formations are active targets for unconventional shale gas production in the Horn River Basin. Understanding gas generation processes, storage and transport is necessary for successful gas recovery from these ultra-low permeability shale reservoirs. Isotope analysis may be an important technique in evaluation of shale gas plays since stable isotope signatures of natural gases hold clues to origin and transport within sedimentary rocks. Carbon isotope ratios ($^{13}\text{C}/^{12}\text{C}$) of hydrocarbon components of natural gas (methane, ethane, propane and butane) are determined by organic matter precursors, gas generation processes and post generation factors.

In conventional systems, stable carbon isotope signatures of natural gas are commonly used as indicators of gas origin (biogenic or thermogenic), maturity, mixing and migration history (Fuex, 1977; Fuex, 1980; Schoell, 1980; Rice and Claypool, 1981; James, 1983; Schoell, 1983; Claypool and Kvenvolden, 1983; Schoell, 1984; Chung et al., 1988; Berner and Faber, 1988; Schoell, 1988; James, 1990; Clayton, 1991; Jenden et al., 1993; Prinzhofer and Huc, 1995; Rowe and Muehlenbachs, 1999a; Rowe and Muehlenbachs, 1999b; Tilley and Muehlenbachs, 2006; Norville and Dawe, 2007) and others. Elements of conventional petroleum systems include the source, reservoir and seal and overburden rock (Magoon and Dow, 1994; Magoon and Schmoker, 2000), however unconventional shale gas systems are self-contained and the shale functions as both source and reservoir as hydrocarbons are extracted directly from the shale during production (Dewitt, 1984; Martini et al., 1998; Curtis, 2002; Shurr and Ridgley, 2002; Hill et al., 2006; Ross and Bustin, 2008; Zumberge et

al., 2012). In chapter 3 and chapter 4 the chemical and stable isotope compositions of shale gases of mud gases and production gases were determined and discussed for shales of the Horn River Group. This study attempts (i) to link findings from the previous two Chapters and (ii) account for the overall observed trends in mud gas and production gas isotope data in the Basin.

The study site is located in the Dilly Creek area of the Horn River Basin, northeast British Columbia; within Map sheet 94/O of the National Topographic System (NTS) (Fig. 5.1). Shale gas wells were drilled with lateral legs completed in the Devonian Muskwa and Otter Park Formations; two of the key shale gas target formations in this region. Paleozoic Horn River Group Formations in the Dilly Creek area have extremely low permeability, generally in the nanodarcy (nd) range with values of approximately 150 to 450 nd (Nexen Corporate Update, 2011). In unconventional shale gas reservoirs hydraulically fracturing is necessary and an artificial fracture network allows flow of natural gas from the reservoir to the well bore in economic quantities. In this study shale gas samples collected for stable isotope analysis include mud gases and production gases hence gases were obtained at stages prior and subsequent to the process of hydraulic fracturing. Mud gas samples were collected from the mud stream during drilling operations and these gases likely are the most representative sample type of in situ reservoir gas. Production gases were sampled after hydraulic fracturing and well treatment and completion phases when the wells were put on production.

Shale gases were analysed to determine carbon isotope ratios ($^{13}\text{C}/^{12}\text{C}$) of methane, ethane, propane and butane (C1-C4). Stable isotope analysis is commonly used for analysis of conventional hydrocarbon reservoirs; however interpretation of carbon isotope signatures of natural gas from shale gas systems provides additional challenges.

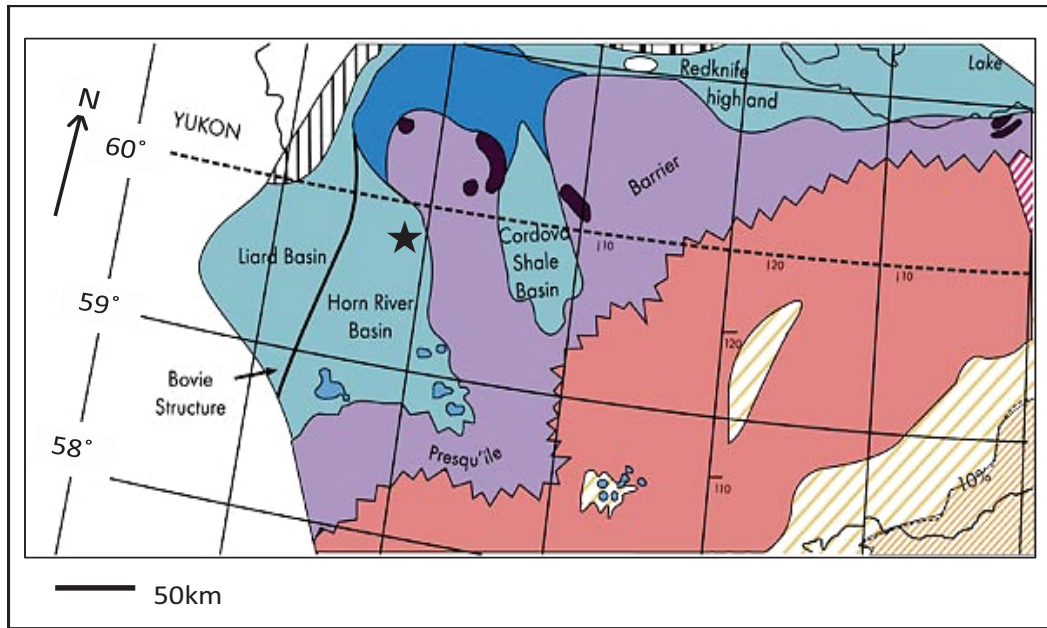


Figure 5.1 Location map showing the study area in the Horn River Basin, Northeast British Columbia using the National Topographic System (modified from British Columbia Ministry of Energy, 2011).

In unconventional shale gas reservoirs (i) the exact mechanism of shale gas generation is not fully understood (Burruss and Laughrey, 2010; Rodriguez and Philp, 2010; Tilley et al., 2011; Tilley and Muehlenbachs, 2013) and (ii) the extent of fractionation that occurs during degassing of the shale including diffusion and adsorption/desorption processes remains unknown (Amann-Hildenbrand et al., 2012; Xia and Tang, 2012). These two factors are significant since they both influence the carbon isotope ratios of shale gases obtained from these resource plays.

Carbon isotope signatures of unconventional shale gases usually differ from those in conventional reservoirs and often ‘isotope reversals’ are observed between $\delta^{13}\text{C}$ values of hydrocarbon components of the gas (Seewald and Whelan, 2005; Burruss and Laughrey, 2010; Tilley et al., 2011; Zumberge et al., 2012; Tilley and Muehlenbachs, 2013). Three stages of maturation have been defined for shale gas systems; pre-rollover, rollover and post rollover stage, each associated with a characteristic range of gas isotope signatures (Tilley and

Muehlenbachs, 2013). In the study area of the Horn River Basin, Upper Devonian Muskwa shales are thermally mature and vitrinite reflectance (R_o) values range from ~ 2.2 to 2.6%. The aim of this paper is to analyse and interpret stable isotope data from Muskwa and Otter Park shale gases of the Horn River Group to enhance understanding of the shale gas system.

5.1.1 Geological background

In the Paleozoic era, the western side of the North American craton represented a passive continental margin setting (Kent, 1994). Late Devonian shales of the Horn River Basin were deposited on the continental shelf during a period of marine transgression (Weissenberger and Potma, 2001) with the main sediment source derived northeast from the craton (Monger and Price, 1979). Low sedimentation rates and rapid sea level rise coupled with increased subsidence and anoxic conditions allowed preservation of organic matter within these sediments (Switzer et al., 1994). Subsequent events included subduction of the oceanic lithosphere and collision of the craton with accreted terrains which resulted in subsidence as Devonian shales were buried and uplifted in the Columbian and Laramide orogenies (Price, 1994).

The Muskwa Formation was originally classified as a Member of the Horn River Formation (Gray and Kassube, 1963) but was later elevated to Formation status (Griffin, 1965; Williams, 1983; Ross and Bustin, 2008). It conformably overlies the Otter Park Formation and is overlain conformably by the Fort Simpson Formation (Fig. 5.2) The Muskwa shale is dark grey to black, organic-rich, siliceous, pyritic and shows high gamma ray activity (Oldale and Munday, 1994).

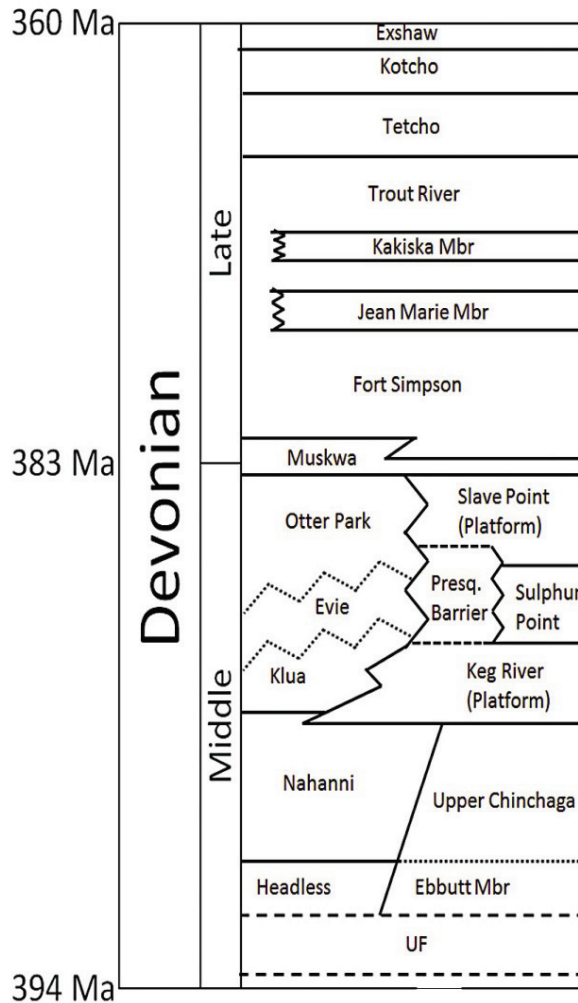


Figure 5.2 Stratigraphy of the Devonian NE British Columbia in the Horn River Basin area (after Close et al., 2012).

5.1.2 Natural Gas Generation

In the study area, the Paleozoic marine Horn River Group shales are presently buried at depths of approximately 2.5 km with vitrinite reflectance values (R_o) between 2.2 to 2.6%. The burial history curve for Devonian strata in this region of the Western Canada Sedimentary Basin (Fig. 5.3) shows maximum burial depths at approximately 7 km before uplift of geological formations. The paleotemperature range for these vitrinite reflectance (R_o) values was calculated using the equation $T = (\ln R_o + 1.68)/0.0124$ (Mukhopadhyay and Dow, 1994).

Paleotemperature values vary between 199°C and 212°C for the Horn River Group Formations and represent the maximum temperatures to which source rocks were exposed. Natural gas in Devonian strata of the Horn River Basin is methane rich and generation occurred during thermal cracking reactions in which complex organic structures were broken down into smaller hydrocarbon molecules. In late stages of thermogenic gas generation, wet gas cracking may play an important role in formation of methane in the reservoir.

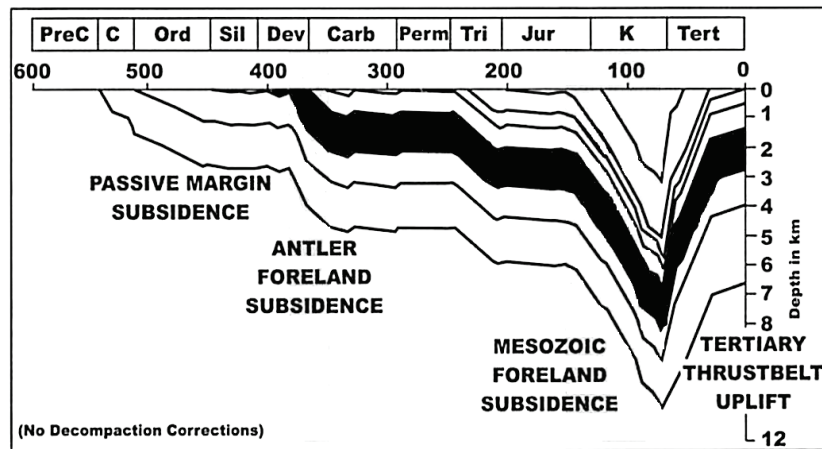


Figure 5.3 Burial curves highlighting Devonian strata in the Sukunka area northeast British Columbia (modified from Root, 2001).

In unconventional shale gas reservoirs the conditions in the shale can be considered near to that of a ‘closed-system’ in which gases generated remain trapped within pores and fractures until their recovery. Pyrolysis experiments have determined the carbon isotope compositions from thermal gas generation in open and closed system conditions (Arneth, 1984; Arneth and Matzigkeit, 1986; Lorant et al., 1998). Under closed system conditions the $\delta^{13}\text{C}$ values of C₂+ hydrocarbon components of natural gas showed ^{13}C enrichment relative to $\delta^{13}\text{C}_{\text{methane}}$. Models for thermogenic gas generation (Rooney et al., 1995; Tang et al., 2000) provide a theoretical approach and the carbon isotope models are useful as comparative reference framework for stable isotope ratios observed in these shale gas reservoirs.

5.1.3 Isotope Fractionation effects during gas transport through the shale matrix

In shale gas systems, natural gas is adsorbed onto kerogen and clays or compressed in pores and fractures (Ramos, 2004; Ross and Bustin, 2008; Ross and Bustin, 2009). Gas flow within pores of the shale matrix and through natural and artificial fractures to the wellbore is essential for hydrocarbon production in these shale gas plays. Various processes are involved as natural gas is transported through the shale matrix and these may include viscous flow, capillary processes, diffusion and adsorption and desorption (Amann-Hildenbrand et al., 2012); however diffusion processes are considered to play a fundamental role in gas transport through the shale matrix (Amann-Hildenbrand et al., 2012; Hu et al., 2012; Freeman et al., 2012).

Isotope fractionation occurs during adsorption, desorption and diffusion of gas in shale (Zhang and Krooss, 2001; Strapoć et al., 2010; Tang and Xia, 2011; Xia and Tang, 2012). Fig. 5.4a and 5.4b show the magnitude of isotope fractionation effects that may occur during natural gas diffusion and desorption in shale. Carbon isotope fractionation effects occur during gas flow in shales as a result of the differences in mobility between the $^{12}\text{CH}_4$ and $^{13}\text{CH}_4$ isotopologues (Zhang and Krooss, 2001; Tang and Xia, 2011). Molecules which contain ^{12}C atoms have higher diffusivity compared to those with ^{13}C atoms. Experimental work by Zhang and Krooss (2001) found as methane diffuses through various samples of shale; the diffused methane became depleted in the heavier (^{13}C) carbon isotope. Effective diffusion coefficients vary for methane (C1), ethane (C2) and propane (C3). Theoretical calculations also show large isotope fractionation effects may occur during gas diffusion through the shale to the wellbore with changes in carbon isotope values ‘up to -30‰, -16‰ and -11‰’ for methane, ethane and propane respectively (Tang and Xia, 2011); although isotope fractionation in geological systems is considered less significant (Xia and Tang, 2012). An experimental approach by (Strapoć et al., 2010) indicated carbon isotope fractionation of C1, C2 and C3 occurs during gas desorption from shale core samples with increases in the $\delta^{13}\text{C}_{\text{methane}}$ value of up to ~12‰ (Fig. 5.4a). It is

evident from these studies that carbon isotope fractionation of methane (CH_4) and higher homologues (C_2H_6 , C_3H_8 , C_4H_{10}) can occur during gas transport processes within low permeability shales.

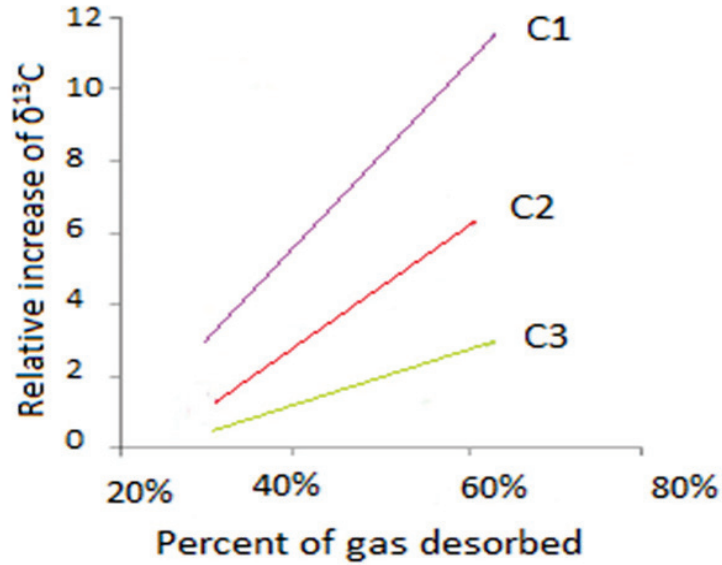


Figure 5.4 (a) Relationship between the relative changes in $\delta^{13}\text{C}$ values of methane, ethane and propane and the fraction of shale gas desorbed from the core (after Strapoc et al., 2010).

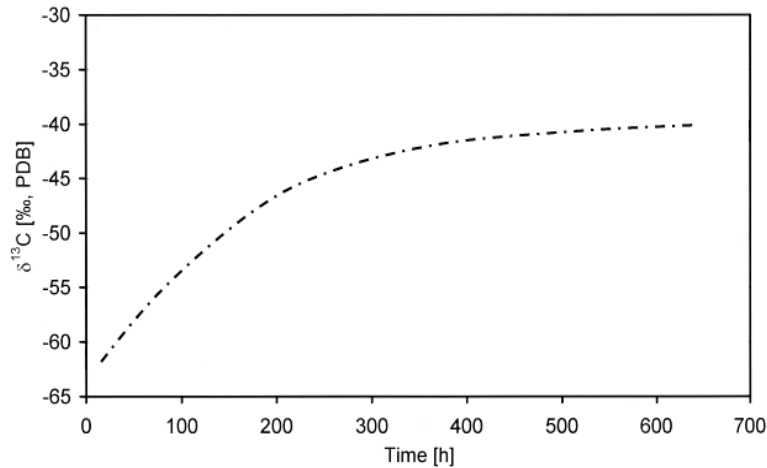


Figure 5.4 (b) Variation in carbon isotope ratios due to isotope fractionation effects during methane gas diffusion in a sample of shale. The dashed line indicates average changes over time until the $\delta^{13}\text{C}$ values approach that of the source where $\delta^{13}\text{C}_{\text{methane}}$ is -39‰ (after Zhang and Kroos, 2001).

5.2 Methods

Shale gas samples for carbon isotope analysis were collected from six wells in the Horn River Basin with lateral lengths of the horizontal wells completed in the Devonian Muskwa and Otter Park gas-rich target formations. Shale gas wells were oriented northwest to southeast in the basin and drilled from three multi-well pads spaced at approximately two kilometer intervals; a-16-I/94-O-08, b-18-I/94-O-08 and c-1-J/94-O-08 (Fig. 5.5a and 5.5b). Approximately one hundred and twenty samples of Horn River Group mud gases and production gases were analysed to determine the carbon isotope ratios ($^{13}\text{C}/^{12}\text{C}$) of methane (CH_4), ethane (C_2H_6), propane (C_3H_8) and butane (C_4H_{10}).

Samples of mud gas were collected from the two shale gas target formations in the Devonian Horn River Group (Table 5.1). During drilling of the wells natural gas liberated from the shale as it is crushed by the drill bit and gas produced from the formation travels up the annulus entrained in the drill mud to the surface where degassing and separation from the drilling mud occurs. Mud gas samples from the Muskwa and Otter Park Formations were collected at the wellhead from the gas flow stream in 110ml aluminium IsoTube[®] containers (IsoTech Laboratories, Inc. Champaign IL) inserted in the gas sampling manifold. Mud gas samples for geochemical analysis were obtained prior to the process of hydraulic fracturing of the shale formation. Produced gas samples were collected subsequent to hydraulic fracturing processes when wells were put on production which allowed gas flow from the reservoir to surface. Samples of production gases were collected at the wellhead in high pressure stainless steel sample cylinders and transferred to Tedlar bags for stable carbon isotope analysis.

Chemical compositions of production gases were measured using gas chromatography by an external commercial laboratory. Stable carbon isotope composition was determined at the University of Alberta, Earth and Atmospheric Science Department using gas chromatography-isotope ratio mass spectrometry. Carbon isotope ratios ($^{13}\text{C}/^{12}\text{C}$) of hydrocarbon components (C1 to C4) of shale gases were measured using a Finnigan-MAT 252 GC CF-IRMS. Carbon isotope

data was reported using standard δ -notation (‰) relative to the VPDB (Vienna Pee Dee Belemnite) standard.

$$\delta^{13}\text{C} (\text{‰}) = \left(\frac{{}^{13}\text{C}/{}^{12}\text{C}_{\text{sample}} - {}^{13}\text{C}/{}^{12}\text{C}_{\text{standard}}}{{}^{13}\text{C}/{}^{12}\text{C}_{\text{standard}}} \right) \times 1000$$

Single analyses were performed on mud gas samples due to limited sample volumes available. Production gases were sampled in duplicate at the well site and isotope analysis was performed in triplicate. The standard deviation values for $\delta^{13}\text{C}_{\text{methane}}$, $\delta^{13}\text{C}_{\text{ethane}}$ and $\delta^{13}\text{C}_{\text{propane}}$ were 0.1, 0.2 and 0.8‰ respectively.

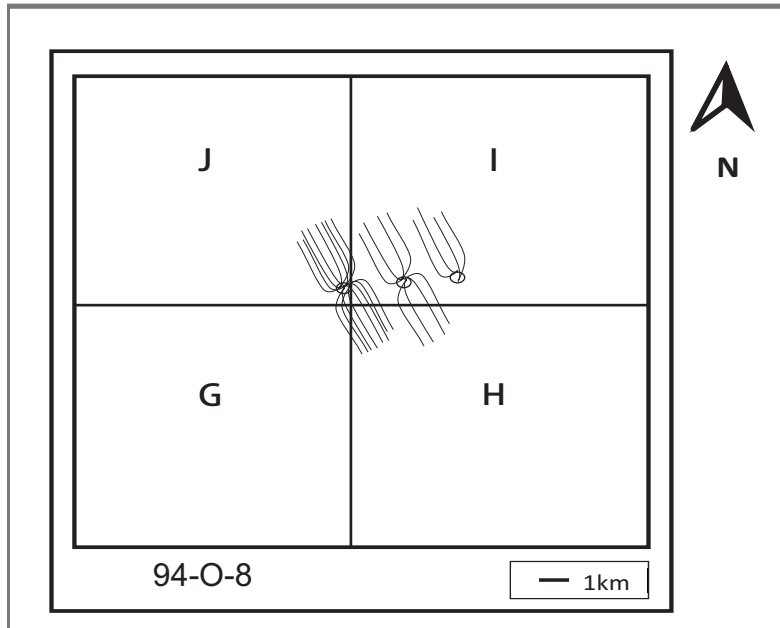


Figure 5.5 Location map indicating the sites of the three well pads in the Horn River Basin. The map (NTS 94/O) shows a section of the NTS 1:50000 map sheet. The horizontal well legs are within the Muskwa and Otter Park Formations of the Horn River Group.

5.3 Results & Discussion

Carbon isotope values ($\delta^{13}\text{C}$) for C1 to C4 hydrocarbon components of Muskwa and Otter Park shale gases are presented in Table 5.1. The mud gases were obtained during drilling and the produced gases taken at various times in the production stage up to approximately 1250 days. Methane carbon isotope ratios ($^{13}\text{C}/^{12}\text{C}$) for shale gases samples were greater than -40‰ and indicative of a thermogenic gas origin (James, 1983; Schoell, 1983; Schoell, 1988; Faber et al., 1992; Norville and Dawe, 2007). Gas wetness values for Muskwa and Otter Park production gas samples were determined from chemical compositions ($\text{C2+}(\%) = [(\sum\text{C2-C4}/\sum\text{C1-C4}) * 100]$) and ranged between 0.14 to 0.53%. These values indicate extremely dry natural gas is present in the shales of the Muskwa and Otter Park Formation of the Horn River Group. Chemical and isotope compositions of Muskwa and Otter Park gases reflect the high thermal maturity of Devonian Horn River shales in the Western Canada Sedimentary Basin.

Table 5.1 Carbon isotope data for mud gases and production gases from the Horn River Basin (Muskwa and Otter Park Formations).

Well #	Formation	Sample type	$\delta^{13}\text{C1}(\text{‰})$	$\delta^{13}\text{C2}(\text{‰})$	$\delta^{13}\text{C3}(\text{‰})$	$\delta^{13}\text{n-C4}(\text{‰})$
1	Muskwa	mud gas	-34.9	-32.2	-28.4	
1	Muskwa	mud gas	-35.1	-33.6	-28.1	
1	Muskwa	mud gas	-34.5	-34.9	-29.6	
1	Muskwa	mud gas	-34.6	-34.9	-28.4	
1	Muskwa	mud gas	-34.9	-33.2	-30.7	-28.7
1	Muskwa	mud gas	-35.2	-34.0	-31.0	-28.6
1	Muskwa	mud gas	-35.3	-35.3	-31.4	-29.2
1	Muskwa	mud gas	-33.7		-29.5	
1	Muskwa	mud gas	-35.2	-34.6	-30.7	
1	Muskwa	mud gas	-34.5	-33.6	-31.2	-28.1
1	Muskwa	mud gas	-35.4	-33.7	-31.0	-28.3
1	Muskwa	mud gas	-35.5	-35.0	-31.2	
1	Muskwa	mud gas	-34.8	-35.4	-31.7	

1	Muskwa	mud gas	-34.6	-34.6	-30.5
1	Muskwa	mud gas	-35.0	-35.1	-38.1
1	Muskwa	production gas	-26.97	-32.58	-36.57
2	Muskwa	production gas	-34.7	-35.7	-37.2
2	Muskwa	production gas	-36.4	-35.7	-35.8
2	Muskwa	production gas	-36.0	-35.6	-37.8
2	Muskwa	production gas	-34.9	-34.6	-38.4
2	Muskwa	production gas	-31.3	-34.1	-37.3
2	Muskwa	production gas	-32.0	-32.0	-39.5
2	Muskwa	production gas	-33.2	-32.2	-39.4
2	Muskwa	production gas	-33.1	-32.2	-37.3
2	Muskwa	production gas	-31.1	-31.9	
2	Muskwa	production gas	-31.5	-29.9	
2	Muskwa	production gas	-30.5	-34.0	
2	Muskwa	production gas	-30.5	-34.0	-32.6
2	Muskwa	production gas	-34.3	-36.7	
2	Muskwa	production gas	-34.2	-36.6	
2	Muskwa	production gas	-35.0	-36.9	
2	Muskwa	production gas	-35.5	-33.5	
3	Muskwa	production gas	-35.8	-32.6	-33.0
3	Muskwa	production gas	-35.9	-35.3	-30.9
3	Muskwa	production gas	-36.0	-36.3	-36.8
3	Muskwa	production gas	-34.7	-37.4	-36.8
3	Muskwa	production gas	-32.1	-34.9	-38.8
3	Muskwa	production gas	-33.5	-33.5	-41.0
3	Muskwa	production gas	-32.0	-34.1	-39.9
3	Muskwa	production gas	-33.1	-32.9	-39.1
3	Muskwa	production gas	-33.1	-33.2	-35.9
3	Muskwa	production gas	-33.9	-32.0	-37.6
3	Muskwa	production gas	-31.5	-30.7	
3	Muskwa	production gas	-31.4	-30.8	
3	Muskwa	production gas	-35.7	-33.6	
3	Muskwa	production gas	-33.0	-35.9	-36.6
3	Muskwa	production gas	-33.6	-35.5	-35.1
3	Muskwa	production gas	-34.6	-36.7	
3	Muskwa	production gas	-34.6	-36.8	
3	Muskwa	production gas	-35.5	-38.1	
3	Muskwa	production gas	-35.9	-36.7	
3	Muskwa	production gas	-34.2	-34.9	
4	Muskwa	production gas	-31.3	-34.7	-37.1

4	Muskwa	production gas	-32.2	-32.4	-41.9
4	Muskwa	production gas	-31.9	-30.8	-37.1
4	Muskwa	production gas	-32.0	-31.6	-39.5
4	Muskwa	production gas	-31.7	-32.1	-36.7
4	Muskwa	production gas	-31.2	-31.7	-38.8
4	Muskwa	production gas	-31.4	-31.9	-37.7
4	Muskwa	production gas	-33.7	-32.3	-39.7
4	Muskwa	production gas	-31.8	-31.0	
4	Muskwa	production gas	-32.9	-35.2	-36.4
4	Muskwa	production gas	-35.7	-35.7	-38.1
4	Muskwa	production gas	-32.9	-35.8	-36.8
4	Muskwa	production gas	-34.3	-35.8	-37.4
4	Muskwa	production gas	-33.7	-36.4	
4	Muskwa	production gas	-34.5	-36.4	
4	Muskwa	production gas	-34.1	-36.4	
4	Muskwa	production gas	-35.0	-36.2	
5	Muskwa	production gas	-35.2	-33.7	-40.6
5	Muskwa	production gas	-35.1	-34.6	-43.4
5	Muskwa	production gas	-35.6	-34.7	-39.0
5	Muskwa	production gas	-36.9	-34.6	-37.6
5	Muskwa	production gas	-36.5	-34.7	-36.0
5	Muskwa	production gas	-35.0	-34.6	-36.2
5	Muskwa	production gas	-38.1	-34.8	-35.7
5	Muskwa	production gas	-34.4	-34.9	-35.2
5	Muskwa	production gas	-36.1	-35.1	-35.8
5	Muskwa	production gas	-36.2	-35.0	-35.6
5	Muskwa	production gas	-37.2	-35.1	-36.7
5	Muskwa	production gas	-35.4	-35.0	
5	Muskwa	production gas	-34.8	-35.1	
5	Muskwa	production gas	-37.0	-35.0	
5	Muskwa	production gas	-36.7	-34.8	
5	Muskwa	production gas	-36.6	-35.2	
5	Muskwa	production gas	-35.8	-35.3	-35.8
5	Muskwa	production gas	-36.1	-35.4	
5	Muskwa	production gas	-36.1	-35.1	-38.2
5	Muskwa	production gas	-36.3	-35.1	-36.3
5	Muskwa	production gas	-36.9	-35.1	-33.8
6	Otter Park	mud gas	-35.7	-32.9	-27.3
6	Otter Park	mud gas	-31.9	-34.3	-27.1
6	Otter Park	mud gas	-33.9	-33.6	-28.1

6	Otter Park	mud gas	-35.4	-34.5	-28.2
6	Otter Park	mud gas	-30.3		
6	Otter Park	mud gas	-33.9	-33.0	-28.3
6	Otter Park	mud gas	-35.9	-37.1	-30.6
6	Otter Park	mud gas	-32.0	-35.6	-35.9
6	Otter Park	mud gas	-34.5	-34.1	-27.8
6	Otter Park	mud gas	-34.3	-34.7	-30.0
6	Otter Park	mud gas	-34.2	-33.8	
6	Otter Park	mud gas	-36.1	-32.2	-28.1
6	Otter Park	mud gas	-33.6		-28.5
6	Otter Park	mud gas	-31.2	-31.4	-27.3
6	Otter Park	mud gas	-34.1		-27.5
6	Otter Park	mud gas	-35.3	-37.4	-26.7
6	Otter Park	mud gas	-36.0	-35.0	-27.4
6	Otter Park	mud gas	-28.0	-39.8	-28.2
6	Otter Park	mud gas	-35.9	-33.6	-29.7
6	Otter Park	mud gas	-37.2	-35.8	
6	Otter Park	mud gas	-35.7	-30.3	
6	Otter Park	mud gas	-36.9	-26.9	
6	Otter Park	mud gas	-35.4		
6	Otter Park	mud gas	-35.4	-33.8	-26.7
6	Otter Park	mud gas	-36.6	-33.5	
6	Otter Park	production gas	-33.6	-34.7	-37.9

In this study shale gases were sampled from three adjacent well pads in the Horn River Basin, hence the geological history is identical and the source (Type II kerogen) and thermal maturity is considered fairly constant. Any variation in carbon isotope signatures of the natural gas would therefore primarily reflect isotope fractionation effects due to (i) gas generation or (ii) gas transport processes during degassing of the shale. Carbon isotope data for mud gases and production gases are presented using the James maturity diagram (James, 1983), isotope cross-plots (methane/ethane and ethane/propane) and the Natural Gas Plot (Chung et al., 1988). The James maturity diagram (Fig. 5.6) shows the average mud gas isotope composition for the Muskwa Formation. The diminutive isotopic separation between the carbon isotope ratios ($^{13}\text{C}/^{12}\text{C}$) of hydrocarbon components reveals the high thermal maturity of the gas.

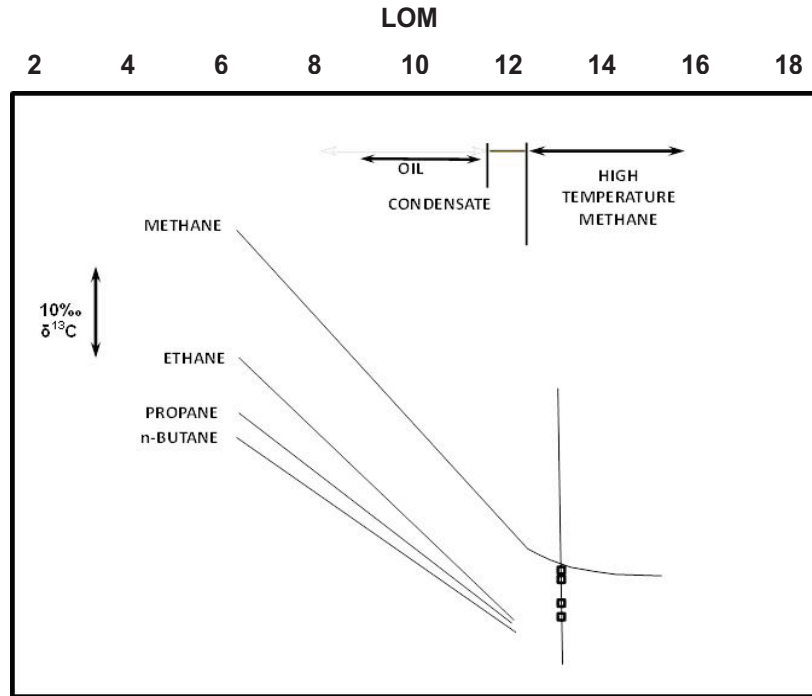


Figure 5.6 The James maturity diagram illustrating Muskwa mud gas (after James, 1983). The plot shows the average $\delta^{13}\text{C}$ values of methane, ethane, propane and butane for all Muskwa mud gases. Isotopic separations between components determine the level of organic maturity (LOM).

The $\delta^{13}\text{C}_{\text{ethane}}$ vs $\delta^{13}\text{C}_{\text{methane}}$ cross-plots and the $\delta^{13}\text{C}_{\text{propane}}$ vs and $\delta^{13}\text{C}_{\text{ethane}}$ cross-plots for Muskwa gases are shown in Fig. 5.7a and Fig.5.7b respectively. In Fig. 5.8a and Fig.5.8b cross-plots for Otter Park gases are presented; $\delta^{13}\text{C}_{\text{ethane}}$ vs $\delta^{13}\text{C}_{\text{methane}}$ and $\delta^{13}\text{C}_{\text{propane}}$ vs and $\delta^{13}\text{C}_{\text{ethane}}$. The high degree of scatter in these plots reflects the variation in carbon isotope ratios ($^{13}\text{C}/^{12}\text{C}$) of shale gases from the Muskwa and Otter Park Formations. In production gas samples from the Muskwa, carbon isotope values ($\delta^{13}\text{C}$) of methane show a wide range from -38.1 to -30.5‰. The $\delta^{13}\text{C}_{\text{propane}}$ vs and $\delta^{13}\text{C}_{\text{ethane}}$ cross-plots for Muskwa gases and Otter Park gases (Fig.5.7b and Fig.5.8b) show differentiation between the carbon isotope ratios of mud gases and production gases which plot in separate regions of the graph.

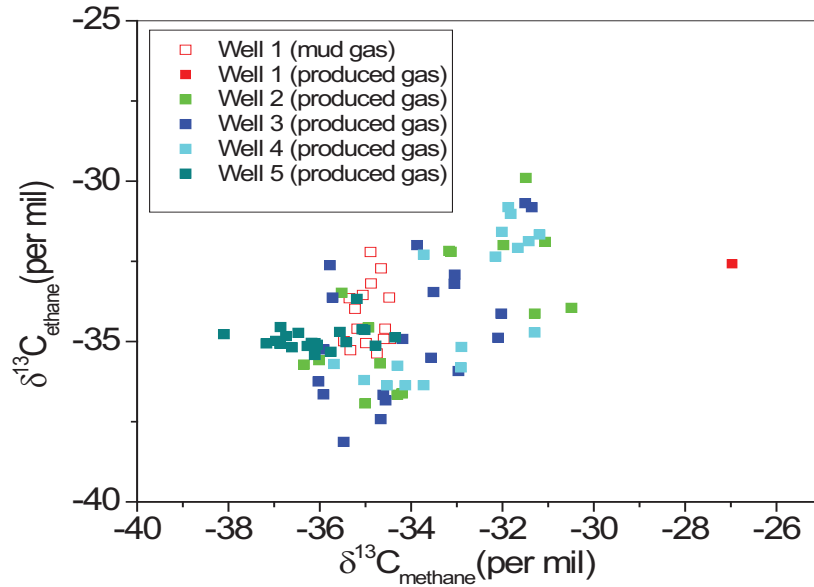


Figure 5.7(a) Cross-plots of $\delta^{13}\text{C}_{\text{ethane}}$ vs $\delta^{13}\text{C}_{\text{methane}}$ gases from the Muskwa. $\delta^{13}\text{C}$ values of methane and ethane for samples of mud gas and production gas are shown for the 5 well locations in the HRB.

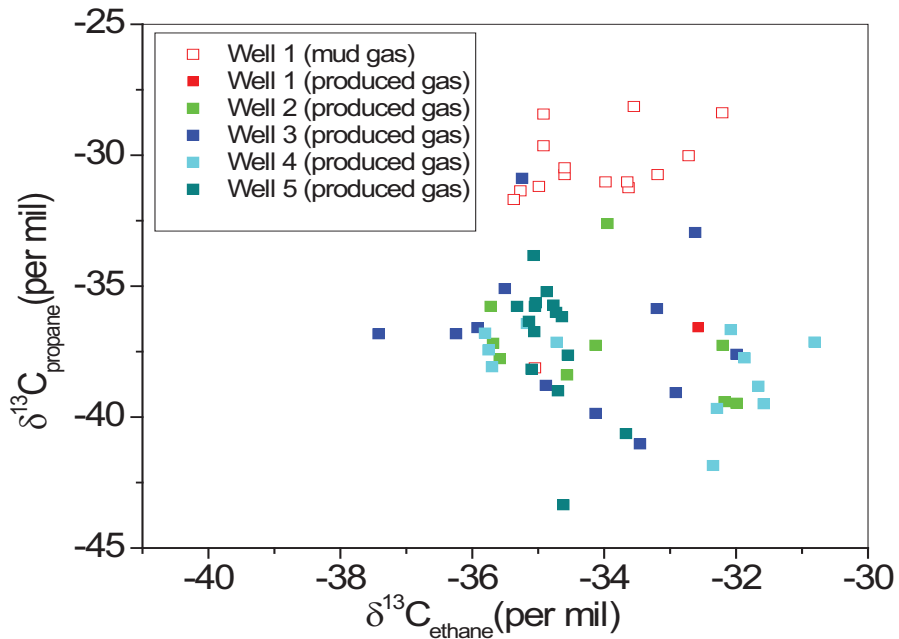


Figure 5.7(b) Cross-plots of $\delta^{13}\text{C}_{\text{propane}}$ vs $\delta^{13}\text{C}_{\text{ethane}}$ gases from the Muskwa. $\delta^{13}\text{C}$ values of methane and ethane for samples of mud gas and production gas are shown for the 5 well locations in the HRB.

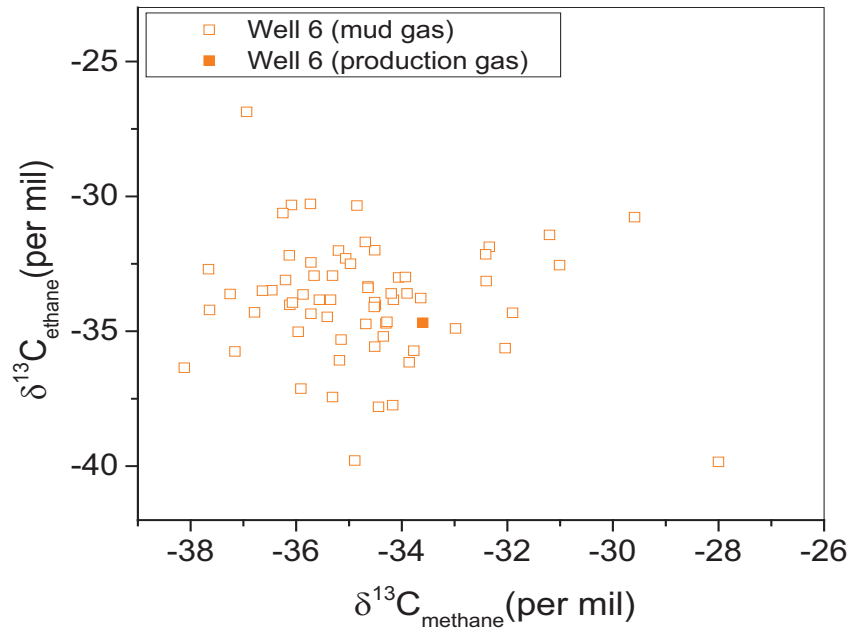


Figure 5.8(a) Cross-plots of $\delta^{13}\text{C}_{\text{ethane}}$ vs $\delta^{13}\text{C}_{\text{methane}}$ gases from the Otter Park $\delta^{13}\text{C}$ values of methane and ethane for samples of mud gas and production gas are shown for the 5 well locations in the HRB.

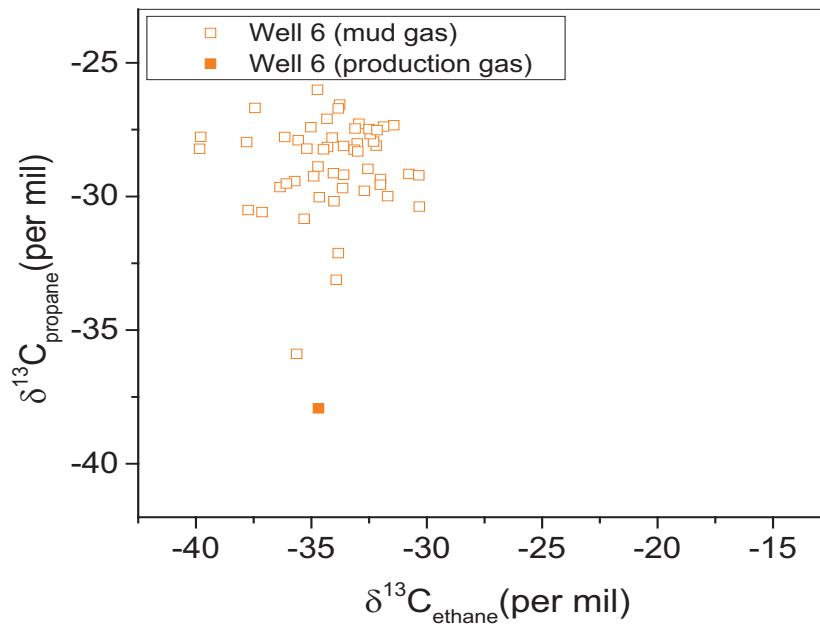


Figure 5.8(b) Cross-plots of $\delta^{13}\text{C}_{\text{propane}}$ vs $\delta^{13}\text{C}_{\text{ethane}}$ gases from the Otter Park. $\delta^{13}\text{C}$ values of methane and ethane for samples of mud gas and production gas are shown for the 5 well locations in the HRB.

In Figs. 5.9 to Fig 5.11 Natural gas plots depict the carbon isotope signatures of shale gases from the Muskwa and Otter Park. In these plots, $\delta^{13}\text{C}$ values of hydrocarbons components (C1-C4) are shown as a function of $1/n$ (the inverse of the number of carbon atoms). The plot was originally used for gases from conventional reservoirs where co-genetic gases show linearity on the plot while gas mixtures or heterogeneity in the source cause deviations (Chung et al., 1988; Rooney et al., 1995). The Natural gas plot is practical for presentation of carbon isotope signatures ($\delta^{13}\text{C}_{\text{methane}}$, $\delta^{13}\text{C}_{\text{ethane}}$, $\delta^{13}\text{C}_{\text{propane}}$ and $\delta^{13}\text{C}_{\text{butane}}$) of natural gas and use has been extended to unconventional shale gas reservoirs (Rodriguez and Philp, 2010; Tilley et al., 2011); however a new approach is required for interpretation of data.

In Fig. 5.9a and Fig. 5.9b Natural gas plots are shown for Well 1 which is completed in the Muskwa Formation. In Well 1 Muskwa mud gases show no isotope reversals whereas Muskwa production gas show full reversal in carbon isotope signature ($\delta^{13}\text{C}_{\text{propane}} < \delta^{13}\text{C}_{\text{ethane}} < \delta^{13}\text{C}_{\text{methane}}$). Fig 5.10 shows production gases for Wells 2 to 5 which are all completed in the Muskwa. It is evident that these production gases from these wells also show isotope reversals in the carbon isotope signatures.

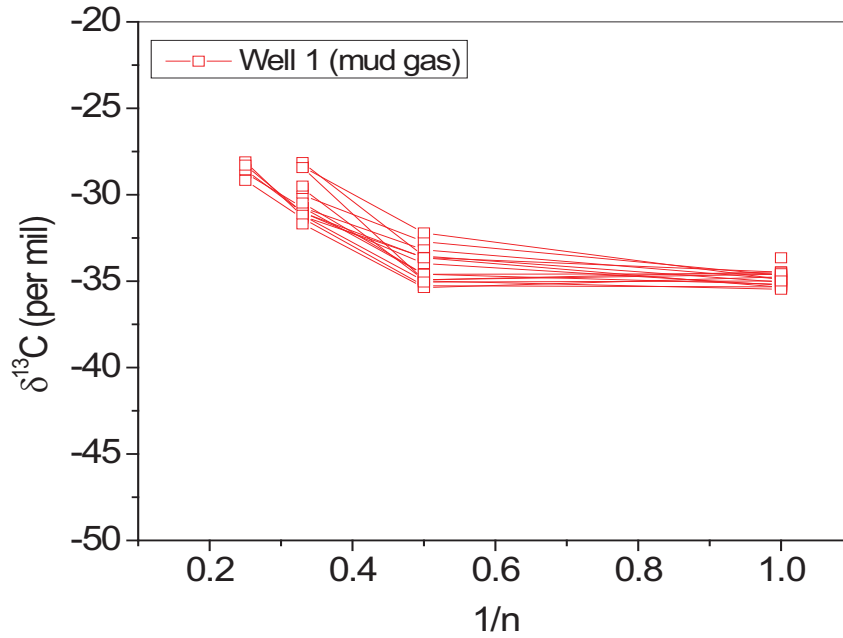


Figure 5.9 (a) The natural gas plot for Muskwa mud gases. $\delta^{13}\text{C}$ values (C1- C4 components) vs $1/n$ are plot where n represents the number of carbon atoms in the hydrocarbon.

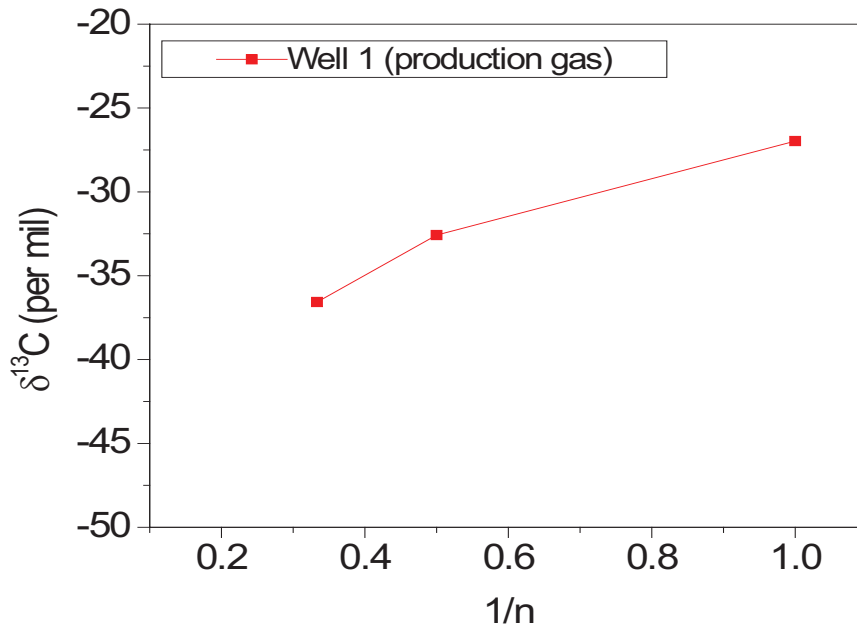


Figure 5.9 (b) The natural gas plot for Muskwa production gas. $\delta^{13}\text{C}$ values (C1- C4 components) vs $1/n$ are plot where n represents the number of carbon atoms in the hydrocarbon.

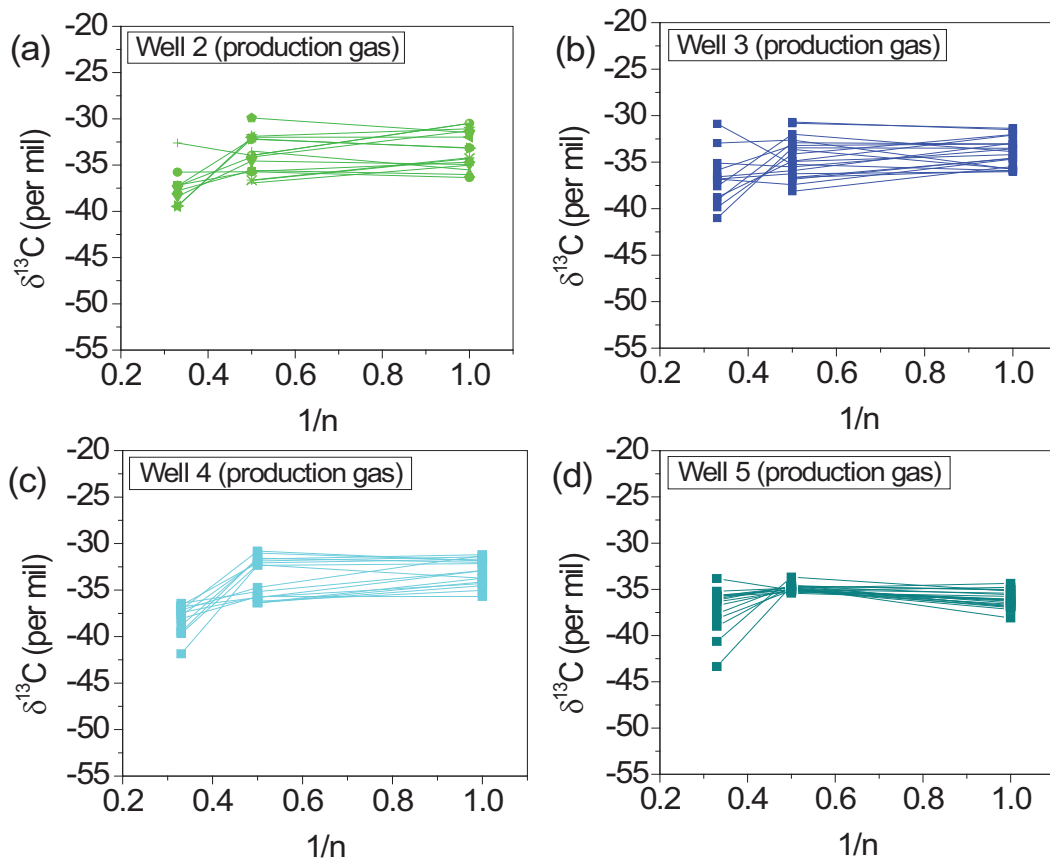


Figure 5.10 Natural gas plots for Muskwa production gases. $\delta^{13}\text{C}$ values (C1-C4 components) vs $1/n$ are plot where n represents the number of carbon atoms in the hydrocarbon.

In Fig. 5.11a and Fig. 5.11b Natural gas plots are shown for Well 6 which is completed in the Otter Park Formation. Mud gases from the Otter Park show mainly non reversed signatures whereas the production gas sampled from this well indicates a reversed gas signature.

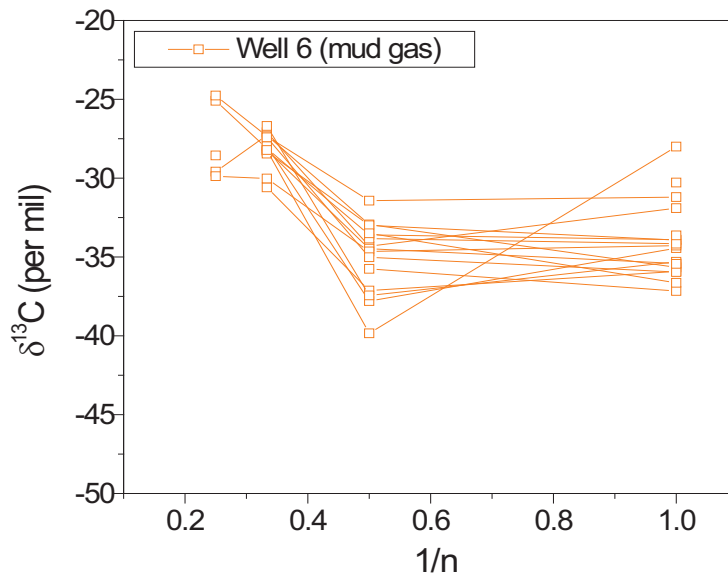


Figure 5.11 (a) The Natural gas plot for Otter Park mud gases. $\delta^{13}\text{C}$ values (C1- C4 components) vs $1/n$ are plot where n represents the number of carbon atoms in the hydrocarbon.

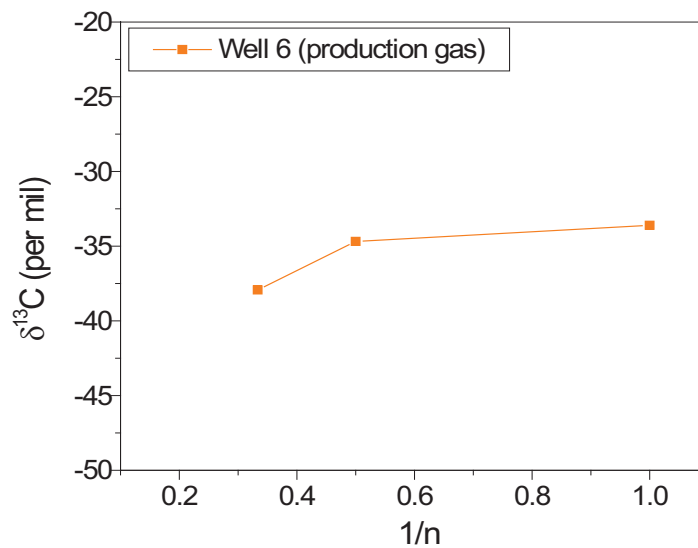


Figure 5.11 (b) The Natural gas plot for Otter Park production gas. $\delta^{13}\text{C}$ values (C1- C4 components) vs $1/n$ are plot where n represents the number of carbon atoms in the hydrocarbon.

A classification scheme for shale gases (Tilley and Muehlenbachs, 2012) is shown in Table 5.2 where gases are grouped into three categories based on their isotope signature: (i) normal (ii) partially reversed and (iii) fully reversed gas.

Table 5.2 Classification scheme for shale gases based on their carbon isotope signatures

Gas Type	Carbon isotope signature
Non- reversed	$\delta^{13}\text{C}_{\text{methane}} < \delta^{13}\text{C}_{\text{ethane}} < \delta^{13}\text{C}_{\text{propane}}$
Partially reversed	(1) $\delta^{13}\text{C}_{\text{ethane}} < \delta^{13}\text{C}_{\text{methane}}$ and $\delta^{13}\text{C}_{\text{ethane}} < \delta^{13}\text{C}_{\text{propane}}$ OR (2) $\delta^{13}\text{C}_{\text{methane}} < \delta^{13}\text{C}_{\text{ethane}}$ and $\delta^{13}\text{C}_{\text{propane}} < \delta^{13}\text{C}_{\text{ethane}}$
Fully reversed	$\delta^{13}\text{C}_{\text{propane}} < \delta^{13}\text{C}_{\text{ethane}} < \delta^{13}\text{C}_{\text{methane}}$

In a large number of mud gases analysed, the carbon isotope signature show no isotopic reversals and $\delta^{13}\text{C}_{\text{methane}} < \delta^{13}\text{C}_{\text{ethane}} < \delta^{13}\text{C}_{\text{propane}} < \delta^{13}\text{C}_{\text{butane}}$. These gases are shown in the natural gas plots (Fig. 5.9a and 5.11a) and $\delta^{13}\text{C}_{\text{ethane}}$, $\delta^{13}\text{C}_{\text{propane}}$ and $\delta^{13}\text{C}_{\text{butane}}$ plot on a straight line with an intercept value of approximately -23‰ which may represent the $\delta^{13}\text{C}$ of the source organic matter. Mud gases are sampled during drilling and contain both ‘free’ and ‘adsorbed’ gas components which are entrained in the drilling fluid as gas is liberated from drill cuttings and produced from the surrounding formation as the bit penetrates the shale. Carbon isotope signatures of production gases from the Muskwa and Otter Park formations are presented in Fig. 5.9b and Fig. 5.11b and indicate partially reversed and fully reversed gases.

In general, carbon isotope signatures ($\delta^{13}\text{C}_{\text{methane}}$, $\delta^{13}\text{C}_{\text{ethane}}$, $\delta^{13}\text{C}_{\text{propane}}$ and $\delta^{13}\text{C}_{\text{butane}}$) of Muskwa and Otter Park shale gases differed for mud gas and production gas samples. The largest variation between the two types of samples was observed for $\delta^{13}\text{C}_{\text{propane}}$ where the average values differed up to ~7 ‰ for mud gases and production gases respectively.

The isotope signatures observed in mud gas samples were characteristic of a mature thermogenic gas where methane is enriched in ^{13}C . In theoretical and experimental investigation (Arneth and Matzigkeit, 1986; Rooney et al., 1995; Lorant et al., 1998; Tang et al., 2000) carbon isotope signatures during thermogenic gas generation in open and closed system conditions show no isotope reversals, although laboratory experiments and theoretical models may not necessarily reflect reactions under geological conditions.

Mud gas samples are collected during drilling and prior to the process of hydraulic fracturing hence gas isotope signatures may be less strongly influenced by transport processes which occur during degassing of shale. Theoretical and experimental studies show large isotope fractionation effects may occur during gas flow through fine grained sedimentary shales which ultimately impact the carbon isotope signature (Zhang and Krooss, 2001; Strapoć et al., 2010; Tang and Xia, 2011; Amann-Hildenbrand et al., 2012; Xia and Tang, 2012; Hu et al., 2012). The initial absence of ‘isotope reversals’ in Muskwa mud gases and subsequent appearance in production gases suggests these reversals may be a result of isotope fractionation effects as gas is transported from the shale to the wellbore during production.

It is noteworthy in published work where ‘isotope reversals’ are reported generally samples of production gases were analysed for carbon isotope ratios; thus it is plausible ‘isotope reversals’ observed in shale gases may be the result of isotope fractionation which occurs during gas transport in ultra-low permeability shales. In one study found in the literature (Schoell et al., 2012) mud gases were analysed for carbon isotope ratios of Paleozoic shale gas. These mud gases were also non-reversed based on their carbon isotope signature hence findings were consistent with the results of this work.

5.4 Conclusions

Devonian Muskwa and Otter Park shale gases from wells in the study region of the Horn River Basin are dry and thermogenic in origin. In general clear differences are observed where mud gases samples exhibited no isotope reversal in their carbon isotope signatures while production gases showed partial or full isotope reversals among hydrocarbon components. Carbon isotope ratios ($^{13}\text{C}/^{12}\text{C}$) of hydrocarbon gas components indicate Muskwa and Otter Park production gases fall within the 'post-rollover zone' as defined in Tilley and Muehlenbachs (2012) and indicative of a highly mature shale gas system; also revealed by vitrinite reflectance (R_o) values of 2.2% to 2.6%. Variation in $\delta^{13}\text{C}$ values among sample type (mud gas or production gas) and within production gases from a single well suggests the sample type and time of collection should be considered during interpretation of stable carbon isotope data from unconventional gas shales. Isotope reversals observed in production gas samples are interpreted to be the result of isotope fractionation effects which occur as gas flows through pores in the shale matrix to the wellbore. The following support this hypothesis: (i) the lack of isotope reversals in mud gases and while production gases showed partial or full reversal (ii) the carbon isotope signatures observed in Muskwa and Otter Park mud gases are characteristic of a mature thermogenic gas (iii) significant isotope fractionation effects are known to occur in shales as gas flows through pores of the rock (iv) theoretical and experimental work show no isotope reversal during gas generation in closed system.

Carbon isotope geochemistry can provide valuable information for elucidation of shale resource plays; however evaluation must be performed within the geological context of the basin. Ultimately understanding processes which occur in the shale gas systems and impact the isotope signatures of the gas may provide data to assist in exploration and development of these unconventional reservoirs.

References Cited

Adams, C., 2012, Summary of Shale Gas Activity in Northeast British Columbia 2011 Oil and Gas Reports 2012-1, BC Ministry of Energy and Mines, Geoscience and Strategic Initiatives Branch.

Amann-Hildenbrand, A., A. Ghanizadeh, and B. M. Krooss, 2012, Transport properties of unconventional gas systems, *Marine and Petroleum Geology*, vol. 31, no. 1, p. 90-99.

Arneth, J. D., 1984, Stable isotope and organo-geochemical studies on phanerozoic sediments of the Williston Basin, North America, *Chemical Geology*, vol. 46, no. 2, p. 113-140.

Arneth, J. D. and U. Matzigkeit, 1986, Variations in the carbon isotope composition and production yield of various pyrolysis products under open and closed system conditions, *Organic Geochemistry*, vol. 10, no. 4-6, p. 1067-1071.

B.C. Ministry of Energy and Mines and National Energy Board, 2011, Ultimate Potential for Unconventional Natural Gas in Northeastern British Columbia's Horn River Basin. Oil and Gas Reports 2011-1, <<http://www.empr.gov.bc.ca/OG/Documents/HornRiverEMA.pdf>> Accessed 10/11, 2013

Berner, U. and E. Faber, 1988, Maturity related mixing model for methane, ethane and propane, based on carbon isotopes, *Organic Geochemistry*, vol. 13, no. 1-3, p. 67-72.

Burruss, R. C. and C. D. Laughrey, 2010, Carbon and hydrogen isotopic reversals in deep basin gas: Evidence for limits to the stability of hydrocarbons, *Organic Geochemistry*, vol. 41, no. 12, p. 1285-1296.

- Chung, H. M., J. R. Gormly, and R. M. Squires, 1988, Origin of gaseous hydrocarbons in subsurface environments: Theoretical considerations of carbon isotope distribution, *Chemical Geology*, vol. 71, no. 1-3, p. 97-104.
- Claypool, G. E. and K. A. Kvenvolden, 1983, Methane and other hydrocarbon gases in marine sediment, *Annual Review of Earth and Planetary Sciences*, vol. 11, p. 299.
- Clayton, C., 1991, Carbon isotope fractionation during natural gas generation from kerogen, *Marine and Petroleum Geology*, vol. 8, no. 2, p. 232-240.
- Close, D., M. Perez, B. Goodway, and G. Purdue, 2012, Integrated workflows for shale gas and case study results for the Horn River Basin, British Columbia, Canada, *The Leading Edge*, vol. 31, no. 5, p. 556-569.
- Curtis, J. B., 2002, Fractured Shale-Gas Systems, *AAPG Bulletin*, vol. 86, no. 11, p. 1921-1938.
- Dewitt, W., 1984, Devonian gas shales and related tight reservoir rocks of Appalachian basin, *AAPG Bulletin*, vol. 68. no.4, p.470.
- Faber, E., W. Stahl, and M. Whiticar, 1992, Distinction of bacterial and thermogenic hydrocarbon gases, *Bacterial gas: Paris, Editions Technip*, p. 63-74.
- Freeman, C., G. J. Moridis, G. E. Michael, and T. A. Blasingame, 2012, Measurement, Modeling, and Diagnostics of Flowing Gas Composition Changes in Shale Gas Wells, *SPE Latin America and Caribbean Petroleum Engineering Conference*, 16-18 April 2012, Mexico City, Mexico.
- Fuex, A. N., 1977, The use of stable carbon isotopes in hydrocarbon exploration, *Journal of Geochemical Exploration*, vol. 7, p. 155-188.

- Fuex, A. N., 1980, Experimental evidence against an appreciable isotopic fractionation of methane during migration, *Physics and Chemistry of the Earth*, vol. 12, p. 725-732.
- Gray, F. F. and J. Kassube, 1963, Geology and stratigraphy of Clarke Lake gas field, British Columbia, *AAPG Bulletin*, vol. 47, no. 3, p. 467-483.
- Griffin, D., 1965, The facies front of the Devonian Slave Point-Elk Point sequence in northeastern British Columbia and the Northwest Territories, *Journal of Canadian Petroleum Technology*, vol. 4, no. 1, p. 13-22.
- Hill, R. J., E. Zhang, Y. Tang, and B. Katz, 2006, Estimating shale gas potential from confined pyrolysis experiments, *Rocky Mountain Natural Gas Geology and Resource Conference Program and Abstracts*, p. 124, 126.
- Hu, Q., Z. Gao, S. Peng, and R. Ewing, 2012, Pore Structure Inhibits Gas Diffusion in the Barnett Shale,
<http://www.searchanddiscovery.netwww.searchanddiscovery.net/documents/2012/50609hu/ndx_hu.pdf> Accessed 09/11, 2012.
- James, A. T., 1983, Correlation of natural gas by use of carbon isotopic distribution between hydrocarbon components, *AAPG Bulletin*, vol. 67, no. 7, p. 1176-1191.
- James, A. T., 1990, Correlation of reservoired gases using the carbon isotopic compositions of wet gas components, *AAPG Bulletin*, vol. 74, no. 9, p. 1441-1458.
- Jenden, P. D., D. J. Drazan, and I. R. Kaplan, 1993, Mixing of thermogenic natural gases in northern Appalachian Basin, *AAPG Bulletin*, vol. 77, no. 6, p. 980-998.

- Kent, D., 1994, Paleogeographic evolution of the cratonic platform-Cambrian to Triassic, Geological Atlas of the Western Canada Sedimentary Basin, p. 69-86.
- Lorant, F., A. Prinzhofer, F. Behar, and A. Huc, 1998, Carbon isotopic and molecular constraints on the formation and the expulsion of thermogenic hydrocarbon gases, *Chemical Geology*, vol. 147, no. 3-4, p. 249-264.
- Magoon, L. and J. Schmoker, 2000, The total petroleum system—The natural fluid network that constrains the assessment unit, US geological survey world petroleum assessment, p. 31.
- Magoon, L.B., and Dow, W.G., 1994, The petroleum system, in Magoon, L.B., and Dow, W.G., eds., *The petroleum system—From source to trap: Tulsa, Okla., American Association of Petroleum Geologists Memoir 60*, p. 3-24.
- Martini, A. M., L. M. Walter, J. M. Budai, T. C. W. Ku, C. J. Kaiser, and M. Schoell, 1998, Genetic and temporal relations between formation waters and biogenic methane: Upper Devonian Antrim Shale, Michigan Basin, USA, *Geochimica et Cosmochimica Acta*, vol. 62, no. 10, p. 1699-1720.
- Monger, J. and R. Price, 1979, Geodynamic evolution of the Canadian Cordillera—progress and problems, *Canadian Journal of Earth Sciences*, vol. 16, no. 3, p. 770-791.
- Mukhopadhyay, P. K. and W. G. Dow, 1994, Vitrinite reflectance as a maturity parameter (applications and limitations), A. C. S. symposium series. American Chemical Society Symposium Series 570, p. 1-24.
- Nexen Corporate Update, 2011,
<http://www.nexencoold.com/~media/Files/Presentations/PDF/Nexen_IRRoaddshow_UBS.ashx> Accessed 01/27, 2014.

Norville, G. A. and R. A. Dawe, 2007, Carbon and hydrogen isotopic variations of natural gases in the southeast Columbus basin offshore southeastern Trinidad, West Indies – clues to origin and maturity, *Applied Geochemistry*, vol. 22, no. 9, p. 2086-2094.

Oldale, H. and R. Munday, 1994, Devonian Beaverhill Lake Group of the western Canada sedimentary basin, *Geological Atlas of the Western Canada Sedimentary Basin*, p. 149-164.

Price, R., 1994, Cordilleran tectonics and the evolution of the Western Canada Sedimentary Basin, *Geological Atlas of the Western Canada Sedimentary Basin*, p. 13-24.

Prinzhofer, A. A. and A. Y. Huc, 1995, Genetic and post-genetic molecular and isotopic fractionations in natural gases, *Chemical Geology*, vol. 126, no. 3-4, p. 281-290.

Ramos, S., 2004, The effect of shale composition on the gas sorption potential of organic-rich mudrocks in the Western Canadian sedimentary basin, M.Sc. thesis University of British Columbia, Vancouver, Canada (2004).

Rice, D. D. and G. E. Claypool, 1981, Generation, accumulation, and resource potential of biogenic gas, *AAPG Bulletin*, vol. 65, no. 1, p. 5-25.

Rodriguez, N. D. and R. P. Philp, 2010, Geochemical characterization of gases from the Mississippian Barnett Shale, Fort Worth Basin, Texas, *AAPG Bulletin*, vol. 94, no. 11, p. 1641-1656.

Rooney, M. A., G. E. Claypool, and H. Moses Chung, 1995, Modeling thermogenic gas generation using carbon isotope ratios of natural gas hydrocarbons, *Chemical Geology*, vol. 126, no. 3-4, p. 219-232.

Root, K. G., 2001, Devonian Antler fold and thrust belt and foreland basin development in the southern Canadian Cordillera: implications for the Western Canada Sedimentary Basin, *Bulletin of Canadian Petroleum Geology*, vol. 49, no. 1, p. 7-36.

Ross, D. J. K. and R. M. Bustin, 2008, Characterizing the shale gas resource potential of Devonian Mississippian strata in the Western Canada sedimentary basin: Application of an integrated formation evaluation, *AAPG Bulletin*, vol. 92, no. 1, p. 87-125.

Ross, D. J. K. and M. Bustin, 2009, The importance of shale composition and pore structure upon gas storage potential of shale gas reservoirs, *Marine and Petroleum Geology*, vol. 26, no. 6, p. 916-927.

Rowe, D. and A. Muehlenbachs, 1999a, Low-temperature thermal generation of hydrocarbon gases in shallow shales, *Nature*, vol. 398, no. 6722, p. 61-63.

Rowe, D. and K. Muehlenbachs, 1999b, Isotopic fingerprints of shallow gases in the Western Canadian sedimentary basin: tools for remediation of leaking heavy oil wells, *Organic Geochemistry*, vol. 30, no. 8, Part 1, p. 861-871.

Schoell, M., U. Bieg, M. Schmitt, A. Jurisch, and B. Nadolny, 2012, Mudgas Isotope Interpretations for Assessment of Paleozoic Shales in Poland Martin Schoell , *SDGG GeoHannover 2012 October 1-3, 2012*.

Schoell, M., 1980, The hydrogen and carbon isotopic composition of methane from natural gases of various origins, *Geochimica et Cosmochimica Acta*, vol. 44, no. 5, p. 649-661.

Schoell, M., 1983, Genetic characterization of natural gases, *AAPG Bulletin*, vol. 67, no. 12, p. 2225-2238.

Schoell, M., 1984, Recent advances in petroleum isotope geochemistry, *Organic Geochemistry*, vol. 6, p. 645-663.

Schoell, M., 1988, Multiple origins of methane in the Earth, *Chemical Geology*, vol. 71, no. 1-3, p. 1-10.

Seewald, J. and J. Whelan, 2005, Isotopic and chemical composition of natural gas from the Potato Hills Field, Southeastern Oklahoma: Evidence for an Abiogenic Origin?

<http://www.searchanddiscovery.com/documents/abstracts/2005research_calgary/abstracts/extended/seewald/seewald.htm> Accessed 10/18, 2013.

Shurr, G. W. and J. L. Ridgley, 2002, Unconventional Shallow Biogenic Gas Systems, *AAPG Bulletin*, vol. 86, no. 11, p. 1939-1969.

Stasiuk, L. D. and M. G. Fowler, 2004, Organic facies in Devonian and Mississippian strata of Western Canada Sedimentary Basin: relation to kerogen type, paleoenvironment, and paleogeography, *Bulletin of Canadian Petroleum Geology*, vol. 52, no. 3, p. 234-255.

Strapoć, D., G. Michael, J. Roper, and Maguire Matt, 2010, Insights into Shale Gas Production & Storage From Gas Chemistry – What Is It Telling Us?

<http://www.searchanddiscovery.com/abstracts/pdf/2011/hedberg-texas/abstracts/ndx_strapoc.pdf> Accessed 09/13, 2013.

Switzer, S., W. Holland, D. Christie, G. Graf, A. Hedinger, R. McAuley, R. Wierzbicki, and J. Packard, 1994, Devonian Woodbend-Winterburn strata of the Western Canada sedimentary basin, *Geological Atlas of the Western Canada Sedimentary Basin: Canadian Society of Petroleum Geologists and Alberta Research Council*, p. 165-202.

Tang, Y. and D. Xia, 2011, Predicting Original Gas in Place and Optimizing Productivity by Isotope Geochemistry of Shale Gas,

<http://www.cspg.org/documents/Conventions/Archives/Annual/2011/204-Predicting_Original_Gas_in_Place_and_Optimizing_Productivity.pdf> Accessed 09/13, 2013.

Tang, Y., J. K. Perry, P. D. Jenden, and M. Schoell, 2000, Mathematical modeling of stable carbon isotope ratios in natural gases, *Geochimica et Cosmochimica Acta*, vol. 64, no. 15, p. 2673-2687.

Tilley, B. and K. Muehlenbachs, 2012, Isotope Systematics of High Maturity Shale Gases in the WCSB Compared to Other North American Shale Gases, <http://www.cspg.org/documents/Conventions/Archives/Annual/2012/026_GC2012_Isotope_Systematics_of_High_Maturity_Shale_Gases.pdf> Accessed 09/11, 2013.

Tilley, B. and K. Muehlenbachs, 2006, Gas maturity and alteration systematics across the Western Canada Sedimentary Basin from four mud gas isotope depth profiles, *Organic Geochemistry*, vol. 37, no. 12, p. 1857-1868.

Tilley, B., S. McLellan, S. Hiebert, B. Quartero, B. Veilleux, and K. Muehlenbachs, 2011, Gas isotope reversals in fractured gas reservoirs of the western Canadian Foothills: Mature shale gases in disguise, *AAPG Bulletin*, vol. 95, no. 8, p. 1399-1422.

Tilley, B. and K. Muehlenbachs, 2013, Isotope reversals and universal stages and trends of gas maturation in sealed, self-contained petroleum systems, *Chemical Geology*, vol. 339, p. 194-204.

Weissenberger, J. A. W. and K. Potma, 2001, The Devonian of western Canada -- aspects of a petroleum system: Introduction, *Bulletin of Canadian Petroleum Geology*, vol. 49, no. 1, p. 1-6.

Williams, G. K., 1983, What does the term 'Horn River Formation' mean? *Bulletin of Canadian Petroleum Geology*, vol. 31, no. 2, p. 117-122.

- Xia, X. and Y. Tang, 2012, Isotope fractionation of methane during natural gas flow with coupled diffusion and adsorption/desorption, *Geochimica et Cosmochimica Acta*, vol. 77, p. 489-503.
- Zhang, T. and B. M. Krooss, 2001, Experimental investigation on the carbon isotope fractionation of methane during gas migration by diffusion through sedimentary rocks at elevated temperature and pressure, *Geochimica et Cosmochimica Acta*, vol. 65, no. 16, p. 2723-2742.
- Zumberge, J., K. Ferworn, and S. Brown, 2012, Isotopic reversal ('rollover') in shale gases produced from the Mississippian Barnett and Fayetteville formations, *Marine and Petroleum Geology*, vol. 31, no. 1, p. 43-52.

CHAPTER 6

6.1 CONCLUSIONS

Stable isotope geochemistry is essential for characterization of natural gas and this study provided insight into the properties of gases from the Horn River Basin; a major emerging Canadian unconventional shale gas play. Integration of various types of data is necessary for reservoir evaluation and the use of stable isotopes is shown to be a complementary analytical tool. In this thesis, each chapter focused on a particular aspect or application of stable isotope geochemistry in analysis of natural gas from formations in the Dilly Creek area of the Horn River Basin and the major conclusions are presented.

6.1.1 Environmental remediation

Variations in carbon ($^{13}\text{C}/^{12}\text{C}$) and hydrogen (D/H) isotope ratios of natural gases obtained from the Devonian Evie shale gas target formation to the Cretaceous Dunvegan Formation are shown using stable isotope geochemistry. In general, carbon isotope values of methane ($\delta^{13}\text{C}_{\text{methane}}$) indicated higher gas maturity with increasing subsurface depth. $\delta^{13}\text{C}_{\text{methane}}$ values of gases ranged from approximately -55‰ at depths near surface to -28‰ in the target shale formation. Carbon isotope values ($\delta^{13}\text{C}$) of Horn River Basin gases denote high thermal maturity and confirm a thermogenic gas origin. Detailed carbon isotope depth profiles created for Nexen HZ TSEA B-018-I/094-O-08 record the subsurface changes in the $\delta^{13}\text{C}$ values of methane, ethane and propane ($\delta^{13}\text{C}_{\text{methane}}$, $\delta^{13}\text{C}_{\text{ethane}}$ and $\delta^{13}\text{C}_{\text{propane}}$) of natural gases collected from these Paleozoic to Cretaceous sedimentary rocks. Using carbon isotope profiles, the depths at which isotope rollover and isotope reversals occur are identified. Carbon isotope data showed the shallowest depth at which isotope reversal is observed between methane and ethane ($\delta^{13}\text{C}_{\text{methane}} > \delta^{13}\text{C}_{\text{ethane}}$) lies within the Paleozoic shales of the Exshaw Formation.

Carbon isotope signatures ($\delta^{13}\text{C}_{\text{methane}}$, $\delta^{13}\text{C}_{\text{ethane}}$ and $\delta^{13}\text{C}_{\text{propane}}$) of Horn River Basin natural gases establish a geochemical fingerprint for this region. In

this study carbon isotope signatures of surface casing vent gases and soil gases from different leaking wells in the basin were matched to carbon isotope depth profiles and the gas origin identified. Other cases involving leaking gas wells in which vertical migration of stray gases occurs along the wellbore to surface can also be addressed since identification of source formations is feasible. Application of this technique is valuable for purposes of environmental remediation.

6.1.2 Flow connectivity in shale gas target formations

Devonian Muskwa and Otter Park Formations of the Horn River are heterogeneous in mineral composition at the Nexen Hz TSEA B-018-I/094-O-08 and Nexen Hz TSEA B-A18-I/094-O-08 well sites. Significant contrast in lateral carbon isotope depth profiles was observed in the Otter Park and Muskwa shale formations. Stable isotope composition analysis indicate natural gases from Horn River Basin shale gas target formations were deep, dry thermogenic gases; consistent with the thermal history of the Basin in this region and the vitrinite reflectance (R_o) values reported for the Dilly Creek region. Various stages are identified in transformation of organic matter to hydrocarbons (Hunt, 1984) and results suggest Horn River Group gases fall with the late catagenesis/ metagenesis stage in the gas window.

Mud gas isotope lateral profiles within the Muskwa and Otter Park target formations for shale gas production reflect differences in flow connectivity within the shale formations. Stable carbon isotope lateral profiles for the Muskwa Formation suggest a higher degree of pore connectivity within the shale of the Muskwa Formation compared to that of the Otter Park Formation. Connectivity in the pores of the Muskwa Formation may have contributed to the overall higher mud gas concentrations observed in this formation; however it does not preclude other factors which may have contributed to higher gas concentrations measured.

Although carbon isotope analysis of natural gas is routinely used in conventional hydrocarbon systems to identify compartmentalization within the reservoir, findings of this study show potential applications in unconventional gas shale formations. Extremely small pore sizes in the nanometer range have been

reported in the literature for gas shales; however limitations may include the resolution of the instruments used for measurements or the analytical techniques employed. Muskwa shales in the Horn River Group were quartz rich compared to the Otter Park shales which contained a higher percentage of clay minerals. It is likely that the difference in mineralogy for these two formations and the shale fabric play an important role in gas distribution and the carbon isotope signatures of the shale gas. Stable isotope geochemistry may be a useful technique for evaluation of pore connectivity in ultra-low permeability shale gas target formations.

6.1.3 Isotope fractionation effects during degassing of the shale reservoir

Variations in the carbon isotope signature of shale gases occur during production and carbon isotope ratios ($^{13}\text{C}/^{12}\text{C}$) of gases differ between wells even amongst those drilled from a single well pad location in the basin. Stable isotope data showed initial ^{12}C methane enrichment and a general trend where gases show increased ^{13}C at later stages of production. It is likely this observed trend is due to the diffusivity differences in the methane isotopologues and theoretical models in current literature also predict such changes may occur during gas production (Tang and Xia, 2011; Xia et al., 2012). As various gas molecules (C1 to C4) traverse the complex shale fabric and move to the wellbore isotope fractionation effects occur and signatures of produced gases may reflect such effects. Periods of well 'shut in' and changes in gas production are accompanied by changes in the carbon stable isotope ratios of shale gases. Temporal variations in carbon and hydrogen stable isotope ratios of hydrocarbon components of shale gases ($\delta^{13}\text{C}_{\text{methane}}$, $\delta^{13}\text{C}_{\text{ethane}}$, $\delta^{13}\text{C}_{\text{propane}}$ and $\delta^{13}\text{C}_{\text{butane}}$ and $\delta\text{D}_{\text{methane}}$) occur during production from Devonian Horn River Group Formations.

6.1.4 Carbon isotope ratios of mud gas vs production gases

During interpretation of stable isotope compositional data from unconventional shale gas plays, the gas sample type selected for analysis should be taken into consideration. In this study stable carbon isotope signatures varied between mud gases and their corresponding production gases from the wells sampled. Gas origin and generation processes are important in determination of the carbon isotope signature of natural gas within sedimentary shale rocks. The mud gas carbon isotope signatures may be the most accurate representation of in situ gas in the reservoir since the rock is crushed releasing the gas from the matrix. In the natural gas plots for both the Otter Park and the Muskwa Formations, mud gas carbon isotope ratios of ethane, propane and butane followed the expected trend resulting in a straight line which intercepts the y-axis at the point which gives the carbon isotope signature of the parent organic matter. The $\delta^{13}\text{C}$ values obtained for the marine source organic matter from these formations fell within the range expected. Propane in the production gas samples were enriched in ^{12}C compared to the samples of mud gases.

Isotope reversals were commonly observed in Horn River Basin production gases in all three shale gas target formations (Muskwa, Otter Park and Evie) including cases of complete isotope reversal where $\delta^{13}\text{C}_{\text{propane}} < \delta^{13}\text{C}_{\text{ethane}} < \delta^{13}\text{C}_{\text{methane}}$. Few cases of isotope reversal were observed in the samples of mud gases especially among ethane, propane and butane components. In the literature where experiments have been conducted to simulate generation in both open and closed system conditions there have been no isotope reversals observed in the carbon isotope ratios of gas components (Arneeth and Matzigkeit, 1986). These results are also in agreement with data from this study in which the gas carbon isotope signatures from mud gas samples showed few isotope reversals and the observed gas signatures were those expected for mature thermogenic gases.

Although key information is available using gas isotope signatures, the geological context is important and must be taken into consideration during reservoir evaluation. While isotope reversal is a diagnostic feature and can be

indicative of maturity of the shale gas system the underlying cause of reversals in natural is still debated. Isotope reversals have been documented in the literature (Zumberge et al., 2009; Burruss and Laughrey, 2010; Rodriguez and Philp, 2010; Tilley et al., 2011; Burruss and Laughrey, 2011; Tilley and Muehlenbachs, 2012; Zumberge et al., 2012; Tilley and Muehlenbachs, 2013). Although several suggestions have been made to account for these reversals in shale gas systems, the new findings of this study indicate that the isotope reversal observed in samples of produced gases may have been caused by the isotope fractionation effects during the degassing of the shale as the gas moves through the pores and fracture system from the reservoir to the wellbore.

This study provided novel insight into the Horn River Basin gases, documented subsurface vertical and lateral carbon and hydrogen isotope variation and demonstrated stable isotope changes during shale gas production. It provided stable isotope data for Horn River Basin shale gases which is not available in the literature at present. While further study is necessary, the value in using stable isotope geochemistry as a tool for reservoir evaluation is shown.

6.2 Future Work

Understanding the shale gas system is essential for successful development of unconventional shale gas reservoirs. This study presented new information regarding stable isotope geochemistry and chemical composition of natural gases from the Horn River Basin, although further investigation is necessary to build on findings of this research. Limitations included the size of the mud gas sample set and the number of wells from which mud gases were obtained. In addition, mud gases were obtained from only two of the three target formations for shale gas production in the Horn River Basin; the Otter Park and Muskwa shale, while no mud gas samples were obtained from the Evie Formation. While findings of this study appeared consistent with some other analytical methods used for determining the connectivity within the Otter Park and Muskwa Formations, it is necessary that natural gases from more wells are

analysed. Carbon isotope depth profiles created mapped the vertical isotope changes through various strata from the Paleozoic to Cretaceous and is shown to be applicable for environmental remediation and identification of gas source leaks from soil gases, and surface casing vent flows; however there exists possibility of some variation due to facies changes across the basin exists hence isotope stratigraphy ought to be performed correlating data from wells across the Basin.

It is known that carbon isotope fractionation can occur during gas transport in shale, however this study lacked samples of core from target formations where the stable isotope changes that occur during desorption could be measured. Although theoretical changes expected during such processes (Tang and Xia, 2011; Xia and Tang, 2012) were considered in interpretation of results including experimental work on gas diffusion in shale (Zhang and Krooss, 2001; Strapóć et al., 2010), it is beneficial if core samples from the Horn River Basin are obtained to conduct measurements on the gas isotope composition over time during desorption of the shale. Petroleum isotope geochemistry is essential for characterization of natural gases hydrocarbon reservoirs and additional research is necessary to develop greater understanding of these unconventional shale gas plays.

References Cited

- Arneeth, J. D. and U. Matzigkeit, 1986, Variations in the carbon isotope composition and production yield of various pyrolysis products under open and closed system conditions, *Organic Geochemistry*, vol. 10, no. 4–6, p. 1067-1071.
- Burruss, R. C. and C. D. Laughrey, 2010, Carbon and hydrogen isotopic reversals in deep basin gas: Evidence for limits to the stability of hydrocarbons, *Organic Geochemistry*, vol. 41, no. 12, p. 1285-1296.
- Burruss, R. C. and C. D. Laughrey, 2011, Isotope reversals and rollovers: The last gasp of shale gas?
<http://www.searchanddiscovery.com/abstracts/pdf/2011/hedberg-beijing/abstracts/ndx_burruss.pdf> Accessed 09/13, 2013.
- Hunt, J. M., 1984, Generation and Migration of Light Hydrocarbons, *Science*, vol. 226, no. 4680, p. 1265-1270.
- Rodriguez, N. D. and R. P. Philp, 2010, Geochemical characterization of gases from the Mississippian Barnett Shale, Fort Worth Basin, Texas, *AAPG Bulletin*, vol. 94, no. 11, p. 1641-1656.
- Strapoć, D., G. Michael, J. Roper, and Maguire Matt, 2010, Insights into Shale Gas Production & Storage From Gas Chemistry – What Is It Telling Us?
<http://www.searchanddiscovery.com/abstracts/pdf/2011/hedberg-texas/abstracts/ndx_strapoc.pdf> Accessed 09/13, 2013.
- Tang, Y. and D. Xia, 2011, Predicting Original Gas in Place and Optimizing Productivity by Isotope Geochemistry of Shale Gas,
<http://www.cspg.org/documents/Conventions/Archives/Annual/2011/204-Predicting_Original_Gas_in_Place_and_Optimizing_Productivity.pdf> Accessed 09/13, 2013.

Tilley, B. and K. Muehlenbachs, 2012, Isotope Systematics of High Maturity Shale Gases in the WCSB Compared to Other North American Shale Gases, <http://www.cspg.org/documents/Conventions/Archives/Annual/2012/026_GC2012_Isotope_Systematics_of_High_Maturity_Shale_Gases.pdf> Accessed 09/11, 2013.

Tilley, B., S. McLellan, S. Hiebert, B. Quartero, B. Veilleux, and K. Muehlenbachs, 2011, Gas isotope reversals in fractured gas reservoirs of the western Canadian Foothills: Mature shale gases in disguise, AAPG Bulletin, vol. 95, no. 8, p. 1399-1422.

Tilley, B. and K. Muehlenbachs, 2013, Isotope reversals and universal stages and trends of gas maturation in sealed, self-contained petroleum systems, Chemical Geology, vol. 339, p. 194-204.

Xia, X., J. Chen, R. Braun, and Y. Tang, 2012, Isotopic reversals with respect to maturity trends due to mixing of primary and secondary products in source rocks, Chemical Geology, vol. 339, p. 205-212.

Xia, X. and Y. Tang, 2012, Isotope fractionation of methane during natural gas flow with coupled diffusion and adsorption/desorption, Geochimica et Cosmochimica Acta, vol. 77, p. 489-503.

Zhang, T. and B. M. Krooss, 2001, Experimental investigation on the carbon isotope fractionation of methane during gas migration by diffusion through sedimentary rocks at elevated temperature and pressure, Geochimica et Cosmochimica Acta, vol. 65, no. 16, p. 2723-2742.

Zumberge, J., K. Ferworn, and J. Curtis, 2009, Gas character anomalies found in highly productive shale gas wells, Geochimica et Cosmochimica Acta Supplement, vol. 73, p. A1539.

Zumberge, J., K. Ferworn, and S. Brown, 2012, Isotopic reversal ('rollover') in shale gases produced from the Mississippian Barnett and Fayetteville formations, *Marine and Petroleum Geology*, vol. 31, no. 1, p. 43-52.

References Cited

- Adams, C., 2012, Summary of Shale Gas Activity in Northeast British Columbia 2011 Oil and Gas Reports 2012-1, BC Ministry of Energy and Mines, Geoscience and Strategic Initiatives Branch.
- Aguilera, R., 2013, Flow Units: From Conventional to Tight Gas to Shale Gas to Tight Oil to Shale Oil Reservoirs, SPE Western Regional & AAPG Pacific Section Meeting, 2013 Joint Technical Conference, Apr 19 - 25, 2013 2013, Monterey, CA, USA.
- Akkutlu, I. Y. and E. Fathi, 2012, Multiscale Gas Transport in Shales With Local Kerogen Heterogeneities, SPE Journal, no. 12, p. pp. 1002-1011.
- Amann-Hildenbrand, A., A. Ghanizadeh, and B. M. Krooss, 2012, Transport properties of unconventional gas systems, Marine and Petroleum Geology, vol. 31, no. 1, p. 90-99.
- Ambrose, R., R. Hartman, M. Diaz Campos, I. Y. Akkutlu, and C. Sondergeld, 2010, New pore-scale considerations for shale gas in place calculations, SPE Unconventional Gas Conference, 23-25 February 2010, Pittsburgh, Pennsylvania, USA.
- Arneth, J. and U. Matzigkeit, 1986, Variations in the carbon isotope composition and production yield of various pyrolysis products under open and closed system conditions, Organic Geochemistry, vol. 10, no. 4-6, p. 1067-1071.
- Arneth, J. D., 1984, Stable isotope and organo-geochemical studies on phanerozoic sediments of the Williston Basin, North America, Chemical Geology, vol. 46, no. 2, p. 113-140.
- B.C. Ministry of Energy and Mines and National Energy Board, 2011, Ultimate Potential for Unconventional Natural Gas in Northeastern British Columbia's Horn River Basin. Oil and Gas Reports 2011-1,

<<http://www.empr.gov.bc.ca/OG/Documents/HornRiverEMA.pdf>> Accessed 10/11, 2013.

Behar, F., M. Vandenbroucke, S. Teermann, P. Hatcher, C. Leblond, and O. Lerat, 1995, Experimental simulation of gas generation from coals and a marine kerogen, *Chemical Geology*, vol. 126, no. 3, p. 247-260.

Behar, F., M. Vandenbroucke, Y. Tang, F. Marquis, and J. Espitalie, 1997, Thermal cracking of kerogen in open and closed systems: determination of kinetic parameters and stoichiometric coefficients for oil and gas generation, *Organic Geochemistry*, vol. 26, no. 5, p. 321-339.

Behar, F., S. Kressmann, J. Rudkiewicz, and M. Vandenbroucke, 1992, Experimental simulation in a confined system and kinetic modelling of kerogen and oil cracking, *Organic Geochemistry*, vol. 19, no. 1, p. 173-189.

Berner, U. and E. Faber, 1988, Maturity related mixing model for methane, ethane and propane, based on carbon isotopes, *Organic Geochemistry*, vol. 13, no. 1-3, p. 67-72.

British Columbia Oil and Gas Commission, 2012, Investigation of observed seismicity in the Horn River Basin, <<http://www.bcogc.ca/node/8046/download>> Accessed 06/04, 2013.

Burruss, R. C. and C. D. Laughrey, 2010, Carbon and hydrogen isotopic reversals in deep basin gas: Evidence for limits to the stability of hydrocarbons, *Organic Geochemistry*, vol. 41, no. 12, p. 1285-1296.

Burruss, R. C. and C. D. Laughrey, 2011, Isotope reversals and rollovers: The last gasp of shale gas?

<http://www.searchanddiscovery.com/abstracts/pdf/2011/hedberg-beijing/abstracts/ndx_burruss.pdf> Accessed 09/13, 2013.

- Bustin, A. M. M. and R. M. Bustin, 2012, Importance of rock properties on the producibility of gas shales, *International Journal of Coal Geology*, vol. 103, p. 132-147.
- Cardott, B., 2006, Gas shales tricky to understand: *AAPG Explorer*, vol. 27, no.11, p 48, 49.
- Carpenter, D. O., 2013, Public health implications of hydraulic fracturing, *Abstracts with Programs - Geological Society of America*, vol. 45, no. 7; 7, p. 182-182.
- Chalmers, G. R., D. J. Ross, and R. M. Bustin, 2012, Geological controls on matrix permeability of Devonian Gas Shales in the Horn River and Liard basins, northeastern British Columbia, Canada, *International Journal of Coal Geology*, vol. 103, p. 120-131.
- Chermak, J. and M. E. Schreiber, 2012, Environmental impact evaluation of hydrocarbon extraction from shales, *Abstracts with Programs - Geological Society of America*, vol. 44, no. 7; 7, p. 313-313.
- Chung, H. M., J. R. Gormly, and R. M. Squires, 1988, Origin of gaseous hydrocarbons in subsurface environments: Theoretical considerations of carbon isotope distribution, *Chemical Geology*, vol. 71, no. 1-3, p. 97-104.
- Claypool, G. E. and K. A. Kvenvolden, 1983, Methane and other hydrocarbon gases in marine sediment, *Annual Review of Earth and Planetary Sciences*, vol. 11, p. 299.
- Clayton, C., 1991, Carbon isotope fractionation during natural gas generation from kerogen, *Marine and Petroleum Geology*, vol. 8, no. 2, p. 232-240.
- Close, D., M. Perez, B. Goodway, and G. Purdue, 2012, Integrated workflows for shale gas and case study results for the Horn River Basin, British Columbia, Canada, *The Leading Edge*, vol. 31, no. 5, p. 556-569.

- Coleman, M. L., T. J. Shepherd, J. J. Durham, J. E. Rouse, and G. R. Moore, 1982, Reduction of water with zinc for hydrogen isotope analysis, *Analytical Chemistry*, vol. 54, no. 6, p. 993-995.
- Corlett, H. and B. Jones, 2011, The influence of paleogeography in epicontinental seas: A case study based on Middle Devonian strata from the MacKenzie Basin, Northwest Territories, Canada, *Sedimentary Geology*, vol. 239, no. 3–4, p. 199-216.
- Curtis, J. B., 2002, Fractured Shale-Gas Systems, *AAPG Bulletin*, vol. 86, no. 11, p. 1921-1938.
- Curtis, M., R. Ambrose, C. Sondergeld, and C. Sondergeld, 2010, Structural characterization of gas shales on the micro-and nano-scales, *Canadian Unconventional Resources and International Petroleum Conference*, 19-21 October 2010, Calgary, Alberta, Canada.
- Danesh, A., 1998, PVT and phase behaviour of petroleum reservoir fluids, vol. 47. Elsevier.
- Dawson, D. and A. Murray, 2011, Applications of Mud Gas Isotope Logging in Petroleum Systems Analysis, http://www.searchanddiscovery.com/abstracts/pdf/2011/hedberg-beijing/abstracts/ndx_dawson.pdf Accessed 10/01, 2013.
- De Wit, M. J., 2011, The great shale debate in the Karoo, *S Afr J Sci*, vol. 107, no. 7/8.
- Dewitt, W., 1984, Devonian gas shales and related tight reservoir rocks of Appalachian basin, *AAPG Bulletin*, vol. 68. no.4, p.470.
- Dieckmann, V., H. J. Schenk, B. Horsfield, and D. H. Welte, 1998, Kinetics of petroleum generation and cracking by programmed-temperature closed-system pyrolysis of Toarcian Shales, *Fuel*, vol. 77, no. 1–2, p. 23-31.

Dong, T. and N. Harris, 2012, Porosity and Pore Sizes in the Horn River Shales, <https://docs.google.com/viewer?a=v&q=cache:bxCSVjGXi2gJ:www.empr.gov.bc.ca/OG/oilandgas/petroleumgeology/UnconventionalGas/Documents/N%2520Harris.pdf+otter+park,+mukswa,+harris&hl=en&gl=ca&pid=bl&srcid=ADGEESgRYliGiaqTy7MdvSBrdaR6afQXqASw0wOa-FaI_yENUQfAU6IBbKKBv6gTJCJhm88m0yVI29TAxjOvTfzpbby55mcQRXRbh-LPMDwXGG6NqSJEnECxMkdoL4-N_r6mV4_g6I5Tp&sig=AHIEtbRIOyNJ2CIFNLK8KBaAWcRCnFiNgw> Accessed 09/11, 2013.

Duggan-Haas, D., R. M. Ross, and K. E. Cronin, 2013, What do you need to understand to teach about hydrofracking? Abstracts with Programs - Geological Society of America, vol. 45, no. 7; 7, p. 284-284.

Ellis, L., A. Brown, M. Schoell, and S. Uchytel, 2003, Mud gas isotope logging (MGIL) assists in oil and gas drilling operation, The Oil and Gas Journal, vol. 101, no. 21, p. 32(8).

Elshahawi, H., O. C. Mullins, M. Hows, S. Colacelli, M. Flannery, J. Zuo, and C. Dong, 2010, Reservoir fluid analysis as a proxy for connectivity in deepwater reservoirs, *Petrophysics*, vol. 51, no. 2.

Faber, E., W. Stahl, and M. Whitar, 1992, Distinction of bacterial and thermogenic hydrocarbon gases, *Bacterial gas: Paris*, Editions Technip, p. 63-74.

Freeman, C., G. J. Moridis, G. E. Michael, and T. A. Blasingame, 2012, Measurement, Modeling, and Diagnostics of Flowing Gas Composition Changes in Shale Gas Wells, SPE Latin America and Caribbean Petroleum Engineering Conference, 16-18 April 2012, Mexico City, Mexico.

Freeman, C., G. Moridis, and T. Blasingame, 2013, Modeling and Performance Interpretation of Flowing Gas Composition Changes in Shale Gas Wells with Complex Fractures, 6th International Petroleum Technology Conference, Mar 26 - 28, 2013, Beijing, China.

Fuex, A. N., 1977, The use of stable carbon isotopes in hydrocarbon exploration, *Journal of Geochemical Exploration*, vol. 7, p. 155-188.

Fuex, A. N., 1980, Experimental evidence against an appreciable isotopic fractionation of methane during migration, *Physics and Chemistry of the Earth*, vol. 12, p. 725-732.

Geoscience BC Report 2012-4, 2013, Results from a Pilot Airborne Electromagnetic Survey, Horn River Basin, British Columbia, <<http://www.geosciencebc.com/s/Report2012-04.asp>> Accessed 10/29, 2013.

Glorioso, J. C. and A. J. Rattia, 2012, Unconventional Reservoirs: Basic Petrophysical Concepts for Shale Gas, SPE/EAGE European Unconventional Resources Conference and Exhibition, 20-22 March 2012, Vienna, Austria.

Gray, F. F. and J. Kassube, 1963, Geology and stratigraphy of Clarke Lake gas field, British Columbia, *AAPG Bulletin*, vol. 47, no. 3, p. 467-483.

Gray, J. and R. Dawe, 1991, Modeling low interfacial tension hydrocarbon phenomena in porous media, *SPE Reservoir Engineering*, vol. 6, no. 3, p. 353-359.

Griffin, D., 1965, The facies front of the Devonian Slave Point-Elk Point sequence in northeastern British Columbia and the Northwest Territories, *Journal of Canadian Petroleum Technology*, vol. 4, no. 1, p. 13-22.

Harris, N. B. and T. Dong, 2013, Characterizing porosity in the Horn River shale, northeastern British Columbia, <http://www.empr.gov.bc.ca/OG/oilandgas/petroleumgeology/Geoscience_Pub/Documents/Geoscience%20Reports%202013%20Web.pdf> Accessed 09/13, 2013.

Hill, D. G. and C. R. Nelson, 2000, Gas Productive Fractured Shales: An Overview and Update, *Gas TIPS*, vol. 6, no. No.2, p. 4-13.

Hill, R. J., E. Zhang, Y. Tang, and B. Katz, 2006, Estimating shale gas potential from confined pyrolysis experiments, Rocky Mountain Natural Gas Geology and Resource Conference Program and Abstracts, p. 124, 126.

Hill, R. J., Y. Tang, and I. R. Kaplan, 2003, Insights into oil cracking based on laboratory experiments, Organic Geochemistry, vol. 34, no. 12, p. 1651-1672.

Horsfield, B., H. Schenk, N. Mills, and D. Welte, 1992, An investigation of the in-reservoir conversion of oil to gas: compositional and kinetic findings from closed-system programmed-temperature pyrolysis, Organic Geochemistry, vol. 19, no. 1, p. 191-204.

Hu, Q., Z. Gao, S. Peng, and R. Ewing, 2012, Pore Structure Inhibits Gas Diffusion in the Barnett Shale, <http://www.searchanddiscovery.net/www.searchanddiscovery.net/documents/2012/50609hu/ndx_hu.pdf> Accessed 09/11, 2012.

Hunt, J. M., 1984, Generation and Migration of Light Hydrocarbons, Science, vol. 226, no. 4680, p. 1265-1270.

Jackson, R. B., A. Vengosh, T. H. Darrah, A. Down, and N. Warner, 2013, Drinking water and shale gas extraction; evidence for water contamination in some locations but not others, Abstracts with Programs - Geological Society of America, vol. 45, no. 7; 7, p. 181-181.

James, A. T., 1983, Correlation of natural gas by use of carbon isotopic distribution between hydrocarbon components, AAPG Bulletin, vol. 67, no. 7, p. 1176-1191.

James, A. T., 1990, Correlation of reservoired gases using the carbon isotopic compositions of wet gas components, AAPG Bulletin, vol. 74, no. 9, p. 1441-1458.

- Javadpour, F., 2009, Nanopores and apparent permeability of gas flow in mudrocks (shales and siltstone), *Journal of Canadian Petroleum Technology*, vol. 48, no. 8, p. 16-21.
- Javadpour, F., D. Fisher, and M. Unsworth, 2007, Nanoscale gas flow in shale gas sediments, *Journal of Canadian Petroleum Technology*, vol. 46, no. 10, p. 55-61.
- Jenden, P. D., D. J. Drazan, and I. R. Kaplan, 1993, Mixing of thermogenic natural gases in northern Appalachian Basin, *AAPG Bulletin*, vol. 77, no. 6, p. 980-998.
- Kent, D., 1994, Paleogeographic evolution of the cratonic platform-Cambrian to Triassic, *Geological Atlas of the Western Canada Sedimentary Basin*, p. 69-86.
- Kotarba, M. J. and M. D. Lewan, 2013, Sources of natural gases in Middle Cambrian reservoirs in Polish and Lithuanian Baltic Basin as determined by stable isotopes and hydrous pyrolysis of Lower Palaeozoic source rocks, *Chemical Geology*, vol. 345, p. 62-76.
- Law, B. E. and J. B. Curtis, 2002, Introduction to Unconventional Petroleum Systems, *AAPG Bulletin*, vol. 86, no. 11, p. 1851-1852.
- Lewan, M., 1997, Experiments on the role of water in petroleum formation, *Geochimica et Cosmochimica Acta*, vol. 61, no. 17, p. 3691-3723.
- Liang, P., J. M. Thompson, and L. Mattar, 2012, Importance of the Transition Period to Compound Linear Flow in Unconventional Reservoirs, *SPE Canadian Unconventional Resources Conference*, 30 October-1 November, Calgary, Alberta, Canada.
- Lorant, F. and F. Behar, 2002, Late generation of methane from mature kerogens, *Energy & Fuels*, vol. 16, no. 2, p. 412-427.
- Loucks, R. G., R. M. Reed, S. C. Ruppel, and D. M. Jarvie, 2009, Morphology, genesis, and distribution of nanometer-scale pores in siliceous mudstones of the

Mississippian Barnett Shale, *Journal of Sedimentary Research*, vol. 79, no. 12, p. 848-861.

Magoon, L. and J. Schmoker, 2000, The total petroleum system—The natural fluid network that constrains the assessment unit, US geological survey world petroleum assessment, p. 31.

Magoon, L.B., and Dow, W.G., 1994, The petroleum system, in Magoon, L.B., and Dow, W.G., eds., *The petroleum system—From source to trap*: Tulsa, Okla., American Association of Petroleum Geologists Memoir 60, p. 3-24.

Martini, A. M., L. M. Walter, J. M. Budai, T. C. W. Ku, C. J. Kaiser, and M. Schoell, 1998, Genetic and temporal relations between formation waters and biogenic methane: Upper Devonian Antrim Shale, Michigan Basin, USA, *Geochimica et Cosmochimica Acta*, vol. 62, no. 10, p. 1699-1720.

Monger, J. and R. Price, 1979, Geodynamic evolution of the Canadian Cordillera—progress and problems, *Canadian Journal of Earth Sciences*, vol. 16, no. 3, p. 770-791.

Montgomery, S. L., D. M. Jarvie, K. A. Bowker, and R. M. Pollastro, 2005, Mississippian Barnett Shale, Fort Worth basin, north-central Texas: Gas-shale play with multi-trillion cubic foot potential, *AAPG Bulletin*, vol. 89, no. 2, p. 155-175.

Moridis, G., T. Blasingame, and C. Freeman, 2010, Analysis of mechanisms of flow in fractured tight-gas and shale-gas reservoirs, SPE Latin American and Caribbean Petroleum Engineering Conference. Society of Petroleum Engineers, 2010.

Morrow, D. W., M. Zhao, and L. D. Stasiuk, 2002, The Gas-Bearing Devonian Presqu'ile Dolomite of the Cordova Embayment Region of British Columbia, Canada: Dolomitization and the Stratigraphic Template, *AAPG Bulletin*, vol. 86, no. 9, p. 1609-1638.

Mukhopadhyay, P. K. and W. G. Dow, 1994, Vitrinite reflectance as a maturity parameter (applications and limitations), A. C. S. symposium series. American Chemical Society Symposium Series 570, p. 1-24.

Mycke, B., K. Hall, and P. Leplat, 1994, Carbon isotopic composition of individual hydrocarbons and associated gases evolved from micro-scale sealed vessel (MSSV) pyrolysis of high molecular weight organic material, *Organic Geochemistry*, vol. 21, no. 6–7, p. 787-800.

Nelson, P. H., 2009, Pore-throat sizes in sandstones, tight sandstones, and shales, *AAPG Bulletin*, vol. 93, no. 3, p. 329-340.

Ness, S., R. Benteau, and S. Leggitt, 2010, Horn River Shales ...Boring and Black? ...or...Beautifully Complex?
<http://cseg.ca/assets/files/resources/abstracts/2010/core/1069_GC2010_Horn_River_Shales.pdf> Accessed 09/11, 2013.

Nexen Corporate Update, 2011,
<http://www.nexencoold.com/~media/Files/Presentations/PDF/Nexen_IRRoadshow_UBS.ashx> Accessed 01/27, 2014.

Ni, Y., J. Dai, X. Yang, Y. Tang, Y. Jin, and J. Chen, 2009, Kinetic modeling of post-mature gas generation: Constraints from high-pressure thermal-cracking of nC₂₄, *Geochimica et Cosmochimica Acta*, vol. 73, no. 13 supplement 1, p. A940.

Norville, G. A. and R. A. Dawe, 2007, Carbon and hydrogen isotopic variations of natural gases in the southeast Columbus basin offshore southeastern Trinidad, West Indies – clues to origin and maturity, *Applied Geochemistry*, vol. 22, no. 9, p. 2086-2094.

Odden, W., T. Barth, and M. Talbot, 2002, Compound-specific carbon isotope analysis of natural and artificially generated hydrocarbons in source rocks and petroleum fluids from offshore Mid-Norway, *Organic Geochemistry*, vol. 33, no. 1, p. 47-65.

Oldale, H. and R. Munday, 1994, Devonian Beaverhill Lake Group of the western Canada sedimentary basin, Geological Atlas of the Western Canada Sedimentary Basin, p. 149-164.

Orem, W. H., L. M. Crosby, C. Tatu, M. S. Varonka, C. DeVera, and M. Engle, 2013, Produced water from shale gas production; organic substances and toxicity testing, Abstracts with Programs - Geological Society of America, vol. 45, no. 7; 7, p. 181-181.

Passey, Q. R., K. Bohacs, W. L. Esch, R. Klimentidis, and S. Sinha, 2010, From oil-prone source rock to gas-producing shale reservoir—geologic and petrophysical characterization of unconventional shale-gas reservoirs, SPE-131350, CPS/SPE International Oil & Gas Conference and Exhibition in China (2010) June 8–10, 2010, Beijing, China

Pedentchouk, N., K. H. Freeman, and N. B. Harris, 2006, Different response of δD values of n-alkanes, isoprenoids, and kerogen during thermal maturation, *Geochimica et Cosmochimica Acta*, vol. 70, no. 8, p. 2063-2072.

Pelzer, E. E., 1966, Mineralogy, geochemistry, and stratigraphy of Besa River Shale, British Columbia, *Bulletin of Canadian Petroleum Geology*, vol. 14, no. 2, p. 273-321.

Price, R., 1994, Cordilleran tectonics and the evolution of the Western Canada Sedimentary Basin, Geological Atlas of the Western Canada Sedimentary Basin, p. 13-24.

Prinzhofer, A. A. and A. Y. Huc, 1995, Genetic and post-genetic molecular and isotopic fractionations in natural gases, *Chemical Geology*, vol. 126, no. 3-4, p. 281-290.

Ramos, S., 2004, The effect of shale composition on the gas sorption potential of organic-rich mudrocks in the Western Canadian sedimentary basin, M.Sc. thesis University of British Columbia, Vancouver, Canada (2004).

- Reynolds, M. M. and D. L. Munn, 2010, Development Update for an Emerging Shale Gas Giant Field - Horn River Basin, British Columbia, Canada, .
- Rice, D. D. and G. E. Claypool, 1981, Generation, accumulation, and resource potential of biogenic gas, AAPG Bulletin, vol. 65, no. 1, p. 5-25.
- Rodriguez, N. D. and R. P. Philp, 2010, Geochemical characterization of gases from the Mississippian Barnett Shale, Fort Worth Basin, Texas, AAPG Bulletin, vol. 94, no. 11, p. 1641-1656.
- Rooney, M. A., G. E. Claypool, and H. Moses Chung, 1995, Modeling thermogenic gas generation using carbon isotope ratios of natural gas hydrocarbons, Chemical Geology, vol. 126, no. 3-4, p. 219-232.
- Root, K. G., 2001, Devonian Antler fold and thrust belt and foreland basin development in the southern Canadian Cordillera: implications for the Western Canada Sedimentary Basin, Bulletin of Canadian Petroleum Geology, vol. 49, no. 1, p. 7-36.
- Ross, D. J. K. and M. Bustin, 2009, The importance of shale composition and pore structure upon gas storage potential of shale gas reservoirs, Marine and Petroleum Geology, vol. 26, no. 6, p. 916-927.
- Ross, D. J. K. and R. M. Bustin, 2008, Characterizing the shale gas resource potential of Devonian Mississippian strata in the Western Canada sedimentary basin: Application of an integrated formation evaluation, AAPG Bulletin, vol. 92, no. 1, p. 87-125.
- Rowe, D. and A. Muehlenbachs, 1999a, Low-temperature thermal generation of hydrocarbon gases in shallow shales, Nature, vol. 398, no. 6722, p. 61-63.
- Rowe, D. and K. Muehlenbachs, 1999b, Isotopic fingerprints of shallow gases in the Western Canadian sedimentary basin: tools for remediation of leaking heavy oil wells, Organic Geochemistry, vol. 30, no. 8, Part 1, p. 861-871.

- Rullkötter, J., D. Leythaeuser, B. Horsfield, R. Littke, U. Mann, P. Müller, M. Radke, R. Schaefer, H. Schenk, and K. Schwochau, 1988, Organic matter maturation under the influence of a deep intrusive heat source: a natural experiment for quantitation of hydrocarbon generation and expulsion from a petroleum source rock (Toarcian shale, northern Germany), *Organic Geochemistry*, vol. 13, no. 4, p. 847-856.
- Sackett, W. M., 1978, Carbon and hydrogen isotope effects during the thermocatalytic production of hydrocarbons in laboratory simulation experiments, *Geochimica et Cosmochimica Acta*, vol. 42, no. 6, Part 1, p. 571-580.
- Schenk, H., R. Di Primio, and B. Horsfield, 1997, The conversion of oil into gas in petroleum reservoirs. Part 1: Comparative kinetic investigation of gas generation from crude oils of lacustrine, marine and fluviodeltaic origin by programmed-temperature closed-system pyrolysis, *Organic Geochemistry*, vol. 26, no. 7, p. 467-481.
- Schmoker, J. W., 2002, Resource-Assessment Perspectives for Unconventional Gas Systems, *AAPG Bulletin*, vol. 86, no. 11, p. 1993-1999.
- Schoell, M., 1980, The hydrogen and carbon isotopic composition of methane from natural gases of various origins, *Geochimica et Cosmochimica Acta*, vol. 44, no. 5, p. 649-661.
- Schoell, M., 1980, The hydrogen and carbon isotopic composition of methane from natural gases of various origins, *Geochimica et Cosmochimica Acta*, vol. 44, no. 5, p. 649-661.
- Schoell, M., 1983, Genetic characterization of natural gases, *AAPG Bulletin*, vol. 67, no. 12, p. 2225-2238.
- Schoell, M., 1984, Recent advances in petroleum isotope geochemistry, *Organic Geochemistry*, vol. 6, p. 645-663.

Schoell, M., 1988, Multiple origins of methane in the Earth, *Chemical Geology*, vol. 71, no. 1-3, p. 1-10.

Schoell, M., U. Bieg, M. Schmitt, A. Jurisch, and B. Nadolny, 2012, Mudgas Isotope Interpretations for Assessment of Paleozoic Shales in Poland Martin Schoell , SDGG GeoHannover 2012 October 1-3, 2012.

Seewald, J. and J. Whelan, 2005, Isotopic and chemical composition of natural gas from the Potato Hills Field, Southeastern Oklahoma: Evidence for an Abiogenic Origin?

<http://www.searchanddiscovery.com/documents/abstracts/2005research_calgary/abstracts/extended/seewald/seewald.htm> Accessed 10/18, 2013.

Shurr, G. W. and J. L. Ridgley, 2002, Unconventional Shallow Biogenic Gas Systems, *AAPG Bulletin*, vol. 86, no. 11, p. 1939-1969.

Smith, J. E., D. A. Morris, and J. G. Erdman, 1971, Migration, Accumulation and Retention of Petroleum in the Earth, *Proc. 8th World Petroleum Congress*, vol. 2, p. 13-26.

Soeder, D. J., 1988, Porosity and Permeability of Eastern Devonian Gas Shale, , vol. 3, no. 1, p. 116-116-124.

Sondergeld, C., R. Ambrose, C. Rai, and J. Moncrieff, 2010, Micro-Structural Studies of Gas Shales. Paper SPE 131771 presented at the SPE Unconventional Gas Conference, Pittsburg, Pennsylvania, USA, 23–25 February 2010.

Stahl, W., 1974, Carbon isotope fractionations in natural gases, *Nature*, vol. 251, no. 5471, p. 134-135.

Stasiuk, L. D. and M. G. Fowler, 2004, Organic facies in Devonian and Mississippian strata of Western Canada Sedimentary Basin: relation to kerogen type, paleoenvironment, and paleogeography, *Bulletin of Canadian Petroleum Geology*, vol. 52, no. 3, p. 234-255.

Strapoć, D., G. Michael, J. Roper, and Maguire Matt, 2010, Insights into Shale Gas Production & Storage From Gas Chemistry – What Is It Telling Us? <http://www.searchanddiscovery.com/abstracts/pdf/2011/hedberg-texas/abstracts/ndx_strapoc.pdf> Accessed 09/13, 2013.

Switzer, S., W. Holland, D. Christie, G. Graf, A. Hedinger, R. McAuley, R. Wierzbicki, and J. Packard, 1994, Devonian Woodbend-Winterburn strata of the Western Canada sedimentary basin, Geological Atlas of the Western Canada Sedimentary Basin: Canadian Society of Petroleum Geologists and Alberta Research Council, p. 165-202.

Tang, Y. and D. Xia, 2011, Predicting Original Gas in Place and Optimizing Productivity by Isotope Geochemistry of Shale Gas, <http://www.cspg.org/documents/Conventions/Archives/Annual/2011/204-Predicting_Original_Gas_in_Place_and_Optimizing_Productivity.pdf> Accessed 09/13, 2013.

Tang, Y., J. K. Perry, P. D. Jenden, and M. Schoell, 2000, Mathematical modeling of stable carbon isotope ratios in natural gases, *Geochimica et Cosmochimica Acta*, vol. 64, no. 15, p. 2673-2687.

Tilley, B. and K. Muehlenbachs, 2006, Gas maturity and alteration systematics across the Western Canada Sedimentary Basin from four mud gas isotope depth profiles, *Organic Geochemistry*, vol. 37, no. 12, p. 1857-1868.

Tilley, B. and K. Muehlenbachs, 2007, Isotopically Determined Mannville Group Gas Families, *Let it Flow: CSPG/CSEG 2007 Convention, Abstracts Volume*, p. 67-69.

Tilley, B. and K. Muehlenbachs, 2012, Isotope Systematics of High Maturity Shale Gases in the WCSB Compared to Other North American Shale Gases, <http://www.cspg.org/documents/Conventions/Archives/Annual/2012/026_GC2012_Isotope_Systematics_of_High_Maturity_Shale_Gases.pdf> Accessed 09/11, 2013.

Tilley, B. and K. Muehlenbachs, 2013, Isotope reversals and universal stages and trends of gas maturation in sealed, self-contained petroleum systems, *Chemical Geology*, vol. 339, p. 194-204.

Tilley, B. J., K. Muehlenbachs, and B. J. Szatkowski, 2001, Compartmentalization of Gas Reservoirs: Insights From Carbon Isotope Ratios, <<http://www.cspg.org/documents/Conventions/Archives/Annual/2001/14-102.pdf>> Accessed 09/11, 2013.

Tilley, B., S. McLellan, S. Hiebert, B. Quatero, B. Veilleux, and K. Muehlenbachs, 2011, Gas isotope reversals in fractured gas reservoirs of the western Canadian Foothills: Mature shale gases in disguise, *AAPG Bulletin*, vol. 95, no. 8, p. 1399-1422.

Ungerer, P. and R. Pelet, 1987, Extrapolation of the kinetics of oil and gas formation from laboratory experiments to sedimentary basins, .

Vengosh, A., 2013, Tracing the impacts of fossil fuels production on the quality of water resources in the United States, *Abstracts with Programs - Geological Society of America*, vol. 45, no. 7; 7, p. 181-181.

Wang, F. P. and R. M. Reed, 2009, Pore Networks and Fluid Flow in Gas Shales, *reSPE Annual Technical Conference and Exhibition*, 4-7 October 2009, New Orleans, Louisiana, 2009, Society of Petroleum Engineers, New Orleans, Louisiana.

Waples, D. W., 2000, The kinetics of in-reservoir oil destruction and gas formation: constraints from experimental and empirical data, and from thermodynamics, *Organic Geochemistry*, vol. 31, no. 6, p. 553-575.

Wei, M., Y. Duan, Q. Fang, R. Wang, B. Yu, and C. Yu, 2013, Mechanism model for shale gas transport considering diffusion, adsorption/desorption and Darcy flow, *Journal of Central South University*, vol. 20, no. 7, p. 1928-1937.

Weissenberger, J. A. W. and K. Potma, 2001, The Devonian of western Canada -- aspects of a petroleum system: Introduction, *Bulletin of Canadian Petroleum Geology*, vol. 49, no. 1, p. 1-6.

Wilhelms, A., E. Rein, C. Zwach, and A. S. Steen, 2001, Application and implication of horizontal well geochemistry, *Petroleum Geoscience*, vol. 7, no. 1, p. 75-79.

Williams, G. K., 1983, What does the term 'Horn River Formation' mean? *Bulletin of Canadian Petroleum Geology*, vol. 31, no. 2, p. 117-122.

Xia, X. and Y. Tang, 2012, Isotope fractionation of methane during natural gas flow with coupled diffusion and adsorption/desorption, *Geochimica et Cosmochimica Acta*, vol. 77, p. 489-503.

Xia, X., J. Chen, R. Braun, and Y. Tang, 2012, Isotopic reversals with respect to maturity trends due to mixing of primary and secondary products in source rocks, *Chemical Geology*.

Zhang, T. and B. M. Krooss, 2001, Experimental investigation on the carbon isotope fractionation of methane during gas migration by diffusion through sedimentary rocks at elevated temperature and pressure, *Geochimica et Cosmochimica Acta*, vol. 65, no. 16, p. 2723-2742.

Zhang, T., G. S. Ellis, S. C. Ruppel, K. Milliken, and R. Yang, 2012, Effect of organic-matter type and thermal maturity on methane adsorption in shale-gas systems, *Organic Geochemistry*, vol. 47, p. 120-131.

Zumberge, J., K. Ferworn, and J. Curtis, 2009, Gas character anomalies found in highly productive shale gas wells, *Geochimica et Cosmochimica Acta Supplement*, vol. 73, p. A1539.

Zumberge, J., K. Ferworn, and S. Brown, 2012, Isotopic reversal ('rollover') in shale gases produced from the Mississippian Barnett and Fayetteville formations, *Marine and Petroleum Geology*, vol. 31, no. 1, p. 43-52.

APPENDIX A –Time Series

CHEMICAL COMPOSITION - MOLE FRACTION (AIR FREE AS RECEIVED)

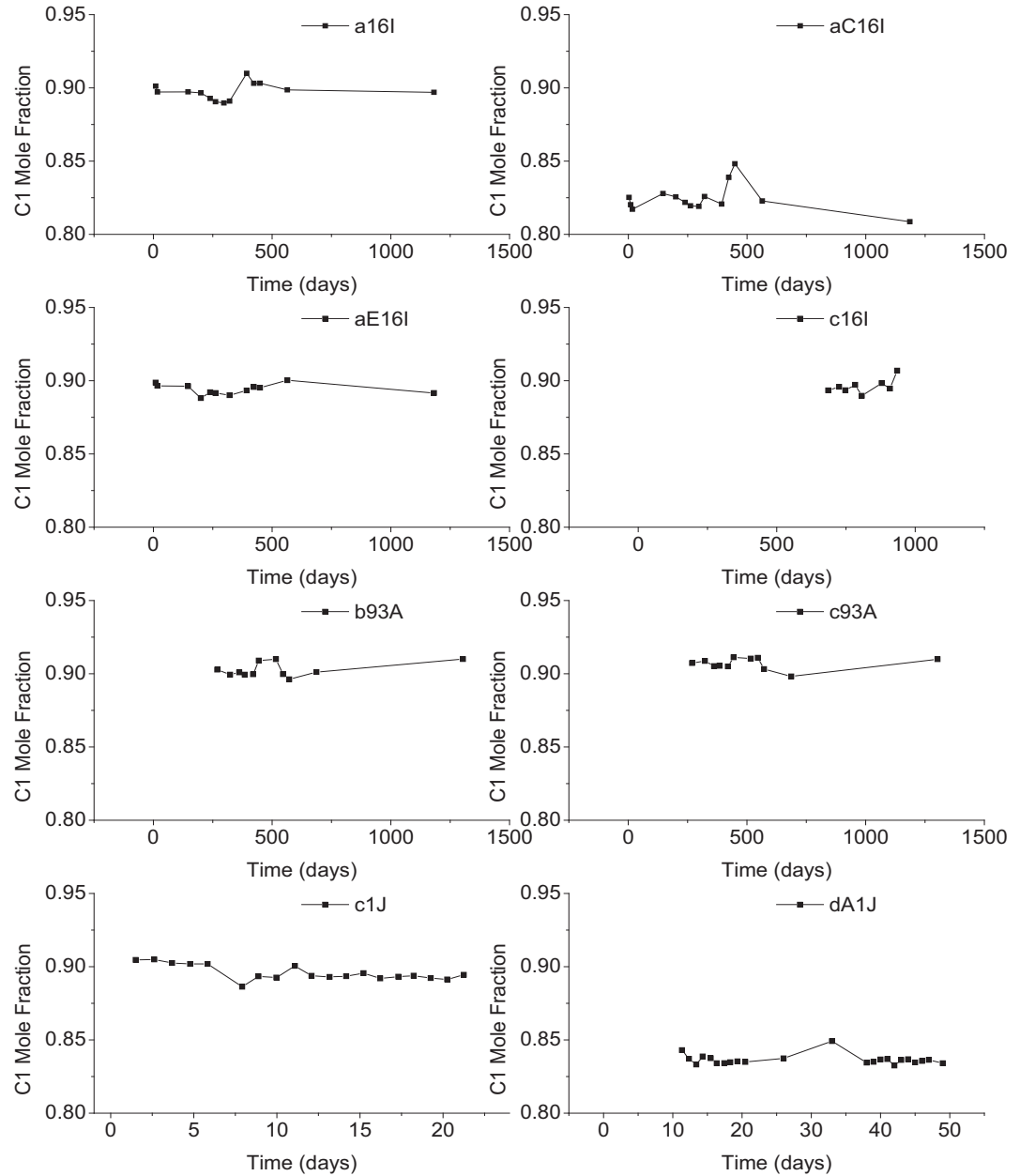


Figure A.1. Variation in methane concentration (mole fraction) for Horn River Group shale gases from 8 well locations- NTS 94/08.

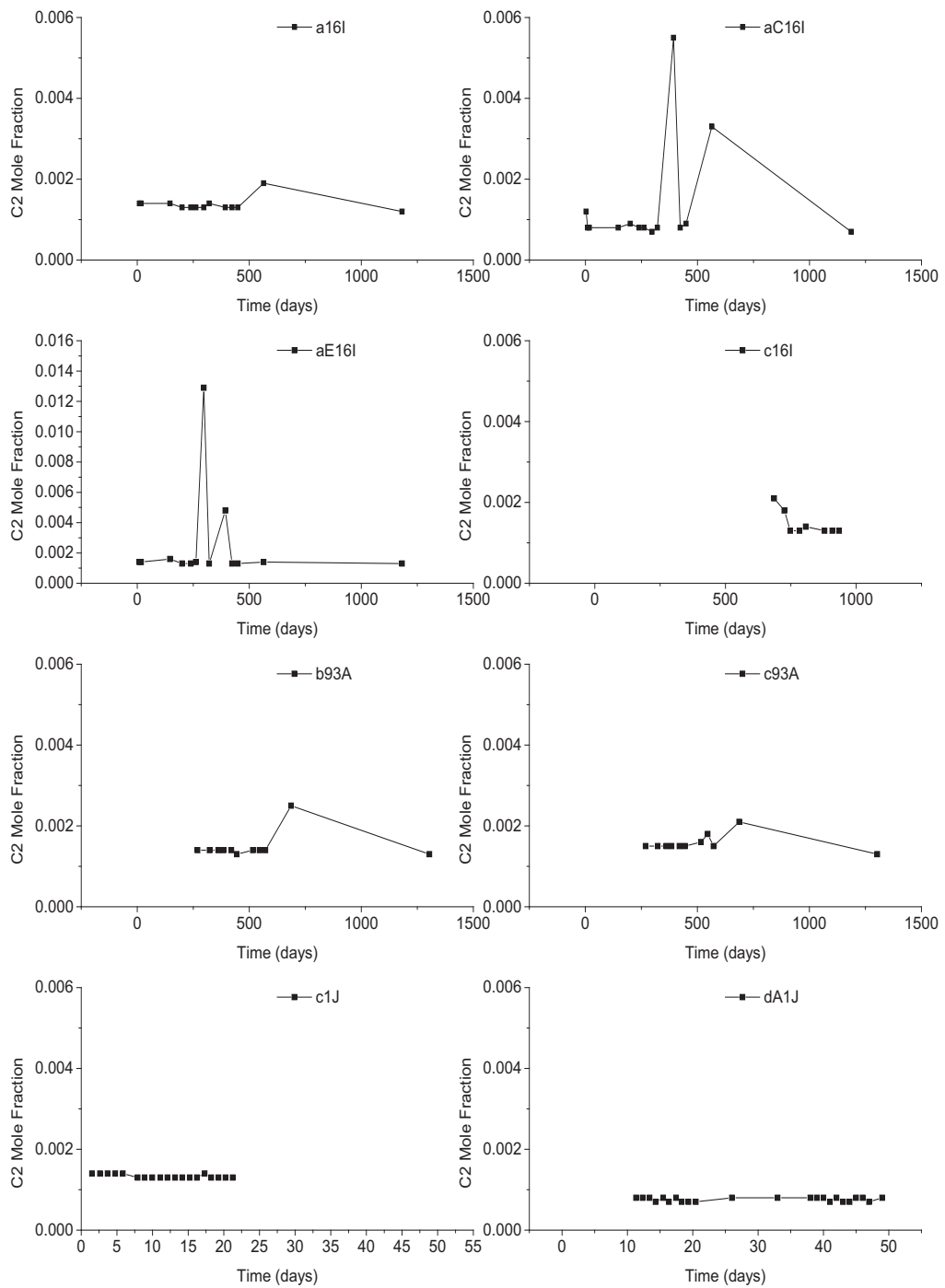


Figure A.2. Variation in ethane concentration (mole fraction) for Horn River Group shale gases from 8 well locations - NTS 94/08.

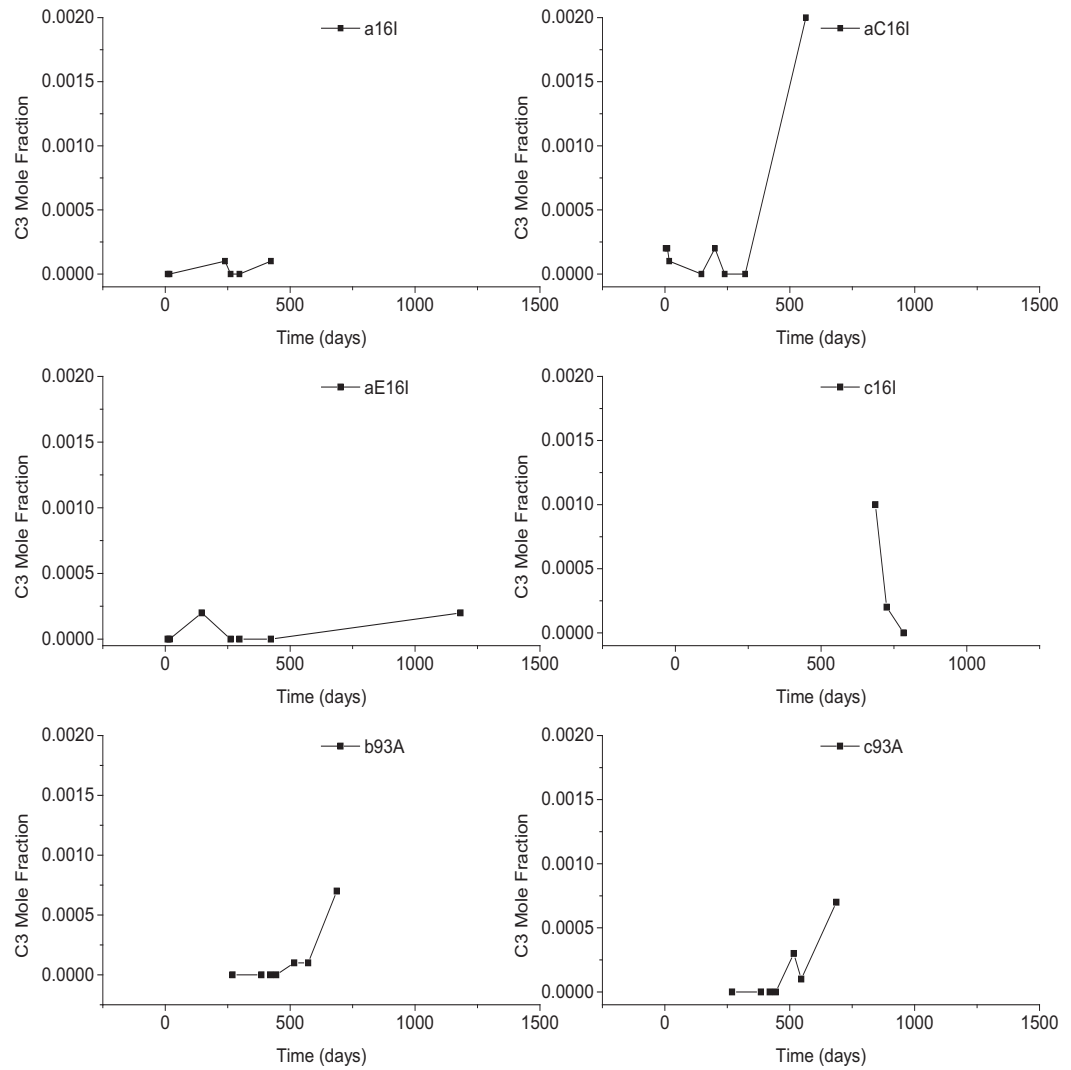


Figure A.3. Variation in propane concentration (mole fraction) for Horn River Group shale gases from 6 well locations - NTS 94/08.

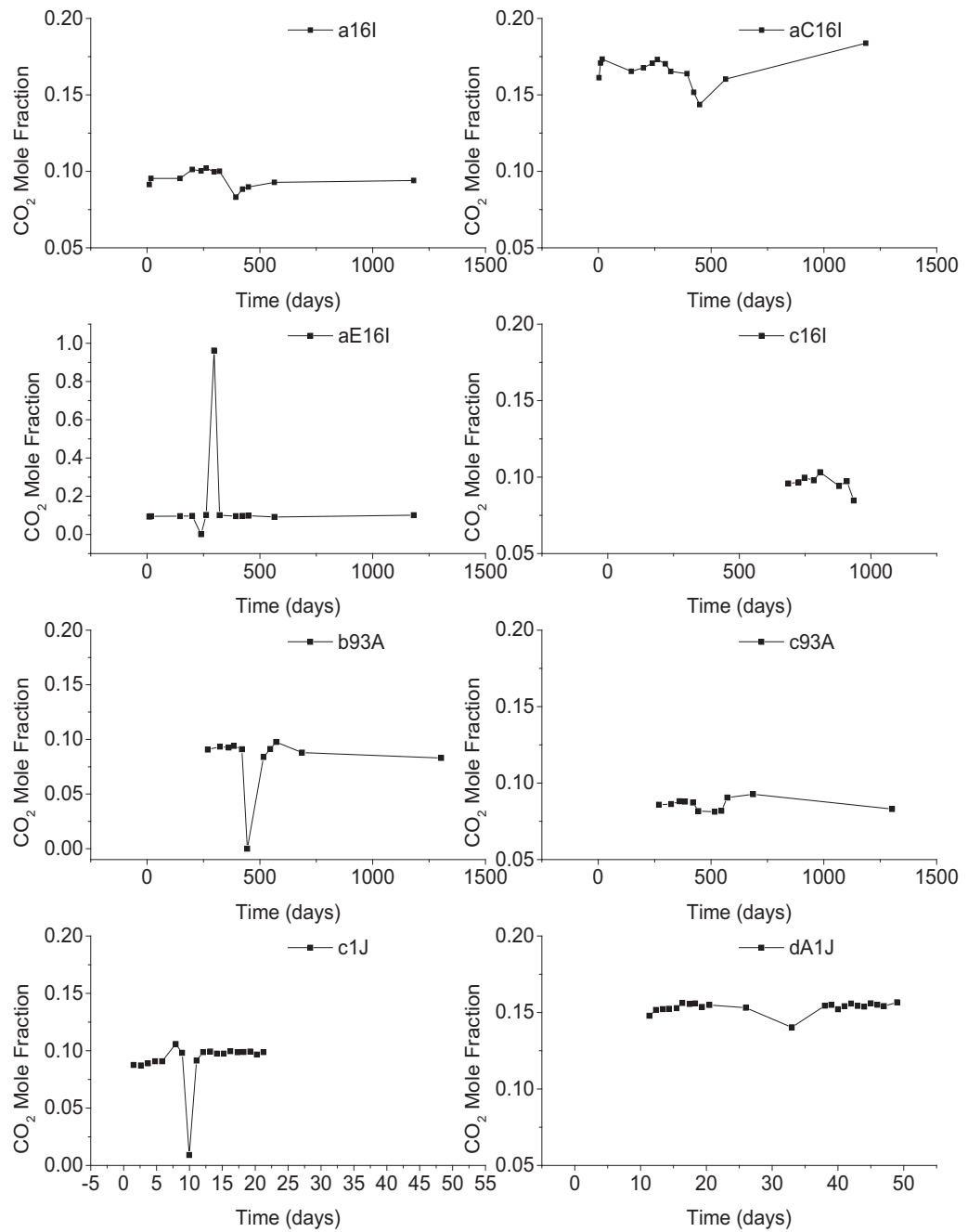


Figure A.4. Variation in carbon dioxide concentration (mole fraction) for Horn River Group shale gases from 8 well locations - NTS 94/08.

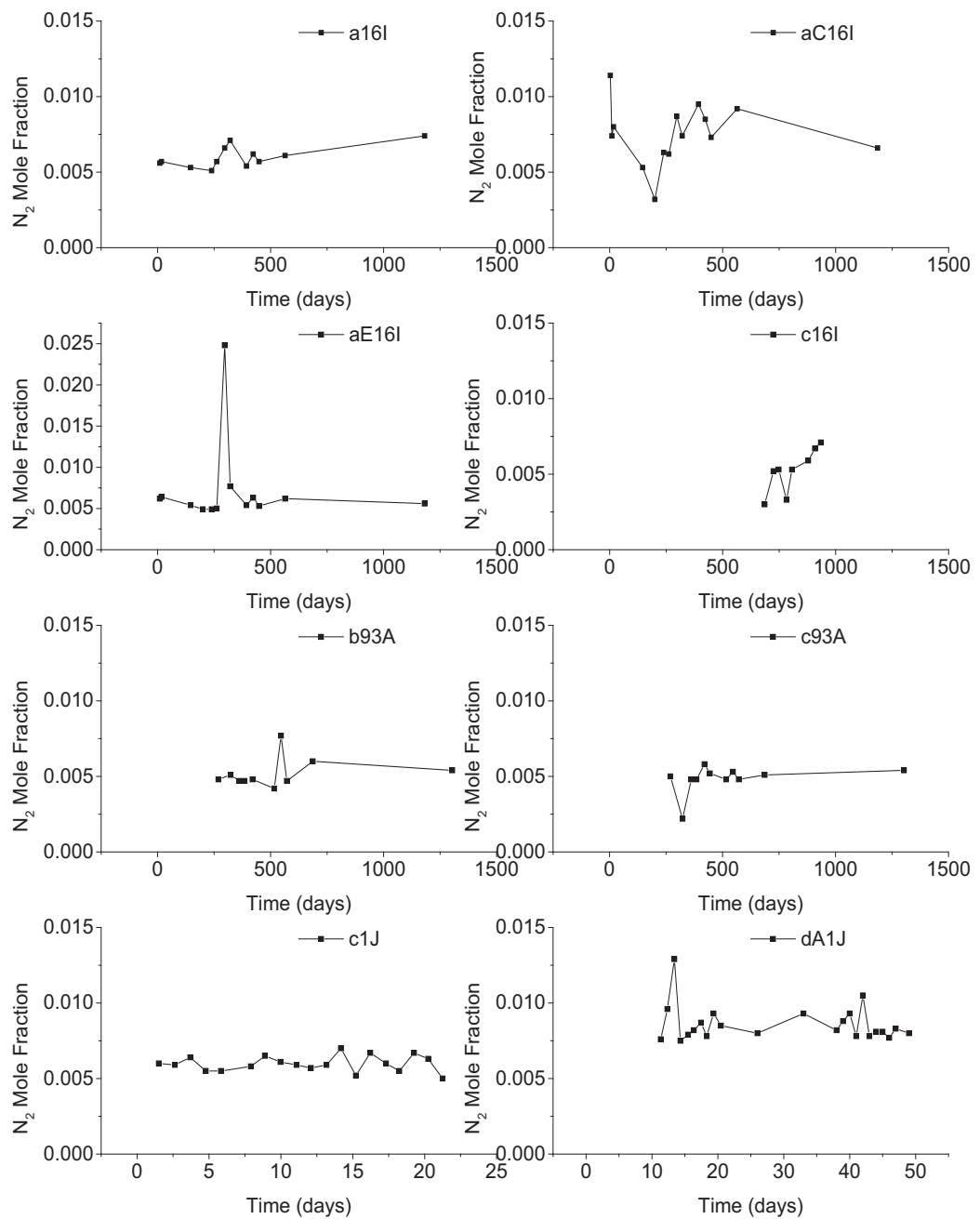


Figure A.5. Variation in nitrogen concentration (mole fraction) for Horn River Group shale gases from 8 well locations - NTS 94/08.

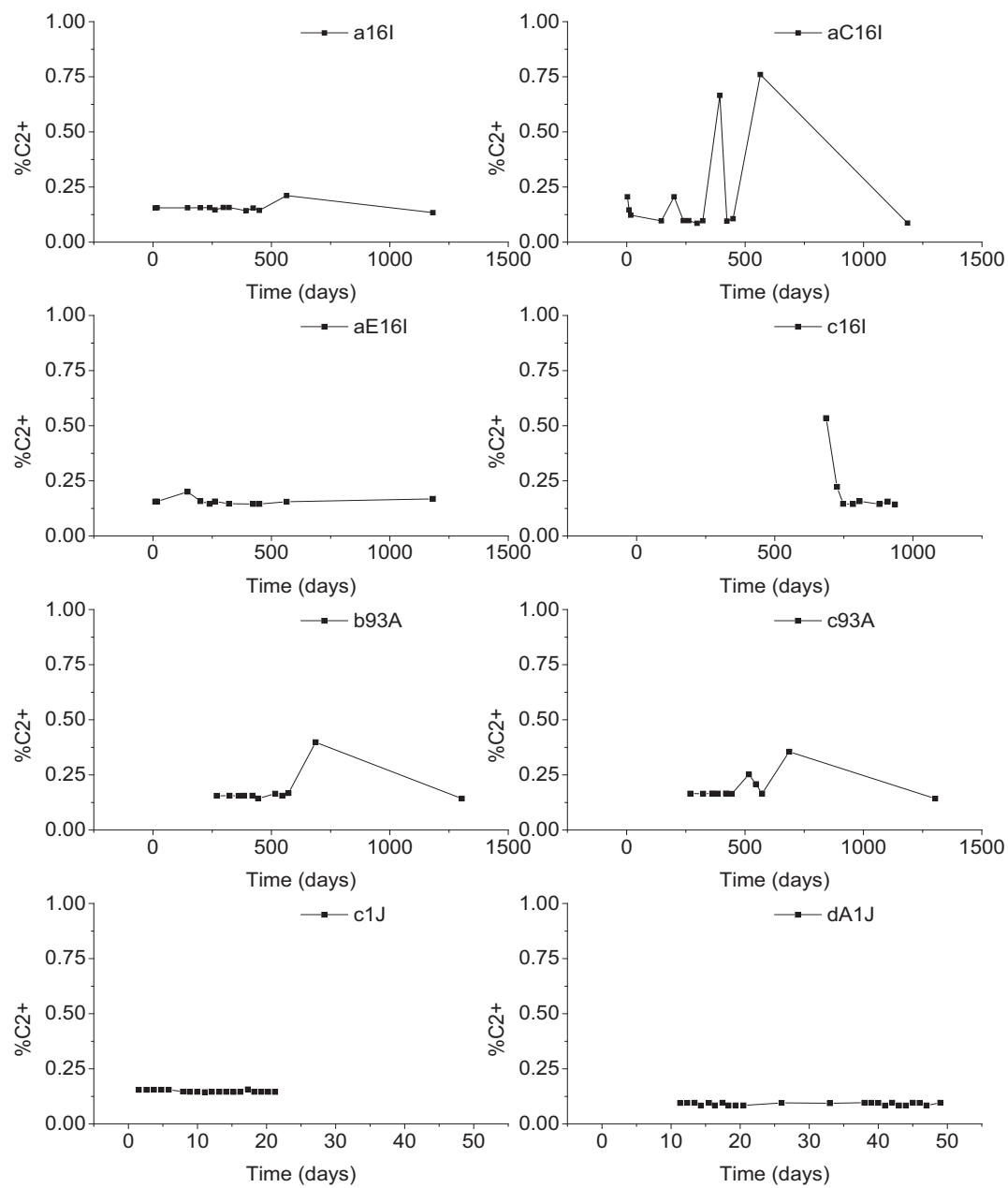


Figure A.6. Variation in gas wetness for Horn River Group shale gases from 8 well locations - NTS 94/08.

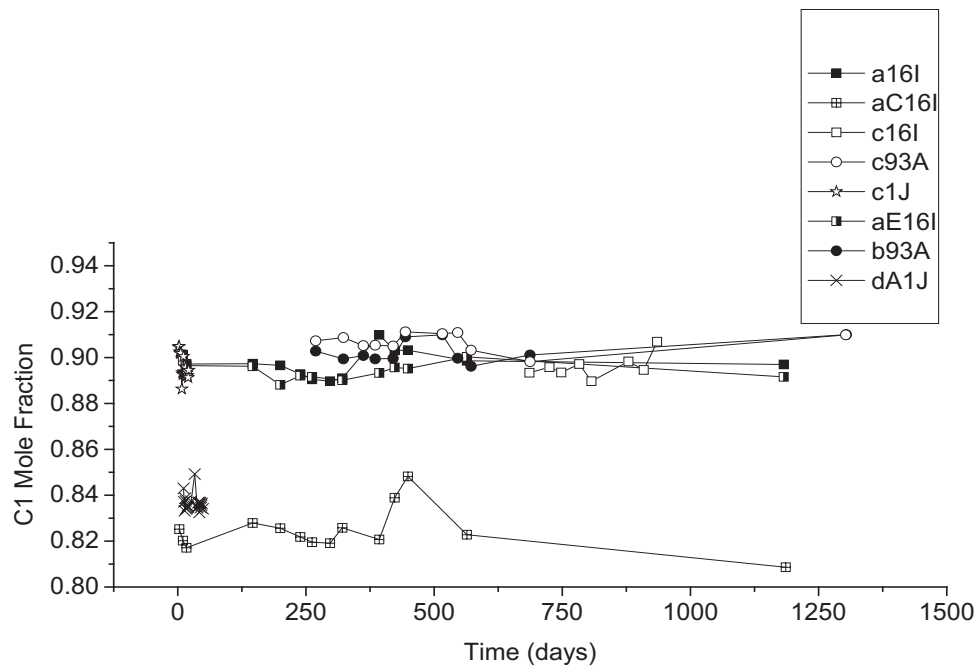


Figure A.7. Overlay plot showing variation in methane concentration (mole fraction) for Horn River Group shale gases from 8 well locations - NTS 94/08.

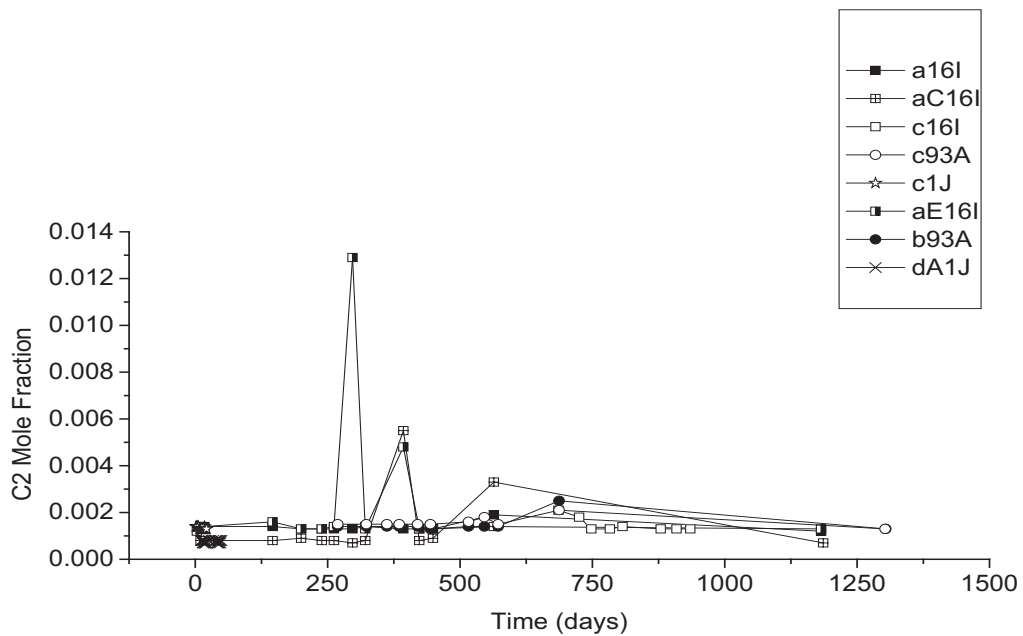


Figure A.8. Overlay plot showing variation in ethane concentration (mole fraction) for Horn River Group shale gases from 8 well locations - NTS 94/08.

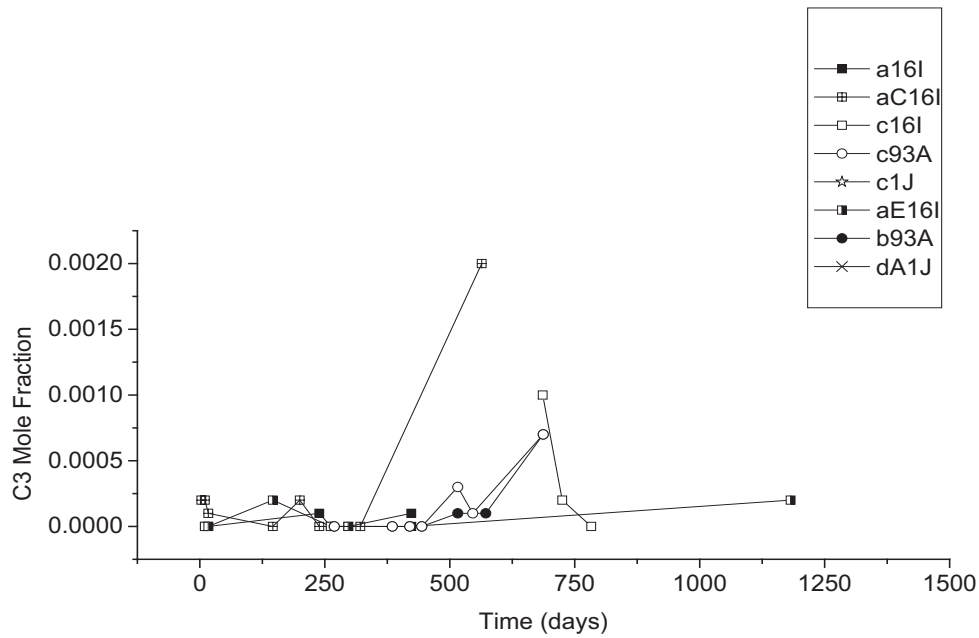


Figure A.9. Overlay plot showing variation in propane concentration (mole fraction) for Horn River Group shale gases from 8 well locations - NTS 94/08.

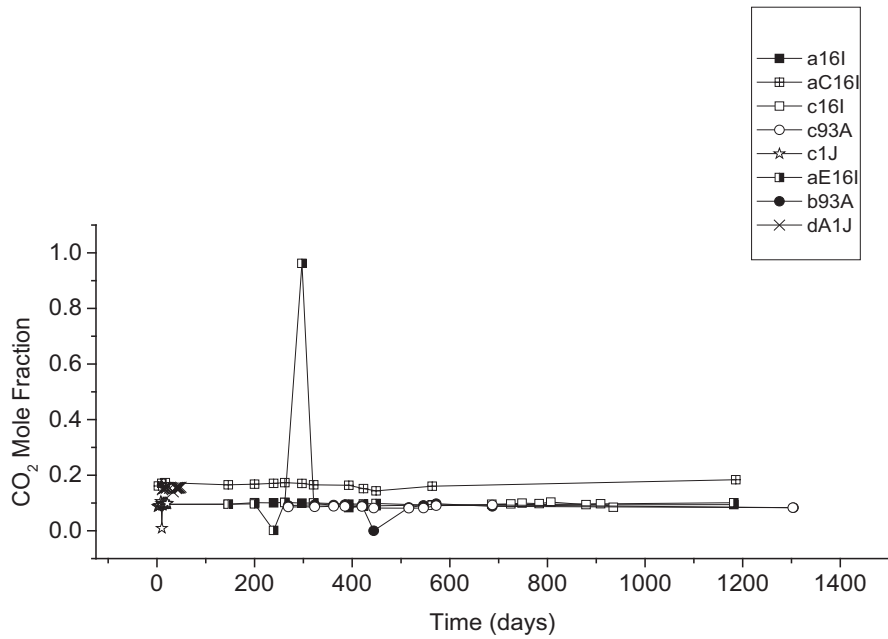


Figure A.10. Overlay plot showing variation in carbon dioxide concentration (mole fraction) for Horn River Group shale gases from 8 well locations - NTS 94/08.

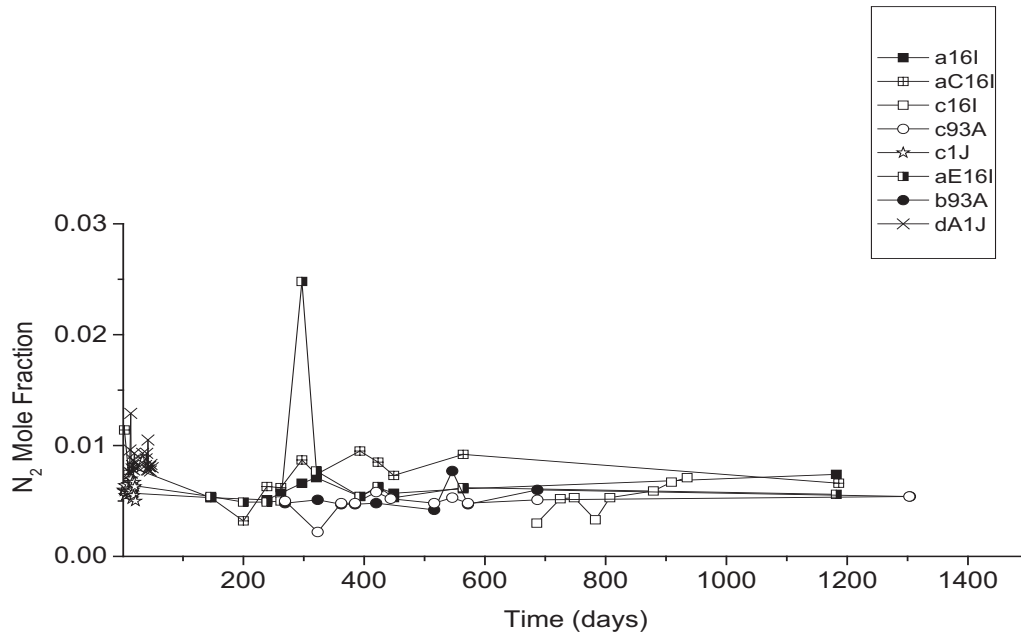


Figure A.11. Overlay plot showing variation in carbon dioxide concentration (mole fraction) for Horn River Group shale gases from 8 well locations - NTS 94/08.

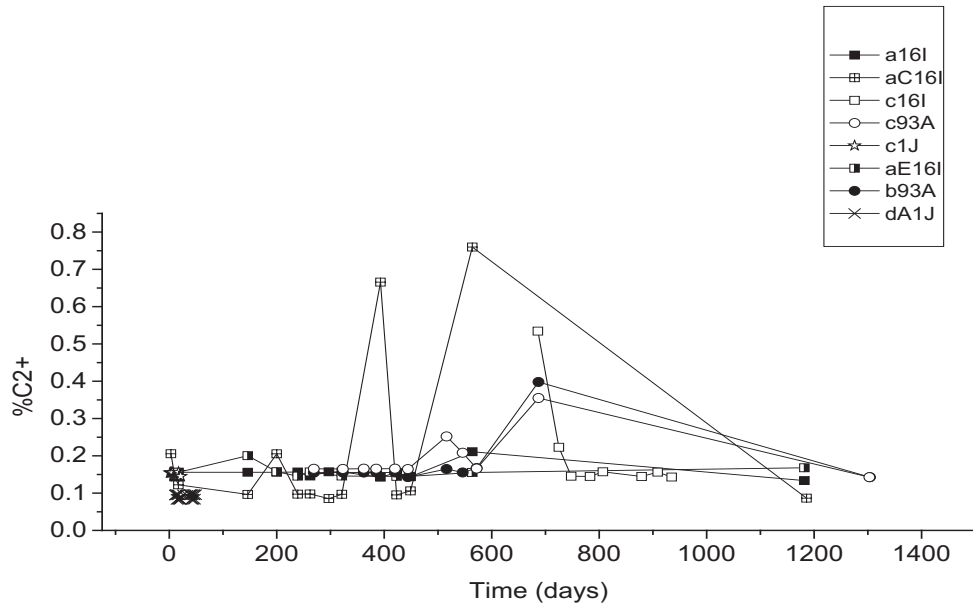


Figure A.12. Overlay plot showing variation in gas wetness for Horn River Group shale gases from 8 well locations - NTS 94/08.

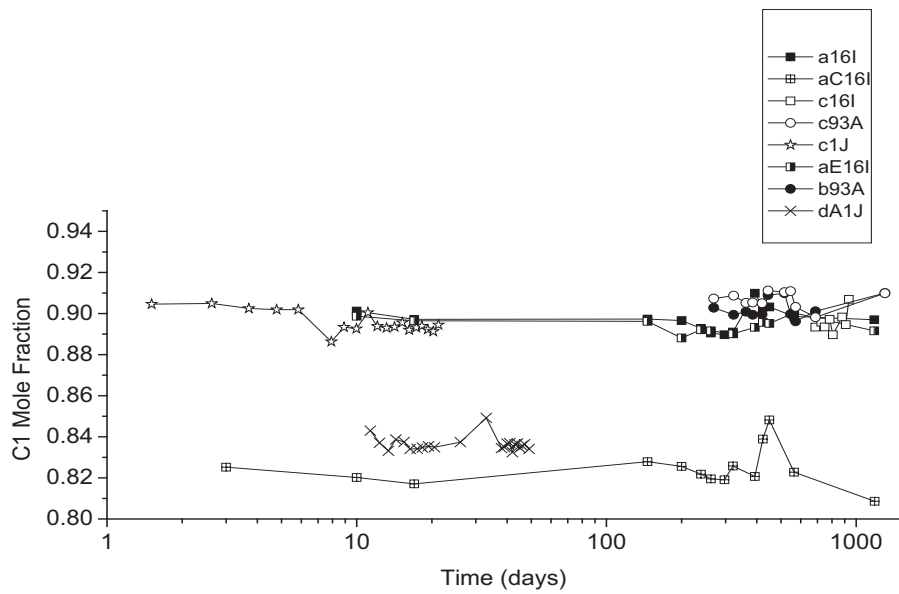


Figure A.13. Overlay plot showing variation in methane concentration (mole fraction) on a logarithmic time scale for Horn River Group shale gases from 8 well locations - NTS 94/08.

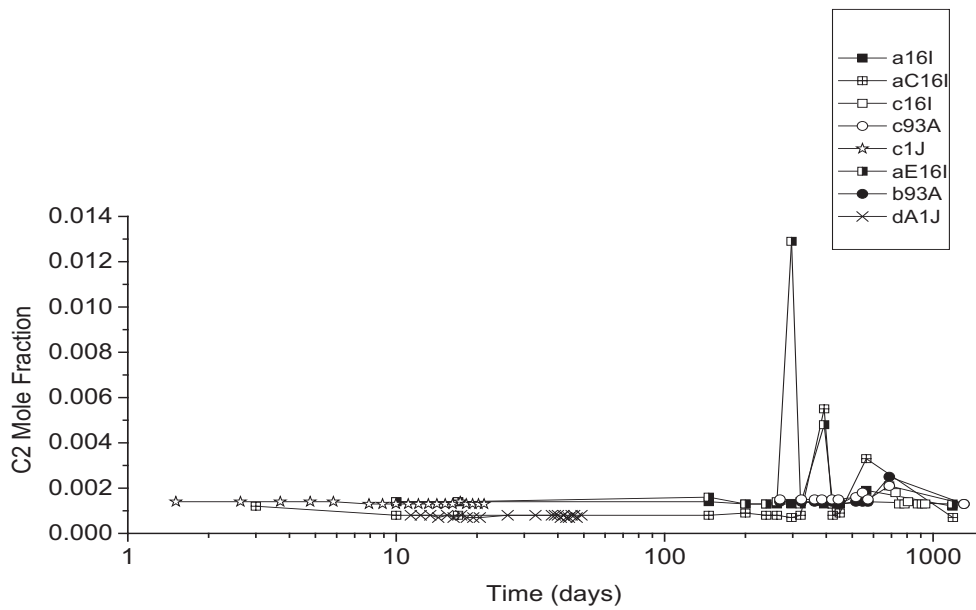


Figure A.14. Overlay plot showing variation in ethane concentration (mole fraction) on a logarithmic time scale for Horn River Group shale gases from 8 well locations - NTS 94/08.

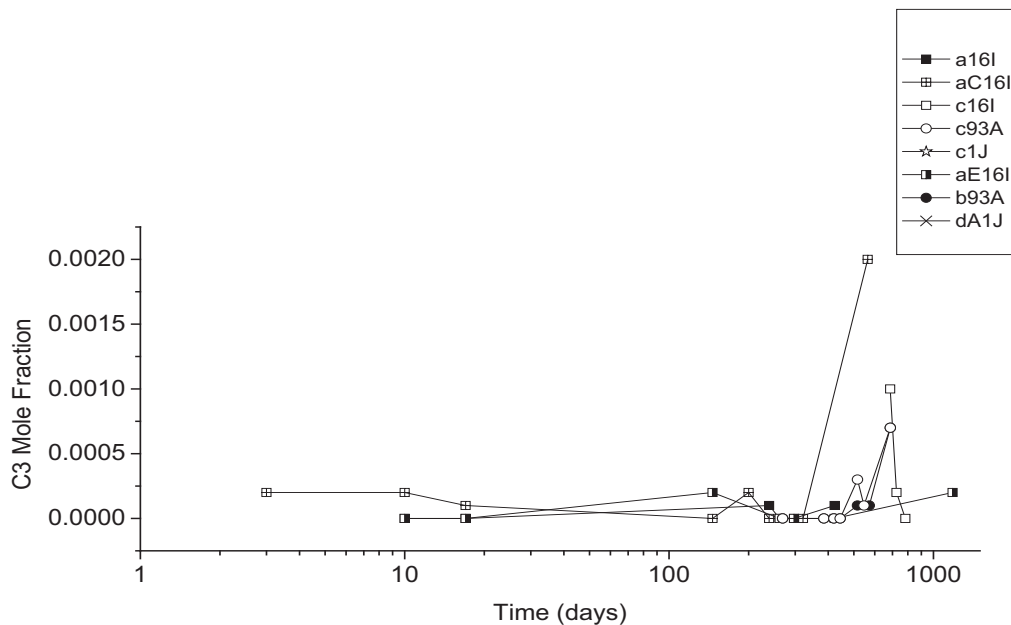


Figure A.15. Overlay plot showing variation in propane concentration (mole fraction) on a logarithmic time scale for Horn River Group shale gases from 8 well locations - NTS 94/08.

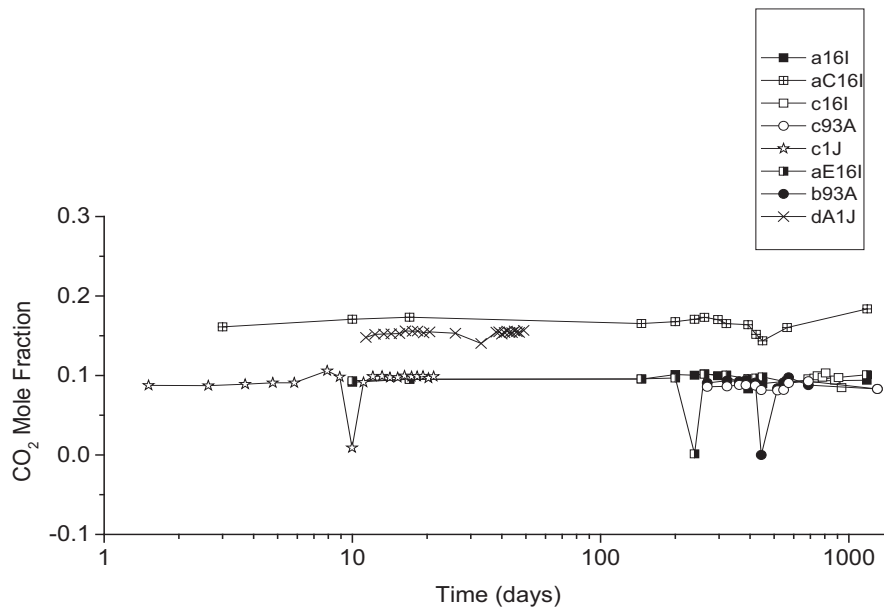


Figure A.16. Overlay plot showing variation in carbon dioxide concentration (mole fraction) on a logarithmic time scale for Horn River Group shale gases from 8 well locations - NTS 94/08.

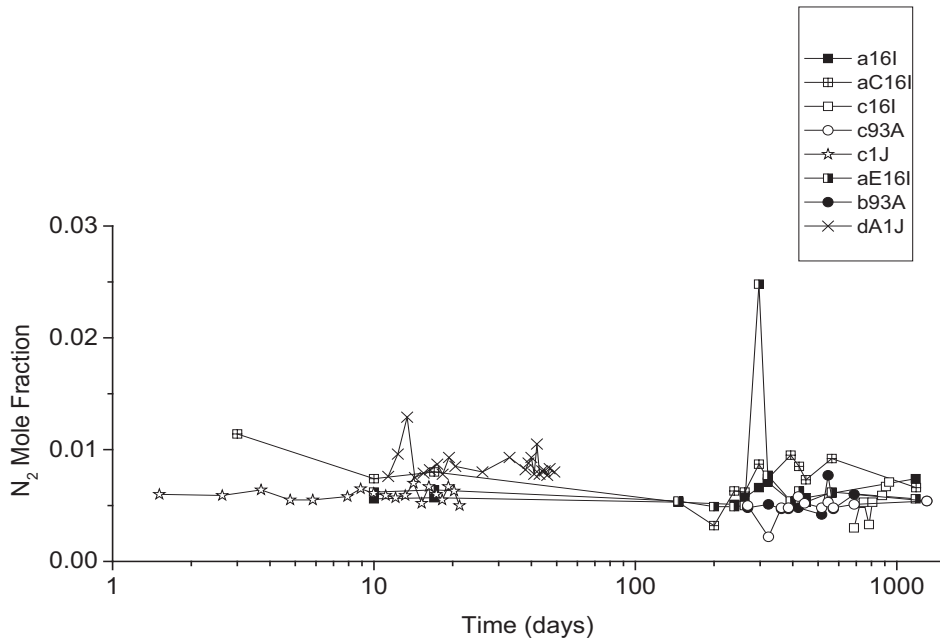


Figure A.17. Overlay plot showing variation in nitrogen concentration (mole fraction) on a logarithmic time scale for Horn River Group shale gases from 8 well locations - NTS 94/08.

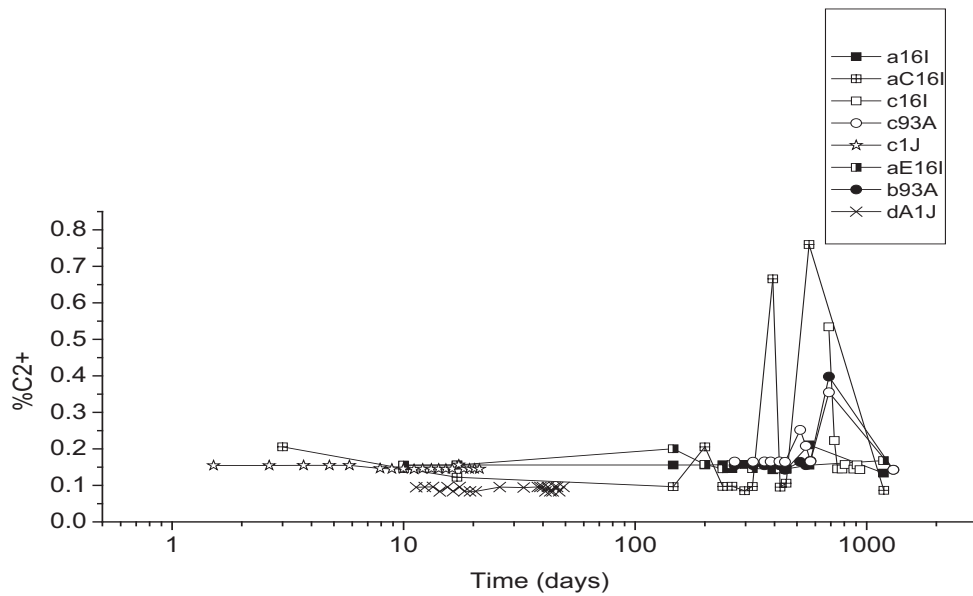


Figure A.18. Overlay plot showing variation in gas wetness on a logarithmic time scale for Horn River Group shale gases from 8 well locations - NTS 94/08.

APPENDIX B1 –Time Series
STABLE ISOTOPE COMPOSITION

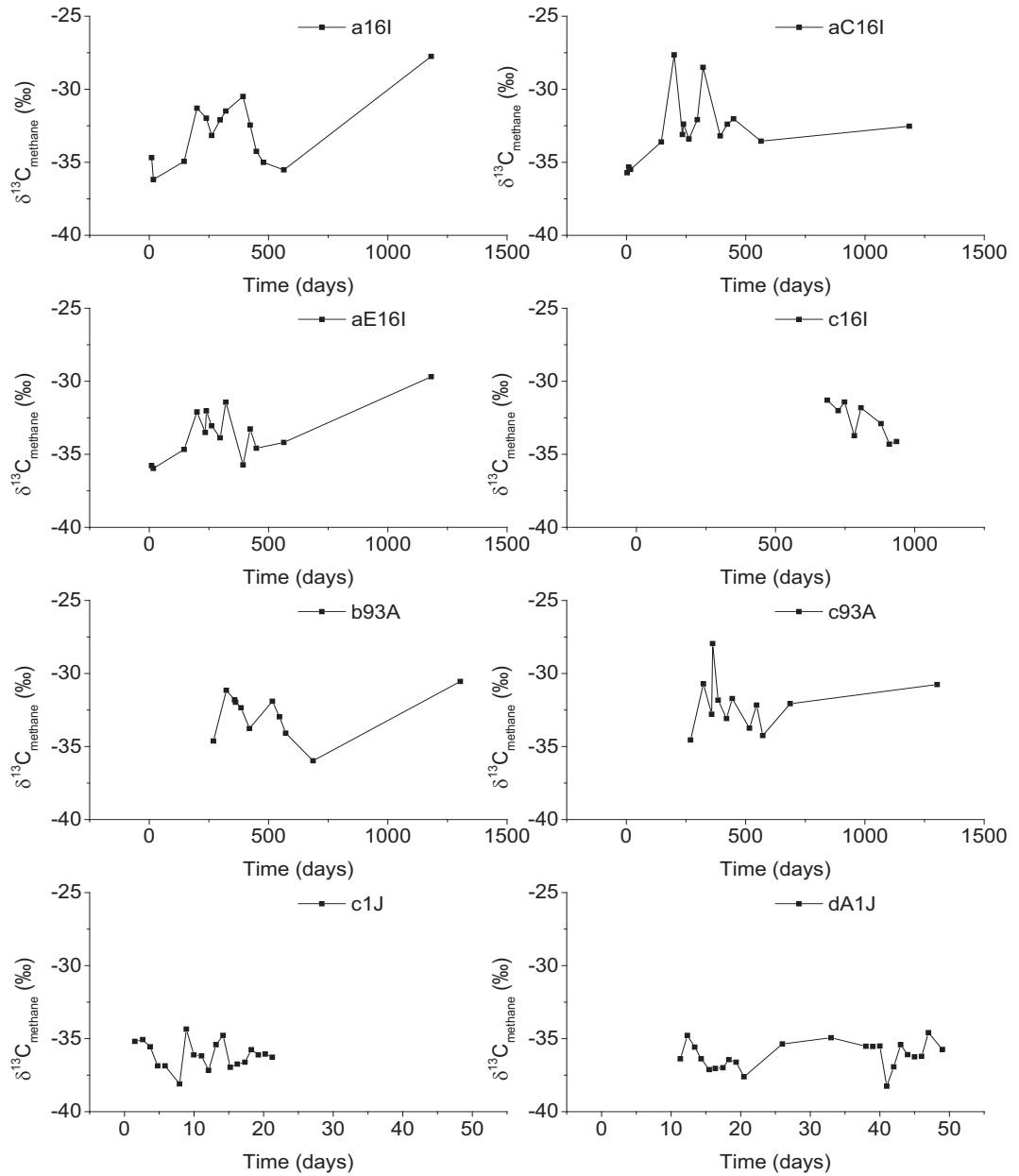


Figure B1.1. Variation in $\delta^{13}\text{C}_{\text{methane}}$ values for Horn River Group shale gases from 8 well locations - NTS 94/08.

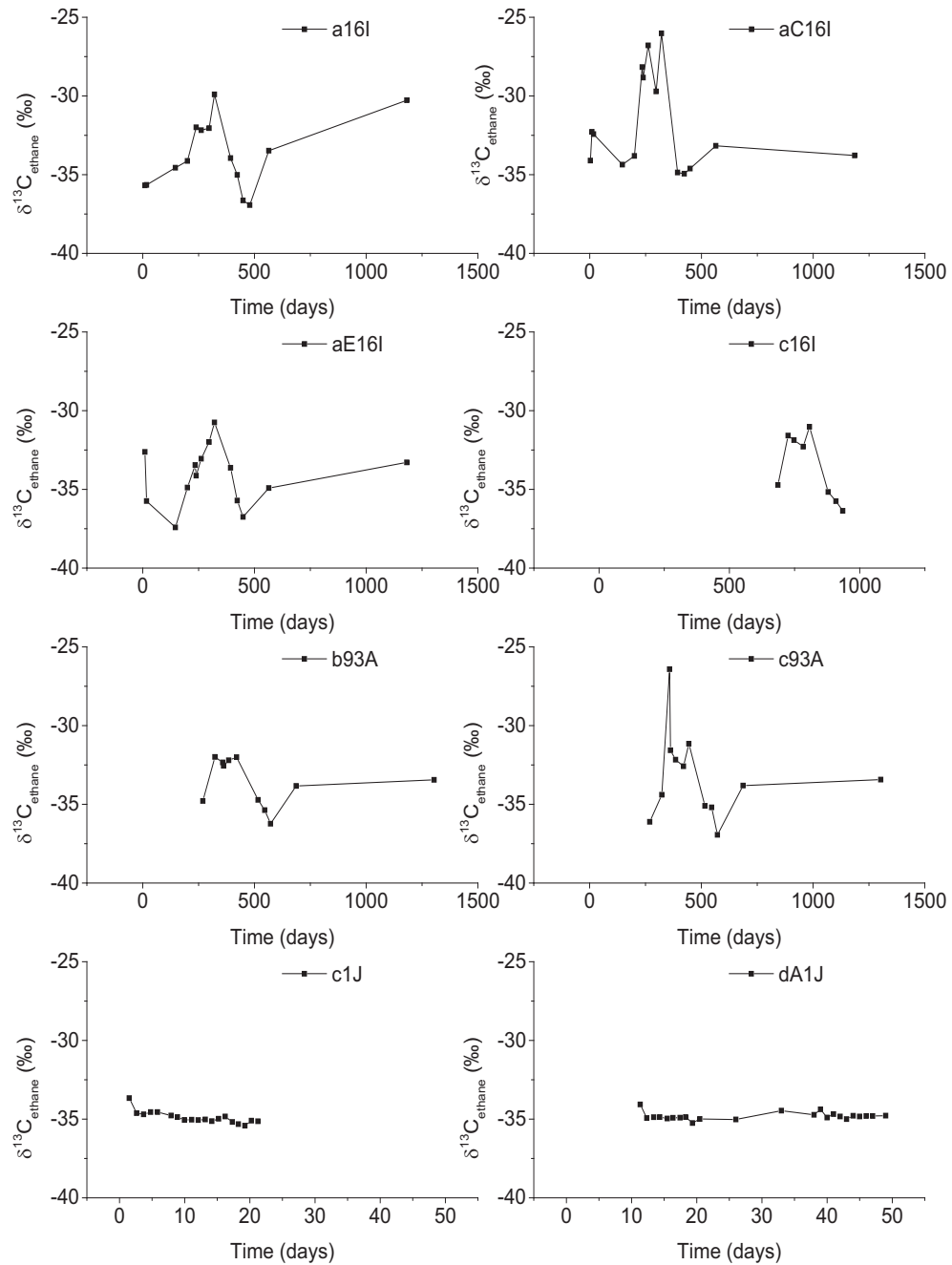


Figure B1.2. Variation in $\delta^{13}\text{C}_{\text{ethane}}$ values for Horn River Group shale gases from 8 well locations - NTS 94/08.

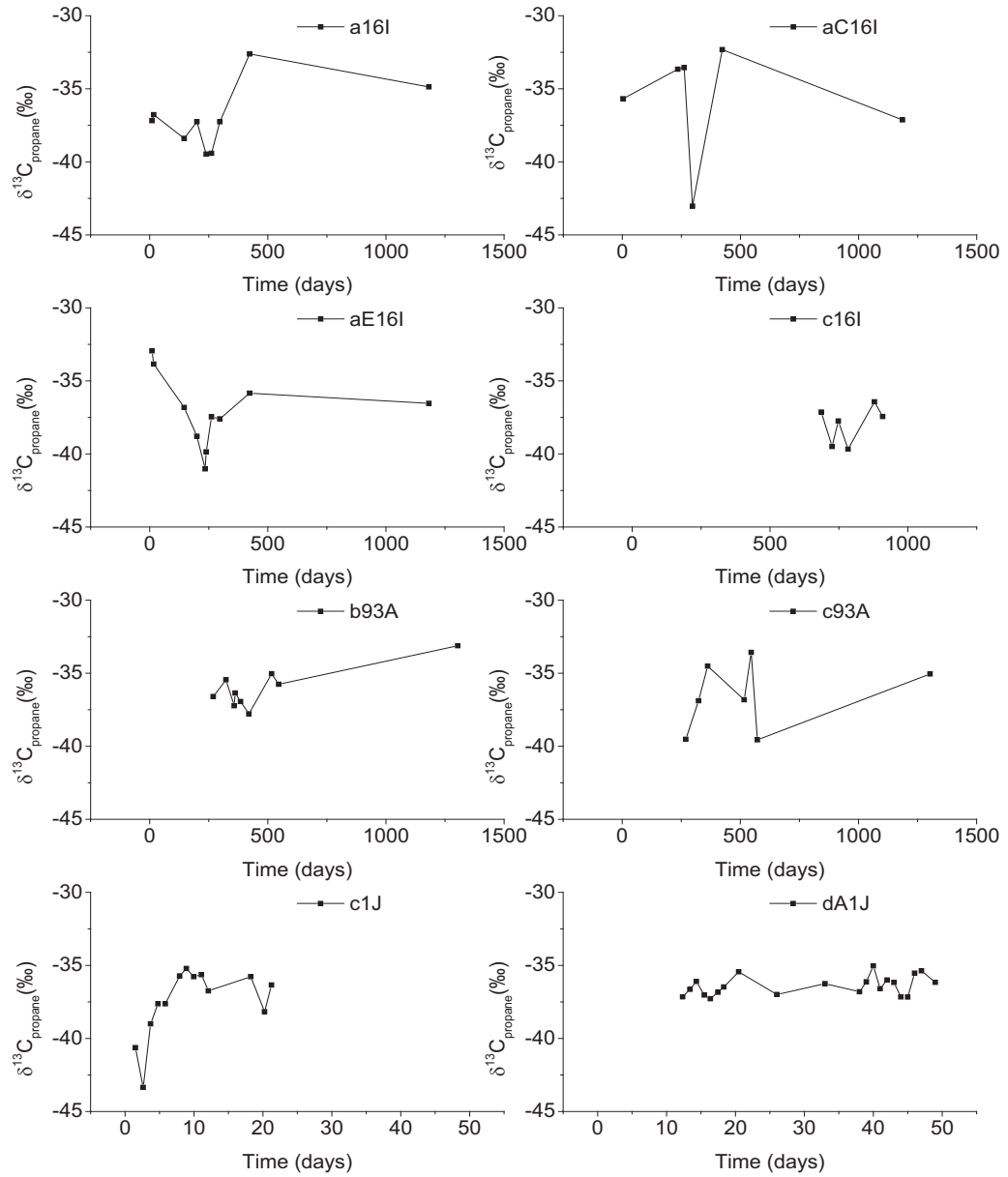


Figure B1.3. Variation in $\delta^{13}\text{C}_{\text{propane}}$ values for Horn River Group shale gases from 8 well locations - NTS 94/08.

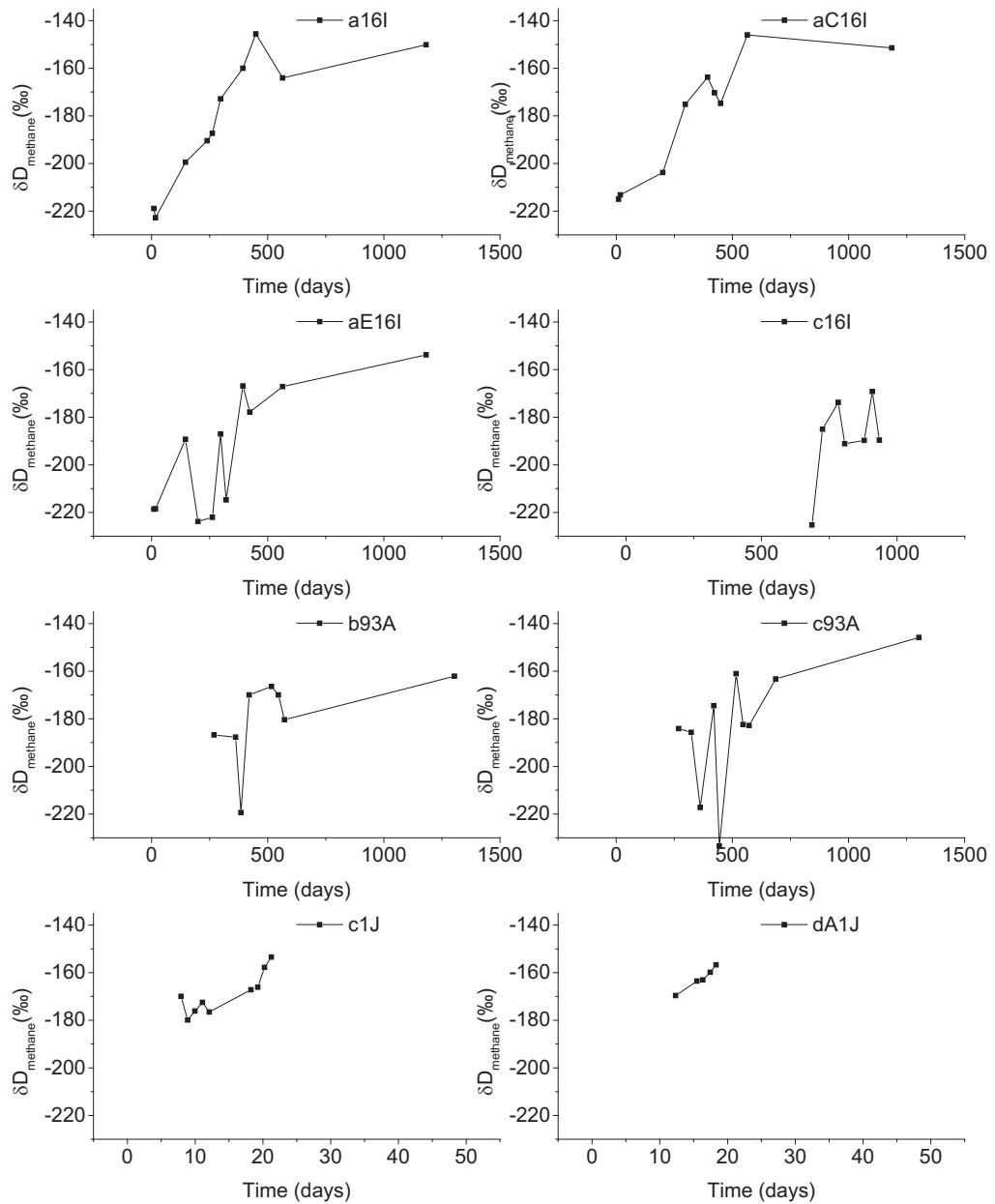


Figure B1.4. Variation in $\delta D_{\text{methane}}$ values for Horn River Group shale gases from 8 well locations - NTS 94/08.

Table B1.1 Carbon isotope ratios of methane and ethane for production gases from 18 wells located at the b-77-H multi-well pad site.

Well	Formation	$\delta^{13}\text{C}_{\text{methane}}(\text{‰})$	$\delta^{13}\text{C}_{\text{ethane}}(\text{‰})$
b-77-H	Muskwa	-36.63	-35.09
b-A77-H	Evie	-34.84	-34.05
b-B77-H	Otter Park	-35.82	-34.89
b-C77-H	Muskwa	-34.95	-34.71
b-D77-H	Evie	-34.74	-33.86
b-E77-H	Otter Park	-35.32	-34.74
b-F77-H	Muskwa	-36.68	-34.39
b-G77-H	Otter Park	-34.25	-34.84
b-H77-H	Evie	NA	NA
b-I77-H	Evie	-35.56	-35.65
b-J77-H	Muskwa	-34.82	-34.3
b-K77-H	Otter Park	-35.94	-34.24
b-L77-H	Muskwa	-35.59	-35.05
b-M77-H	Evie	-31.81	-33.44
b-N77-H	Otter Park	-35.73	-34.97
b-O77-H	Muskwa	-36.57	-34.65
b-P77-H	Evie	-35.37	-33.50
b-Q77-H	Otter Park	-35.11	-34.26

NA –Not available

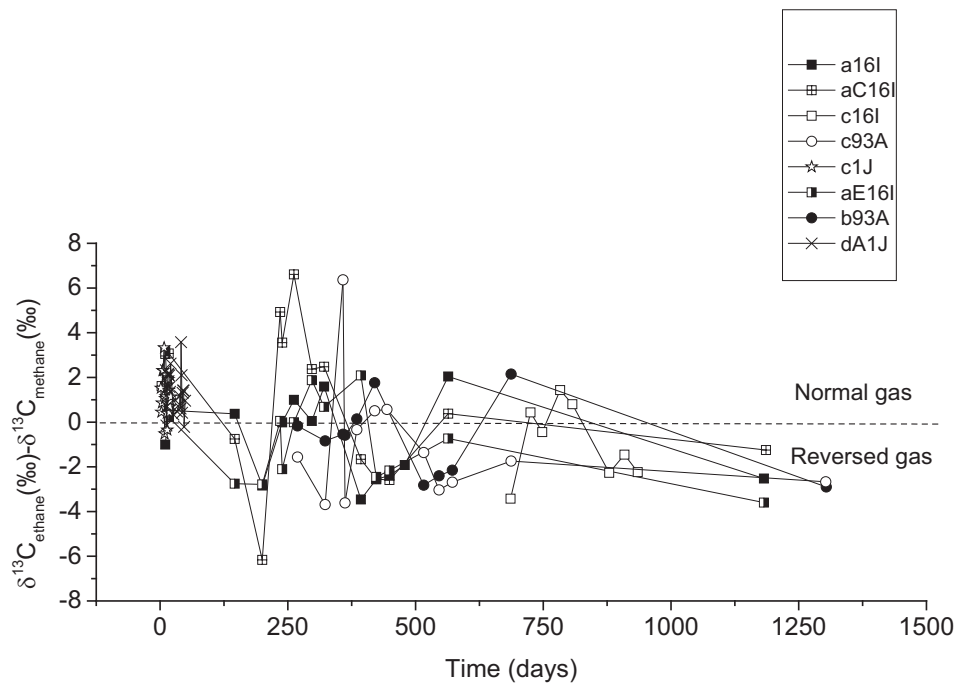


Figure B1.5. Overlay plot of $\delta^{13}\text{C}_{\text{ethane}} - \delta^{13}\text{C}_{\text{methane}}$ for Horn River Group shale gases from 8 well locations - NTS 94/08.

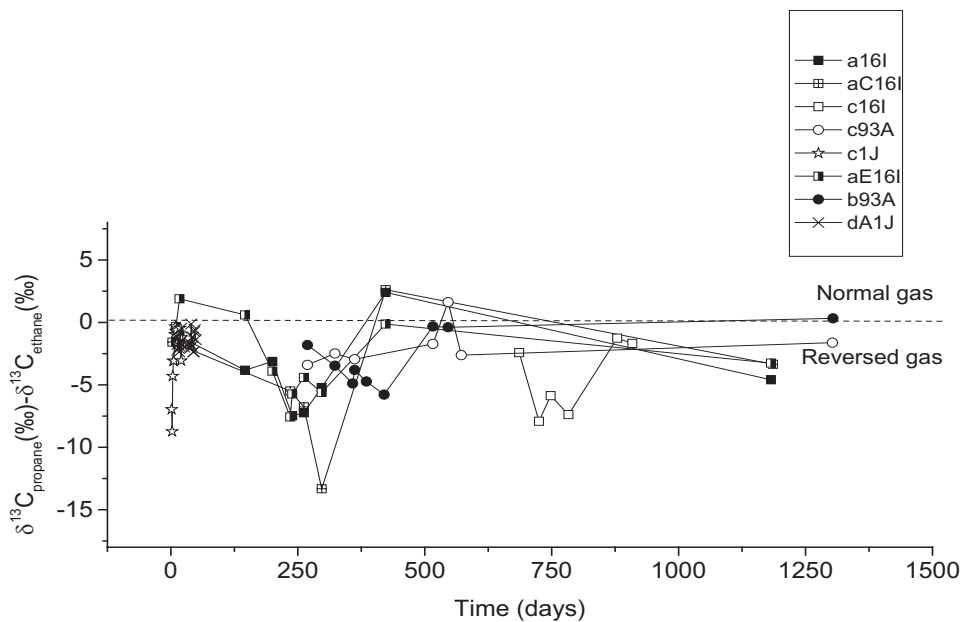


Figure B1.6. Overlay plot of $\delta^{13}\text{C}_{\text{propane}} - \delta^{13}\text{C}_{\text{ethane}}$ for Horn River Group shale gases from 8 well locations - NTS 94/08.

APPENDIX B2 – Isotope Cross-plots

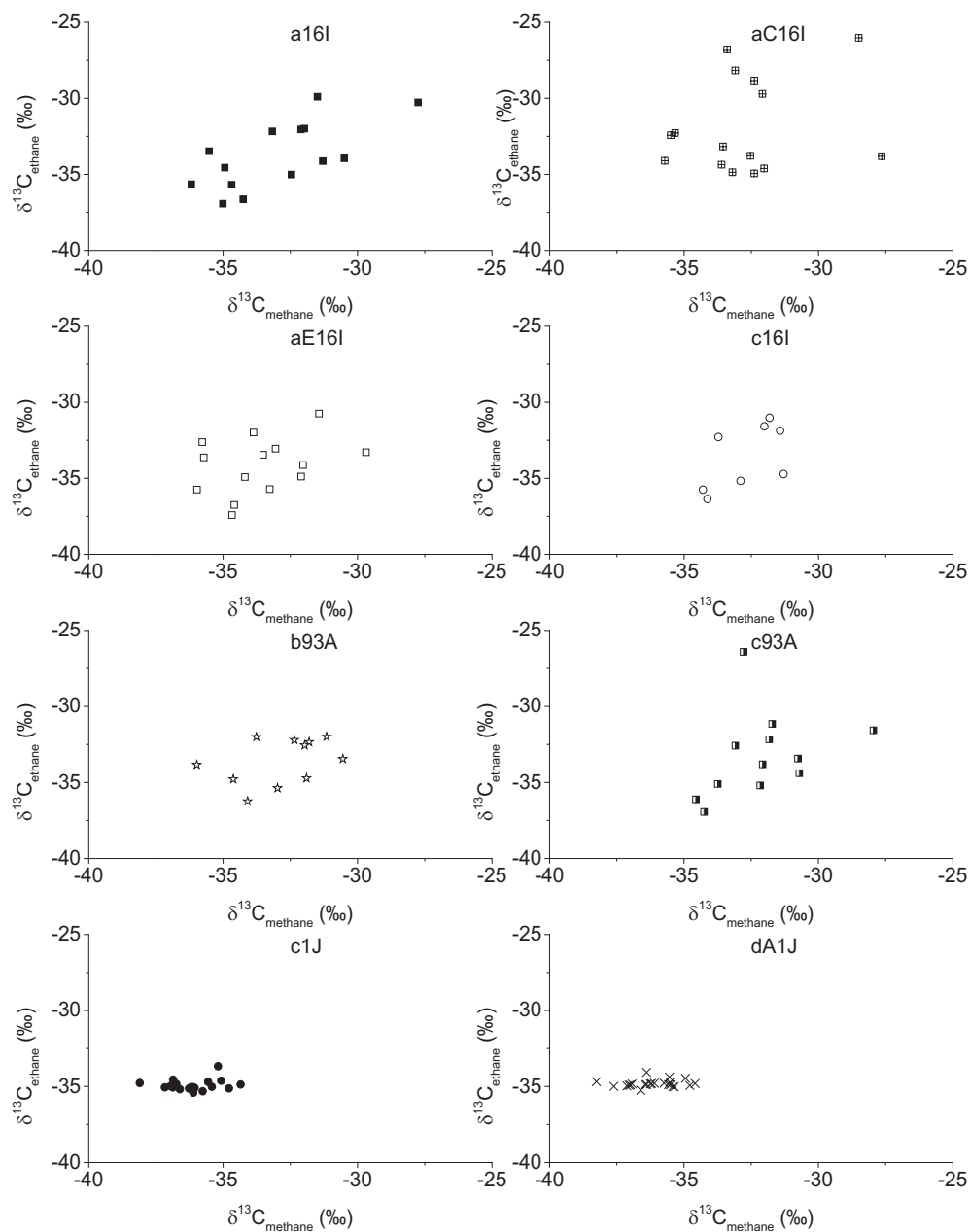


Figure B2.1. Isotope cross-plot showing $\delta^{13}\text{C}_{\text{ethane}}$ vs $\delta^{13}\text{C}_{\text{methane}}$ for Horn River Group shale gases from 8 well locations - NTS 94/08.

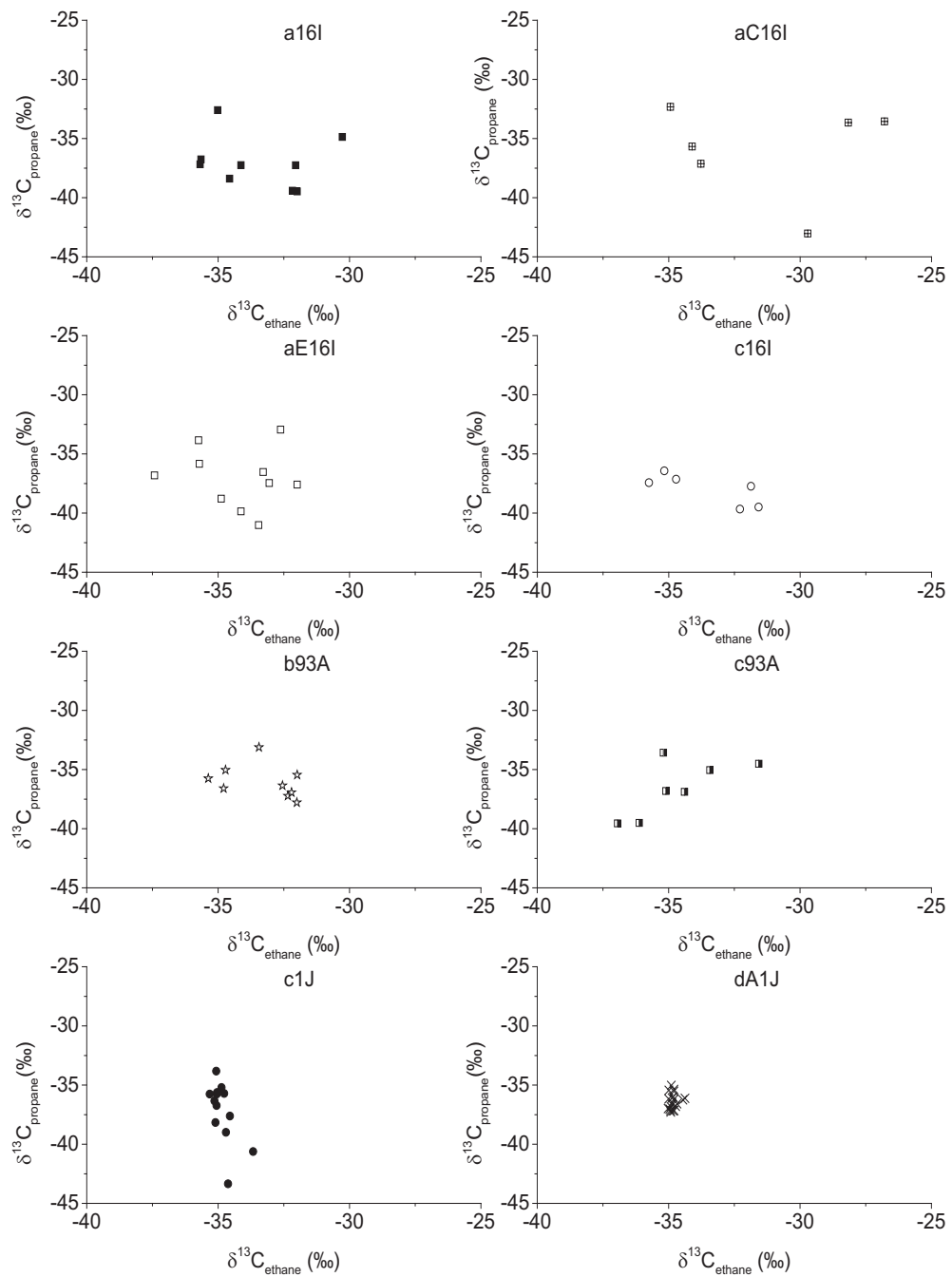


Figure B2.2. Isotope cross-plot showing $\delta^{13}\text{C}_{\text{propane}}$ vs $\delta^{13}\text{C}_{\text{ethane}}$ for Horn River Group shale gases from 8 well locations - NTS 94/08.

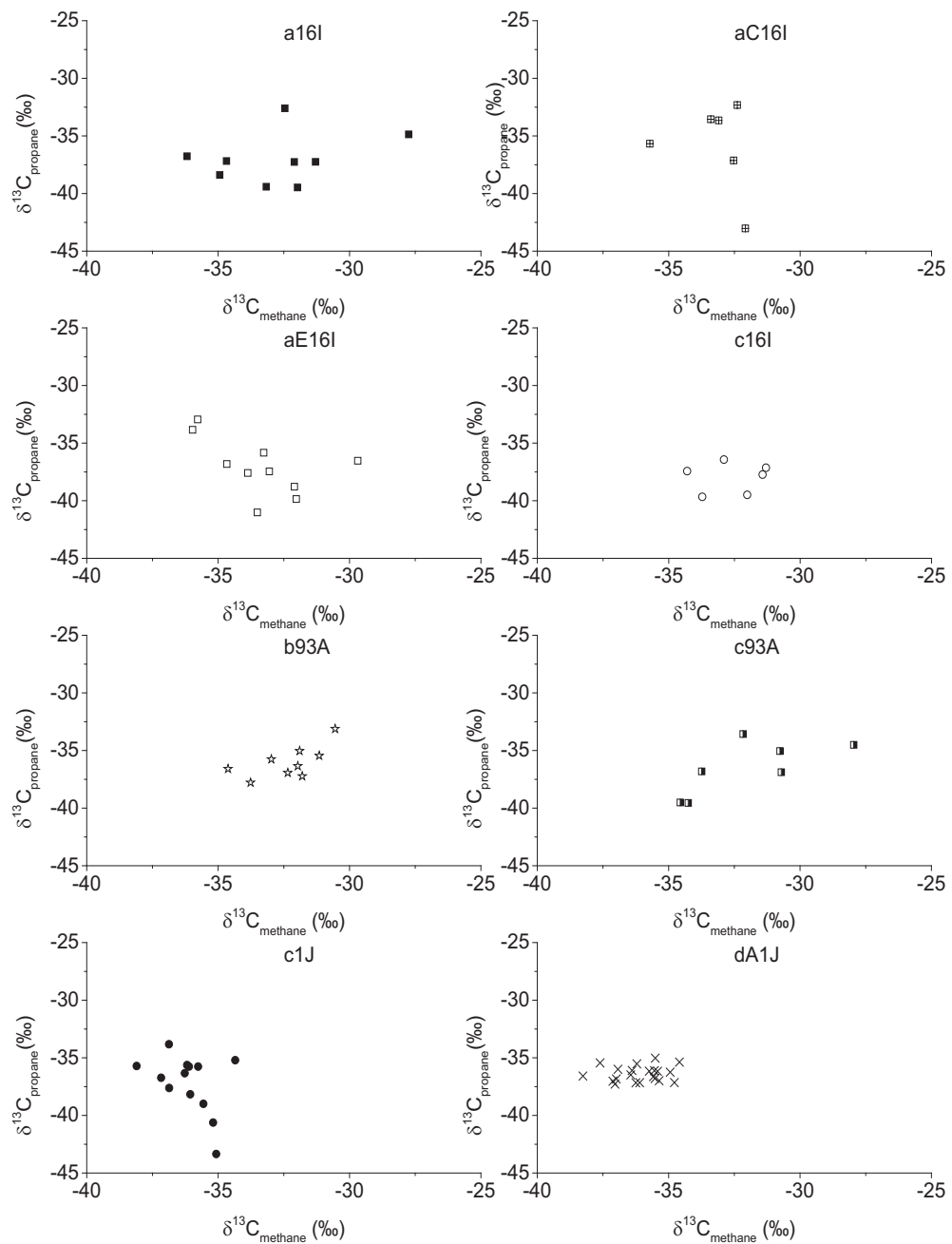


Figure B2.3. Isotope cross-plot showing $\delta^{13}\text{C}_{\text{propane}}$ vs $\delta^{13}\text{C}_{\text{methane}}$ for Horn River Group shale gases from 8 well locations - NTS 94/08.

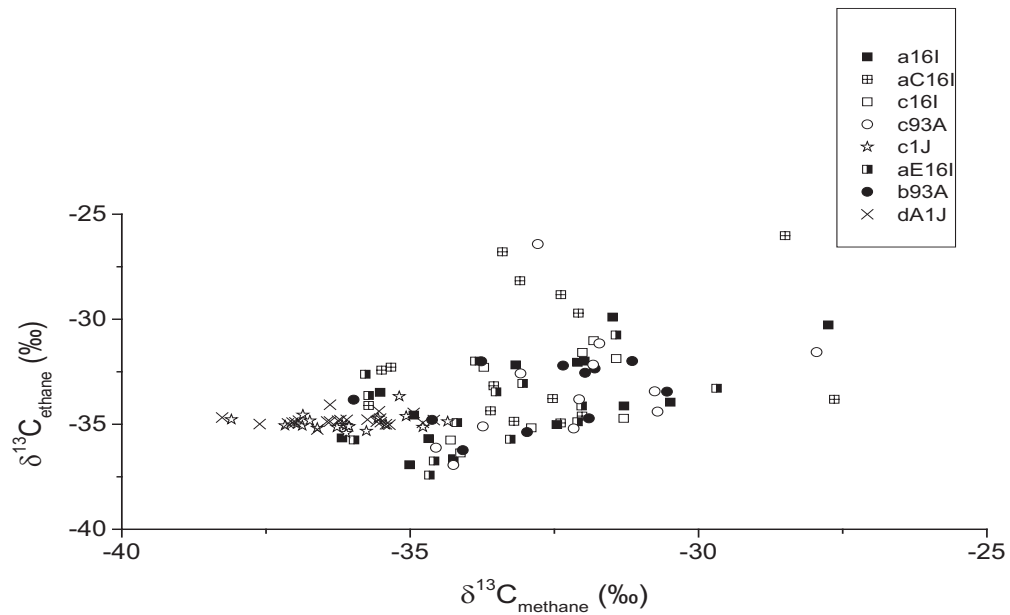


Figure B2.4. Overlay plot of $\delta^{13}\text{C}_{\text{ethane}} - \delta^{13}\text{C}_{\text{methane}}$ for Horn River Group shale gases from 8 well locations - NTS 94/08.

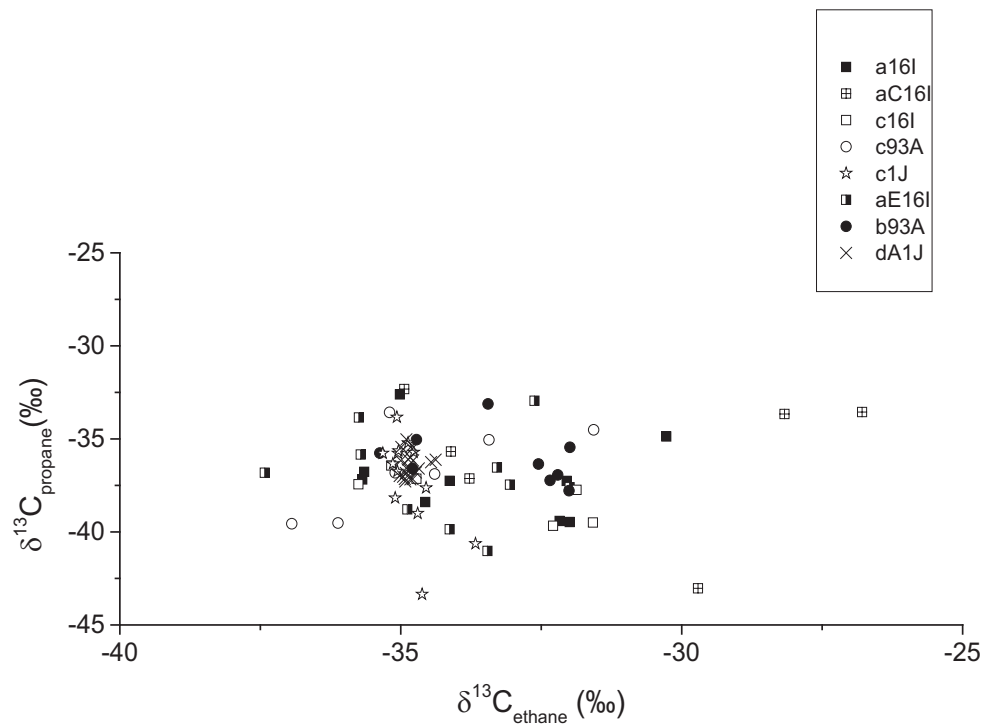


Figure B2.5. Overlay plot of $\delta^{13}\text{C}_{\text{propane}} - \delta^{13}\text{C}_{\text{ethane}}$ for Horn River Group shale gases from 8 well locations - NTS 94/08.

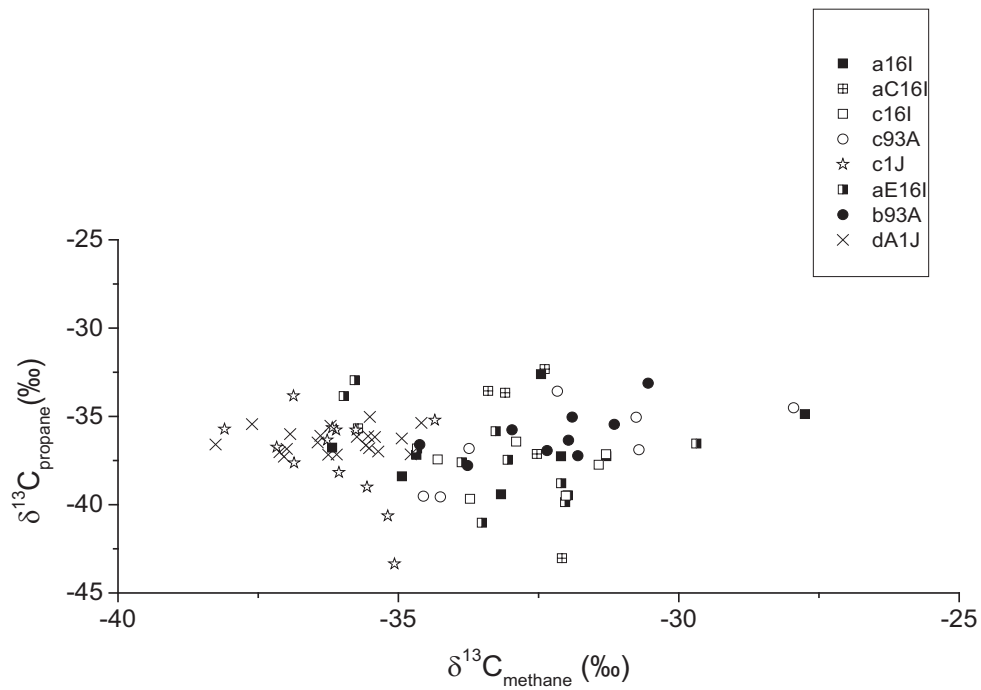


Figure B2.6. Overlay plot of $\delta^{13}\text{C}_{\text{propane}} - \delta^{13}\text{C}_{\text{methane}}$ for Horn River Group shale gases from 8 well locations - NTS 94/08.

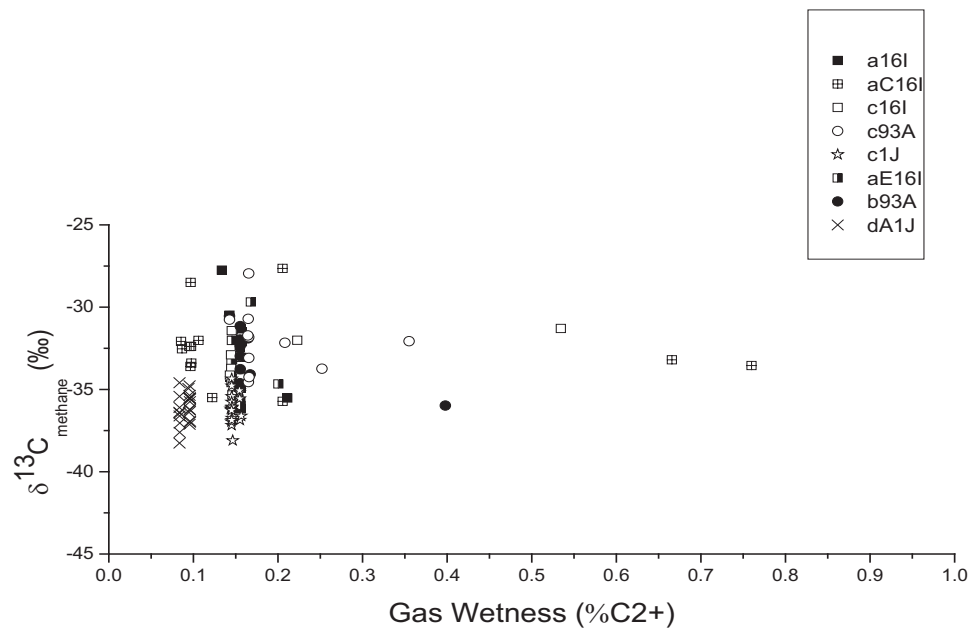


Figure B2.7. Overlay plot of $\delta^{13}\text{C}_{\text{methane}}$ vs gas wetness for Horn River Group shale gases from 8 well locations - NTS 94/08.

APPENDIX C1 - Time Series

GAS PRODUCTION

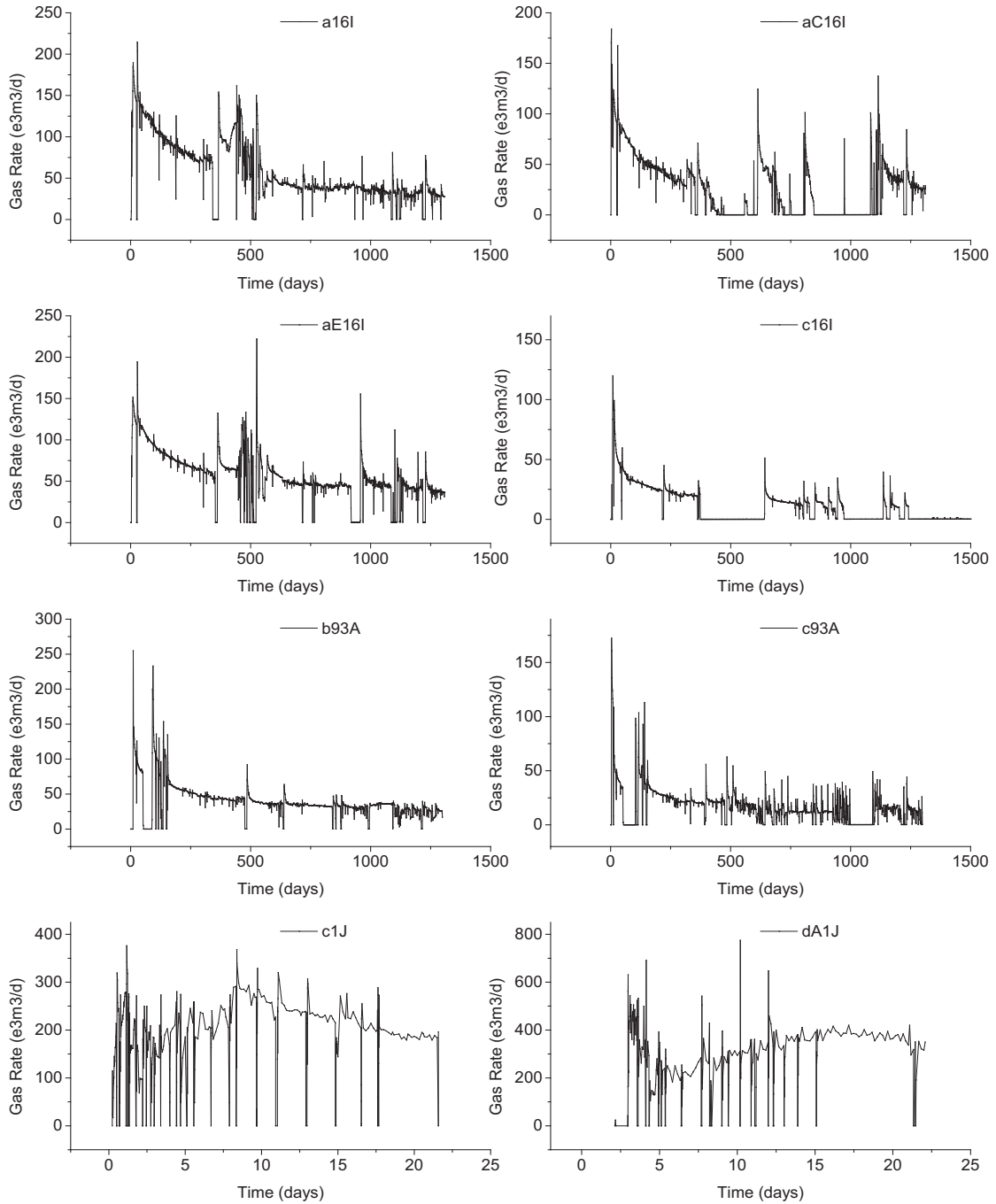


Figure C1.1. Gas production decline curves for Horn River Group shale gases from 8 well locations - NTS 94/08.

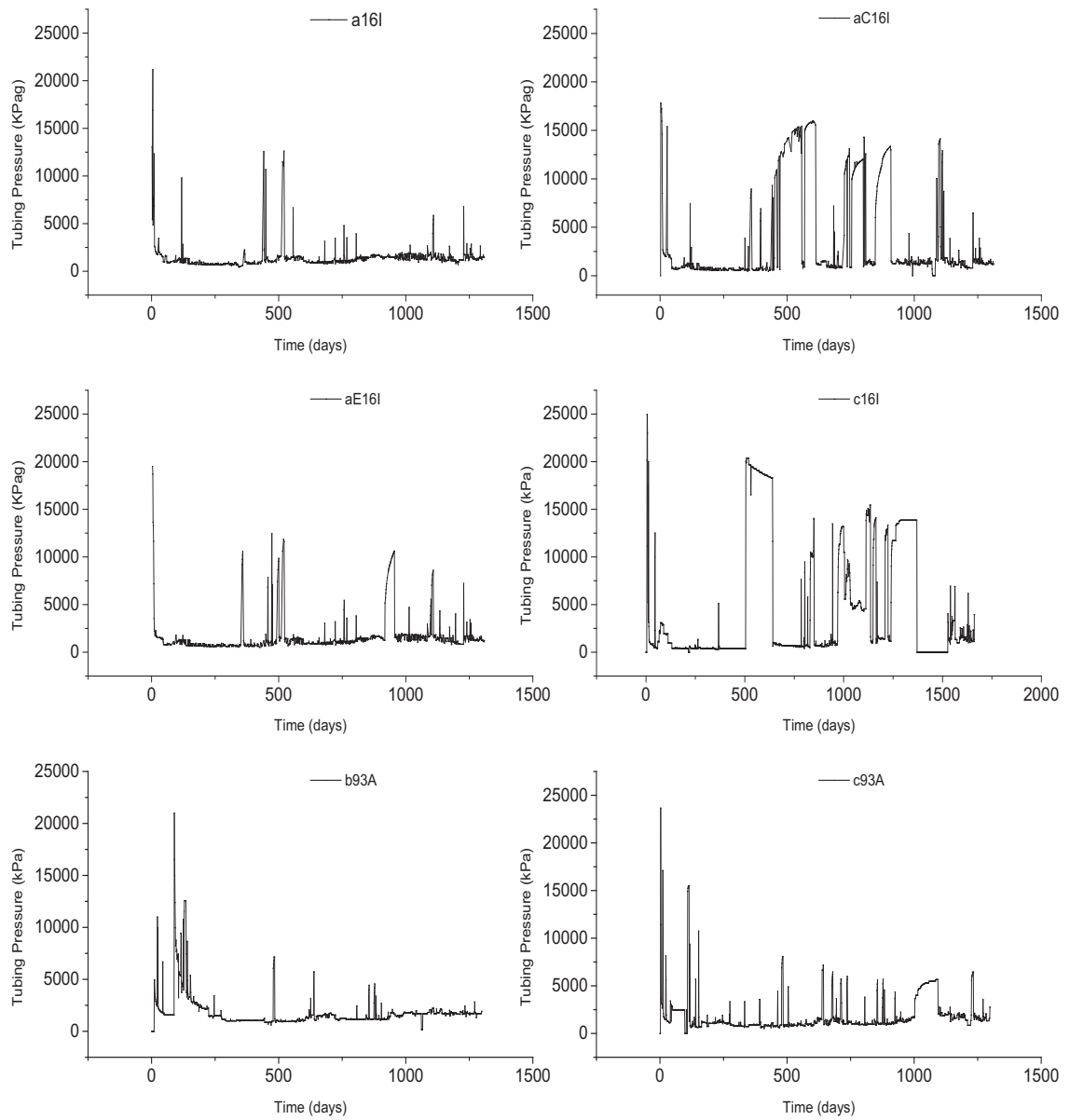


Figure C1.2. Variation in tubing pressure for Horn River Group shale gases from 6 well locations - NTS 94/08.

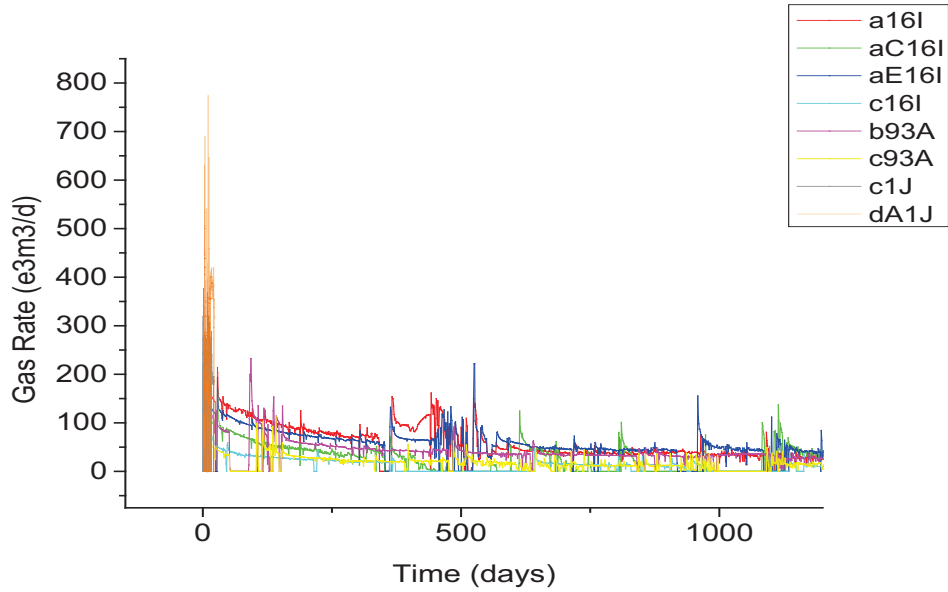


Figure C1.3. Gas production decline curves for Horn River Group shale gases from 8 well locations - NTS 94/08.

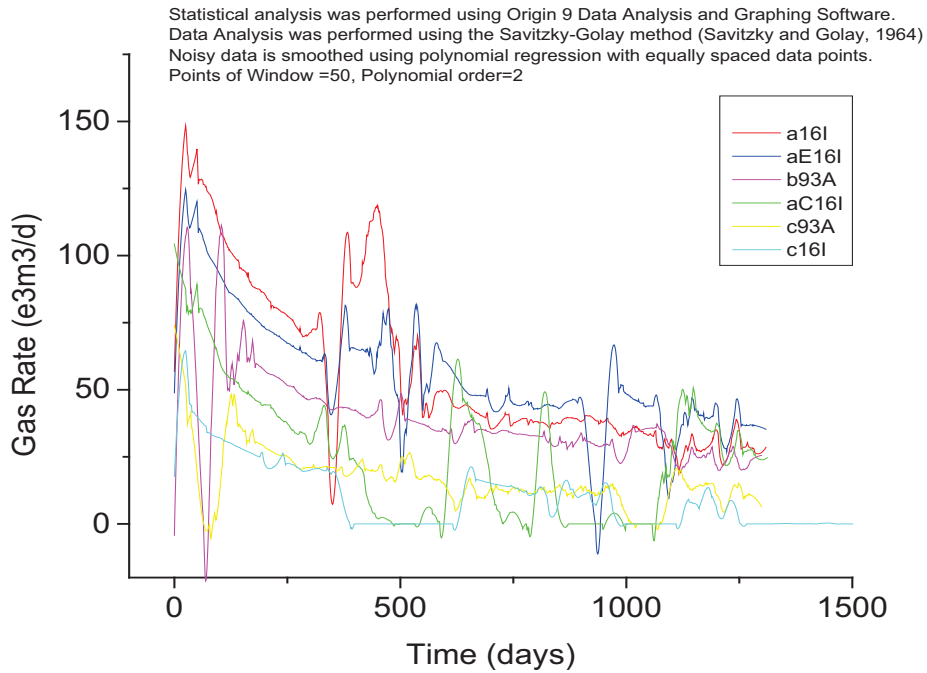


Figure C1.4. Gas production decline curves for Horn River Group shale gases from 6 well locations - NTS 94/08.

APPENDIX C2

GAS PRODUCTION AND STABLE ISOTOPES

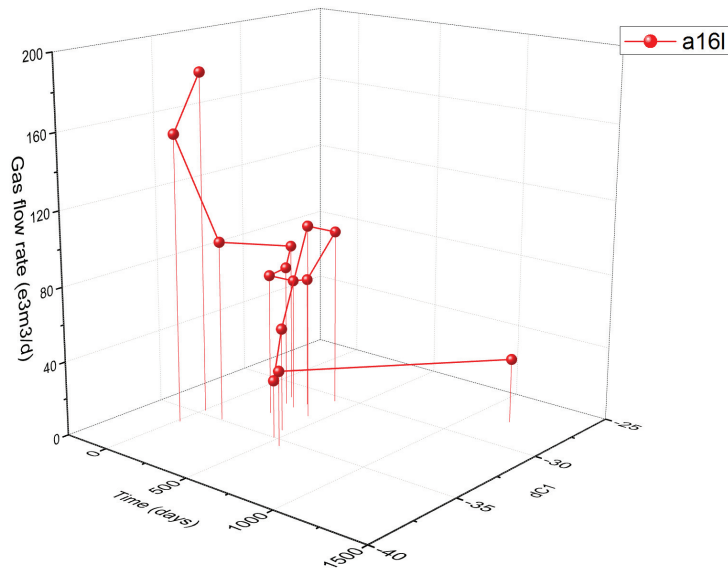


Figure C2.1. 3D plot showing variation in gas flow rate and $\delta^{13}\text{C}_{\text{methane}}$ with time for well a16I - NTS 94/08.

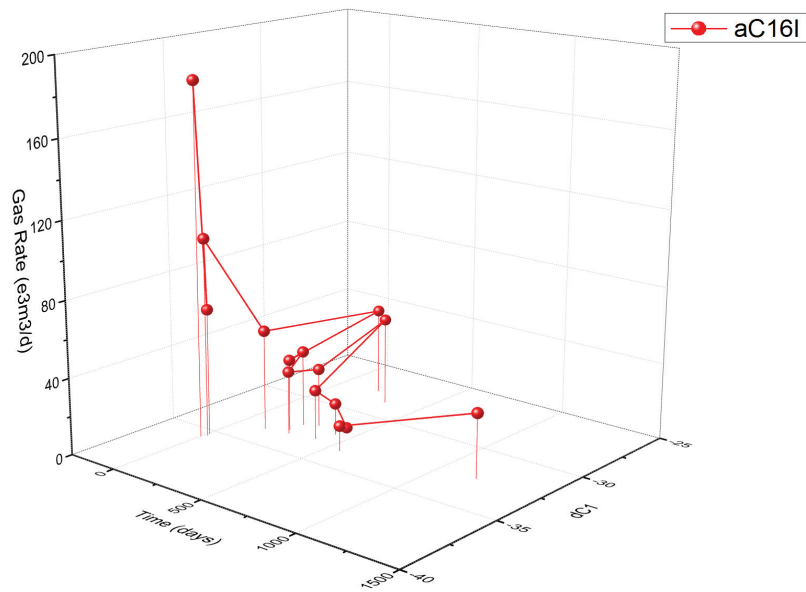


Figure C2.2. 3D plot showing variation in gas flow rate and $\delta^{13}\text{C}_{\text{methane}}$ with time for well aC16I - NTS 94/08.

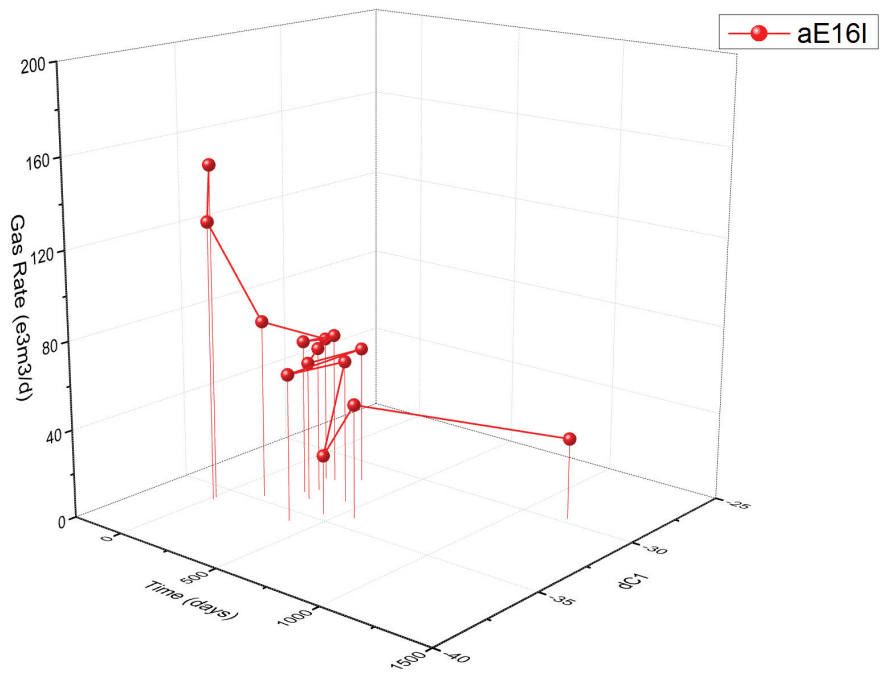


Figure C2.3. 3D plot showing variation in gas flow rate and $\delta^{13}\text{C}_{\text{methane}}$ with time for well aE16I - NTS 94/08.

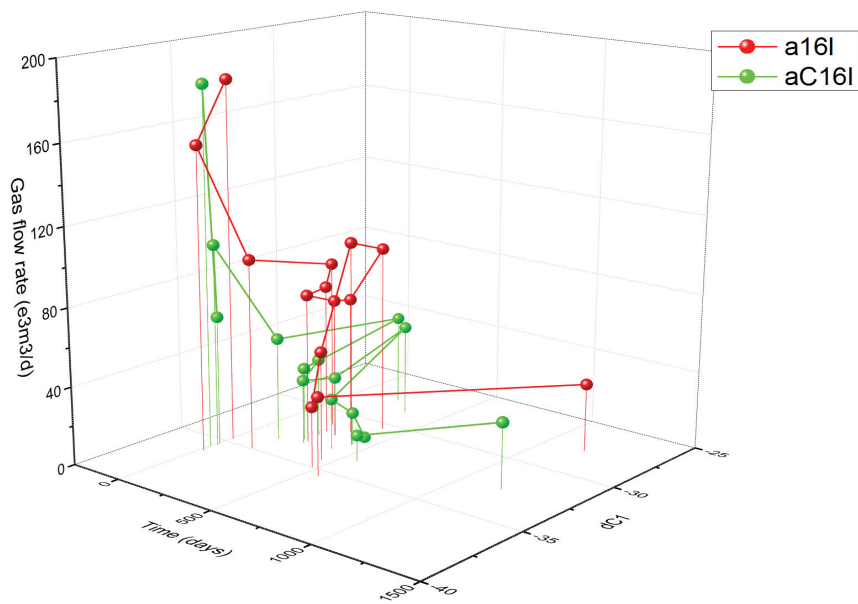


Figure C2.4. Overlay 3D plot showing variation in gas flow rate and $\delta^{13}\text{C}_{\text{methane}}$ with time for wells a16I and aC16I - NTS 94/08.

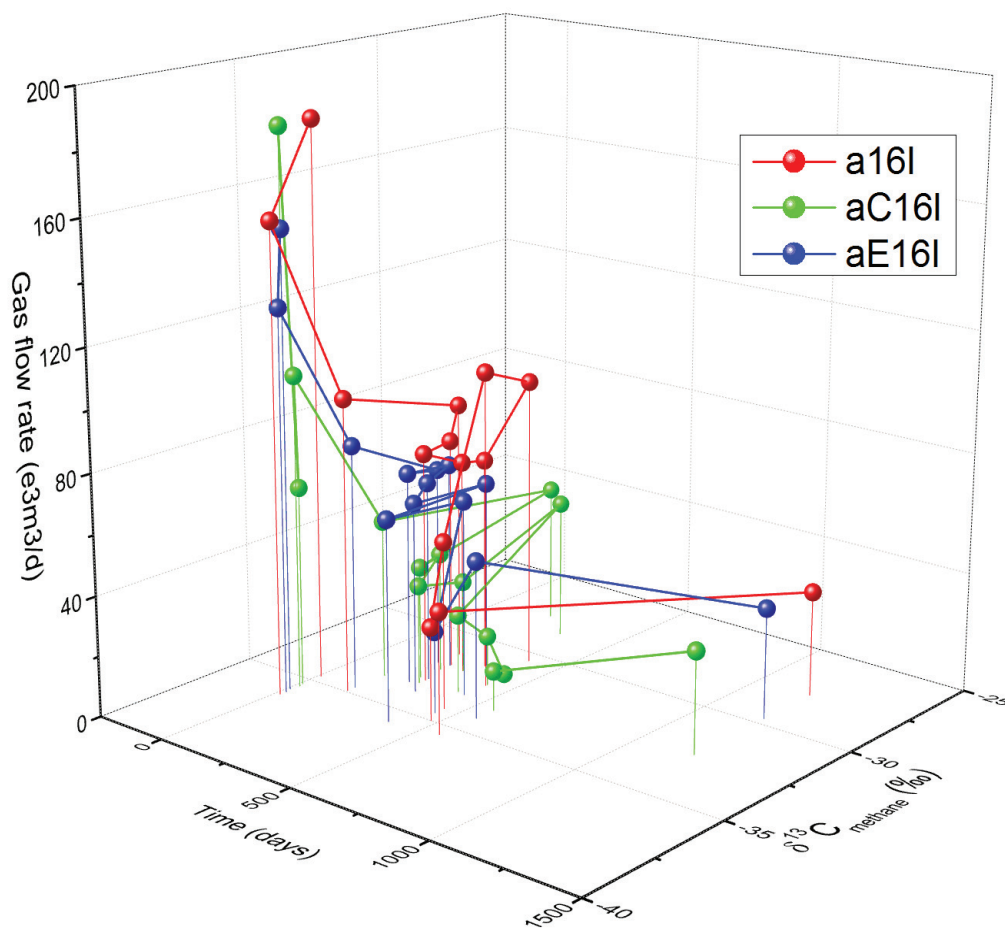


Figure C2.5. Overlay 3D plot showing variation in gas flow rate and $\delta^{13}\text{C}_{\text{methane}}$ with time for three wells at the a16I multi-well pad site (a16I and aC16I and aE16I) - NTS 94/08.

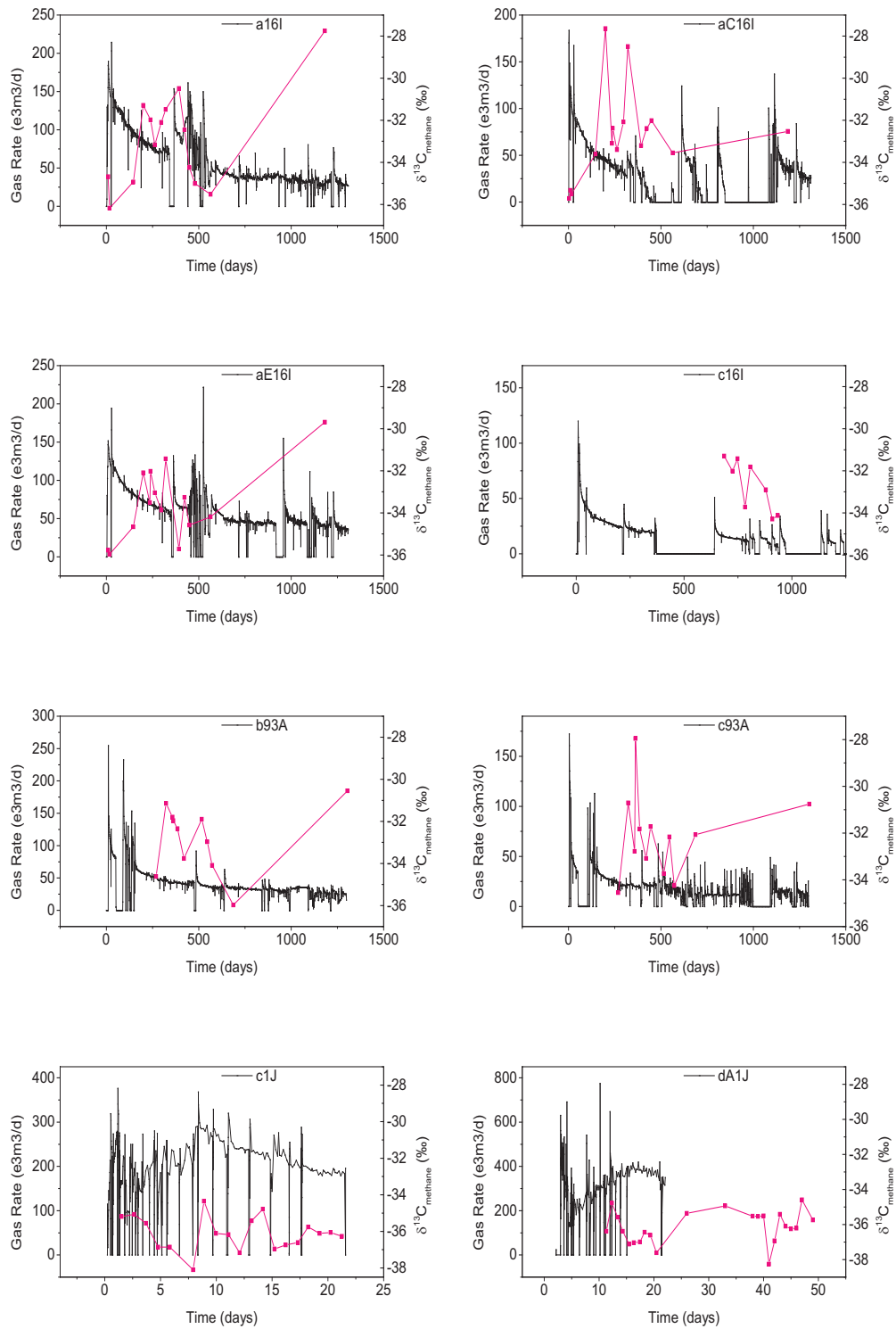


Figure C2.6. Overlay plots of gas production rate and methane carbon isotope values ($\delta^{13}\text{C}_{\text{methane}}$) vs time for Horn River Group shale gases from 8 well locations - NTS 94/08.

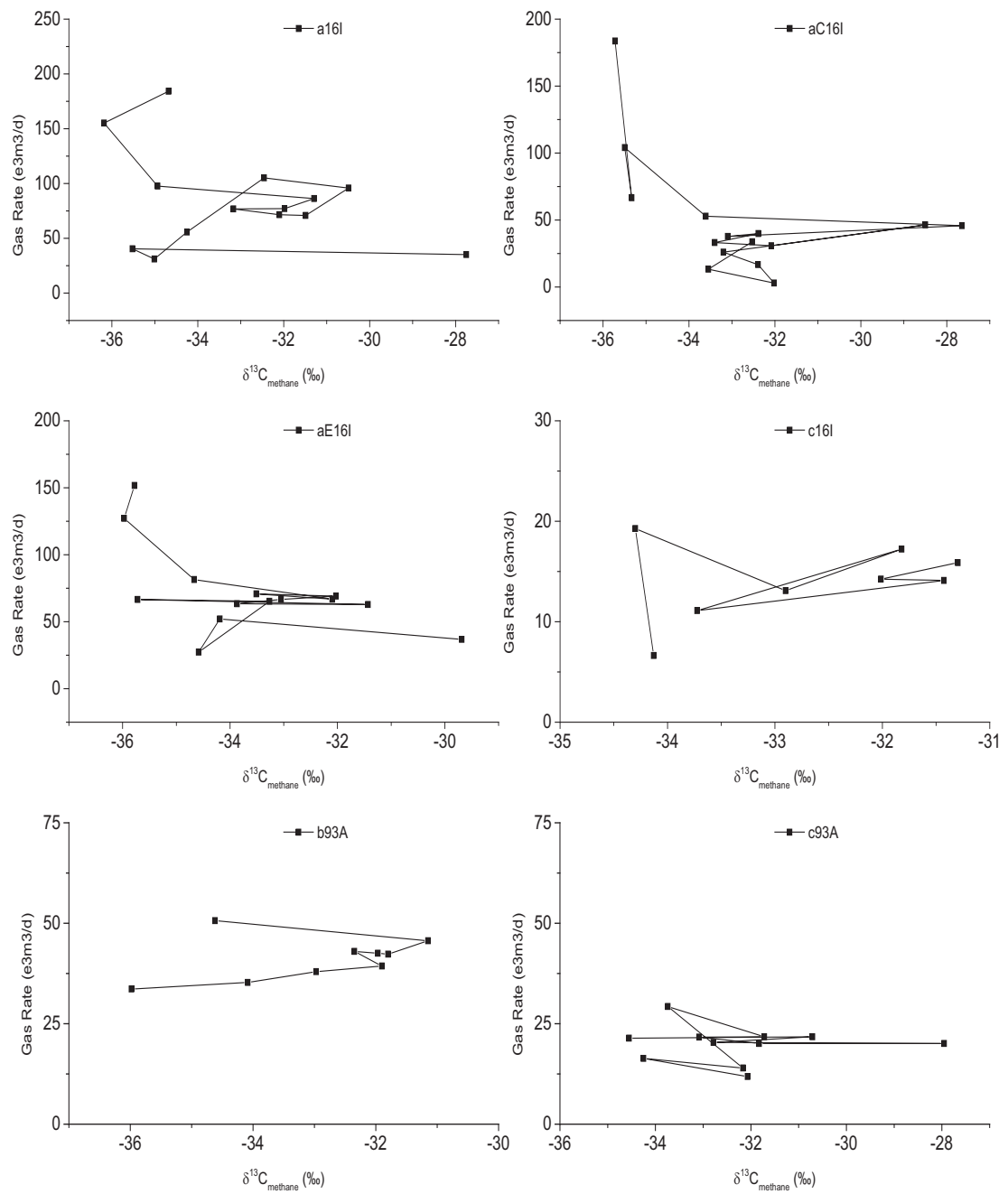


Figure C2.7. Gas rate vs methane carbon isotope values ($\delta^{13}\text{C}_{\text{methane}}$) for Horn River Group shale gases from 6 well locations - NTS 94/08.

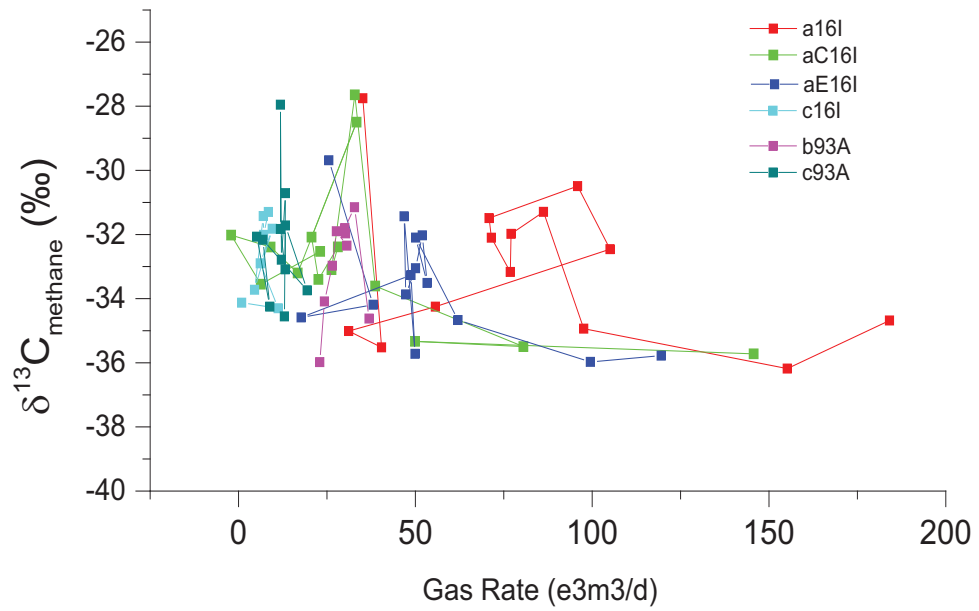


Figure C2.8. Overlay plot showing methane carbon isotope values ($\delta^{13}\text{C}_{\text{methane}}$) vs gas rate for Horn River Group shale gases from 6 well locations - NTS 94/08.

APPENDIX D – The Natural Gas Plot

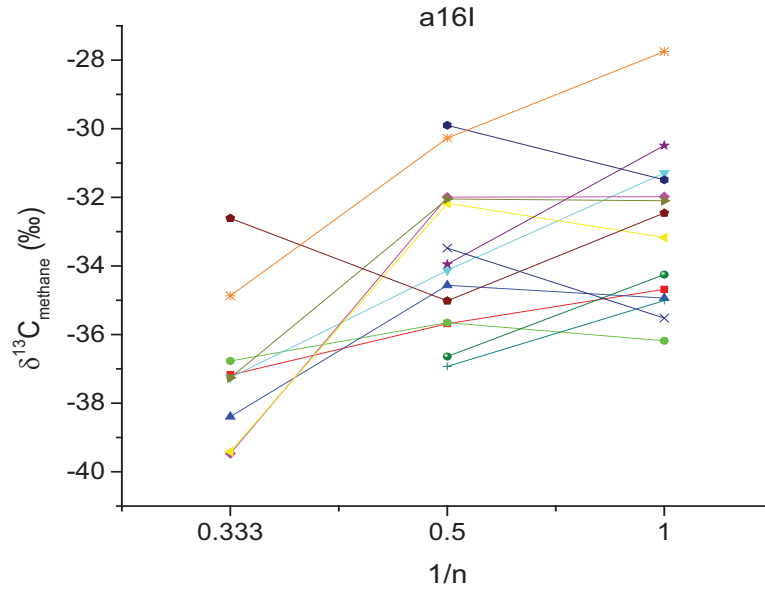


Figure D.1. The natural gas plot for well a16I (NTS 94/08). $\delta^{13}\text{C}$ values vs $1/n$ are shown where n represents the number of carbon atoms in the hydrocarbon.

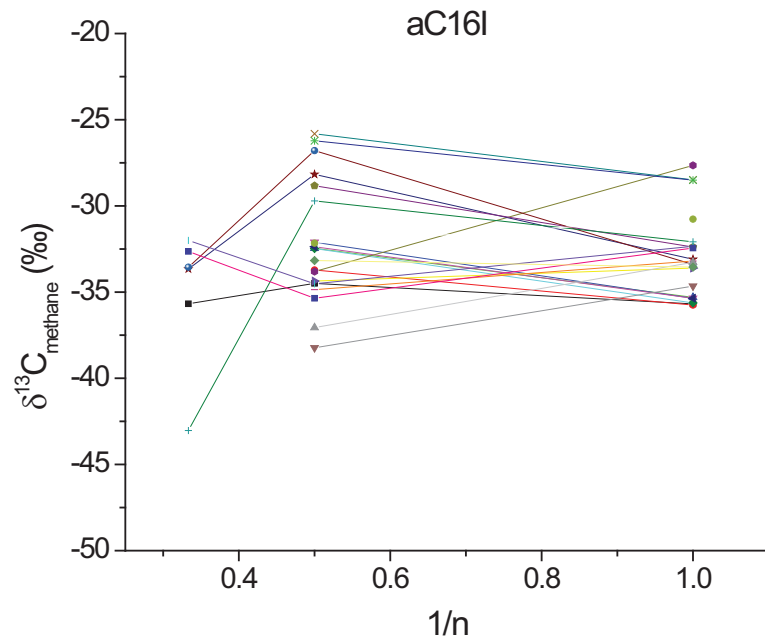


Figure D.2. The natural gas plot for well aC16I (NTS 94/08). $\delta^{13}\text{C}$ values vs $1/n$ are shown where n represents the number of carbon atoms in the hydrocarbon.

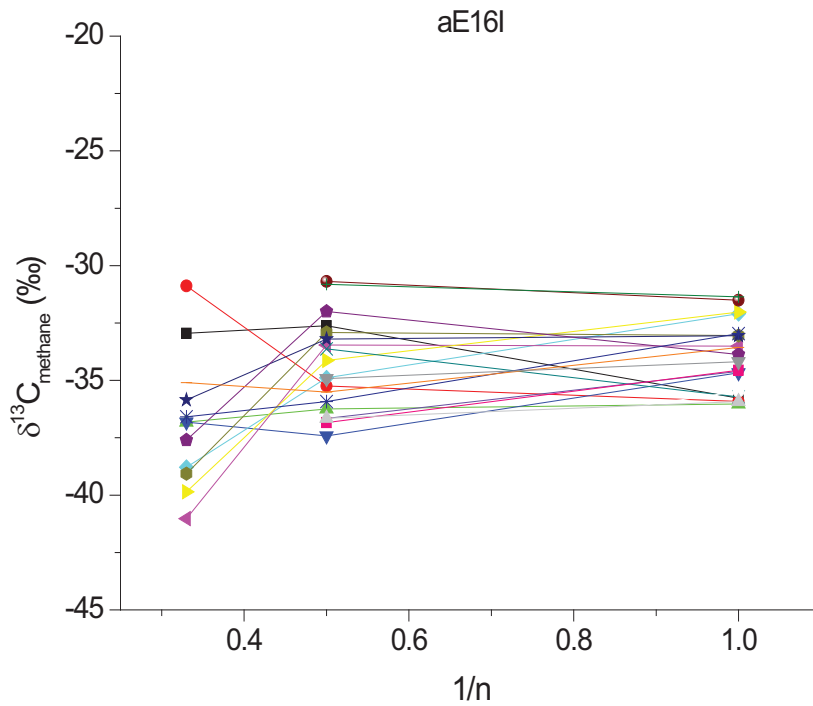


Figure D.3. The natural gas plot for well aE16I (NTS 94/08). $\delta^{13}\text{C}$ values vs $1/n$ are shown where n represents the number of carbon atoms in the hydrocarbon.

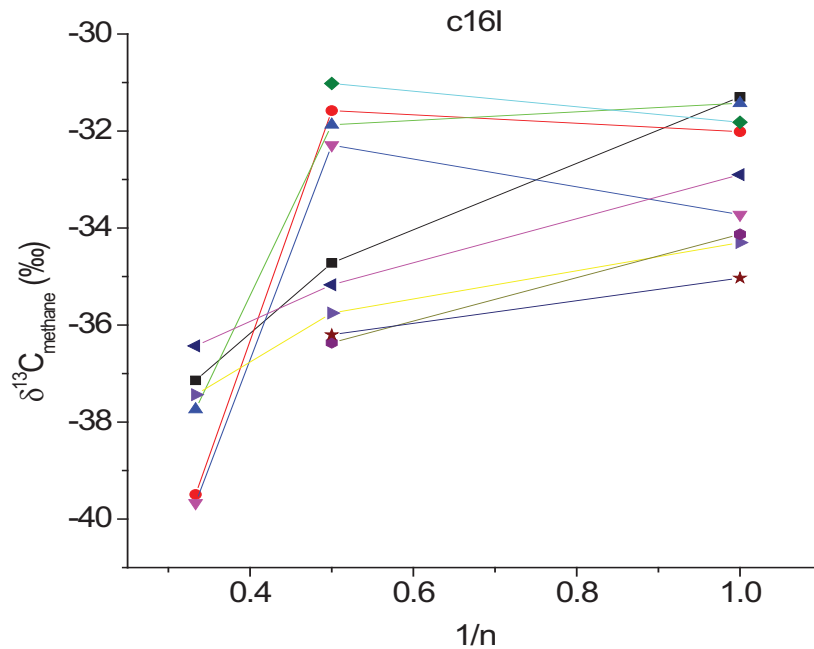


Figure D.4. The natural gas plot for well c16I (NTS 94/08). $\delta^{13}\text{C}$ values vs $1/n$ are shown where n represents the number of carbon atoms in the hydrocarbon.

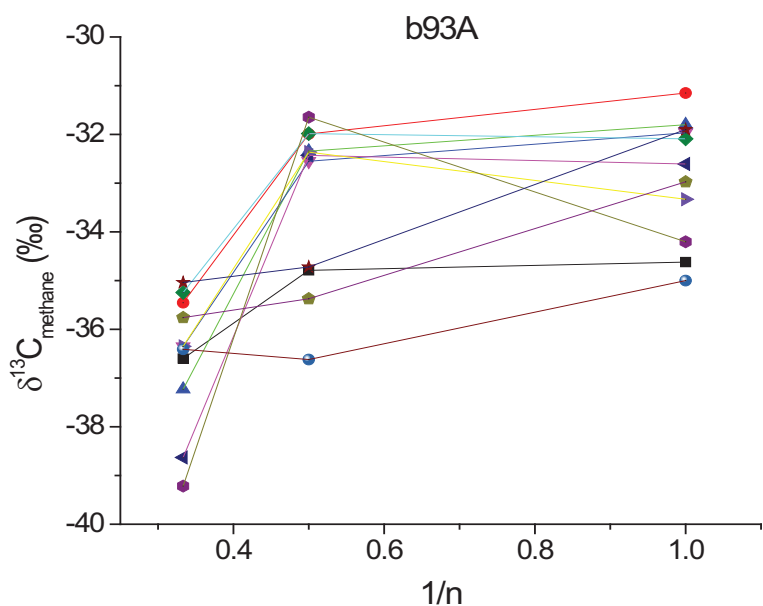


Figure D.5. The natural gas plot for well b93A (NTS 94/08). $\delta^{13}\text{C}$ values vs $1/n$ are shown where n represents the number of carbon atoms in the hydrocarbon.

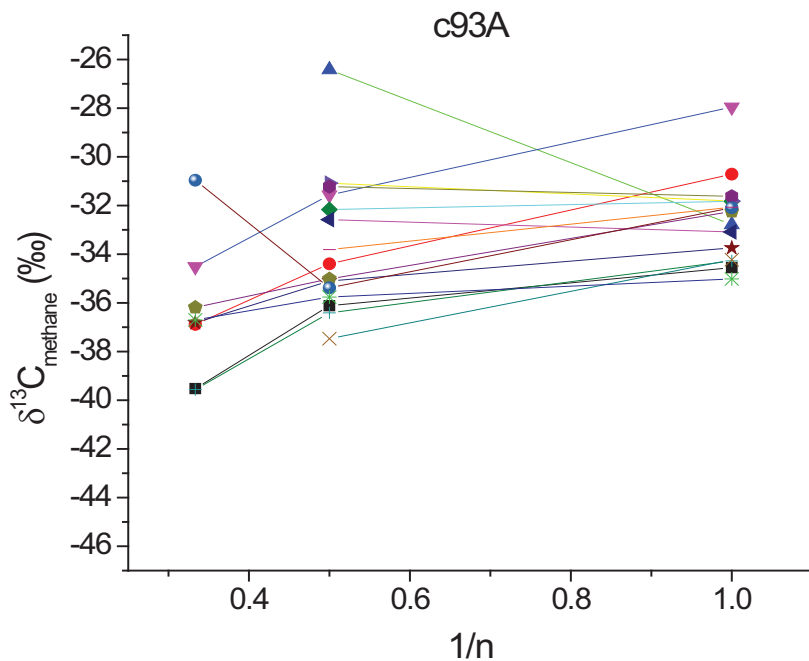


Figure D.6. The natural gas plot for well c93A (NTS 94/08). $\delta^{13}\text{C}$ values vs $1/n$ are shown where n represents the number of carbon atoms in the hydrocarbon.

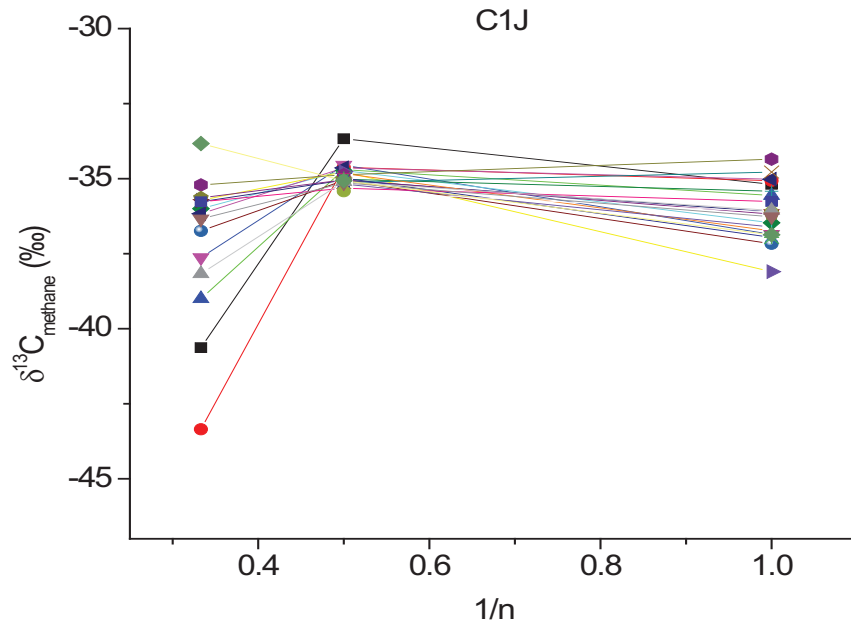


Figure D.7. The natural gas plot for well c1J (NTS 94/08). $\delta^{13}\text{C}$ values vs $1/n$ are shown where n represents the number of carbon atoms in the hydrocarbon.

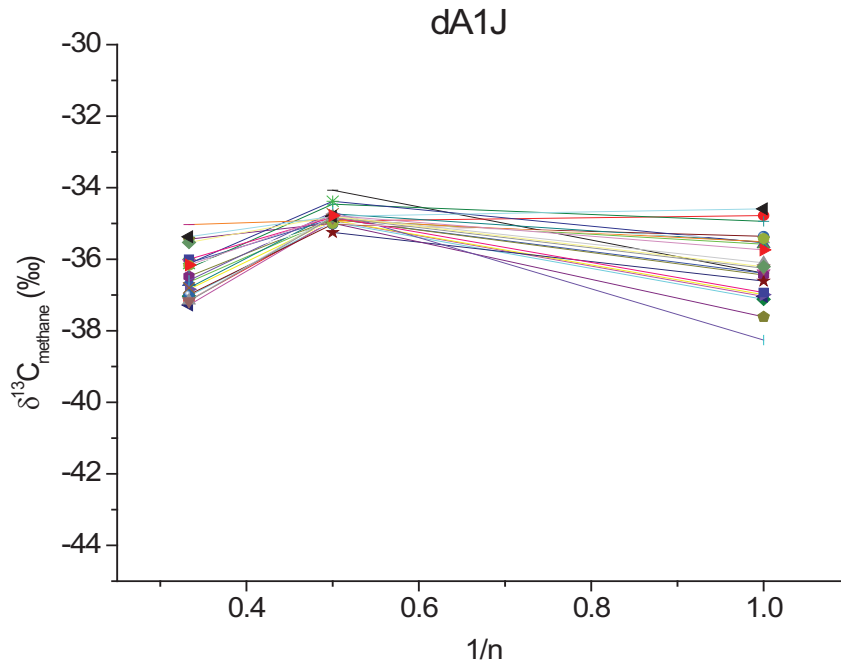


Figure D.8. The natural gas plot for well dA1J (NTS 94/08). $\delta^{13}\text{C}$ values vs $1/n$ are shown where n represents the number of carbon atoms in the hydrocarbon.

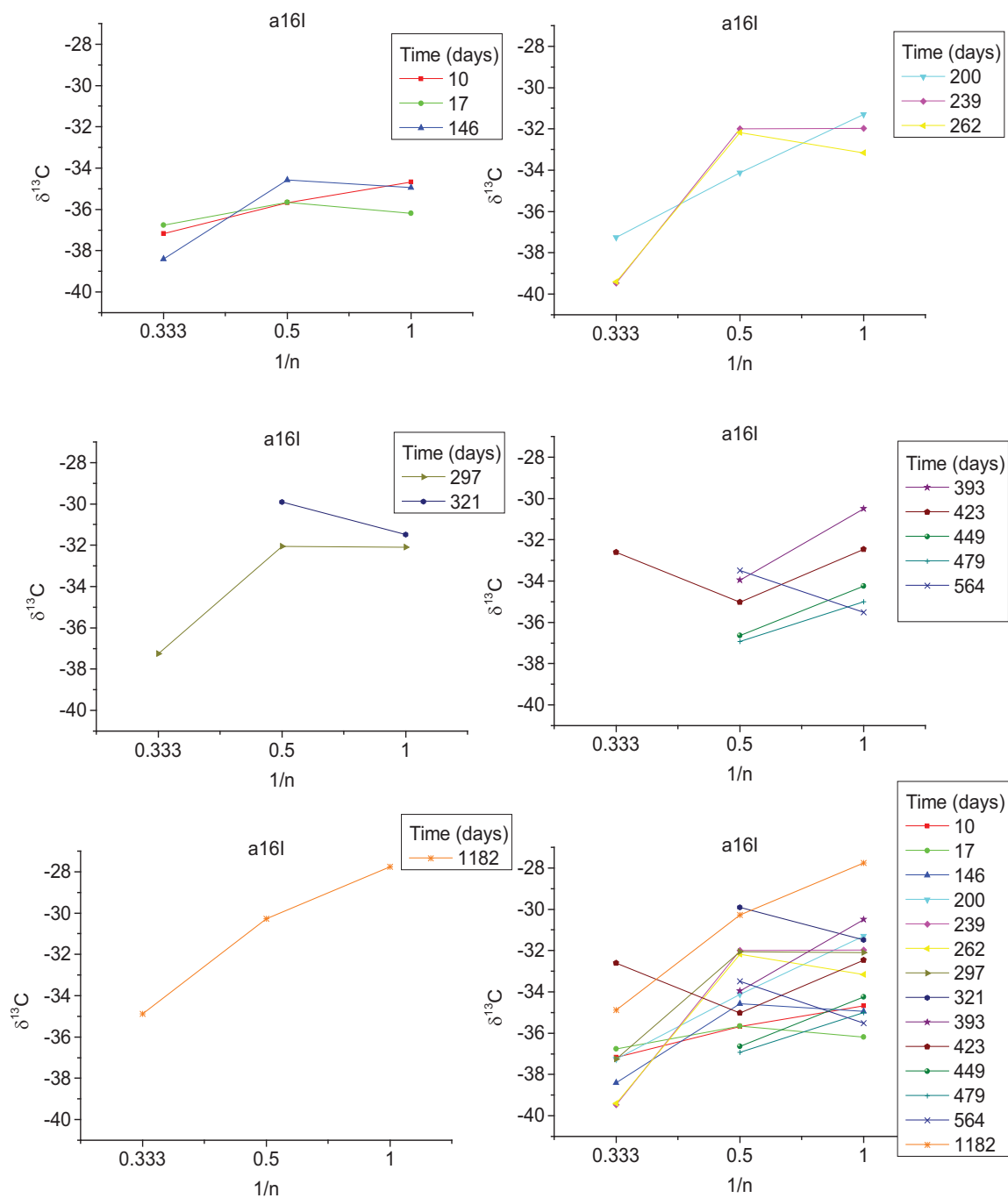


Figure D.9. Natural gas plots for well a16I (NTS 94/08) showing variation in carbon isotope signatures of gases over time. $\delta^{13}\text{C}$ values vs $1/n$ are shown where n represents the number of carbon atoms in the hydrocarbon.

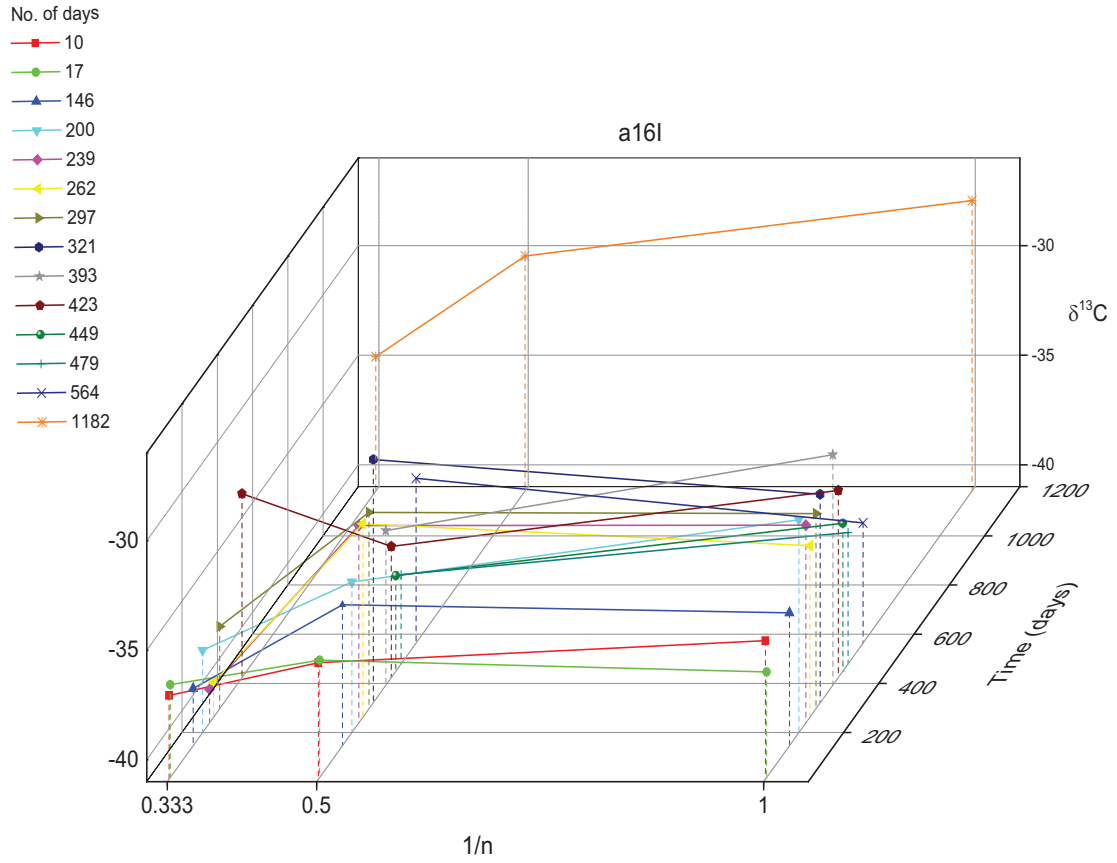


Figure D.10. 3D natural gas plot for well a16I (NTS 94/08) showing variation in carbon isotope signatures of gases over time. $\delta^{13}\text{C}$ values vs $1/n$ are shown where n represents the number of carbon atoms in the hydrocarbon.